Mechanisms of platelet activation in vaccine-induced thrombotic thrombocytopenia and heparin-induced thrombocytopenia

Richard John Buka

UNIVERSITY OF BIRMINGHAM

A thesis submitted to the
University of Birmingham for the degree of
DOCTOR OF PHILOSOPHY

Department of Cardiovascular Sciences
College of Medicine and Health
University of Birmingham
March 2025

Abstract

Vaccine-induced immune thrombocytopenia with thrombosis (VITT) and heparin-induced thrombocytopenia (HIT) are disorders mediated by antibodies against platelet factor 4 (PF4), an abundant, positively charged, platelet-derived chemokine. In VITT, immune complexes consisting of PF4 and anti-PF4 antibodies form and activate platelets through the low-affinity immune receptor FcγRIIA whereas in HIT, the immune complexes also contain the anticoagulant heparin. Both heparin and PF4 are known to activate platelets independently. Heparin acts through platelet endothelial aggregation receptor 1 (PEAR1) but the mechanism of activation by PF4 is unknown.

The aims of this thesis were therefore to firstly ascertain the mechanism of platelet activation by PF4 and then to investigate whether PF4 and heparin play a role in directly activating platelets in VITT and HIT. A third, separate aim was to investigate endothelial activation in VITT and HIT to elucidate any differences that may contribute to the common occurrence of cerebral venous sinus thrombosis in VITT but not in HIT.

Herein, PF4 is shown to lead to platelet aggregation, α-granule release, and spreading in a dose-dependent manner starting at 10 µg/mL (1.28 µM). This occurs through binding to the thrombopoietin receptor c-Mpl and signalling through Janus kinase 2 (JAK2), a process that can be blocked by the JAK2 inhibitor, ruxolitinib, and a c-Mpl blocking antibody. Next, it was shown that blockade of the PF4-c-Mpl interaction and downstream signalling could reduce platelet aggregation to sera and isolated immunoglobulin G from patients with VITT. There was no such clear effect with HIT sera and antibodies. However, blockade of the heparin-PEAR1 interaction with an inhibitory anti-PEAR1 nanobody did lead to reduction in platelet aggregation and α-granule release to HIT sera and antibodies. These findings may have therapeutic relevance when developing targeted therapies for use in these disorders. Endothelial cell work showed no direct induction of endothelial activation by VITT or HIT sera or antibodies, nor did they lead to platelet recruitment.

Publications arising from this thesis

1. Richard J Buka*, Samantha J Montague*, Luis A Moran, Eleyna M Martin, Alexandre Slater, Steve P Watson, Phillip L R Nicolson. **PF4 activates the c-Mpl-Jak2 pathway in platelets**. *Blood*. 2024;141(1)64-69. DOI: 10.1182/blood.2023020872. *Equal contribution (joint first authorship).

2. Richard J Buka, Sue Pavord. **Anti-platelet factor 4 immunothrombotic syndromes**. *Br J Haematol*. 2024;205(4):1291-1295. 10.1111/bjh.19663.

3. Eleyna M Martin, Joanne C Clark, Samantha J Montague, Luis A Morán, Ying Di, Lily J Bull, Luke Whittle, Florije Raka, Richard J Buka, Idrees Zafar, Caroline Kardeby, Alexandre Slater, Steve P Watson. **Trivalent nanobody-based ligands mediate powerful activation of GPVI, CLEC-2, and PEAR1 in human platelets whereas FcγRIIA requires a tetravalent ligand.** *J Thromb Haemost*. 2024;22(1):271-285. 10.1016/j.jtha.2023.09.026.

4. Phillip LR Nicolson, Samantha J Montague, Richard J Buka, Anthony Calvert, Jo-Ann I Shepherd, Yi Zhang, Jing Jing Wang, Jack Sharman, Eman Hassan, James Harrison, Errin Lawrence, Phillip El-Dalil, Dhruv Parekh, Husam Osman, Tom P Gordon, Ishac Nazy, Theodore Warkentin, William Lester. **Anti-PF4 mediated thrombocytopenia and thrombosis associated with acute cytomegalovirus infection displays both HIT-like and VITT-like characteristics**. 2025. *Br J Haematol.* doi.org/10.1111/bjh.20092

5. Phillip LR Nicolson, Simon T Abrams, Gayatri Amirthalingam, Kevin Brown, Richard J Buka, Mark J Caulfield, Joshua Gardner, David Goldblatt, Charlotte Lovatt, Sam J Montague, Dean J Naisbitt, Alan Parker, Sue Pavord, Mary E Ramsay, Jonathan AC Sterne, Cathie LM Sudlow, Cheng Hock Toh, Steve P Watson, Guozheng Wang, Angela M Wood, William Whiteley, Munir Pirmohamed. **Understanding Mechanisms of Thrombosis and Thrombocytopenia with Adenoviral SARS-CoV-2 Vaccines: A Comprehensive Synopsis**. In press. *Efficacy and Mechanism Evaluation.*

Acknowledgements

I was supported to start this work through funding from the UK Department of Health and Social Care via the National Institute for Health and Care Research (NIHR) (NIHR135073). Further funding was provided by the British Heart Foundation (BHF), first through a dedicated scholarship and later via a BHF Accelerator Grant.

This research would not have been possible without the infrastructure at the University of Birmingham, particularly the laboratory shared by the Birmingham Platelet Group within the Institute of Biomedical Research. I am very appreciative of the estates, technical, and laboratory management staff who contribute to the upkeep of these research spaces. The Department of Cardiovascular Sciences, where this research was conducted, benefits from support by the NIHR Biomedical Research Centre (NIHR203326) and the British Heart Foundation Accelerator (BHF) (AA/18/2/34218).

Firstly, I am incredibly grateful to my two direct PhD supervisors, Dr Pip Nicolson and Dr Samantha Montague. Without Pip's organisation, lateral thinking, and hard work, the opportunities that enabled this research would not have materialised. It has been a joy to be mentored by Pip and I think he has also enjoyed the process, describing it as attempting to steward an excited puppy. Pip played a vital role in recruiting local patients with VITT and meticulously storing the countless sequential samples that formed the foundation of this work. Sam has provided world-class training in laboratory techniques, instilling a structured, detail-focused approach. Most importantly, she has kept my feet on the ground, ensuring accountability through monthly reports. Her experience in scientific writing and attention to detail greatly shaped our joint first author publication and would not have been possible without her.

Prof Steve Watson has been an invaluable mentor, offering wisdom and guidance. In many ways, we are kindred spirits, sharing an excitement for new discoveries, and I hope to maintain the same enthusiasm he has demonstrated throughout his career. I am also sincerely

appreciative of Dr Gill Lowe, who has provided clinical mentorship, encouraged forward-thinking, and facilitated future opportunities. Prof Roy Bicknell has been an excellent sounding board for bigger ideas and has offered valuable careers afvice.

The Birmingham Platelet Group has provided an incredibly supportive working environment, making daily lab life a joy. Their dedication and work ethic continue to be an inspiration. Firstly, the willingness of many members of the group, their families, and others in and around the university to give blood for healthy volunteer experiments is pivotal and none of this work could have been done without this altruism. Several aspects of this work were performed with significant support from others. A special mention goes to Dr Luis Moran, who generously dedicated time to teaching me core laboratory techniques, always with a smile. No question, request for help, or task was ever too much trouble. His idea to send a small cut-out from a platelet lysate SDS-PAGE led to the discovery described in Chapter 3. Dr Jenefa Begum kindly provided cultured endothelial cells and advice. Jenefa was an absolute pleasure to work with, never asking for anything except the odd bit of blood in return. Thank you also to her boss, Prof. Asif Iqbal for facilitating this vital help. Dr Beata Grygielska's assistance with endothelial cell culture was greatly appreciated. Dr Eleyna Slater conducted surface plasmon resonance experiments and contributed to nanobody manufacturing, alongside Dr. Rachel Lamerton, who also maintained essential lab equipment, was always willing to help me (especially with the daftest and most naïve questions) and is now a wonderful friend. Dr Alex Slater shared his expertise in protein structure, helping me navigate AlphaFold and produce figures in PyMOL Ying Di played a crucial role in developing nanobodies and managed all shipping logistics - saving me from having to grapple with an unfathomable, archaic process. Ying's ability to fix expensive machines without judgment, always with a smile, has been truly invaluable. Dr Steve Thomas provided expert guidance on microscopy and performed platelet spreading analysis using bespoke code, championed health and safety measures, and shared excellent hill-walking recommendations. I am also grateful to Dr Julie Rayes for her thoughtful feedback on my first- and second-year reports, insightful experimental advice for Chapter 5,

and generosity in lending me antibodies. Dr Ingrid Dumitriu's expert review of my reports, enthusiastic support, and constructive feedback also shaped the direction of my future experiments. Dr. Natalie Poulter has been a tremendous help in her role as postgraduate research lead, particularly in navigating the ever-expanding list of mandatory requirements. Prof Neil Morgan's input during laboratory meetings has been greatly valued, as has his generosity in letting me watch football in his office. Prof. Paul Harrison initially agreed to supervise my PhD for a different project that was later shelved due to early successes in this one. His support made it possible for me to apply for this post, and his periodic enthusiastic encouragement has meant a great deal. Particular appreciation also goes to the management staff, including Gayle Halford, who provided a warm welcome when I joined the group, as well as Donna Wiles and Holly Hoar for their expertise in navigating the complexities of contracts and finance. My final-year BMedSc student, Mitchell Hall, deserves recognition as the first undergraduate I have supervised. His patience in managing my chaotic ideas and style has been greatly appreciated. Hugo Lagonotte, who visited from Université de Tours, displayed remarkable aptitude in quickly learning and expertly performing platelet aggregation enabling him to assist with experiments in Chapter 4.

Beyond the lab, the NIHR VITT consortium, led by Prof Sir Munir Pirmohamed, played a key role in making this work possible. Dr Sue Pavord provided the opportunity to contribute to a short review piece, and her ongoing encouragement has been uplifting. I also value the insightful feedback received from Dr Simon Abrams, Prof Alan Parker, and their teams during monthly collaborator meetings. Discussions with Dr Joseph Aslan and Prof Ian Hitchcock on JAK2 and c-Mpl have been instrumental, as have those with Prof Yves Gruel and Dr Jérôme Rollin on HIT. A special note of appreciation goes to Prof Gruel and Dr Rollin for providing the monoclonal HIT-like antibody, 5B9.

I also acknowledge the committee and members of HaemSTAR, an organisation I am privileged to chair, as well as collaborators on other clinical research projects that I have been able to keep moving during quieter moments. This is also an opportunity to recognise previous

supervisors and mentors who have offered guidance, encouragement, and career advice, including occasional reality checks. Prof Mark Cobbold, Dr Hugo de la Peña, Prof M Thirumala Krishna, Prof Ben Willcox, Dr Carrie Willcox, Dr Mab Salim, Dr Fiyaz Mohammed, Prof Charlie Craddock, Dr Christine Wright, Dr David Sutton, and Dr Jane Graham have all played a role in shaping my journey.

Outside of work, I am deeply appreciative of my wife, Holly, who has provided a counterbalance to becoming entirely consumed by research. Over the past few years, she has nurtured and entertained our (now) three children with more love than I ever thought possible. She is a wonderful mother, a quite incredible human being, and exceptionally talented at planning holidays. To my children, Joey, Autumn, and Jasper, you are my greatest source of joy and a constant reminder to take breaks and have fun. To our great friends Jacky and Dan, thank you for being a refuge when I have needed it; always somewhere to go with the kids when at a final loose end. They are a second family and some lovely camping trips have been the ultimate distraction from platelets and thrombosis. Finally, my heartfelt gratitude extends to my wider family. My parents, Mary and George, and in-laws, Paula and Allen, have stepped in with emergency childcare, sustenance, and much parenting of two adults in their 30s who should usually know better. Rob, Sophie, Dan, Abi, George, Helen, Alan, and all the kids have brought fun and laughter along the way, for which I am truly grateful.

Dedication

This work is dedicated to the patients and the families of those who died from vaccine-induced immune thrombocytopenia with thrombosis, and those who continue to suffer the after-effects of this disease.

I also dedicate this to my wife Holly, and three children, Joey, Autumn, and Jasper, without whom this would have all been completed much quicker and to a higher standard.

Contents

List of Figures

List of Tables

Abbreviations

5-HT	5-hydroxytryptophan
ACKR1	Atypical chemokine receptor 1
ADAMTS13	A disintegrin and metalloproteinase with thrombospondin type 1 motif, member 13
ADP	Adenosine diphosphate
AEBSF	4-(2-aminoethyl) benzenesulfonyl fluoride hydrochloride
aPTT	Activated partial thromboplastin time
APOH	Apolipoprotein H
AS	Ankylosing spondylitis
ATP	Adenosine triphosphate
AUC	Area under curve
AUC min^{-1}	Area under curve per minute
Bad	Bcl-2-associated agonist of cell death
BHF	British Heart Foundation
BSA	Bovine serum albumin
CD	Cluster of differentiation
CD40L	CD40 ligand
CHO cells	Chinese hamster ovary cells
CLEC-2	C-type lectin-like receptor 2
CLIA	Chemiluminescence immunoassay
COVID-19	Coronavirus disease 2019
CRP	Collagen-related peptide
CS	Chondroitin sulfate
CSA	Chondroitin 4-O-sulfate A
CSB	Chondroitin 4-O-sulfate B
CSC	Chondroitin 6-O-sulfate
CSD	Chondroitin 2,6-O-sulfate
CSE	Chondroitin 4,6-O-sulfate
CSB	Chondroitin 4-O-sulfate with iduronic acid
CVST	Cerebral venous sinus thrombosis
CXCL	C-X-C motif ligand
CXCL4	CXC motif ligand 4
CXCR	C-X-C motif receptor
CXCR3	CXC Chemokine Receptor 3
CXCR3b	CXC Chemokine Receptor 3b
cAMP	Cyclic adenosine monophosphate
c-Cbl	Casitas B-lineage lymphoma protein
c-Mpl	Cellular myeloproliferative leukemia virus oncogene
DMSO	Dimethyl sulfoxide
DNASE1	Deoxyribonuclease
DNA	Deoxyribonucleic acid
DTT	Dithiothreitol
ECMO	Extracorporeal membranous oxygenation
EGF	Epidermal growth factor
ELISA	Enzyme-linked immunosorbent assay

EM	Electron microscopy
EMI	Elastin microfibril interface
ERK	Extracellular signal-regulated kinases
ERK1/2	Extracellular signal-regulated kinases 1 and 2
FcγRIIA	Fc gamma receptor IIa
FGF2	Fibroblast growth factor 2
Gal	Galactose
GalNAc	N-acetylated galactosamine
GAG	Glycosaminoglycan
GATA-3	GATA-binding protein 3
GlcA	Glucuronic acid
GlcNAc	N-acetylated glucosamine
GlcNS	N-sulfated glucosamine
GP130	Glycoprotein 130
GPVI	Glycoprotein VI
GRB2	Growth factor receptor-bound protein 2
GWAS	Genome wide association study
HDMECs	Human dermal microvascular endothelial cells
HIPA	Heparin-induced platelet activation
HIT	Heparin-induced thrombocytopenia
HS	Heparan sulfate
HSC	Haematopoietic stem cell
HUVECs	Human umbilical vein endothelial cells
IC50	Inhibitory concentration 50%
ICAM-1	Intercellular adhesion molecule 1
IGFR1	Insulin-like growth factor receptor 1
Ig	Immunoglobulin
IKK	IkappaB kinase
IL-8	Interleukin 8
IL1R1	Interleukin 1 receptor type 1
ITAM	Immunoreceptor tyrosine-based activation motif
JAK2	Janus kinase 2
JNK	c-Jun N-terminal kinase
KD	Dissociation constant
LFIA	Lateral flow immunoassay
LIGam	Latex gel immunoassay
LRP1	Low-density lipoprotein receptor-related protein 1
LTA	Light transmission aggregometry
MAPK	Mitogen-activated protein kinase
MEA	Multiplate electrode aggregometry
MK	Megakaryocyte
MGUS	Monoclonal gammopathy of uncertain significance
MOPS	3-(Morpholin-4-yl)propane-1-sulfonic acid
mAb	Monoclonal antibody
mTOR	Mammalian target of rapamycin
mTORC	Mammalian target of rapamycin complex
ND	Not done
ND50	Neutralising dose 50
NET	Neutrophil extracellular trap

NETosis	Neutrophil extracellular trap formation
NETs	Neutrophil extracellular traps
NIHR	National Institute for Health and Care Research
NHS	National Health Service
NHSBT	National Health Service Blood and Transplant
OD	Optical density
PaGIA/PIFA	Particle gel immuno and immunofiltration assay
PBS	Phosphate buffered saline
PDGF	Platelet-derived growth factor
PDK1	Phosphoinositide-dependent kinase 1
PF4	Platelet factor 4
PF4v	PF4 variant
PI3K	Phosphoinositide 3-kinase
PKCδ	Protein kinase C delta type
PLCγ2	Phospholipase C gamma 2
POSTN	Periostin
PRP	Platelet rich plasma
PS	Phosphatidylserine
PTGDS	Prostaglandin D2 synthase
RT	Room temperature
SARS-CoV-2	Severe acute respiratory syndrome coronavirus 2
SDS-PAGE	Sodium dodecyl sulfate polyacrylamide gel electrophoresis
SHC	Src homology 2 domain-containing protein
SOS	Son of sevenless
SPR	Surface plasmon resonance
SRA	Serotonin release assay
STAT	Signal transducer and activator of transcription
STAT3/5	Signal transducer and activator of transcription 3/5
Syk	Spleen tyrosine kinase
TBK	TANK-binding kinase
Th1	T helper cell 1
Th2	T helper cell 2
Tiam1	T-cell lymphoma invasion and metastasis 1
TLR	Toll-like receptor
TNFα	Tumour necrosis factor α
TPO	Thrombopoietin
TRAP	Thrombin receptor activating peptide
TXA2	Thromboxane A2
TULA-2	T-cell ubiquitin ligand-2
TYK2	Tyrosine kinase 2
VCAM-1	Vascular cell adhesion molecule 1
VEGF	Vascular endothelial growth factor
VITT	Vaccine-induced immune thrombocytopenia with thrombosis
vWF	Von Willebrand factor
β2-GPI	β2-Glycoprotein I

Word count: 37,456

1. General introduction

On 29th December 2021, the UK became the first country in the world to issue emergency approval for the ChAdOx1 nCoV-19 vaccine against Severe Acute Respiratory Syndrome Coronavirus 2 (SARS-CoV-2) (Medicines and Healthcare products Regulatory Agency, 2020). This approval was based on a global trial that randomised over 30,000 participants in a 2:1 ratio to vaccination or placebo, reporting a significant reduction in symptomatic and severe Coronavirus Disease 2019 (COVID-19) (Falsey et al., 2021). Over the ensuing months and years, billions of individuals were vaccinated worldwide, and it has been estimated that in the first year of vaccination, 14.4 million lives were saved, which represents the single biggest public health achievement in the history of humanity (Watson et al., 2022).

However, in March 2021 reports began to emerge of rare patients presenting to hospitals across Europe who had a sudden onset of unexplained blood clots in the context of a low platelet count. The combination of thrombocytopenia and thrombosis is unusual and has a short differential diagnosis. Moreover, the blood clots were often at unusual sites such as the veins that drain blood from the brain and bowel. It was soon recognised that these patients, who had recently received ChAdOx1 nCoV-19, were afflicted with a disorder that closely resembled heparin-induced thrombocytopenia (HIT), an infrequent, idiosyncratic adverse effect of treatment with the anticoagulant heparin (Schultz et al., 2021; Greinacher et al., 2021; Scully et al., 2021). The new disorder, termed vaccine-induced immune thrombocytopenia with thrombosis (VITT), was associated with high morbidity and mortality (Pavord et al., 2021), and for survivors the physical and psychological effects are profound and long-lasting (Bennett et al., 2023a, 2023b).

In response to the urgent need for research into VITT, a grant was awarded by the UK National Institute for Health and Care Research (NIHR) to a consortium of academics across the UK.(National Institute for Health and Care Research, 2021) The work in this thesis, which

focuses on platelet activation in VITT and HIT, initially stemmed from this funding and was later supported by funding from the British Heart Foundation (BHF).

1.1. Platelets

Platelets are small, anucleate cells, 2-4 μm in diameter that are key components of the haemostatic system and contribute to numerous physiological and pathological processes. They are key players in thrombotic diseases where they mediate blood clot formation by responding to vessel injury, aggregating with other platelets and provide a surface for the activation of clotting factors. As such, antiplatelet drugs are vital therapies that are proven to save lives (Antithrombotic Trialists' Collaboration, 2002; Stanger et al., 2023).

Platelets are produced in the bone marrow from megakaryocytes, specialised myeloid cells that in a healthy human adult produce 2,000 to 3,000 platelets each, and collectively 100 billion platelets per day (Carminita et al., 2024). The process of platelet production is highly dependent on thrombopoietin (TPO), a hormone that is produced at constant rate in the liver and drives megakaryocyte differentiation and maturation (Hitchcock and Kaushansky, 2014). TPO binds to the cellular myeloproliferative leukaemia protein (c-Mpl) on megakaryocytes which leads to signalling through the Janus kinase and signal transducer and activator of transcription (JAK-STAT) pathway and induction of megakaryocyte transcriptional programmes (Hitchcock et al., 2021).

1.1.1. Platelet activation

Platelets circulate in the bloodstream in a quiescent state until they become activated by a range of stimuli including fixed, membrane-bound ligands, soluble ligands, and biomechanical forces. At sites of vascular injury, platelets adhere to proteins either on endothelial cells or on the subendothelial matrix. A key protein in this process is subendothelial collagen which is exposed at sites of injury. Multimers of von Willebrand factor (vWF) anchor to exposed collagen and subsequently bind platelets through the glycoprotein Ib-V-IX complex (Lenting et al., 2024). Collagen also directly activates platelets through glycoprotein VI (GPVI) and integrin α2β1 (Nuyttens et al., 2011; Perrella et al., 2021). Numerous other interactions of activating ligands and respective receptors on platelets trigger various downstream signalling pathways

that lead to, and reinforce, platelet activation. Generally, fixed ligands such as collagen and vWF signal through phosphorylation cascades involving Src family kinases and phospholipase C gamma 2 (PLCγ2) whilst soluble activators such as thrombin and adenosine diphosphate (ADP) interact with G protein coupled receptors (Offermanns, 2006).

Whilst there are numerous signalling pathways, a key convergence downstream of the various activatory signals is the mobilisation of calcium ions (Ca^{2+}), which contributes to shape change, granule secretion, and integrin activation leading to aggregation (Varga-Szabo et al., 2009). Shape change can be measured investigationally by microscopic examination of platelet spreading on agonist-coated coverslips (Khan et al., 2020).

1.1.2. Platelet granules

Platelets contain three types of granules, α-granules, dense granules, and lysosomes, and the release of α granules and dense granules is an important step in platelet activation (Gremmel et al., 2024; Yao and Kahr, 2024). Selected constituents and functions of α- and dense granules are summarised in Table 1.1.

Dense granules are acidic, membrane associated, intracellular compartments measuring 150 nm in diameter, each platelet containing 3-8 (Heijnen and van der Sluijs, 2015). They contain relatively few different molecules, each at high concentrations including ADP, adenosine triphosphate (ATP), Ca^{2+}, pyrophosphate, polyphosphates, magnesium ions (Mg^{2+}) and potassium ions (K^{+}) (Heijnen and van der Sluijs, 2015). These molecules are released quickly on platelet activation and are crucial in positively reinforcing platelet activation (Heijnen and van der Sluijs, 2015). Platelet activation is further reinforced by *de novo* synthesis and secretion of thromboxane A_2 (TXA_2) from arachidonic acid via the cyclooxygenase pathway. TXA_2 acts in both an autocrine and a paracrine manner via the thromboxane A2 receptor (TxA_2R) (Mumford et al., 2010).

Within a single platelet, there are also 50-80 α-granules, (Heijnen and van der Sluijs, 2015) which contain a much larger range of proteins with diverse biological roles. These include

those with roles in haemostasis such as factor V, fibrinogen, vWF, proteins that are both pro- and anti-angiogenic, growth factors, proteases, necrotic factors, and other cytokines (Yao and Kahr, 2024).

Granule release is an experimental marker of platelet activation. A well-established assay is flow-cytometry for P-selectin, which on release from α-granules, incorporates into the platelet membrane where it can be detected by antibody binding (Jourdi et al., 2023). This is a method used for the diagnosis of VITT and HIT, and is used in this thesis. Dense granule secretion can be quantified by measuring ATP-mediated oxidation of luciferin by luciferase and resultant fluorescence (Dawood et al., 2007). Dense granule and lysosome secretion can also be assessed by flow cytometry for CD63 (Jourdi et al., 2023). Secretion from dense granules is also measured as a marker of platelet activation for the diagnosis of HIT in the serotonin release assay (SRA) which detects release of serotonin containing ^{14}C after pre-incubation and uptake of ^{14}C-serotonin into platelets (Warkentin et al., 2015).

Table 1.1. Major constituents of platelet α and dense granules.

5-HT: 5-hydroxytryptophan; ADP: adenosine diphosphate; ATP: adenosine triphosphate; CD40L: CD40 ligand; CXCL: CXC motif chemokine ligand; EGF: epidermal growth factor; MCP-1: monocyte chemoattractant protein-1; MIP-Iα: macrophage inflammatory protein-1 beta PAI-1: plasminogen activator inhibitor; PDGF: platelet-derived growth factor; PF4: platelet factor 4; RANTES: regulated upon activation, normal T cell expressed and secreted; TGFβ: transforming growth factor β; VEGF: vascular endothelial growth factor; vWF: von Willebrand factor.

α granules		**Dense granules**	
Molecule	**Function**	**Molecule**	**Function**
Adhesion proteins		**Feeback mediators**	
Fibrinogen	Platelet adhesion, thrombus formation	ADP	Compounding platelet activation and thrombus formation
vWF		ATP	
P-selectin	Cell adhesion	5-HT (serotonin)	
Thrombospondin-1	Thrombus formation	Ca^{2+} and Mg^{2+}	
Fibronectin	Platelet adhesion and tissue repair		
Vitronectin	Cell adhesion and migration		
Regulation of fibrinolysis		**Polyphosphates**	
PAI-1	Antifibrinolytic	Inorganic polyphosphate	Procoagulant
Alpha-2-antiplasmin			
Chemokines			
PF4 (CXCL4)	Multiple		
CD40L	Inflammation		
CXCL1 (GRO-α)	Leukocyte recruitment and activation, inflammation		
CXCL5			
CXCL7 (NAP-2)			
CXCL8 (IL-8)			
CCL2 (MCP-1)			
CCL3 (MIP-Iα)			
CCL4 (MIP-Iβ)			
CCL5 (RANTES)			
Cytokines			
VEGF	Proangiogenic		
TGFβ	Inflammation		
EGF	Cell proliferation and wound healing		
PDGFβ			

1.1.3. Aggregation and procoagulant platelets

Following platelet adhesion and activation, the membrane protein, integrin $\alpha_{IIb}\beta_3$ undergoes a conformational change mediated by “inside-out” signalling. Integrin $\alpha_{IIb}\beta_3$ is the dominant platelet integrin with each cell containing ~100,000 copies (Janus-Bell and Mangin, 2023). This leads to crosslinking of platelets through the binding of fibrinogen and vWF leading to the formation of stable platelet aggregates (Janus-Bell and Mangin, 2023). Aggregation can be measured in platelet rich plasma (PRP) or isolated washed platelets by light transmission aggregometry whereby platelets are exposed to agonists whilst being stirred. Aggregated platelets clump together allowing more light transmission which can be measured by a detector (Cattaneo et al., 2013). Aggregation can also be measured in whole blood by impedence where platelets adhere to and aggregate around electrodes in response to agonists (Morel-Kopp et al., 2016). Both methods can be used in the diagnosis of HIT (Arachchillage et al., 2023). Integrin $\alpha_{IIb}\beta_3$ can also be measured in its active form by flow cytometry as a surrogate for the functional readout of aggregation (Savi et al., 2005).

Very strong activating signals can result in the formation of procoagulant platelets. These are platelets that expose phosphatidylserine (PS) on the extracellular surface of the plasma membrane which allows the binding of coagulation factors leading to thrombin generation and fibrin deposition (Agbani and Poole, 2017). Procoagulant platelet formation can be measured by flow cytometry for PS exposure using fluorophore-labelled Annexin-V, a protein that can bind PS at high affinity in a Ca^{2+} manner (Boersma et al., 2005; Jourdi et al., 2023). Again, this can be used as a marker of platelet activation in the diagnosis of HIT.

1.2. Chemokines

Chemokines are immune molecules that function through controlling the circulation, adhesion, and activation of immune cells in tissues (Schulz et al., 2016). From a single proto chemokine that first emerged in evolution 650 million years, they have expanded in number through gene duplication (DeVries et al., 2006) and humans possess over 40 distinct genes coding for individual proteins (Hughes and Nibbs, 2018). These proteins and their receptors form a complex network where many individual chemokines can bind to several receptors and vice-versa (Hughes and Nibbs, 2018).

Chemokines are classified into four main subfamilies: C, CC, CXC, and CX3C, names that refer to the presence and distribution of conserved cysteine residues; all chemokines possess two conserved cytokine bridges, except C chemokines which contain only one (Hughes and Nibbs, 2018). CXC chemokines (which include PF4) are characterised by two N-terminal cysteine residues separated by a single amino acid and are further subclassified by the presence or absence of an N-terminal ELR motif (Glu-Leu-Arg) which precedes the first N-terminal cysteine. ELR positive chemokines including interleukin-8 (IL-8, a.k.a. CXCL8) are pro-angiogenic and potent neutrophil attractants whereas ELR negative chemokines are very weakly neutrophil attractant and generally angiostatic (Rollins, 1997).

1.3. Platelet factor 4 (PF4)

First purified in the 1950s, PF4, also known as CXC motif ligand 4 (CXCL4), was the first chemokine discovered. It is an abundant protein that is stored in, and released from, platelet α-granules upon activation. PF4 is expressed only by eutherian (placental) mammals (Nomiyama et al., 2013) and evolutionary aspects are further discussed in section 6.2. A timeline of key discoveries in the understanding of PF4 and its biology is presented in Figure 1.1.

Although PF4 can be expressed in other cell types including mast cells, microglia (De Jong et al., 2008), monocytes (Schaffner et al., 2005; Vandercappellen et al., 2007), T cells (Shi et al.,

2014), and dendritic cells (Maier et al., 2009; van Bon et al., 2014), it is predominantly associated with platelets (Barber et al., 1972). It is stored in platelet α-granules in complex with the intracellular proteoglycan, serglycin which, in platelets, is decorated with the negatively charged glycosaminoglycan (GAG), chondroitin sulfate (CS) (Woulfe et al., 2008). After platelet activation, PF4 is released from α-granules into the endoluminal space where it can then interact with glycans that coat the surface of platelets, other cellular blood components, and endothelial cells, as well as with other molecules. These interactions are discussed below.

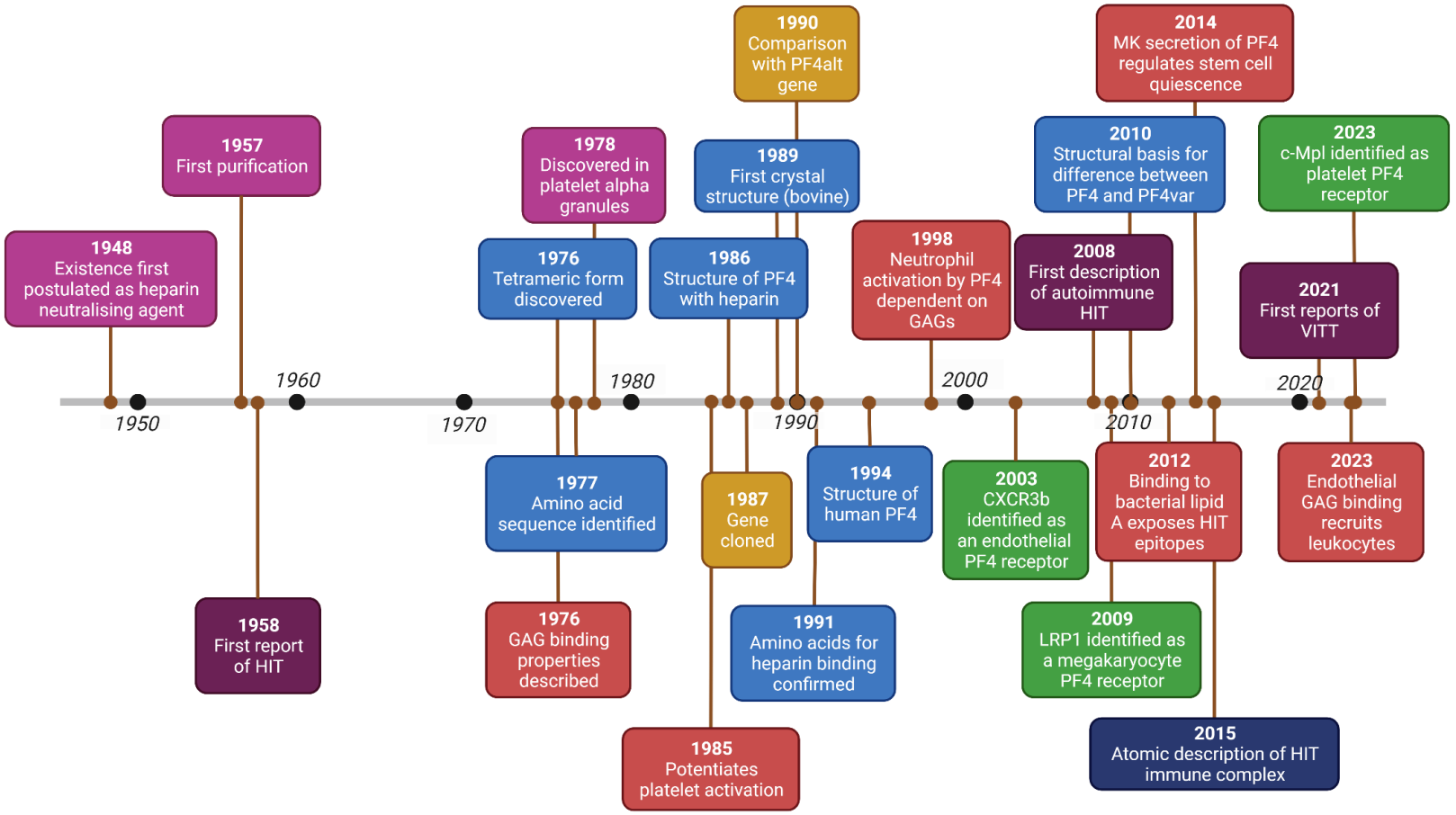

Figure 1.1. Timeline of key discoveries concerning PF4.

Magenta: purification and biological location; purple: clinical implications; red: functional effects; yellow: genetics; green: receptors; blue: structural biology; dark blue: structure of interaction with polyanions. GAG: glycosaminoglycan, HIT: heparin-induced thrombocytopenia, LRP1: low-density lipoprotein receptor-related protein-1, MK: megakaryocyte, VITT: vaccine-induced immune thrombocytopenia with thrombosis. See Appendix 1 for references.

1.3.1. Structure of PF4

The PF4 gene, which sits on chromosome 4 in a cluster of 12 other CXC chemokines (Tunnacliffe et al., 1992), codes for a 101 amino acid protein which includes a leader-sequence that is cleaved to yield a 70-amino acid chain. This forms a 7.8 kDa protein that combines as two homodimers to form an asymmetric tetramer (Zhang et al., 1994; Poncz et al., 1987). A striking characteristic of tetrameric PF4 is the equatorial ring of positive charge formed by a lysine-rich KKVIKK C-terminus sequence that facilitates binding to negatively charged GAGs and which is key to its diverse biological roles (Figure 1.2A).

In some primates (humans, great apes, and old-world monkeys), the PF4 gene has been duplicated and altered giving rise to another chemokine, PF4 variant (PF4v or CXCL4L1) (Struyf et al., 2004). The mature amino acid sequence of PF4v differs by only three amino acids: P58L, K66e, and L67H (Eisman et al., 1990) but this has a major effects on the structure of the tetramer such that the α-helices swing out into the aqueous space, leading to a loss of the globular structure of PF4 (Kuo et al., 2013) (Figure 1.2B). Functionally, this results in weaker binding to GAGs but much stronger inhibition of endothelial cell migration (Dubrac et al., 2010). In addition to these changes, the cleaved leader sequence is markedly different. Lasagni et al. transfected a range of human cells including endothelial, arterial smooth muscle, monocytes, T cells and various cancer cell lines with PF4 and PF4v and compared their synthesis, storage and release (Lasagni et al., 2007). Whilst PF4 was stored in electron-dense cytoplasmic granules and released following stimulation, PF4v was constitutively synthesised and released. It has not been confirmed whether this is the case in platelets.

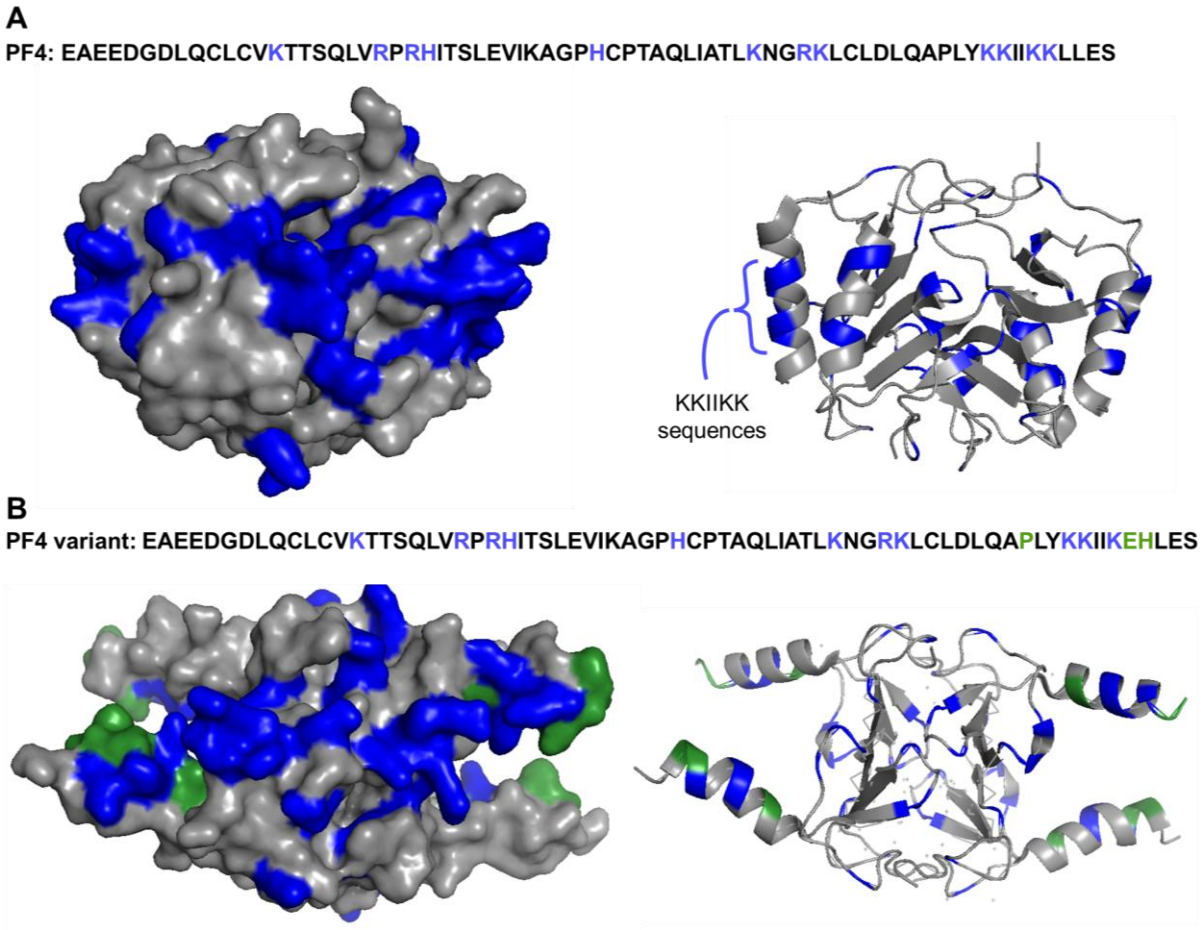

Figure 1.2. The structure of tetrameric PF4 (A) and PF4 variant (B) with associated amino acid sequences of one monomer.

Denoted in blue are positively charged amino acids and denoted in green are the three amino acid substitutions in PF4 variant compared with PF4. For PF4, the positively charged C-terminus KKIIKK sequence is marked on one alpha helix. Figure created in PyMOL using structural information from (A) (Zhang et al., 1994) and (B) (Kuo et al., 2013)

1.3.2. Functions of PF4

The biological functions of PF4 are diverse. It is known to be involved in immune cell activation, thromboinflammation, haemostasis and thrombosis, negative regulation of haematopoiesis, prevention of haematopoietic stem cell ageing, and negative regulation of angiogenesis (Table 1.2). PF4 acts through numerous receptors including CXC chemokine receptor 3b (CXCR3b) (Lasagni et al., 2003), CC chemokine receptor 1 (CCR1) (Fox et al., 2018), LRP1 (Lambert et al., 2009), and cluster of differentiation (CD)11b (Lishko et al., 2018) but most functions are dependent on interactions with negatively charged GAGs such as chondroitin and heparan sulfate (HS) that coat the surfaces of cells in the blood and the endoluminal vasculature. Of note is a 40-year-old observation that PF4 can potentiate the activation of platelets to low dose thrombin which has been proposed to be due to an interaction with GAGs (Capitanio et al., 1985; Kowalska et al., 2010). However, although a mechanism by which PF4 may induce intracellular signalling in cells through the crosslinking of GAGs has been theorised (Petersen et al., 1998, 1999; Kasper et al., 2007), this has not been shown experimentally. Considering its role in coagulation more widely, PF4 has been reported to have both pro-haemostatic/thrombotic and anti-haemostatic/thrombotic roles depending on context. In addition to neutralisation of HS-induced enhancement of antithrombin activity, which is discussed further in section 1.3.3.1, PF4 activates protein C and decreases activation of thrombin activatable fibrinolysis inhibitor (Slungaard and Key, 1994; Slungaard et al., 2003; Kowalska et al., 2007; Mosnier, 2011), demonstrating anticoagulant properties. In contrast, it is known to reduce activated protein C-mediated activation of protein S (Preston et al., 2009), bind to vWF and inhibit its cleavage and inactivation by a disintegrin and metalloproteinase with thrombospondin type 1 motif, member 13 (ADAMTS13) (Nazy et al., 2020) and contribute to the formation of stable fibrin clots (Amelot et al., 2007). The functions of PF4, receptors, and reliance on GAG interactions are presented in Table 1.2.

Table 1.2. Categorised functions of PF4.

The table highlights the most pertinent, functional roles of PF4 and includes information on the affected tissue, receptor and intracellular signalling mediating the function (if known), and whether this role is glycosaminoglycan-dependent. ADAMTS13: a Disintegrin and Metalloproteinase with a Thrombospondin Type 1 motif, member 13; cAMP: cyclic adenosine monophosphate; CCL: Chemokine (C-C motif) ligand;CCR: C-C chemokine receptor; CD: cluster of differentiation; CHO cells: Chines hamster ovary cells; CXCL: C-X-C motif ligand; CXCR: C-X-C motif receptor; FGF2: fibroblast growth factor 2; GAG: glycosaminoglycan; GATA-3: GATA-binding protein 3; HS: heparan sulfate; HUVEC: human umbilical vein endothelial cells; IFNγ: interferon gamma; IKK: IkappaB kinase; IL-2: interleukin 2; IRF; interferon regulator factor; JAK2: Janus kinase 2; LDLR: low density lipoprotein receptor; LRP1: lipoprotein-related receptor 1; Mac-1: Macrophage-1 antigen; MAPK: mitogen-activated protein kinase; MPN: myeloproliferative neoplasm; NA: not applicable; NETs: neutrophil extracellular traps; pDC: plasmacytoid dendritic cell; PF4: platelet factor 4; PI3K: Phosphoinositide 3-kinase; STAT: signal transducer and activator of transcription; TBK; TANK-binding kinase; Th1: T helper cell 1; Th2: T helper cell 2; TLR: toll-like receptor; VEGF: vascular endothelial growth factor; VITT: vaccine-induced immune thrombocytopenia and thrombosis; vWF: von Willebrand factor.

Function	Cell type / tissue	Receptor/binding partner	Signalling	GAG/polyanion-dependent?	Reference
Endothelial proliferation and angiogenesis					
Inhibition of angiogenesis	Endothelial cells	Not reported	Not reported	Yes - activity associated with heparin-binding region	(Maione et al., 1989)
In the absence of its heparin binding domain, PF4 still inhibits angiogenesis	Endothelial cells	Not reported	Not reported	No - PF4 lacking heparin binding site still had an effect	(Maione et al., 1991)
Inhibits mitogenic activity of VEGF in cancer by inhibiting binding to receptor	Endothelial cells	Not reported	Not reported	Yes - PF4 interferes with VEGF121-heparin binding	(Gengrinovitch et al., 1995)
Impaired HUVEC proliferation	Endothelial cells	Not reported	Impaired downregulation of p21Cip1/WAF1	No - GAG independent mechanism	(Gentilini et al., 1999)
Inhibits FGF2-induced endothelial cell proliferation via an intracellular mechanism	Endothelial cells	Not reported	Decreased ERK phosphorylation	No - same effect in HS-neg CHO cells	(Sulpice et al., 2002)
Inhibition of endothelial growth	Endothelial cells	CXCR3b	Increased cAMP and p21 transcription	Not reported	(Lasagni et al., 2003)
Inhibits VEGF synthesis + disrupts KDR-mediated signal transduction	Endothelial cells	Not CXCR3b	Inhibits MAPK signalling	Not reported	(Sulpice et al., 2004)
PF4 heterodimerisation with CXCL8 inhibits endothelial activation and proliferation	Endothelial cells	PF4 + CXCL8 blocks CXCL8 interaction with CXCR2	Not reported	Not reported	(Nesmelova et al., 2005)
Haematopoiesis					
Binds to CD34+ HPCs and enhances binding to stroma. PF4 binds to and blocks IL-8 mediated activation.	Haematopoietic progenitor cells	Suggested - chondroitin-sulfate-containing moiety	Not reported	Yes - lack of binding after chondroitinase	(Dudek et al., 2003)
Inhibition of megakaryocyte terminal differentiation	Megakaryocytes	LRP1	Not reported	Not reported	(Lambert et al., 2009)
Megakaryocyte PF4 secretion leads to maintenance of HSC quiescence	Haematopoietic stem cells	Not reported	Not reported	Not reported	(Bruns et al., 2014)
Inhibition of HSC ageing	Haematopoietic stem cells	CXCR3, LDLR	Not reported	Not reported	(Zhang et al., 2024)
Haemostasis & thrombosis					
Platelet activation and potentiation	Platelets	Not reported	Not reported	Not reported	(Capitanio et al., 1985)
Enhancement of protein C generation by binding glycanated forms of thrombomodulin and protein C	Endothelial cells	NA	NA	Yes	(Dudek et al., 1997)

Neutralises heparan sulfate enhanced antithrombin inactivation of factor Xa	Endothelial cells	NA	NA	Yes	(Fiore and Kakkar, 2003)
PF4 contributes to thrombosis but PF4-null mice had no bleeding diathesis	NA	NA	NA	NA	(Eslin et al., 2004)
Alters structure of fibrin - seals blood clots	Blood vessels	NA	NA	Yes - fibrin is a glycoprotein	(Amelot et al., 2007)
Binds to vWF and inhibits ADAMTS13 activity	Blood vessels	NA	NA	Not reported	(Nazy et al., 2020)
Platelet activation and potentiation	Platelets	Not reported	Not reported	Yes	(Dickhout et al., 2021)
Platelet activation and potentiation + signalling role in platelet activation in VITT	Platelets	c-Mpl	JAK2	Not reported	(Buka et al., 2024)
Thromboinflammation					
Retention of low-density lipoprotein on endothelial cell surface	Endothelial cells	Low density lipoprotein receptors	Not reported	Yes - effect lost with PF4 variants that lacked heparin binding	(Sachais et al., 2002)
PF4 knockout reduces atherosclerosis in mice	NA	Not reported	Not reported	Not reported	(Sachais et al., 2007)
Downregulates atheroprotective haemoglobin receptor CD163	Macrophages	Not reported	Not reported	Yes	(Gleissner et al., 2010a)
Stabilises NETs and prevents degradation	Neutrophils - NETs	NA	NA	Yes (chromatin/DNA)	(Ngo et al., 2023)
Immunity & inflammation					
Neutrophil activation	Neutrophils	GAGs	Not reported	Yes	(Petersen et al., 1999)
Monocyte survival and differentiation	Monocytes	Not reported	Not reported	Inferred	(Scheuerer et al., 2000)
Reduces T cell proliferation, IFNy production, and IL-2 production	T cells	GAGs	Not reported	Yes	(Fleischer et al., 2002)
Phagocytosis	Phagocytes	Not CXCR3b	Not Gi proteins or increased intracellular calcium	Not reported	(Pervushina et al., 2004)
Endothelial activation: increases endothelial E-selectin expression	Endothelial cells	LRP1	NF-kappa-β	Inferred	(Yu et al., 2005)
Induces regulatory T cell proliferation	T cells	Not reported	Not reported	Yes - inhibited by heparin	(Liu et al., 2005)
Differential effects of PF4 on T_h1 and T_h2 cytokine production	T cells	CXCR3	Downregulation of Tbet, upregulation of GATA-3 transcription	Not reported	(Romagnani et al., 2005)
Intracellular calcium release and T cell migration	T cells	CXCR3	Not reported	Yes	(Mueller et al., 2008)
PF4 and CCL5 heterophilic interaction - monocyte arrest on endothelium	Monocytes	Not reported	Not reported	Yes	(Von Hundelshausen et al., 2005)
Monocyte respiratory burst, survival, cytokine expression	Monocytes	Not reported	Rapid activation of PI3K, Syk, and p38 MAPK and delayed activation of Erk	Yes	(Kasper et al., 2007)
Monocyte differentiation - M4 phenotype	Monocyte-derived macrophages	Not reported	Not reported	Not reported	(Gleissner et al., 2010b)
Neutrophil lung infiltration associated with CCL5-PF4 heterotetramers	Lung / neutrophils	Not reported	Not reported	Not reported	(Grommes et al., 2012)
Kills malarial parasites	Red cells	Duffy antigen	Not reported	Yes – Duffy antigen is glycoprotein	(McMorran et al., 2012)
Predominant protein secreted by pDCs in systemic sclerosis and drives fibrosis	pDCs (production)	Not reported	Not reported	Not reported	(van Bon et al., 2014)
Differential effects of PF4 and PF4 variant	Monocytes	Not reported	Not reported	Not reported	(Gouwy et al., 2016)
Induces CD4+ T cells to secrete IL-17 + differentiation of naïve CD4+ T to Th17-cytokine producing cells. Unknown whether direct or indirect.	T cells, monocytes, pDCs	Not reported	Not reported	Not reported	(Affandi et al., 2018)
Drives monocyte migration	Monocytes	CCR1	Not reported	Yes	(Fox et al., 2018)
Monocyte receptor	Monocytes	Mac-1 (CD11b) integrin	Not reported	Yes. Also, Mac-1 PF4 binding mediated by positively charged amino acids	(Lishko et al., 2018)

Produced by pDCs → promotion of fibrosis by potentiation of TLR9-induced IFN	pDCs	Not reported	Secretion under control of PI3K. Potentiates TLR8- but also TLR9-induced IFN production	Not reported	(Ah Kioon et al., 2018)
Differentiation of pro-fibrotic monocyte-derived DCs – sensitizes monocyte-derived DCs to TLR-ligand responsiveness	pDCs	NA	Not reported but → upregulation of CD83, CD86 and MHC class I	Not reported	(Silva-Cardoso et al., 2017)
Organizes "self" and microbial DNA into liquid crystalline immune complexes - amplify TLR9-mediated pDC-hyperactivation and interferon-α production.	pDCs	GAGs; independent of CXCR3	Not reported	Yes	(Lande et al., 2019)
Contributes to fibrosis in MPN	Megakaryocytes, stromal cells	Not reported	JAK/STAT and profibrotic pathways in macrophages	Not reported	(Gleitz et al., 2020)
Drives fibrosis	Endothelial cells and fibroblasts	Not reported	Not reported	Not reported	(Affandi et al., 2022)
Regulation of TLR8 responses, superinduction of inflammatory genes	Monocytes	Not reported	MAPK & IRF pathways, TBK1/IKKε-IRF5 axis		(Yang et al., 2022)
Widespread recruitment of immune cells independent of chemokine receptors	Endothelium	GAGs	Not reported	Yes	(Gray et al., 2023)
Other					
Heterotetramerization with CXCL12 inhibits CXCR4-CXCL12-mediated migration of breast cancer cells	Breast cancer cells	CXCR4	Not reported	Not reported	(Nguyen et al., 2022)
Cognition-enhancing effects of exercise are mediated by PF4 which reverses cognitive decline in aged mice.	Immune cells → indirect effects on brain	Not reported	Not reported	Not reported	(Leiter et al., 2023)

1.3.3. Interaction of PF4 with glycans

Cell surface glycans (sugars) exist in two main forms bound to proteins: proteoglycans and glycoproteins. Proteoglycans are heavily glycosylated proteins consisting of a core protein with long, covalently attached glycosaminoglycan (GAG) chains. These GAGs are made up of repeating disaccharide units (up to ~80 sugar residues) consisting of various combinations of an alternating amino sugar and a uronic acid (Falet et al., 2022). These combinations produce four main families of GAG: chondrotin sulfate (CS), heparin or heparan sulfate, keratan sulfate, and hyaluronic acid (Table 1.3). Uronic acids impart negative charge and additional sulfation of the amino sugar adds further negative charge and complexity.

Another term, “glycoprotein”, refers to proteins that contain short chain, branching polysaccharides termed N- and O-glycans (consisting of ~10 sugar residues). These are linked to nitrogen atoms of asparagine, and oxygen atoms of serine or threonine residues in the protein backbone respectively. Glycans can be further modified with the addition of negatively charged sialic acid residues which are incidentally important for preventing platelets being removed from the circulation by the hepatic Ashwell-Morrell receptor (Lee-Sundlov et al., 2022). The differential expression of the enzymes that produce and attach GAGs and glycans, and those that bring about sulfation and sialylation allows for highly tuneable tissue, and cell-specific patterns, which in turn regulates chemokine activity.

Table 1.3 Predominant constituents of glycosaminoglycans (GAGs).

Each glycosaminoglycan is made up of repeating disaccharide units consisting of a uronic acid and an amino sugar. N-sulfation and N-acetylation further modify the amino sugars with sulfation imparting negative charge. GalNAc: N-acetylated galactosamine; GlcNAc: N-acetylated glucosamine, GlcNS: N-sulfated glucosamine, GlcA: glucuronic acid, IdoA: iduronic acid, Gal: galactose. *Subtypes of chondroitin sulfate depend on position of sulfation of GalNAc: CSA: chondroitin 4-O-sulfate, CSC: chondroitin 6-O-sulfate, CSD: chondroitin 2,6-O-sulfate, CSE: chondroitin 4,6-O-sulfate. CSB: form of chondroitin 4-O-sulfate with IdoA (L-iduronic acid) instead of GlcA as the uronic acid. NK: not known.

Glycosaminoglycan	Amino sugar	Predominant uronic acid	K_D (μM) for PF4 binding
Chondroitin sulfate*			
CSA	GalNAc	GlcA	4.4 (Loscalzo et al., 1985)
CSC	GalNAc	GlcA	4.4 (Loscalzo et al., 1985)
CSD	GalNAc	GlcA	0.6 (Loscalzo et al., 1985)
CSE	GalNAc	GlcA	0.3 (Loscalzo et al., 1985)
Dermatan sulfate (CSB)	GalNAc	IdoA	2.9 (Loscalzo et al., 1985)
Heparin/heparan sulfate			
Heparan sulfate	GlcNAc	GlcA	2.3 (Loscalzo et al., 1985)
Heparin	GlcNS	IdoA	0.16-0.04 (Loscalzo et al., 1985; Dudek et al., 1997; Stringer and Gallagher, 1997; Lord et al., 2017)
Hyaluronic acid	GlcNAc	GlcA	NK
Keratan sulfate	GlcNAc	Gal	NK

1.3.3.1. Heparin

The strongest interaction of PF4 with a GAG is with heparin as it is the most negatively charged GAG (Loscalzo et al., 1985; Petersen et al., 1999) (Table 1.3). Heparin is widely used in medicine as an anticoagulant and is the drug of choice for numerous indications thanks to its rapid onset, predictable pharmacokinetics, and reversibility. The mechanism of anticoagulation of heparin is by binding positively charged lysine residues on antithrombin via a distinctive pentasaccharide sequence (containing a middle 3-O-sulfated glucosamine) that is found on about one third of heparin chains (de Agostini et al., 1990). This leads to major enhancement of antithrombin's activity and its ability to inactivate thrombin, factor IXa, factor Xa, and factor XIa (Mulloy et al., 2016).

Despite its medical use, anticoagulation is not heparin's physiological role; its principal function is to control the correct formation of secretory granules in mast cells (Humphries et al., 1999; Forsberg et al., 1999). Heparan sulfate (HS), the major GAG that covers the endoluminal surface in the vasculature (Reitsma et al., 2007) is structurally similar to heparin but is less heavily sulfated and less negatively charged (Xu and Esko, 2014). Nevertheless, a small proportion of HS chains also contain the aforementioned antithrombin-binding pentasaccharide sequence and bind antithrombin, albeit to a lesser extent than heparin (Mertens et al., 1992). HS therefore functions as a natural anticoagulant through enhancement of antithrombin activity.

PF4 has been shown to effectively neutralise the anticoagulant effect of heparin in rats and in a human phase I trial (Cook et al., 1992; Dehmer et al., 1995). Fiore and Kakkar showed that 20 nM PF4 inhibited 75% of factor Xa inactivation by antithrombin on HS (Fiore and Kakkar, 2003). They found that this occurred by interference with the formation of the factor Xa-antithrombin complex on the HS chain. These findings demonstrate that PF4 could be deployed as a reversal agent for heparin although protamine sulfate, another positively charged molecule is used clinically and is widely accepted (Levy et al., 2023). The interaction between PF4 and other GAGs aside from heparin manifests in the presentation of HIT where the risk of thrombosis can persist after stopping heparin, and where the disease can also present spontaneously without the patient ever being exposed to heparin (Greinacher et al., 2017). This is discussed in more detail in Chapter 4.

GAGs are not only important for PF4's *activity*. Although it was previously accepted that PF4 forms tetramers at physiological pH and concentration (Mayo and Chen, 1989; Moore et al., 1975; Deuel et al., 1977), using native mass spectrometry, Niu et al. found a near-total absence of tetramers under such conditions (Niu et al., 2020). Although a few tetramers emerged at higher ionic strength, only the addition of short chain polyanions permitted tetramers at physiological ionic strength. This important observation essentially suggests that PF4 cannot act as a tetramer without the presence of polyanions and is consistent with prior

observations that GAGs can also stabilise or induce chemokine oligomerisation (Lau et al., 2004; Salanga et al., 2014). In some studies, anti-angiogenic properties of PF4 have been shown to not be dependent on GAG-binding (Maione et al., 1991; Gentilini et al., 1999; Sulpice et al., 2002). Furthermore, C-terminus peptides of PF4 have been shown to conserve functionality to inhibit megakaryopoiesis (Gewirtz et al., 1989; Lebeurier et al., 1996) and inhibit angiogenesis (Maione et al., 1991; Jouan et al., 1999; Hagedorn et al., 2001; Vandercappellen et al., 2010). Together, these data suggest that not all activity of PF4 is dependent on negative charge, and, given the findings from the native mass spectrometry work of Niu et al. this suggests that there is some monomeric activity. This is consistent with the knowledge that other chemokines activate their receptors as monomers (Crijns et al., 2020).

1.4. Anti-PF4 mediated immunothrombotic syndromes

1.4.1. Heparin-induced thrombocytopenia (HIT)

Heparin entered clinical practice in the 1930s but it was not until 1958 that a surgical case series documented the occurrence of recurrent arterial thrombosis in patients treated with heparin (Weismann and Tobin, 1958). This condition, now known as HIT, is characterised by heparin-dependent anti-PF4 antibodies that activate platelets.

In HIT, long, negatively charged heparin polysaccharide molecules bind to the positively charged equatorial region of two or more PF4 tetramers. This neutralises positive charges and facilitates close approximation of these PF4 molecules, the merging of their hydrophobic surfaces, and the formation of a single charge cloud and a stable structure (Greinacher et al., 2006). The assembly of these complexes is exothermic, and the energy produced facilitates structural rearrangement of PF4 that exposes neoepitopes (Kreimann et al., 2014; Nguyen et al., 2015). This altered PF4 is then bound by anti-PF4/heparin antibodies to form large immune complexes that activate platelets and leukocytes by crosslinking the low-affinity immune receptor Fc gamma receptor IIA (FcγRIIA) (Kelton et al., 1988). FcγRIIA is discussed in more detail in section 1.5.1.

Classically, HIT presents with a fall in a patient's platelet count 5-10 days after heparin exposure and this is accompanied by a high risk of thrombosis (Arachchillage et al., 2023). Anti-PF4/heparin antibodies are in fact very common in patients treated with unfractionated heparin and become detectable in between 8 to 50% of patients treated with unfractionated heparin, rates differing with medical or surgical context (Warkentin et al., 2000; Everett et al., 2007; Sokolovic et al., 2016; Vayne et al., 2019). These antibodies are also infrequently detected in patients treated with low molecular weight heparin and the synthetic pentasaccharide, fondaparinux (Warkentin et al., 2005a). However, the development of *platelet activating* anti-PF4/heparin antibodies, and therefore HIT, is much rarer. Unfractionated heparin exposure during cardiac surgery is associated with the highest risk of HIT where it occurs in ~0.5% (Dhakal et al., 2018; Aguayo et al., 2018), with HIT occurring to

a lesser extent in other surgical and medically unwell patients. HIT can also occur rarely in patients exposed to low molecular weight heparin (Martel et al., 2005).

Anti-PF4/heparin antibodies are also readily detectable in patients with intercurrent illness, who have not received heparin. In patients with sepsis, antibodies are frequently detectable by enzyme-linked immunosorbent assay (ELISA) although the majority are of low optical density (OD < 1.0) (Maharaj and Chang, 2018) indicating that the potential for them to activate platelets *in vitro* is low. Furthermore, in this study, the ELISA method used detected not only immunoglobulin (Ig)G, but IgM, and IgA as well, which is known to decrease the specificity of the assay as these latter two subclasses are not often associated with platelet activation (Juhl et al., 2006). Severe COVID-19 infection is also associated with a high frequency of anti-PF4/heparin antibodies, and that their presence is associated with disease severity (Ueland et al., 2022; Liu et al., 2022), however these studies also focused on IgG, IgM, and IgA, and did not measure the platelet activating potential of these antibodies. Anti-PF4/heparin antibodies are also detectable in 1-5% of healthy individuals, but the majority of these antibodies are again of low optical density and positivity varies according to the different commercially available assays (Arepally and Hursting, 2008). Further, where tested, these antibodies are not platelet-activating and likely reflect immune responses to common infections (Hursting et al., 2010; Nicolson et al., in press a). These observations are consistent with the theory that the anti-PF4/heparin immune response allows the adaptive immune system to sense and target negative charge with PF4 forming a bridge between the innate and adaptive immune system (Greinacher and Warkentin, 2023). However, Zhu et al. noticed that antibodies targeting the COVID-19 receptor binding domain had the same unusual molecular characteristics as anti-PF4/heparin antibodies (Zhu et al., 2024). They found that of 130 patients who were hospitalised with COVID-19, 80% had these cross-reacting IgG antibodies and 41% activated platelets in a PF4-dependent manner. Notably however, this study did not see thrombocytopenia in these patients. It is unclear which is the driving immune response in this situation – is the anti-COVID response first generating appropriate antibodies

that are cross-reacting, is the opposite true, or are both these possibilities playing a role? However, what these data do demonstrate is an additional mechanism by which anti-PF4/heparin antibodies can be generated, and a possible further explanation for the prothrombotic phenotype of COVID-19 (Zhu et al., 2024).

As discussed previously, PF4 not only binds to heparin, but also to other negatively charged GAGs (Okayama et al., 1986; Loscalzo et al., 1985). These non-heparin GAGs can induce the same conformational change in PF4 as caused by heparin binding, leading to epitope exposure and binding of anti-PF4/heparin antibodies to form immune complexes. As such, immune complexes can form at the surface of platelets and leukocytes even in the absence of heparin. Although this is known to happen on the surface of platelets (Rauova et al., 2006), PF4 forms antigenic complexes on monocytes more efficiently than on platelets (Rauova et al., 2010) as monocytes express heparan sulfate and dermatan sulfate which have higher binding affinities for PF4 than chondroitin sulfate, the predominant platelet surface GAG (Okayama et al., 1986; Loscalzo et al., 1985).

Importantly, Krauel et al. showed that PF4 binds to gram-negative bacteria via lipid A at the cell surface, a process that exposes PF4-heparin epitopes (Krauel et al., 2011, 2012). PF4 has also been shown to bind to other pathogens including adenovirus (Baker et al., 2021), human immunodeficiency virus 1 (Parker et al., 2016), and SARS-Cov2 (Nguyen et al., 2024). Bacteria are strongly negatively charged, more so than eukaryotic cells (Wilson et al., 2001), and thus negative charge can act as a danger signal for the immune system. However, effector molecules of the adaptive immune system including antibodies and T cell receptors only recognise structure, not charge. Thus, it has been proposed that the binding of PF4 to pathogens, induction of conformational change in PF4, and binding of anti-PF4 antibodies, leads to recognition of these immune complexes by Fc receptors on innate immune cells and thus plays a role in host defence (Greinacher and Warkentin, 2023).

So, the evidence demonstrates that the generation of anti-PF4/heparin antibodies is a physiological immune response, but it is perturbed in HIT where heparin therapy floods the

system with more negative charge than would be seen in nature. Still, spontaneous HIT-like syndromes in individuals with no prior heparin exposure have been reported (Greinacher et al., 2017) demonstrating that there is an evolutionary trade-off for this immune response, and that it can sometimes go wrong.

1.4.2. Vaccine-induced immune thrombocytopenia with thrombosis

VITT is also characterised by platelet activating anti-PF4 antibodies but in contrast to HIT, most of these antibodies are not dependent on the presence of negatively charged GAGs to recognise PF4 (Greinacher et al., 2021; Huynh et al., 2021). Instead, high-affinity, monoclonal or oligoclonal antibodies bind to the heparin-binding region of PF4, themselves overcoming the repellent positive charges of PF4 molecules and forming immune complexes (Huynh et al., 2021; Kanack et al., 2022; Greinacher et al., 2022). Although PF4 has been shown to bind to the surface of ChAdOx1 and form stable complexes (Baker et al., 2021) the sequence of events leading to the generation of VITT antibodies is uncertain.

The clinical presentation of VITT is discussed in more detail in section 1.4.4.2 but one of the most striking features is the high frequency of thrombosis in the cerebral veins, large avalvular veins that drain the brain. An otherwise very rare site of thrombosis in the general population, about 50% of all patients with VITT had cerebral venous sinus thrombosis (CVST). In this context, Huynh et al. found that patients with CVST were much more likely to have anti-PF4 antibodies that bind in similar regions to HIT antibodies *in addition to* VITT antibodies targeting the heparin-binding regions (Huynh et al., 2023), Similarly, sera from some patients with HIT can activate platelets independent of heparin and have also been shown to have VITT-like antibodies targeting the heparin-binding region (Warkentin, 2023b; Nguyen et al., 2017; Warkentin et al., 2023a). In contrast to HIT, the addition of low, therapeutic concentrations of heparin disrupts immune complex formation and blocks platelet activation *in vitro* (Cines and Greinacher, 2021; Warkentin et al., 2023a). Heparin-independent reactivity is typical of the so-called “autoimmune” HIT-like syndromes which have atypical clinical characteristics and are

summarised in Table 1.4. The differences in antibody binding regions on PF4 in relation to positively charged amino acids and heparin binding sites are summarised in Figure 1.3. Still, as discussed, it should be noted that the binding sites shown in Figure 1.3. are a simplification. Labelling a case as HIT- or VITT-like based on antibody binding epitopes is therefore not straightforward and there is cross-over (Huynh et al., 2023; Warkentin, 2023b; Nicolson et al., 2025).

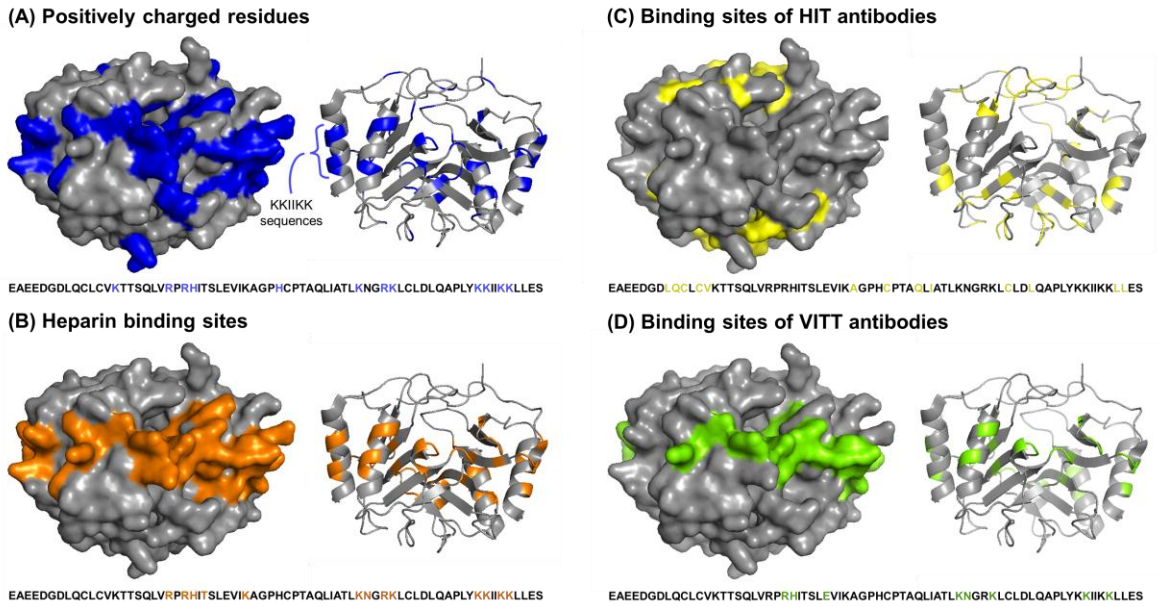

Figure 1.3. Anti-PF4 antibody binding sites in anti-PF4 mediated immunothrombotic disorders.

Adapted from Buka and Pavord, 2024. (A) positively charged amino acids shown in blue, (B) heparin binding sites shown in orange, (C) Typical HIT antibody binding sites in yellow, (D) Typical VITT antibody binding sites shown in green – based on n=5 VITT cases, (Huynh et al. 2021). It should be noted that there is however overlap as patients with atypical HIT syndromes can have VITT-like antibodies and HIT-like antibodies are also detected in some patients with VITT.

Table 1.4. Anti-PF4 immunothrombotic syndromes.

HIT: heparin-induced thrombocytopenia; VITT: vaccine-induced immune thrombocytopenia with thrombosis. *Considered autoimmune (aHIT) as both heparin-dependent and heparin-independent PF4 antibodies are present. Clinical outcomes of aHIT are often more severe. **Up to 42 days if isolated DVT/PE

HIT and HIT-like syndromes	
Classic HIT	Usually occurs 5-10 days after first heparin exposure
Autoimmune HIT	
Rapid onset HIT	Immediate reaction with use of heparin after recent exposure
*Delayed onset HIT**	Platelet count fall begins or worsens after stopping heparin
*Persisting (refractory) HIT**	Persistent thrombocytopenia >1 week from stopping heparin
Spontaneous HIT	Occurs without exposure to heparin
*Fondaparinux induced HIT**	Occurs with exposure to fondaparinux
VITT and VITT-like syndromes	
VITT	Occurs 5-30** days after adenoviral vaccination
Spontaneous VITT	Occurs without vaccine exposure

1.4.3. Spontaneous anti-PF4 immunothrombotic syndromes

In addition to the classical presentations of HIT and VITT, it is now clear that clinically significant anti-PF4 antibodies can occur spontaneously in the absence of heparin or vaccine exposure. Both acute VITT-like and HIT-like syndromes have been reported often connected to mild, intercurrent infection particularly adenovirus (Warkentin et al., 2023b; Uzun et al., 2023; Dimopoulou et al., 2024; Lambert and Warkentin, 2025) but also cytomegalovirus (Nicolson et al., 2025) and after human papilloma virus vaccination (Johansen et al., 2022). Look-back exercises have identified patients with recurrent thrombosis who on further assessment have been found to have platelet activating anti-PF4 antibodies (Schönborn et al., 2023). Population-based studies have shown that individuals with monoclonal gammopathy of uncertain significance (MGUS), a pre-malignant condition with a small risk of progression to multiple myeloma, have a high risk of thrombosis (Kristinsson et al., 2010). Recently patients with MGUS have been shown to have paraproteins formed of anti-PF4 antibodies and one patient required systemic anti-myeloma therapy to successfully prevent recurrent thrombotic events (Kanack et al., 2024; Salmasi et al., 2024). Rather than a rare, isolated patient, Padmanabhan has also reported that of 134 patients with MGUS and a history of thrombosis, four had PF4 and heparin-dependent, platelet activating antibodies that were inhibitable with high concentrations of heparin and blockade of FcγRIIA (Pabmanabhan et al., 2024). This novel data suggests that the anti-PF4 immune response may be an important driver of MGUS and therefore multiple myeloma, as well as thrombosis in these conditions. Notably, these patients tested negative on anti-PF4 ELISA, and two tested negative by the serotonin-release assay (discussed below) suggesting atypical VITT-like antibody epitopes on PF4 that are not detected by this assay (Pabmanabhan et al., 2024).

1.4.4. Clinical aspects

1.4.4.1. HIT

HIT should be suspected in any patient who has recently received heparin and has a decrease in their platelet count (Arachchillage et al., 2023). It is classically characterised by the onset of thrombocytopenia 5 to 10 days after the first exposure to heparin. Notably, it is a fall in platelet count, typically ≥30%, rather than absolute thrombocytopenia ($<150\times10^9$/mL) that is important; patients may have platelet counts in the normal range. Clinically, even though HIT generally occurs in hospitalised, monitored patients, 50% of patients have thrombosis at diagnosis indicating its intensely prothrombotic phenotype as well as delayed diagnosis (Arepally and Padmanabhan, 2021). Less commonly, patients with HIT may also display skin necrosis or experience acute systemic reactions to injections of heparin (Warkentin et al., 2005b).

Several scoring systems have been developed to assess the likelihood of HIT in order to streamline and reduce unnecessary laboratory testing (Lo et al., 2006; Cuker et al., 2010; Nilius et al., 2022). Of these pre-test probability scores, the 4Ts score, which is the most widely used, assigns a score of between 0 and 8 based on the degree of **T**hrombocytopenia, **T**iming of platelet count fall, presence of **T**hrombosis or other sequelae, and the presence of other causes for **T**hrombocytopenia (Lo et al., 2006). The parameters of the 4Ts score are summarised in Table 1.5.

Patients can then be categorised as either low (≤ 3), intermediate (4 to 5), or high (6 to 8) risk of HIT. A low score is reliably predictive of the patient not having HIT (negative predictive value: 0.998) whilst ~14% and ~64% patients with intermediate and high-risk scores have HIT (Cuker et al., 2012). It is recommended that in patients with an intermediate or high-risk score, heparin should be stopped and an alternative non-heparin anticoagulant started whilst the patient is investigated (Cuker et al., 2018; Arachchillage et al., 2023).

Table 1.5. The 4Ts score.

The 4Ts score is a clinical scoring system that can be used to assess the pre-test probability of HIT. Patients are assigned a score of between 0 and 8 categorising them as either low (0-2), intermediate (3-6) or high (7-8) risk of having HIT (Lo et al., 2006). Patients with an intermediate or high risk score should have heparin stopped, be started on an alternative, non-heparin anticoagulant, and referred for diagnostic testing.

	Score		
	0	**1**	**2**
Thrombocytopenia	Platelet count fall <30% OR platelet nadir <10	Platelet count fall 30–50% OR platelet nadir 10–19	Platelet count fall >50% AND platelet nadir ≥20
Timing of platelet count fall	Platelet count fall <4 days without recent exposure	Consistent with days 5–10 fall, but not clear; onset after day 10 OR fall ≤1 day (prior heparin exposure 30–100 days ago)	Clear onset between days 5–10 OR platelet fall ≤1 day (prior heparin exposure within 30 days)
Thrombosis or other sequelae	None	Progressive OR recurrent thrombosis; non-necrotizing skin lesions; suspected thrombosis (not proven)	New thrombosis OR skin necrosis; acute systemic reaction post-intravenous heparin bolus
Other causes for thrombocytopenia	Definite	Possible	None apparent

There are numerous diagnostic tests that can be broadly subcategorised as (1) qualitative screening tests, (2) semi-quantitative tests that detect anti-PF4 antibodies, and (3) functional assays that determine the ability of patient serum to activate platelets in the presence of low concentration heparin (0.1 to 0.5 IU/mL). The semi-quantitative and functional assays also incorporate a “heparin neutralisation step” whereby the assay is repeated in the presence of high concentration heparin (10 to 100 IU/mL) with the expectation that this will block reactivity as this higher concentration disrupts immune complex formation. These assays are summarised in Table 1.6.

Table 1.6. Assays used in the diagnosis of heparin-induced thrombocytopenia.

Test
Screening tests
Lateral flow immunoassay (LFIA)
Particle gel immuno and immunofiltration assay (PaGIA/PIFA)
Latex gel immunoassay (LIGam)
Semi-quantitative immunoassays
Enzyme linked immunosorbent assay (ELISA)
Chemiluminescence immunoassay (CLIA)
Functional platelet activation assays
Flow cytometry-based platelet activation
Heparin-induced platelet activation (HIPA)
Light transmission aggregometry (LTA)
Multiplate electrode aggregometry (MEA)
Serotonin release assay (SRA)

Generally, patient serum is first subjected to a screening test and/or a semi-quantitative antibody test which exhibit high sensitivity but lower specificity. Positive samples are then referred for testing by a functional platelet activation assay which have high specificity (Arachchillage et al., 2023). As described above, anti-PF4/heparin antibodies are frequently found in unwell individuals but platelet activating antibodies are much rarer and diagnostic of HIT. This said, the results of pre-test probability scoring in combination with the magnitude of an immunoassay result can be used in a Bayesian calculator to assign a probability of HIT. For example, a high-risk 4Ts score with an ELISA OD >2.39 yields a 96% probability of HIT (Nilius et al., 2022). Another approach along the same lines is the algorithm suggested Table 1.7 which does not mandate functional testing where the probability is high (Cuker, 2014; Raschke et al., 2017).

Nonetheless, it is optimal to perform a functional platelet assay in all patients with a positive semi-quantitative test. The gold-standard functional assay is the serotonin release assay (SRA) which has a sensitivity and specificity of over 95%. However, this assay detects release of serotonin containing a radioactive isotype of Carbon - Carbon-14 (^{14}C) and as such requires specialised equipment and training. As such, other widely used methods have been

developed. Flow cytometry based assays can either measure P-selectin expression after release from platelet α-granules or annexin-V binding which is a measure of phosphatidylserine exposure. This is the method used by the UK reference laboratory at National Health Service (NHS) Blood and Transplant (NHSBT), Filton (National Health Service Blood and Transplant, 2023). Flow cytometry has been shown to have sensitivity and specificity similar to the SRA (Tardy-Poncet et al., 2021). The heparin-induced platelet activation (HIPA) assay also has good concordance with the SRA (Gonthier et al., 2021) but although LTA has comparable specificity, its sensitivity is lower (Brodard et al., 2020).

Table 1.7. Algorithm for interpretation of ELISA optical density in the context of pre-test probability score.

Based on (Cuker, 2014) and (Raschke et al., 2017).

4Ts score Pre-test probability	**Low risk (0-3)** <1% probability	**Intermediate (4-5)** ~10% probability	**High risk (6-8)** ~50% probability
ELISA result (OD)			
Negative Anti-PF4 <0.6 Likelihood ratio ~0.04	0% probability HIT HIT is excluded	0% probability HIT HIT is excluded	~10% probability Functional assay Stop heparin ?? Empiric tx for HIT
Indeterminate Anti-PF4 0.6-1.5 Likelihood ratio ~1.2	<2% probability HIT unlikely Consider functional assay	~12% probability Functional assay Stop heparin ?? Empiric tx for HIT	~55% probability Functional assay Stop heparin Empiric tx for HIT
Positive Anti-PF4 1.5-2 Likelihood ratio ~7	~7% probability HIT Functional assay Stop heparin ?? Empiric tx for HIT	~50% probability Functional assay Stop heparin Empiric tx for HIT	~90% probability HIT largely ruled in Stop heparin Empiric tx for HIT
Strongly positive Anti-PF4 (>2) Likelihood ratio ~70	~42% probability Functional assay Stop heparin Empiric tx for HIT	91% probability HIT largely ruled in Stop heparin Empiric tx for HIT	99% probability HIT is ruled in. Stop heparin Empiric tx for HIT

1.4.4.2. VITT

VITT should be suspected in patients with platelets <150×10^9/mL or >50% decrease in platelet count who have new thrombosis or severe persistent headache presenting 5-30 days post vaccination, or up to 42 days if only presenting with deep vein thrombosis or pulmonary embolism (Schönborn et al., 2024). Characteristically, D-dimer is ≥8 times the upper limit of normal and fibrinogen is low. Thrombosis can occur at any site but as stated previously, over half of all patients had CVST with other unusual sites of thrombosis such as the portal vein also common (Pavord et al., 2021). Possible mechanisms for the preponderance of CVST in VITT are discussed in more detail in section 5.1.1. In contrast to HIT, as patients are previously well and are not in hospital being monitored, almost all present with thrombosis, although several cases of so called “pre-VITT” in patients presenting with headache, thrombocytopenia but no thrombosis, have been reported (Salih et al., 2021). Although estimates vary, the incidence of VITT after the first dose of ChAdOx1 is likely to be between 1 in 25,000 and 1 in 70,000 with rates higher in younger people (Schultz et al., 2021; Medicines and Healthcare products Regulatory Agency, 2022). In the UK, a seminal case series of 220 patients showed that 85% of affected individuals were younger than 60 years of age (Pavord et al., 2021). Cases of VITT have also been reported after vaccination with the two other adenoviral vector vaccines, Ad26.COV2.S, and Gam-COVID-Vac/Sputnik V, but at much lower rates (See et al., 2022; Herrera-Comoglio and Lane, 2022). There have also been scattered reports of possible VITT following vaccination with mRNA-based vaccines, but these patients did not have complete diagnostic work-up, or had results not wholly consistent with VITT (Sangli et al., 2021; Lin et al., 2023).

In the UK, one third of patients with VITT died but early recognition and aggressive treatment with intravenous immunoglobulin, plasma exchange, and anticoagulation is effective (Pavord et al., 2021). In Australia, the vaccination programme was delayed by several weeks compared to Europe, so by the time patients started presenting with VITT, it had already been

described. Thus, patients with VITT in Australia were recognised sooner and treated more quickly with a resultant mortality of only 5% (Tran et al., 2023).

In patients with clinical suspicion for VITT, the diagnosis can be confirmed using similar principles to HIT – the demonstration of platelet activating, anti-PF4 antibodies (Handtke et al., 2021). Typically, rapid screening tests designed for the diagnosis of HIT are negative in VITT and semi-quantitative immunoasssays are positive. Low dose heparin that is expected to enhance platelet functional responses in HIT has an abrogating effect in VITT, thus functional HIT tests require adapting for VITT. Instead of heparin, low concentration PF4 can be used to enhance responses (Handtke et al., 2021; Schönborn et al., 2023).

1.5. Relevant platelet receptors

1.5.1. Fc-gamma receptor IIA (FcγRIIA)

FcγRIIA (CD32a) mediates platelet activation in anti-PF4 immunothrombotic syndromes. It is a platelet immunoreceptor tyrosine-based activation motif (ITAM) receptor that becomes activated when crosslinked by IgG molecules such as those contained in immune complexes or in other contexts as discussed below. Platelets contain two other ITAM receptors, glycoprotein VI (GPVI) and C-type lectin-like receptor 2 (CLEC-2) and all three have shared downstream signalling pathways (Lee and Bergmeier, 2016). ITAM receptors are characterised by the presence of a conserved amino acid sequence in the cytoplasmic tail of the receptor: a tyrosine followed by two amino acids then a leucine or an isoleucine (YxxL/I), with two of these patterns usually separated by 6-8 amino acids: Yxx(I/L)x(6-12)Yxx(I/L) (Rayes et al., 2019). This sequence is important for signal transduction and is found in a variety of immune cells.

Fcγ receptors are a group of receptors that recognise IgG. This class includes six receptors, five are activating: FcγRI, FcγRIIA, FcγRIIC, FcγRIIIA, and FcγRIIIB, and one is inhibitory, FcγRIIB (Bournazos et al., 2020). They are differentially expressed on a range of myeloid and lymphoid cells, but platelets only express FcγRIIA and FcγRIIB. FcγRIIA is also expressed on neutrophils, monocytes, eosinophils, macrophages, and dendritic cells (Bournazos et al., 2020). Human platelets express about 1,000 copies of FcγRIIA (Huang et al., 2021; Burkhart et al., 2012) which structurally comprises two extracellular Ig-like domains, the second of which mediates binding to IgG.

All Fcγ receptors, aside from FcγRI, are low-affinity receptors that cannot be activated by monomeric IgG (Bournazos et al., 2020). Thus, they require IgG that is multimeric in order to provide sufficient avidity to enable cellular activation (Arman and Krauel, 2015). The physiological role of these receptors is to bind to the Fc regions of immunoglobulins that have opsonised pathogens. In this context, multivalent binding leads to crosslinking of the Fc receptors and, in the case of the activatory receptors, activation of the FcR-expressing cell.

Crosslinking of platelet FcγRIIA induces robust and rapid platelet activation resulting in aggregation and granule release (Arman and Krauel, 2015). Pathological FcγRIIA activation occurs in response to immune complexes such as those seen in anti-PF4 immunothrombotic syndromes (Kelton et al., 1988) systemic lupus erythematosus (Duffau et al., 2010; Berlacher et al., 2013) and with drug-dependent antibodies (Meyer et al., 2009; Gao et al., 2009). The receptor also facilitates clearance of immune complexes which, in contrast contributes to reducing inflammation thus illustrating a balance between pro- and anti-thromboinflammatory activity (Huang et al., 2011). These known ligands for FcγRIIA are listed in Table 1.8 in addition to other non-naturally occurring ligands that have been developed as either research tools or therapeutics.

It should be noted that FcγRIIA is only present in higher order primates; murine platelets do not express any Fc receptor (Trist et al., 2014; Hogarth et al., 2014; Lejeune et al., 2019). In the context of HIT, whilst mice can generate anti-PF4/heparin antibodies (Zheng et al., 2013) these do not activate mouse platelets, and mice do not develop HIT. Thus, in murine models of HIT, double knock-in of human FcγRIIA and PF4 is required to successfully recapitulate the phenotype of HIT (Reilly et al., 2001).

Table 1.8. Known ligands for FcγRIIA.

CD40L: cluster of differentiation 40 ligand; HIT: heparin-induced thrombocytopenia; GP: glycoprotein; IgG: immunoglobulin G; mAb: monoclonal antibody; VITT: vaccine-induced immune thrombocytopenia with thrombosis.

Naturally occurring	References
Physiological	
IgG-opsonised bacteria	Many, reviewed: (Arman and Krauel, 2015)
IgG-opsonised influenza	(Boilard et al., 2014)
Pathological	
Immune complexes containing anti-PF4 antibodies	
HIT sera / isolated antibodies	(Kelton et al., 1988)
VITT sera / isolated antibodies	(Smith et al., 2021)
Drug-dependent antibodies	(Meyer et al., 2009; Gao et al., 2009)
Immune complexes in systemic lupus erythematosus	(Duffau et al., 2010; Berlacher et al., 2013)
Non-naturally occurring	
Mouse anti-human FcγRIIA antibody, IV.3, crosslinked by anti-mouse IgG	(Arman et al., 2014; Zhou et al., 2016)
IgG coated beads	(Antczak et al., 2011)
Aggregated IgG	(Worth et al., 2006)
Antibodies against other platelet membrane receptors	
Anti-CD9 mAb	(Taylor et al., 2000; Stolla et al., 2011)
Anti-GPVI mAb	(Gardiner et al., 2008)
Anti-CD151 mAb	(Gardiner et al., 2008)
Anti-GPIX mAb	(Stolla et al., 2011; Taylor et al., 2000; Zhou et al., 2016)
Monoclonal anti-PF4 antibodies (KKO, 5B9, 1E12).	
KKO HIT-like mAb	(Arepally et al., 2000)
5B9 HIT-like mAb	(Kizlik-Masson et al., 2017)
1E12 VITT-like mAb	(Vayne et al., 2021a)
Tetravalent llama anti-human FcγRIIA nanobody	(Martin et al., 2024)
Immune complexes containing anti-CD40L mAb and CD40L	(Robles-Carrillo et al., 2010; Langer et al., 2005; Amirkhosravi et al., 2014)

1.5.1.1.1. FcγRIIA polymorphisms

FcγRIIA exists in human populations in two common allelic forms that are defined by either an arginine or histidine at position 131 (R131 or H131) of the amino acid chain (Warmerdam et al., 1990). In Caucasians, ~25% of individuals are H131 homozygous, ~35% R131 homozygous, and the remainder heterozygous (van Schie and Wilson, 2000). This is a clinically important polymorphism and R131 homozygotes are at higher risk of severe sepsis (Vidarsson et al., 2014; Endeman et al., 2009; Beppler et al., 2016), nephritis in systemic lupus erythematosus (Duits et al., 1995; Haseley et al., 1997), and thrombosis in HIT (Carlsson et al., 1998). FcγRIIA R131 has a lower affinity for IgG2 than H131 (Bruhns et al., 2009) resulting in reduced IgG2 antibody-dependent immune responses (Vidarsson et al., 2014), thus explaining the higher risk of sepsis as IgG2 antibodies are produced in a T cell independent manner in response to bacterial polysaccharide antigens and individuals homozygous for R131 therefore mount a weaker immune response against these infections. In HIT, anti-PF4/heparin antibodies are predominantly of IgG1 subclass (Arepally et al., 1997). In R131 individuals, reduced binding of IgG2 (which makes up ~30% of all plasma IgG (Vidarsson et al., 2014)) increases the availability of binding sites for IgG1 and IgG3-containing immune complexes (Rollin et al., 2015).

A study involving nearly 100 patients with HIT and over 300 controls reported that polymorphisms in the protein tyrosine phosphatase CD148, a protein that regulates Src (a pivotal kinase in FcγRIIA downstream signalling) were associated with frequency of HIT (Rollin et al., 2012). 276P and 326Q polymorphisms were protective against the development of HIT, and detailed *in vitro* work found hyporesponsiveness and decreased phosphorylation of effectors downstream of FcγRIIA in platelets from these individuals in after crosslinking of FcγRIIA (Rollin et al., 2012). Zhou et al. screened 147 healthy individuals for responsiveness to FcγRIIA activation and performed gene expression profiling. They identified downregulation of the protein phosphatase, T cell ubiquitin ligand-2 (TULA-2) as being independently associated with hyper-responsiveness to FcγRIIA activation (Zhou et al., 2015). They further

showed that knockdown and knockout of TULA-2 in human FcγRIIA-expressing mice enhanced FcγRIIA mediated platelet activation, and worsened thrombocytopenia and increased thrombin generation in a model of HIT (Zhou et al., 2015, 2016). These studies demonstrate that complex, interacting processes govern responsiveness to FcγRIIA-induced stimulation. However, in the study of CD148 polymorphisms, the controls were heparin-exposed cardiac surgery patients who either did not have any anti-PF4/heparin antibodies, or who had detectable antibodies that were non-platelet activating (Rollin et al., 2012). Therefore, it is unclear why patients who are higher responders to FcγRIIA stimulation are more likely to develop platelet activating anti-PF4/heparin antibodies (as defined by the ability of patient serum to activate platelets from high responding healthy donors) rather than just being more prone to thrombosis when these antibodies develop. Genetic factors that govern the generation of anti-PF4/heparin antibodies as well as those that activate platelets have not been elucidated.

1.5.2. Platelet endothelial aggregation receptor-1

Platelet endothelial aggregation receptor-1 (PEAR1) is a type-1 transmembrane protein that belongs to the multiple epidermal growth factor (EGF)–like domain family of proteins (Nanda et al., 2005). Principally expressed on endothelial cells and platelets, it comprises one extracellular elastin microfibril interface (EMI) domain and 15 extracellular EGF-like repeats (Nanda et al., 2005). The intracellular component contains five proline-rich regions, which facilitate docking of SH3 domain-containing proteins such as Src family kinases and phosphoinositide-3 kinase (PI3K), and four tyrosine residues (Nanda et al., 2005). Human platelets contain ~1800 copies of PEAR1 (Burkhart et al., 2012; Huang et al., 2021) but cell surface expression is increased by release of PEAR1 from α-granules on activation (Kauskot et al., 2012).

PEAR1 was first shown to become activated during platelet aggregation to other agonists, and that this activation could be blocked by the integrin $\alpha_{IIb}\beta_3$ inhibitor eptifibatide which abrogates platelet aggregation (Nanda et al., 2005). However, it was also shown that PEAR1 activation could occur during platelet centrifugation, but this was not blocked by eptifibatide. It was later demonstrated that this process occurs through the binding of an unidentified platelet surface ligand to the EMI domain of PEAR1 leading to rapid phosphorylation and signalling through PI3K which results in enhancement of integrin $\alpha_{IIb}\beta_3$ activation (Kauskot et al., 2012).

1.5.2.1. PEAR1 in the context of HIT

Prior to, and independently of, the work on PEAR1 described above, it was known that therapeutic administration of heparin in humans leads to transient thrombocytopenia and to detectable increases in markers of platelet activation and renders platelets hyperresponsive to activation by ADP and thrombin receptor activating peptide (TRAP) (Xiao and Théroux, 1998). It was also shown that heparin potentiates integrin $\alpha_{IIb}\beta_3$ signalling (Gao et al., 2011).

More recently, sulfated polysaccharides belonging to the dextran and fucoidan families have been shown to induce robust platelet activation through interaction with the 13th EGF repeat

of PEAR1 (Kardeby et al., 2019). Kardeby subsequently showed that heparin sulfate conjugated to an albumin core could stimulate aggregation of washed platelets, platelet rich plasma (PRP) and whole blood. Unconjugated heparin and low molecular weight heparin both also stimulated aggregation in washed platelets but not in PRP or whole blood, and there was significant inter-donor variability in responses. Aggregation to all three agonists was blocked by a llama-derived nanobody to the 13th EGF-like repeat of PEAR1 (Kardeby et al., 2023). This nanobody, nanobody 138 (Nb138) is used in this thesis and nanobodies are further introduced later. The ligands and activating stimuli for PEAR1 are summarised in Table 1.9.

Table 1.9. Known ligands and activating stimuli for PEAR1 in platelets.

EGF: epidermal growth factor; EMI: elastin microfibril interface; FcεR1α: Fc epsilon receptor 1 alpha.

Naturally occurring	**PEAR1 binding**	**Reference**
Platelet contact – ligand unknown	EMI domain	(Nanda et al., 2005)
FcεR1α	13th EGF-like repeat	(Sun et al., 2015)
Fucoidan	13th EGF-like repeat	(Kardeby et al., 2019)
Heparin sulfate	13th EGF-like repeat	(Kardeby et al., 2023)
Non-naturally occurring		
Centrifugation – ligand unknown	EMI domain	(Nanda et al., 2005)
Synthetic glycopolymers	13th EGF-like repeat	(Kardeby et al., 2019)
Albumin-linked heparin sulfate	13th EGF-like repeat	(Kardeby et al., 2023)
Low molecular weight heparin	13th EGF-like repeat	(Kardeby et al., 2023)
Trivalent nanobodies	13th EGF-like repeat	(Martin et al., 2024)

Single nucleotide polymorphisms (SNPs) in PEAR1 have been associated with variability in healthy donors' platelet responses to range of agonists. Herrea-Galeano et al. screened 1,486 healthy individuals from families with a history of premature coronary artery disease for PEAR1 variants (Herrera-Galeano et al., 2008). They found that a SNP in the promoter region of PEAR1 (rs2768759) was correlated with increased platelet aggregation to ADP, collagen, and adrenaline and increased resistance to aspirin. Numerous other studies have reported associations between SNPs in PEAR1 (particularly in intron 1) and platelet function and resistance to antiplatelets (Ansari et al., 2021). Furthermore, Stimpfle et al. demonstrated that,

in a large cohort of patients undergoing percutaneous coronary intervention, homozygous carriers of the PEAR1 minor allele rs12566888 had significantly worse outcomes (Stimpfle et al., 2018).

Despite the pivotal role for heparin in HIT, the role of the heparin-PEAR1 interaction has never been investigated. Healthy donors' platelet responses to HIT sera are characteristically variable (Warkentin et al., 1992) and it is unknown whether PEAR1 has any role in in this. Further, it is unknown whether variants in PEAR1 have any role in the pathogenesis of thrombosis in HIT; PEAR1 variants were not reported as disease modifiers in the largest genome wide association study (GWAS) of HIT which involved 1,269 patients with proven HIT (Karnes et al., 2015). However, given the relatively small sample size, and low sensitivity for GWAS in detecting associations, particularly when effect sizes are small, this does not rule out an association (Stringer et al., 2011). Thus, the role of PEAR1 in HIT has not previously been evaluated and it may contribute to platelet activation through the heparin-PEAR1 interaction as well as contact-induced integrin $\alpha_{IIb}\beta_{III}$ activation. To elucidate the relative contribution, novel tools are required to specifically inhibit these different processes. Camelid-derived nanobodies have been developed in the Birmingham Platelet Group and are introduced in section 1.6.

1.5.3. Cellular myeloproliferative leukaemia protein (c-Mpl)

c-Mpl is a JAK-associated receptor found on haematopoietic stem cells, megakaryocytes and platelets (Hitchcock et al., 2021). Platelets contain several JAK-associated receptors including the IL-6 receptor subunit glycoprotein 130 (GP130), insulin-like growth factor receptor 1 (IGFR1), and the TPO receptor, c-Mpl (Burkhart et al., 2012; Huang et al., 2021). These proteins are named after the dual-faced Roman god of doors, gates and transitions, Janus, reflecting their dual phosphate transferring domains. One domain is active as a kinase, and the other as a negative regulator of the first domain's kinase activity (Seavey and Dobrzanski, 2012). JAKs are a family of four kinases: JAK1, JAK2, JAK3, and tyrosine kinase 2 (TYK2).

They are significant in many physiological and disease processes and mediate cellular activation downstream of receptors of the type I and type II cytokine receptor superfamily (Hu et al., 2021). This is a group of receptors that includes those that bind interferons, many interleukins, colony stimulating factors, and hormones including erythropoietin and TPO. JAKs are constitutively associated with cytoplasmic domains of cytokine receptors and on ligand-receptor binding become phosphorylated and activated. Active JAKs then phosphorylate the cytoplasmic tail of the receptor which leads to binding and phosphorylation of effectors including the STATs (Hu et al., 2021). There are seven STATs: STAT1, STAT2, STAT3, STAT4, STAT5a, STAT5b, and STAT6 and various combinations of JAKs and STATs are found in different cell types (Casanova et al., 2012).

In megakaryocytes, the binding of TPO to c-Mpl and induction of downstream signalling is the key driver of platelet production (Hitchcock and Kaushansky, 2014). Inherited mutations that render c-Mpl dysfunctional result in congenital amegakaryocytic thrombocytopenia which is characterised by profound thrombocytopenia and a propensity for leukaemia (Van Den Oudenrijn et al., 2000). Similarly, activating mutations in c-Mpl and JAK2 can drive abnormal proliferation of myeloid cells as seen in myeloproliferative neoplasms (Cross et al., 2021). The TPO molecule has two distinct binding sites for c-Mpl – one low-affinity and one high-affinity – through which it binds to and dimerises c-Mpl (Tsutsumi et al., 2023). This results in JAK2 activation which induces phosphorylation of STAT3 and STAT5, mitogen-activated protein kinase (MAPK)/extracellular signal-regulated kinases (ERK), and PI3K (Miyakawa et al., 1995; Yamada et al., 1995; Miyakawa et al., 1996, 2000; Sattler et al., 1995; Ezumi et al., 1995; Drachman et al., 1999; Tsutsumi et al., 2023). These pathways drive the activation of megakaryocyte-specific transcriptional programmes resulting in expression of megakaryocyte-specific genes.

TPO is produced in the liver at a constant rate and circulating TPO binds to c-Mpl which is retained on mature platelets (Hitchcock and Kaushansky, 2014). Here, it becomes internalised, reducing TPO levels and thus reducing the amount that reaches the bone marrow

(Fielder et al., 1996). As such, the higher the platelet count, the less TPO that reaches the bone marrow, and the fewer platelets that are produced (Kuter, 2013). A second negative regulatory mechanism is the activation of a second receptor Casitas B-lineage lymphoma protein (c-Cbl), also by TPO which is an E3 ubiquitin ligase that ubiquitinates c-Mpl and marks it for degradation (Saur et al., 2010).

In addition to this role, TPO has been shown to potentiate platelet activation (Ezumi et al., 1995, 1999; Van Willigen et al., 2000; Moore et al., 2019; Pasquet et al., 2000) and at high concentrations has been shown to induce platelet aggregation (Hammond et al., 1998; Pasquet et al., 2000). At lower concentrations, TPO can support platelet adhesion to vWF (Van Os et al., 2003). Although TPO has been reported to contribute to platelet activation in several disease states (Lupia et al., 2006, 2009, 2022), the true physiological relevance of this is debatable. Indeed, the physiological relevance of JAK signalling in platelets in general is unclear.

1.5.3.1. JAK2 in platelets

There is evidence of JAK/STAT activation in platelets in response to platelet stimulation by thrombin (Rodríguez-Liñares and Watson, 1994) and through GPVI (Parra-Izquierdo et al., 2022; Babur et al., 2020) and CLEC-2 (Izquierdo et al., 2020). However, JAK2 is not crucial to any of the key mechanisms of platelet activation, either through ITAM-receptors, or G-protein coupled receptors. Inhibition of JAK2 kinase activity is reported to diminish platelet activity (Lu et al., 2014; Parra-Izquierdo et al., 2022) although when used in patients, JAK2 inhibitors do not significantly increase the risk of bleeding; indeed, some increase the risk of thrombosis (Mehta et al., 2020). Conversely, patients with myeloproliferative disorders, who often have activating mutations in JAK2, have an increased risk of thrombosis. However, in some patients, especially those with more extreme thrombocytosis, there is a risk of bleeding due to acquired von Willebrand syndrome which is caused by vWF consumption (Barbui et al., 2013). JAK2 knockout mice have severe thrombocytosis due to dysregulated TPO turnover (Meyer et al., 2014). These mice also show a bleeding diathesis and impaired thrombus

formation with impaired responses through GPVI and CLEC-2 but not through G-protein coupled receptors (Eaton et al., 2021).

Much of the role of JAK2 in platelets has been studied in the context of the activating V617F mutation which is pathognomic for myeloproliferative neoplasms. Humans with JAK2 V617F mutated essential thrombocythaemia have been shown to have hypoactive platelets with impaired signalling through the PI3K/Rap1 pathway resulting in loss of the potentiating effect of TPO (Moore et al., 2013). Several groups have investigated the effects of the activating JAK2 V617F mutation in murine knock-in models. Hobbs et al. reported the phenotype of JAK2V617F mice, under the control of a Mx1-Cre system induced by polyinosinic-polycytidylic acid (pIpC) treatment administered at 10 days of age, which targets JAK2 V617F to haematopoietic cells (Hobbs et al., 2013). These mice had thrombocytosis (~1,600×10^9/L), enhanced responsiveness to platelet agonists independent of platelet count, enhanced thrombus formation *in vitro*, and reduced tail bleeding. Another murine model of JAK2 V617F using non-inducible Tie2-Cre mice which targets the mutation to haematopoietic and endothelial cells also described mice with thrombocytosis but compared to Mx1-Cre mice, platelet counts were much higher (>2,500×10^9/L) (Etheridge et al., 2014). Platelets from these mice showed no difference in their aggregaton responses but counterintuitively, *in vivo* thrombus formation was significantly attenuated. Wild type mice, transplanted with HSCs from Tie2-Cre mice had thrombocytosis but no observed difference in thrombus formation or bleeding. In contrast, Tie-Cre mice transplanted with wild-type HSCs (and thus only expressing JAK2 V617F in endothelial cells had no thrombocytosis but did have delayed and unstable thrombus formation (Etheridge et al., 2014). Lamrani reported findings from a murine polycythaemia/myelofibrosis model where haematopoietic stem cells from JAK2 V617F Vav-Cre or SCLCreER knock-in mice were transplanted into lethally irradiated wild type mice so as to remove any contribution of endothelial V617F expression (Lamrani et al., 2014). The study reported hyporesponsive platelets, increased tail bleeding, and attenuated thrombosis after injury. These conflicting reports indicate the complex and context-dependent role

specifically of the JAK2 V617F mutation in thrombosis and haemostasis. However, the wider physiological importance of JAK2 in physiological platelet activation is still unclear.

1.6. Nanobodies

Conventional antibodies (immunoglobulins) are composed of two light chains and two heavy chains linked together by a disulfide bridge (Figure 1.4A) The immunoglobulin classes, A, D, E, G, and M are determined by the heavy chain fragment crystallisable (Fc) region and this is responsible for the effector functions of antibodies including binding to and activation of Fc receptors. Antigen recognition is mediated by the fragment antigen-binding (Fab) regions, which consist of the variable domains of both the heavy (V_H) and light (V_L) chains (Gutierrez and Desiderio, 2024). In camelid species such as camels, llamas and alpacas, whilst their IgG1 antibodies are also composed of light and heavy chains, their IgG2 and IgG3 antibodies are heavy chain only (Hamers-Casterman et al., 1993). Thus the antigen recognition domain is formed of a variable heavy chain-only domain (V_{HH}) but these remain high affinity for target antigens. In the same manner as conventional antibodies, heavy chain-only antibodies can be raised against a wide range of antigens and these services are available commercially (Harmsen and De Haard, 2007). The V_{HH} domain can be easily expressed alone to produce single domain antibodies – nanobodies – which have a molecular weight of only 15 kDa compared to 150 kDa for a full IgG molecule. The differences between conventional antibodies, heavy chain antibodies, and nanobodies are represented in Figure 1.4.

In research, nanobodies have numerous advantages over conventional antibodies including their ease of expression in a variety of systems, stability, and ease of engineering for various purposes (Harmsen and De Haard, 2007). For example, whilst monovalent nanobodies can be used as inhibitors of platelet receptors, linkers can be inserted into the constructs to produce polyvalent nanobodies that can cluster and activate receptors (Martin et al., 2024). The size of nanobodies allows more precise targeting of regions within larger proteins to inhibit specific functions related to those regions. For example, caplacizumab is a nanobody that

targets the A1 domain of vWF inhibiting the interaction between vWF and the platelet receptor GPIb and is used to excellent therapeutic effect in thrombotic thrombocytopenic purpura (Scully et al., 2019). In this thesis, nanobody technology is utlised to specifically block the heparin-binding 13th EGF like repeat of PEAR1 and these studies are described in Chapter 4.

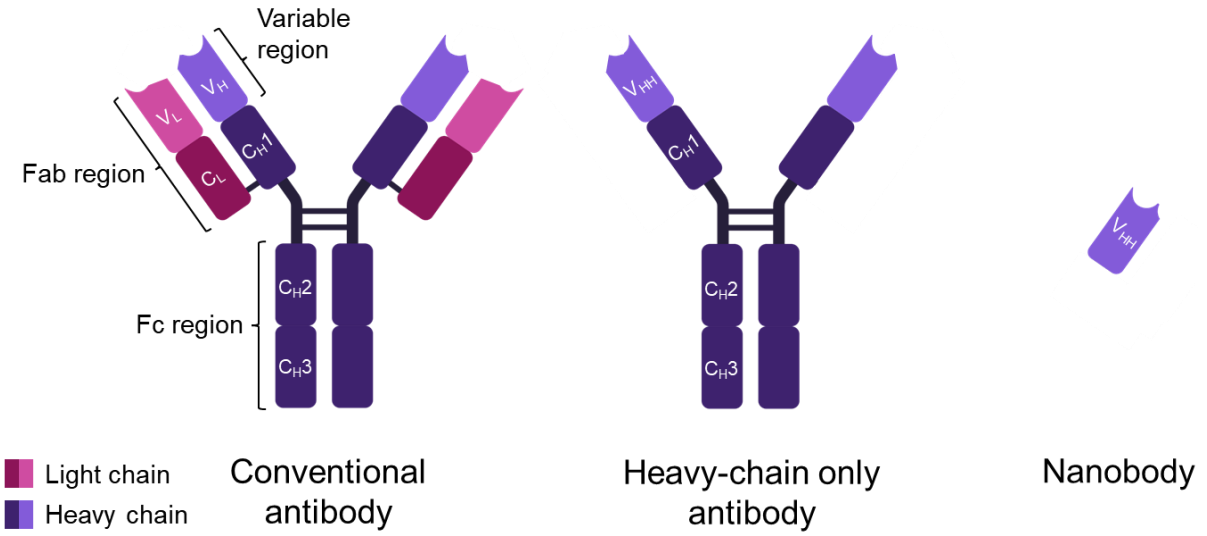

Figure 1.4. Schematic showing of the difference between conventional antibodies heavy-chain only antibodies, and nanobodies.

Conventional antibodies are composed of two light chains (red/pink) and two heavy chains (purple) linked by a disulfide bridge. Both light chains and heavy chains are composed of variable (V) and constant domains. The antigen binding site is formed by the variable regions of the heavy and light chains (V_H and V_L). Heavy-chain only antibodies are composed of only heavy chains linked by a disulfide bridge and an antigen binding site formed by only the variable heavy chain only domain (V_{HH}). Nanobodies, formally known as single-domain antibodies, consist of a single variable heavy chain only domain.

1.7. Aims of the thesis

It has been known since the 1980s that platelets are activated in HIT through binding of Fc regions of antibodies in immune complexes to FcγRIIA (Kelton et al., 1988). As discussed above, it is also known that both PF4 and heparin activate platelets but their contributions to platelet activation in HIT and VITT have not been investigated. The mechanism of heparin-induced platelet activation is now understood but PF4's mechanism of activation is yet to be elucidated. Here, it is hypothesised that both free, and immune complex-bound PF4 contribute to platelet activation in VITT as do PF4 and heparin in HIT.

Finally, a key mystery in the pathophysiology and presentation of VITT is the preponderance for cerebral venous sinus thrombosis. This is introduced in more detail in Chapter 5. It was hypothesised that differential interactions of platelets and endothelial cells in response to stimulation with combinations of PF4, heparin, HIT and VITT antibodies, in this anatomical location may contribute to the observed phenomena.

Thus, the aims are to:

1. Characterise and investigate the mechanism of platelet activation to PF4.
2. Investigate the role of PF4-mediated platelet activation in VITT and HIT.
3. Investigate the role of heparin-mediated platelet activation in HIT.
4. Investigate the interactions between platelets, endothelial cells, PF4, heparin, HIT and VITT antibodies and sera.

2. Methods

2.1. Materials

2.1.1. Agonists

Reagent	Source
1E12 VITT-like monoclonal antibody	Dr Jérôme Rollin, Prof Yves Gruel (Tours, France)
5B9 HIT-like monoclonal antibody	Dr Jérôme Rollin, Prof Yves Gruel (Tours, France)
Collagen (equine tendon)	Takeda (Linz, Austria).
Collagen-related peptide, cross-linked (CRP)	CambCol Laboratories (Cambridge, UK)
Crosslinked IV.3 IV.3 Goat anti-mouse IgG secondary antibody	 Ying Di, (University of Birmingham, UK) Invitrogen (Thermo Fisher Scientific, Waltham, USA)
Heparin (PL 29831/0111)	Wockhardt (Wrexham, UK)
KKO HIT-like monoclonal antibody (MA5-17641)	Thermo Fisher Scientific (Waltham, USA)
Platelet factor 4, purified from human blood	Chromatec (Greifswald, Germany)
Platelet factor 4, purified from human blood	Prof Doug Cines (Philadelphia, USA)
Platelet factor 4, purified from human blood	Dr Simon Abrams, Dr Guozheng Wang (Liverpool, UK)
Recombinant thrombopoietin (HZ-1248)	Proteintech (Rosemont, USA)
VITT IgG isolated from patient plasma	Dr Luis Moran, Dr Samantha Montgaue, Dr Margaret Goodall (University of Birmingham, UK)

2.1.2. Inhibitors

Reagent	Target	Source
Dasatinib	Src	Sigma-Aldrich (Merck, Darmstadt, Germany).
Eptifibatide	Integrin $\alpha_{IIb}\beta_3$	GSK (Brentford, UK)
Goat anti-human c-Mpl (PA5-47042)	c-Mpl	Invitrogen (Thermo Fisher Scientific, Waltham, USA)
KU-0063794	mTOR	Selleckchem (Houston, USA)
Niclosamide	STAT3, mTOR	Selleckchem (Houston, USA)
PRT-030618	Syk	Sigma-Aldrich (Merck, Darmstadt, Germany)
Ruxolitinib	JAK1 JAK2	Stratech Scientific (Ely, United Kingdom)
SH4-54	STAT3 STAT5	Selleckchem (Houston, USA)
STAT5 inhibitor	STAT5	Cayman Chemicals
Stattic	STAT3	Cayman Chemicals
TGX-221	PI3K p110β	Selleckchem (Houston, USA)
Wortmannin	PI3K	Selleckchem (Houston, USA)
WYE-354	mTOR	Selleckchem (Houston, USA)

2.1.3. Antibodies

All anti-human unless stated. AF: Alexa Fluor; APC: allophycocyanin; Cy5: cyanine5; Cy7: cyanine7; ELISA: enzyme-linked immunosorbent assay; FC: flow cytometry; FITC: fluorescein isothiocyanate; HRP: horseradish peroxidase; IP: Immunoprecipitation; M: Microscopy; PE: phycoerythrin; WB: Western Blot.

Reagent	**Host species**	**Use**	**Source**
AF-488 PAC1 (activated integrin $\alpha_{IIb}\beta_3$)	Mouse	FC: 1/100	Santa Cruz (Dallas, USA)
AF-488-PF4 (sc-398979)	Mouse	M: 1/100	Santa Cruz (Dallas, USA)
AF-488-phalloidin	Mouse	M: 1/750	(Thermo Fisher Scientific, Waltham, USA)
AF-647-PF4 (sc-398979)	Mouse	M: 1/100	Santa Cruz (Dallas, USA)
AF-647-phalloidin	Mouse	M: 1/750	(Thermo Fisher Scientific, Waltham, USA)
Anti-mouse IgG HRP conjugate secondary antibody	Rabbit	WB: 1/3000 to 1/10000	Amersham Biosciences (GE Healthcare, Buckinghamshire, UK)
Anti-rabbit IgG HRP conjugate secondary antibody	Goat	WB: 1/3000 to 1/10000	Amersham Biosciences (GE Healthcare, Buckinghamshire, UK)
Anti-thrombopoietin	Rabbit	ELISA	Antibodies.com (Cambridge, UK)
APC anti-CD62P (P-selectin), Clone AK4	Mouse	FC: 1/100	Biolegend (San Diego, USA)
APC-Cy7-CD62P (P-selectin), Clone AK4.	Mouse	FC: 1/100	Biolegend (San Diego, USA)
APC-Cy7-IgG1κ isotype (clone MOPC-21)	Mouse	FC: 1/100	Biolegend (San Diego, USA)
APC-Cy7-VCAM1 (CD106) FAB5649A	Mouse	FC: 1/100	Biolegend (San Diego, USA)
APC-IgG1κ isotype (clone MOPC-21)	Mouse	FC: 1/100	Biolegend (San Diego, USA)
FITC-CD31 (11-0311-82)	Mouse	M: 1/100	Thermo Fisher Scientific (Waltham, USA)
FITC-CD41 (5B12)	Mouse	FC: 1/100	Dako (Agilent, Santa Clara, USA)
FITC-ICAM1 (CD54) (322720)	Mouse	FC: 1/100	Biolegend (San Diego, USA)
FITC-IgG1κ isotype (clone MOPC-21)	Mouse	FC: 1/100	Biolegend (San Diego, USA)
Hoechst 33342 (62249)	NA	M: 1/10000	Thermo Fisher Scientific (Waltham, USA)
JAK2 (D2E12)	Rabbit	IP: 1/100	Cell Signaling Techology (Danvers, USA)
PE-Cy5-IgG1κ isotype (clone MOPC-21)	Mouse	FC; 1/100	Biolegend (San Diego, USA)
PE-Tissue factor	Mouse	FC: 1/100	Biolegend (San Diego, USA)
Phospho-c-Mpl (06-944)	Rabbit	WB: 1/1000	Sigma-Aldrich (Merck, Darmstadt, Germany)
Phospho-STAT3 (D3A7, Tyr705)	Rabbit	WB: 1/1000	Cell Signaling Techology (Danvers, USA)

Phospho-STAT5a/b (05-495Ab, Tyr694/699)	Mouse	WB: 1/1000	Sigma-Aldrich (Merck, Darmstadt, Germany)
Phosphotyrosine (4G10, 05-1050)	Mouse	WB: 1/1000	Sigma-Aldrich (Merck, Darmstadt, Germany)
Syk (4D10, sc-1240)	Mouse	WB: 1/1000	Santa Cruz Biotechnology (Dallas, USA)

2.1.4. Recombinant proteins

ELISA: enzyme linked immunosorbent assay; LTA: light transmission aggregometry; SPR: surface plasmon resonance,

Reagent	Species	Target	Use	Source
c-Mpl (TpoR) (4444-TR)	Recombinant, human-derived	NA	SPR, ELISA	Biotechne (R&D Systems, Minneapolis, USA)
Nanobody 138 (Nb138)	Recombinant llama-derived	PEAR1	FC, LTA	Developed by Birmingham Platelet Group. Batch produced by Dr Eleyna Slater, Dr Rachel Lamerton, and Hugo Lagonotte (University of Birmingham, UK)

2.1.5. Endothelial cell culture

Reagent	Source
Human dermal microvascular endothelial cells (C-12212)	Promocell (Heidelberg, Germany)
Human umbilical vein endothelial cells	Promocell (Heidelberg, Germany)
Endothelial cell growth medium (C-22020)	Promocell (Heidelberg, Germany)
Endothelial growth medium supplement mix (C-39211)	Promocell (Heidelberg, Germany)
Opti-MEM™ Reduced Serum Medium	Gibco™, Thermo Fisher Scientific (Waltham, USA)
Trypsin / EDTA 0.03% / 0.04% (C-41010)	Promocell (Heidelberg, Germany)
Trypsin neutralising solution (C-41110)	Promocell (Heidelberg, Germany)
Freezing medium cryo-SFM (C29912)	Promocell (Heidelberg, Germany)
Glass bottom 20 mm centre confocal dishes (734-2906)	VWR (Avantor, Lutterworth, UK).

2.1.6. Other reagents

Reagent/material	Source
Immun-Blot polyvinylidene fluoride membrane	Biorad (Hercules, USA)
Non-fatty acid free Bovine Serum Albumin (BSA)	First Link (UK) Ltd (Birmingham, UK).
Novex NuPAGE Bis-Tris Protein Gels 4 to 12%, Mini, 1.5 mm – 10-15 lanes	Invitrogen (Thermo Fisher Scientific (Waltham, USA)
Nunc™ MicroWell™ 96-Well Microplates	Thermo Scientific (Thermo Fisher Scientific (Waltham, USA)
NuPAGE™ MOPS (3-(N-morpholino)propanesulfonic acid) SDS Running Buffer	Invitrogen (Thermo Fisher Scientific (Waltham, USA)
Protein A sepharose Fastflow beads	GE Healthcare (Chicago USA)
SuperSignal™ West Pico PLUS Chemiluminescent Substrate (34580)	Thermo Fisher Scientific (Waltham, USA)
Transblot Turbo western blotting buffer	Biorad (Hercules, USA)
TMB (3,3′,5,5′-Tetramethylbenzidine) substrate	Sigma-Aldrich (Merck, Darmstadt Germany)

2.1.7. VITT IgG

IgG was isolated from the plasma of a patient with VITT collected after plasma exchange. Work included in this thesis using this reagent is published (Buka et al., 2024). Plasma was passed through protein A columns after which IgG collected on columns was eluted, collected and concentrated. Eluate was dialysed into phosphate buffered saline (PBS) and protein concentration measured by NanoDrop (Thermo Fisher Scientific, Waltham, USA). Control IgG was isolated from the plasma of a healthy donor previously known to be a high responder to FcγRIIA stimulation. These reagents were produced by Dr Luis Moran, Dr Samantha Montague, and Dr Margaret Goodall, University of Birmingham. Approval for this was included in the project ethical approval via the University of Birmingham Human Bioresource Centre as detailed in section 2.4.

2.1.8. Nanobody 138

Nanobody 138 against the 13th EGF repeat of PEAR1 was generated in collaboration with VIB Nanobody Core (Ixelles, Belgium). This nanobody was produced, developed, and characterised in the Birmingham Platelet Group as part of programme of work that included

development of nanobodies against PEAR1, glycoprotein VI (GPVI), C-type lectin-ike receptor 2 (CLEC-2) and FcγRIIA (Martin et al., 2024). The work has been led by Dr Eleyna Slater (née Martin) and Prof Steve Watson, with extensive testing by Ying Di and significant academic development also done by Dr Joanne Clark. Dr Caroline Kardeby first established Nb138 as a research tool (Kardeby et al., 2023). The nanobody used in this thesis was made in-house by Dr Eleyna Slater, Dr Rachel Lamerton, and Hugo Lagonotte.

2.1.8.1. Nanobody production

A llama was immunised by VIB by subcutaneous injection with 100 to 150 µg of soluble recombinant PEAR1 EGF-like repeat 12-13 on days 0, 7, 14, 21, 28, and 35. Following this, blood was collected on day 40 and lymphocytes isolated. Lymphocytes were used to construct a variable domain of heavy chain only antibody (VHH) library which consisted of over 100 million unique VHH clones which were selected for those that contained appropriately sized inserts in the phagemid vector. Three rounds of selection were conducted using a receptor-specific antigen immobilised on a solid surface (concentration: 100-200 µg/mL), with enrichment for phages displaying antigen specificity evaluated after each cycle. Following this, colonies identified as positive were tested using ELISA to detect receptor antigen-specific nanobodies within crude periplasmic extracts.

2.1.8.2. Expression and purification of Nb from bacterial E. coli WK6 cells

Nanobody constructs containing an N-terminal PelB signal sequence were received from VIB in a pMECS-GG vector. The PelB sequence directs the expressed nanobody to the periplasmic space of *E. coli* which facilitates their extraction. Monovalent Nb138 was expressed using the WK6 *E. coli* strain (VIB Nanobody Core, Belgium) as follows. Nanobody constructs received in the pMECS-GG vector contain an N-terminal PelB signal sequence that targets the nanobody to the perisplasmic space of *E. coli* allowing their extraction from the periplasm. Divalent nanobodies were expressed using the WK6 *E. coli* strain (provided by VIB) as follows. WK6 *E. coli* colonies that had been transformed with Nb138 construct where

incubated for 16-24 hours in Luria-Bertani broth supplemented with ampicillin 100 μg/mL. A 1:300 dilution of the overnight cultures was prepared in 1 L of Terrific Broth (TB) medium (2.3 g/L KH_2PO_4, 16.4 g/L $K_2HPO_4 \cdot 3H_2O$, 12 g/L tryptone, 24 g/L yeast extract, 0.4% v/v glycerol), supplemented with 100 μg/mL ampicillin. These cultures were agitated at 180 rpm at 37°C until the optical density at 590 nm was between 0.6 and 0.9. 1 mM β-D-thiogalactoside (IPTG) was added to induce nanobody expression and cultures were incubated for a further 16 hours, agitated at 180 rpm at 28°C. Cultures were centrifuged for 15 min at 3,000 rpm to pellet *E. coli* cells that contained nanobody. Supernatant was discarded and cells resuspended in TES buffer (0.2 M tris pH 8, 0.5 mM EDTA, 0.5 M sucrose) and gently agitated at 4°C for one hour following which the cell suspension was further two times diluted in a 4x dilution of TES buffer and incubated for another hour at 4°C. Soluble proteins were isolated by centrifugation at 8000 rpm for 30 min at 4°C, removing insoluble protein and cell debris, and producing supernatant containing nanobody and other proteins that had been extracted from the periplasmic. Nanobody was purified using nickel-affinity column chromatography. Nanobody was expressed with C-terminal His_6-HA tags which was removed by on-column cleavage of a thrombin recognition sequence by addition of thrombin to nanobody bound to nickel-nitrilotriacetic acid beads (1-2 units thrombin per mg protein). Columns were incubated overnight in cleavage buffer (20 mM Tris pH 8.4, 150 nM NaCl, 2.5 mM Ca^{2+}) at room temperature (RT) to achieve near 100% cleavage. Residual thrombin was removed by passing the untagged nanobody solution through a 1 mL benzamidine column (Cytiva). Subsequently, the sample was dialysed into PBS or subjected to further purification using size exclusion chromatography on a HiLoad 26/600 Superdex 75 pg column (Cytiva) when necessary, to achieve highly pure nanobody samples. The concentration of the purified nanobody was quantified using a NanoDrop spectrophotometer (ND-1000, Geneflow), measuring absorbance at 280 nm as per the manufacturer's instructions.

Nb138 was previously tested for binding to PEAR1 by SPR (Martin et al., 2024) and for the ability to block binding of FcεR1α to PEAR1 using avidity-based extracellular interaction

screening (Kardeby et al., 2023). Nb138 was also previously shown to inhibit platelet aggregation to fucoidan (Kardeby et al., 2023).

2.2. Protein purity

PF4 formulations were assessed for purity using sodium dodecyl sulfate polyacrylamide gel electrophoresis (SDS-PAGE) under reducing conditions. 5 to 20 µg of each PF4 formulation at 1 mg/mL (mass according to the manufacturer's labelling), dissolved in PBS was added to 5X SDS-reducing buffer (supplemented with dithiothreotol [DTT]). Protein was loaded into individual wells of a 10-lane graduated 4-12% gel along with a molecular weight marker (5 µL). Electrophoresis was carried out in NuPAGE™ MOPS (3-(Morpholin-4-yl)propane-1-sulfonic acid) SDS running buffer (Invitrogen, Thermo Fisher Scientific, Waltham, USA) first at 80 V for 10 min then at 120 V until the molecular weight marker showed optimal separation. The gel was removed from the casing and covered with Coomassie blue, microwaved 4 times (1200 kW) for 30 s and then placed on a rocker for 1 h. The gel was rinsed with water and left on the rocker overnight after which it was imaged using an Odyssey XF Imager (Li-COR Biosciences, Cambridge, UK).

2.3. Blood collection and platelet preparation

Blood was taken from consenting patients or healthy, drug-free volunteers, into vacutainers containing 3.2% sodium citrate or into serum separator tubes (Becton, Dickinson and Company, Franklin Lakes, USA). Platelet rich plasma (PRP) was obtained by centrifugation at 200 *g* for 20 min at RT in the presence of acid citrate dextrose (ACD – 120 mM sodium citrate, 110 mM glucose, 80 mM citric acid, 10% final volume). Washed platelets were obtained by centrifugation of PRP at 1,000 *g* for 10 min using 0.2 µg/mL PGI_2 and resuspended in modified Tyrode's-HEPES buffer (134 mM NaCl, 0.34 mM Na_2HPO_4, 2.9 mM KCl, 12 mM $NaHCO_3$, 20 mM HEPES (4-(2-hydroxyethyl)-1-piperazineethanesulfonic acid), 5 mM glucose, 1 mM $MgCl_2$; pH 7.3). Platelet poor plasma (PPP) was then removed and the pellet resuspended in 25 mL modified Tyrode's-HEPES buffer and centrifuged again at 1000 *g* for

10 min in the presence of 3 mL ACD and 0.2 µg/mL PGI_2. Platelets were resuspended in 2 mL modified Tyrode's-HEPES buffer and counted after dilution of 8 µL in 192 µL PBS (1 in 25) using a XP-300™ Automated Hematology Analyzer (Sysmex, Irvine, USA). Platelet concentration was adjusted to 2×10^7/mL, 1, 2, or 4×10^8/mL depending on the experiment and rested for at least 30 min to allow the effect of PGI_2 to wear off prior to any functional experiments.

2.4. Approvals and ethics

Blood was acquired from healthy donors under approval from the University of Birmingham Science, Technology, Engineering and Mathematics Ethical Review Committee (ERN_11-0175AP21). Serum and plasma samples from patients with VITT and HIT were acquired from University Hospitals Birmingham NHS Foundation Trust and NHS Blood and Transplant and this collection was authorised by the University of Birmingham Human Bioresource Centre (15/NW/0079). All samples were obtained in accordance with the Declaration of Helsinki.

2.5. Platelet function testing

2.5.1. Light transmission aggregometry

Platelet aggregation was measured by light transmission aggregometry (LTA) at 37°C, stirring at 1200 rpm using a Model 700 or Model 490 4+4 aggregometers (ChronoLog, Havertown, USA). Washed platelets were used at a concentration of 2×10^8/mL in a reaction volume of 250-300 µL. Platelets were warmed to 37°C for at least 5 min prior to the addition of agonists. Before stirring, platelets were pre-incubated sequentially with inhibitors or buffer controls (dimethyl sulfoxide [DMSO] or PBS) for at least 5 min each. After incubation with inhibitors, potentiators including PF4, TPO, and heparin, or buffer control (PBS) were added (sequentially where applicable) and again incubated for 5 min. Details of the concentrations used are described in the figure legends. After completion of pre-incubation steps, platelets were stirred for 1 min before the addition of agonists. Aggregation data was generated using Aggrolink 8 software (Chronolog, Havertown, USA). Quantitation of platelet aggregation data

is presented as area under curve (AUC) per minute (AUC min^{-1}) as this incorporates both magnitude and dynamics of the response. AUC compared to maximum aggregation is visually represented in Figure 2.1.

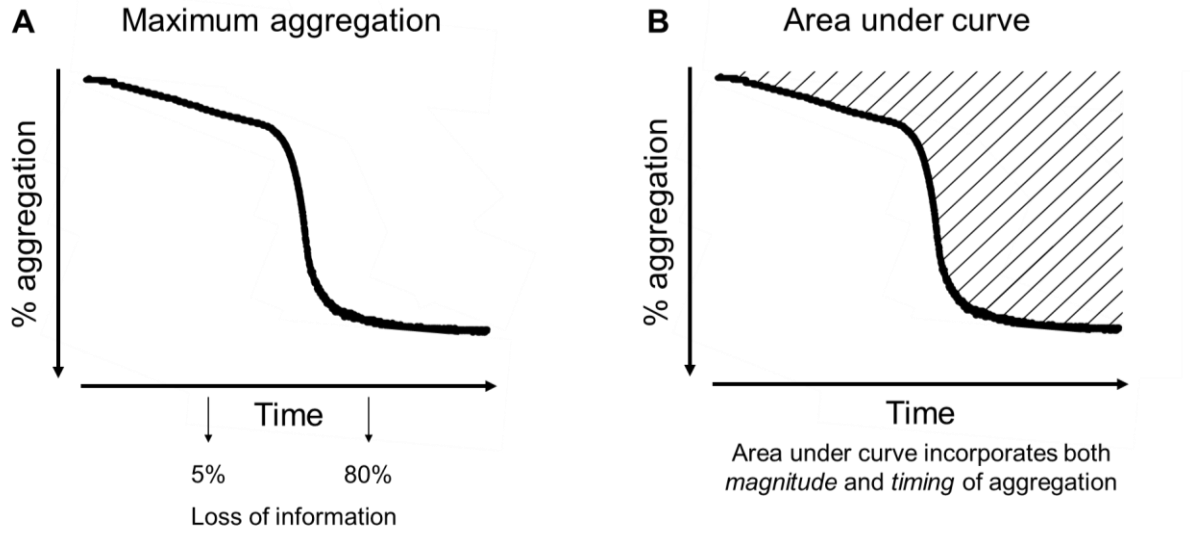

Figure 2.1. Comparison of quantitation of platelet aggregation by maximum aggregation and area under curve.

(A) Example aggregation trace showing delayed aggregation with 5% aggregation at the earlier time point and 80% aggregation at the later time point, hence loss of information. (B) The same aggregation trace showing area under curve which incorporates both magnitude and speed of aggregation.

2.5.2. Flow cytometry

For experiments assessing the effect of inhibitors on platelet activation to PF4 and TPO, washed platelets were used at 2×10^8/mL. Platelets at RT, were added to wells of a round-bottom 96 well plate and pre-incubated with inhibitors or vehicle controls (DMSO or PBS) for 5 min before addition of PF4 50 µg/mL, TPO 100 ng/mL, or vehicle control (PBS). The final reaction volume was 50 µL. Platelets were incubated at RT for 45 min before addition of 50 µL PBS containing mouse anti-human APC-CD62P (P-selectin) antibody or isotype control (final concentration: 1/100). Platelets were incubated in the dark for 20 min after which 200 µL PBS was added. The plate was analysed on a CytoFLEX LX flow cytometer (Beckman

Coulter, Indianapolis, USA). Percentage positive values were defined according to the isotype control.

For experiments using HIT-like monoclonal antibodies (5B9 and KKO) or patient sera, ± heparin 0.5 IU/mL, ± Nb138 100 nM, reagents were added to PBS to yield a final volume of 25 µL in wells of a round bottom 96-well plate. 25 µL washed platelets at 2×10^8/mL were added, and the plate was agitated on a shaker (350 rpm) for 60 min at RT. After this, 50 µL PBS containing mouse anti-human APC-CD62P (P-selectin) antibody, mouse-PAC1 (FITC-anti-human integrin $\alpha_{IIb}\beta_3$ antibody) (final concentrations: 1/100), or relevant isotype controls were added, incubated, and analysed as above.

2.5.3. Platelet spreading

Glass coverslips were placed in wells of a 24 well flat bottom plate and coated with PF4 (10 to 100 µg/mL), TPO (10 to 100 ng/mL), or collagen 50 µg/mL at RT for 60 min. Wells were then blocked with heat denatured, filtered bovine serum albumin (BSA) 5 mg/mL (in PBS) for 60 min at RT and washed three times in PBS. 300 µL platelets at 2×10^7/mL were pre-incubated with inhibitors or vehicle controls (DMSO or PBS) for 5 min then added to each well and plates incubated at 37°C for 45 min. Liquid was then aspirated and plates washed once with modified Tyrode's-HEPES buffer and then fixed with formalin for 10 min after which wells were washed three times with PBS. Platelets were stained for 20 min in the dark at RT with AF488-phalloidin or AF-647 phalloidin made up at 1/750 concentration in 1% bovine serum albumin (BSA) and 2% goat serum. Wells were once again washed three times with PBS and then mounted onto glass slides for imaging. Platelets were imaged using a Zeiss Axio Observer 7 microscope (Carl Zeiss AG, Oberkocken, Germany) at 63X magnification using fluorescence intensity emitted at 520 nm.

Analysis was conducted by Dr Steve Thomas, University of Birmingham, using a customised Cellpose 2.0 model to segment images of adhered platelets (Pachitariu and Stringer, 2022). Analysis was conducted after finetuning of the *cyto2* model on a subset of the data following

which the model was run on all images. Using a Random Forest supervised machine learning model, segmented cells were classified as follows: (1) unspread, (2) spikey/noduly, and (3) fully spread. The Random Forest model parameters were: Tree depth = 3, Number of trees = 100, trained with the Napari Accelerated Pixel And Object Classification (APOC) plugin (Pachitariu and Stringer, 2022). To train the model, the following object features were used: mean intensity, minimum intensity, maximum intensity, sum intensity, standard deviation intensity, pixel count and shape. To support the training process, a tailored Jupyter notebook was employed to generate a single tiled image from the training dataset, which included both raw data and Cellpose segmentations saved as .npy files. The image was subsequently annotated using Napari before the classifier was trained with APOC. Another Jupyter notebook was utilized to perform predictions on the complete dataset and compute additional cell-level measurements, such as area and circularity. Both notebooks can be accessed at https://github.com/JeremyPike/cell-classification.

2.6. Protein phosphorylation

2.6.1. Western blotting

Washed platelets at 4×10^8/mL were incubated at RT with eptifibatide 9 µM for 10 min. Platelets were further pre-incubated sequentially with inhibitors or vehicle controls and/or potentiators or vehicle controls as described in section 2.5.1. Reactions were terminated with the addition of 5X SDS reducing sample buffer. The buffer consisted of 4% SDS, 0.5 M Tris buffer, 30% glycerol, 1 M 2-mercaptoethanol, and bromphenol blue titrated to colour. Samples were placed on ice, transferred to Eppendorf tubes and stored at -20°C until use. Prior to western blotting, samples were heated at 100°C for 5 min then loaded onto lanes of 4-12% SDS-PAGE gels. Protein was separated by electrophoresis in NuPAGE™ MOPS (3-(Morpholin-4-yl)propane-1-sulfonic acid) SDS running buffer (Invitrogen, Thermo Fisher Scientific, Waltham, USA) at between 80 and 120 V then transferred to methanol-activated polyvinylidene fluoride membranes using a Biorad Transblot Turbo in transfer buffer. Membranes were then blocked in 4% BSA in TBS-T (Tris-buffered saline [200 mM Tris, 1.37 M NaCl; pH 7.6] with 0.2%

Tween20) for 60 min on a rocker at RT before being incubated in antibodies made up in 4% BSA in TBS-T for 16-24 hours at 4°C on a rocker. Membranes were then rinsed three times in TBS-T before three 10 min washes in TBS-T and stained with HRP-conjugated anti-mouse or anti-rabbit IgG secondary antibodies for 60 min at RT on a rocker. Secondary antibodies were used at 1:10000 apart from anti-phospho STAT3/5 (1:5000) and anti-JAK2 (1:2000). Membranes were once again rinsed three times and washed three times and developed using SuperSignal™ West Pico PLUS Chemiluminescent Substrate (Thermo Fisher Scientific, Waltham, USA). Blots were imaged using an Odyssey XF Imager (Li-COR Biosciences, Cambridge, UK) and band quantification was performed in Li-COR Image Studio version 6.0 (Li-COR Biosciences, Cambridge, UK).

2.6.1.1. Membrane stripping

To probe for loading controls, membranes were stripped using stripping buffer containing 2% SDS ± 1% 2-mercaptoethanol. Membranes first incubated in stripping buffer containing 2-mercaptoethanol for 20 min at 65°C then in stripping buffer without 2-mercaptoethanol, again for 20 min at 65°C. Membranes were washed 3 times in TBS-T, blocked for 60 min in 4% BSA then processed as described above.

2.6.2. Immunoprecipitation

Platelets at 4×10^8/mL were prepared as described in section 2.6.1 but reactions were instead halted by the addition of ice-cold 2X Nonidet P-40 lysis buffer containing protease inhibitors 4-(2-aminoethyl) benzenesulfonyl fluoride hydrochloride) (AEBSF) (200 µg/mL), aprotinin (10 µg/mL), leupeptin (10 µg/mL), pepstatin (1 µg/mL), and sodium orthovanadate (5 µM). Samples were incubated overnight at 4°C on rotation with 1.5 µg/mL JAK2 antibody followed by 2 hours with protein A Sepharose beads. Samples were eluted in 3X SDS reducing sample buffer and boiled for 5 min. Lysates were western blotted as described in section 2.6.1.

2.6.3. Mass spectrometry

Mass spectrometry for phosphorylated proteins in platelets induced by PF4 50 µg/mL (12.8 µM) was performed by Dr Jinglei Yu and Dr Todd Mize of the Advanced Mass Spectrometry Facility, College of Life and Environmental Sciences, University of Birmingham, UK. Surface plasmon resonance

Surface plasmon resonance (SPR) experiments were conducted by Eleyna Slater, University of Birmingham and performed using a Biacore T200 instrument (GE Healthcare, Chicago, USA). Recombinant c-Mpl (Bio-Techne, Minneapolis, USA) was conjugated onto a CM5 chip using amine-coupling to the surface coated with carboxymethylated dextran. Reference surfaces were blocked using ethanolamine 1 M, pH 8. Sensorgrams were double reference subtracted with two technical replicates injected per cycle in addition to 3 experimental replicates. The experiments were performed at 25°C with PF4 and TPO flowed over at a rate of 30 µL/min in HBS-EP running buffer (0.01 M HEPES pH 7.4, 0.15 M NaCl, 3 mM EDTA, 0.005% v/v surfactant P20). Multi-cycle kinetic assays were used with at least five concentration points between 0.1 and 10 times the estimated K_D. Each concentration of the analytes, PF4 and TPO, was run as follows; 120 s injection, 900 s dissociation, 30 s regeneration with 10 mM Glycine pH 1.5 and a 300 second stabilisation period. Kinetic analysis was performed using Biacore T200 Evaluation Software version 3.2 and used a global fitting to a 1:1 binding model. Methods are also published previously (Buka et al., 2024).

2.7. Enzyme-linked immunosorbent assay (ELISA)

These experiments were conducted by Samantha Montague, University of Birmingham. TPO binding to c-Mpl and subsequent interference by PF4 was measured with a c-Mpl-TPO ELISA. Nunc MaxiSorp 96-well plates were coated with recombinant c-Mpl 1 µg/mL by incubation at 4°C for 16-24 hours. Wells were washed in PBS-T (PBS with 0.2% Tween) four times then blocked with 1% BSA-PBS at RT for 60 min. Wells were then washed four times with PBS before addition of TPO (1, 10, 100 ng/mL) and incubated for 60 min at RT. To test the effect of PF4 on TPO binding, wells were pre-incubated with increasing concentrations of PF4 (1-

100 µg/mL) for 15 min at RT before the addition of TPO. Wells were then washed again and incubated with anti-c-Mpl antibody (0.1 µg/mL) for 60 min at RT. Wells were then washed and incubated with anti-rabbit-HRP antibody (1/5000) for 60 min at RT. Wells were then washed again after which 100 µL TMB (3,3',5,5'-tetramethylbenzidine) substrate was added for 15 min, before stopping the reaction with H_2SO_4 1 M. Plates were read at 450 nm using a plate reader. Results are representative of 3-4 experimental replicates.

2.8. 3D protein structure prediction

3D structures of firstly a PF4 tetramer with c-Mpl, and secondlyTPO with c-Mpl were modelled using AlphaFold 3.0 (Jumper et al., 2021) using the user-friendly online interface, AlphaFold Server Beta (Google DeepMind, n.d.). Predicted local distance difference test (pLDDT) scores, a per-residue measure of the confidence in the predicted structure, were used to rank the predictions. The scores are interpreted as follows: >90 indicates high accuracy, 70-90 suggests good modelling, 50-70 indicates low confidence and should be treated with caution, and <50 suggests a ribbon-like appearance unsuitable for interpretation. To merge structure predictions, files were loaded into the PyMOL Molecular Graphics System, version 3.1 (Schrödinger, New York, USA) and aligned by c-Mpl.

2.9. Endothelial cell assays

2.9.1. Endothelial cell culture

500,000 cryopreserved human dermal microvascular endothelial cells (HDMECs) or human umbilical vein endothelial cells (HUVECs) (Promocell, Heidelberg, Germany) were thawed in sterile conditions at 37°C for 2 min. The cryovial was rinsed in 70% ethanol and opened under a laminar flow bench. Cells were transferred to a T25 flask containing 10 mL pre-warmed endothelial growth media and incubated overnight at 37°C. After 16-24 h, media was replaced and then every 2-3 days thereafter until 90% confluency was reached. Media was aspirated and cells were then detached using trypsin / EDTA 0.04% / 0.03% for at least 2 min at RT until detachment could be visualised, with the process assisted by manual agitation. 2 mL trypsin

neutralising solution was added and liquid containing cells was poured into a 15 mL falcon tube. Cells were centrifuged at 200 *g* for 5 min after which supernatant was aspirated and 10 mL fresh endothelial growth medium added. Cells were then seeded in two T25 flasks and again incubated at 37°C until 90% confluency reached, changing media every two days. For the second passage, cells were split into two T75 flasks, and for the third and fourth passage, each T75 flask was split into three T75 flasks. Cells were then cryopreserved by detachment and centrifugation as described above before resuspension of the contents of one T75 flask in 1.5 mL freezing medium, cryo-SFM. Cells were frozen in cryovials at -80°C overnight and then transferred to liquid nitrogen. For experiments, one cryovial was thawed at 37°C for 2 min, washed in 5 mL endothelial growth media and resuspended in 5 mL media. Cells were then incubated in a T25 flask for 1-2 days before detaching, washing and counting using a haemocytometer. HMDECs were seeded at 180,000 cells per dish in gelatine-coated glass-bottom confocal dishes overnight. HUVECs were seeded at between 25,000 and 100,000 cells per well of a 24 well flat bottom plate depending on when experiments were due to take place, timed for cells to arrive at >90% confluence on the day of experiments. Cell culture and seeding of HMDECs was performed by Dr Jenefa Begum, Prof Asif Iqbal's group, University of Birmingham.

2.9.2. Microscopy

Glass-bottom dishes containing confluent endothelial cells were washed once with 500 µL serum free endothelial growth media after which PF4 10, 50 or 100 µg/mL in 400 µL serum free endothelial growth media was added (or media only control). Cells were incubated at 37°C for 60 min after which they were washed once in 500 µL serum free media. Anti-PF4 and anti-CD31 antibodies were added at 1:100 dilution in 400 µL media and incubated at 37°C for 30 min. Cells were washed again as above and then fixed in 4% paraformaldehyde for 10 min. Paraformaldehyde was removed and cells covered with 400 µL media containing 0.01% Hoechst 33342 for 3 min at RT after which they were washed once with 1 mL PBS and re-covered with PBS for imaging. Cells were imaged using a Zeiss Axio Observer 7 microscope

(Carl Zeiss AG, Oberkocken, Germany) at 60X magnification and Zen imaging software version 3.11 (Carl Zeiss AG). Fields where endothelial cells were >95% confluent were imaged with the user blinded to the PF4-channel. Ten fields from five distinct areas of the dish were imaged. Images were processed using the open source image processing package Fiji (Image J), version 1.54f (Schindelin et al., 2012) and quantitation of PF4 binding to endothelial cells performed by 'Analzye Particles' analysis using a consistent colour threshold.

For assessment of platelet adherence to PF4-treated endothelial cells, HMDECs were incubated with PF4 10-200 µg/mL for 3 hours at 37°C and washed three times in serum-free endothelial growth media. Platelets at 2×10^7/mL in 50% modified Tyrode's-HEPES buffer and 50% serum free endothelial cell growth media were added and incubated for 30 min at 37°C after which dishes were washed in warm endothelial growth media and incubated with anti-AF647-CD31 and FITC-CD41 antibodies for 20 min. Dishes were again washed then fixed in 4% paraformaldehyde, washed and stained with Hoechst 33342 for 3 min. Cells were washed and covered with PBS ready for visualisation by microscopy as described above. For these experiments, the user did not observe the FITC-CD41 channel when taking images.

2.9.3. Flow cytometry

HUVECs were prepared as described in section 2.9.1 and used when >90% confluent. Supernatant was removed and wells were washed once with Opti-MEM low serum media. Cells were then stimulated with combinations of PF4 10-100 µg/mL, heparin 0.5 IU/mL, VITT IgG 100 µg/mL, KKO 20 µg/mL, VITT, HIT, or control sera 3-10% final concentration, in Opti-MEM low serum media for 4 hours at 37°C. Tumour necrosis factor α (TNFα) (100 ng/mL) was used as a positive control. Cells were then covered with 200 µL RT trypsin / EDTA 0.04% / 0.03%, for 2-3 min until detached at which point 200 µL trypsin neutralising solution was added. Suspended cells were then collected into Eppendorf tubes at centrifuged at 200 *g* for 3 min. Supernatant was removed and cells were resuspended in ice cold PBS containing 10% foetal calf serum (FCS) and blocked on ice for 15 min. Tubes were once again centrifuged at

200 *g* for 3 min after which supernatant was removed and cells were resuspended in 100 µL ice cold 1% FCS in PBS containing antibodies against ICAM1, VCAM1, P-selectin, and tissue factor. Cells were incubated on ice for 20 min after which they were transferred to a 96 well round bottom plate and analysed by flow cytometry using a CytoFLEX LX flow cytometer (Beckman Coulter, Indianapolis, USA). Compensation was achieved using individually stained compensation beads and applied to the data in FlowJo version 10.3 (BD Biosciences, Ashland, USA). Percentage positive values were defined according to the isotype control.

For experiments that aimed to detect platelets adhered to HUVECs by flow cytometry, HUVECs were pre-activated with low dose TNFα (1 ng/mL) in Opti-MEM for 3 hours at 37°C. Cells were then washed once with Opti-MEM, and stimulants and platelets (2×10^8/mL) added together in 50% modified Tyrode's-HEPES buffer and 50% Opti-MEM. The plate was incubated at 37°C for 30 min to allow for platelet attachment after which wells were washed three times with Opti-MEM. Cells were trypsinised, processed, and analysed as described above.

2.10. Statistical analysis

Quantitative data are presented as mean ± standard deviation with the threshold for statistical significance set at $P < 0.05$. Prior to significance testing, data were tested for normality using the Shapiro-Wilk test with alpha set at 0.05. All data was paired unless indicated. For testing the significance of differences between two groups, the paired t-test and Wilcoxon matched-pairs signed rank test were used for normally, and non-normally distributed data respectively. For testing the significance of differences between more than one group, one-way analysis of variance (ANOVA) with Bonferroni post-test and the Friedman test were used for normally and non-normally distributed data respectively. On occasions where the presence of missing data precluded use of the one-way ANOVA, a mixed effects analysis was used. On the one occasion that data was unpaired, statistical testing of difference between groups was conducted using a t-test. Statistical testing of correlation was performed by Spearman's rank correlation coefficient. Missing data was treated as missing at random. Statistical testing of

differences was conducted on all histograms unless stated and for each, all groups (bars) that are shown in the graph were included in the analyses. Statistical significance was defined as $p < .05$ and significance labelled with asterixis according to the following thresholds: *< .05, **< .01, ***< .001, ****< .0001. All bars were compared with every other bar in the graphs, but only statistically significant comparisons are displayed. Statistical analyses were performed using GraphPad Prism 9.5.1 (San Diego, California USA). Biorender (www.biorender.com, Toronto, Canada) and PyMOL Molecular Graphics System, version 3.1 (Schrödinger, New York, USA) were used for illustrations.

3. PF4 activates platelets through c-Mpl and JAK2 signalling

3.1. Acknowledgements

Some of the data detailed in this Chapter and in Chapter 4 are included in the published study, Buka RJ and Montague SJ et al., PF4 activates the c-Mpl–Jak2 pathway in platelets, Blood. 2024 Jan 4;143(1):64-69. Some of the experiments were performed by other members of the Birmingham Platelet Group and these contributions are indicated throughout.

3.2. Introduction

The key observation that preludes this chapter is that, as mentioned in Chapter 1, PF4 is known to potentiate platelet activation to low dose agonists such as thrombin and collagen (Capitanio et al., 1985). It has been proposed that this could be due to charge effects – PF4 binding to negatively charged GAGs on the platelet surface neutralising the repellent negative force between platelets, facilitating apposition, agglutination, and aggregation (Kowalska et al., 2010). However, it is known that other chemokines including CCL17, CCL22, CXCL12, and CXC3L1, can activate platelets via receptor-dependent mechanisms (Gleissner et al., 2008). Thus, PF4 may also act through a receptor-dependent mechanism with associated downstream signalling. Supporting this possibility is the observation that PF4 at micromolar concentrations can induce platelet aggregation and α-granule secretion (Dickhout et al., 2021) demonstrating the propensity of PF4 to induce or support activating signalling cascades rather than simply facilitating platelet apposition.

Given that PF4 activates and potentiates platelets, is implicated in thrombosis, and is central to the pathophysiology of anti-PF4 immunothrombotic syndromes, investigating the mechanism by which PF4 has its effects on platelets is a valid endeavour. The addition of PF4 is known to enhance platelet activation in diagnostic assays of HIT and VITT which is assumed to be mediated by increased immune complex formation (Padmanabhan et al., 2016).

However, I hypothesised that in addition to being a focus of immune complex formation, PF4 might also contribute to the pathogenesis of HIT and VITT through direct platelet activation. As such, the aim of this chapter was to characterise platelet activation by PF4 and investigate the mechanism by which this might occur.

3.3. Results

3.3.1. 10 µg/mL (1.28 µM) PF4 is required to potentiate platelet responses to VITT serum

The addition of PF4 to functional diagnostic assays of VITT enhances platelet reactivity and hence the sensitivity of these assays (Warkentin and Greinacher, 2022). Indeed, functional assays for HIT have been adapted for VITT through replacement of exogenous heparin with PF4 although the precise amount of PF4 added is variable (Handtke et al., 2021; Greinacher et al., 2021; Smith et al., 2021). The Birmingham Platelet Group has previously used PF4 at a standard concentration of 10 µg/mL (1.28 µM) in LTA (Smith et al., 2021; Montague et al., 2022). Using serum from a patient with VITT that was previously shown not to activate platelets without additional PF4 (48 year old female, 203 days post vaccination, patient 7 in (Montague et al., 2022)), at least 10 µg/mL PF4 was required to result in platelet aggregation Moreover, weak aggregation was seen with PF4 alone (Figure 3.1).

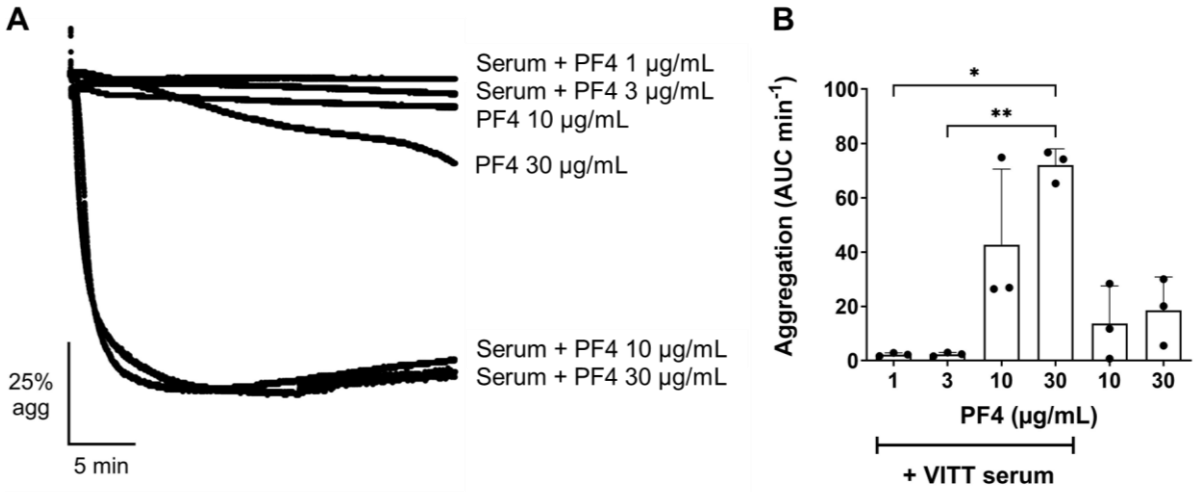

Figure 3.1. Potentiation of platelet aggregation to VITT serum requires at least 10 µg/mL PF4.

Platelet activation to PF4 and VITT serum was assessed by LTA. Pre-warmed platelets (2×10^8/mL) at 37 °C were pre-incubated with PF4 1-30 µg/mL for 5 min, then stirred at 1200 rpm for 1 min before addition of VITT serum (6.7% final concentration). (A) Representative aggregation traces, (B) Quantification of aggregation (area under curve per minute [AUC min-1] for 30 min, n=3). Statistical testing of differences by one-way ANOVA. *P < .05, **P < .01.

3.3.2. PF4 induces platelet aggregation in a dose-dependent manner

Thus, the ability of PF4 to induce platelet aggregation alone was investigated further. In washed platelets, aggregation to PF4 alone occurred in a dose-dependent manner, first occurring in some donors at 10 µg/mL and peaking at 50 µg/mL (1.28 to 12.8 µM) (Figure 3.2A). In some donors, the aggregation trace was biphasic, characterised by a gradual initial slope followed by a more rapid second phase of robust aggregation after about 10-15 min. Whilst the first phase occurred in all donors, the second phase, leading to over 50% aggregation, only occurred in about one third of donors (Figure 3.2Aii). Donors where the second phase occurred are hereon referred to as *responders*. The dose response relationship was bell-shaped; increasing the dose to 100 µg/mL had limited additional effect, and in 3/4 donors where full aggregation had occurred at 50 µg/mL, aggregation was reduced or absent (Figure 3.2A). Increasing concentrations of PF4 resulted in a faster onset of the second phase of aggregation rather than marked increase in the percentage maximum aggregation. There was no aggregation across this concentration range in PRP from healthy volunteers who were responders in washed platelets (Figure 3.2B) suggestive of PF4 binding to plasma proteins.

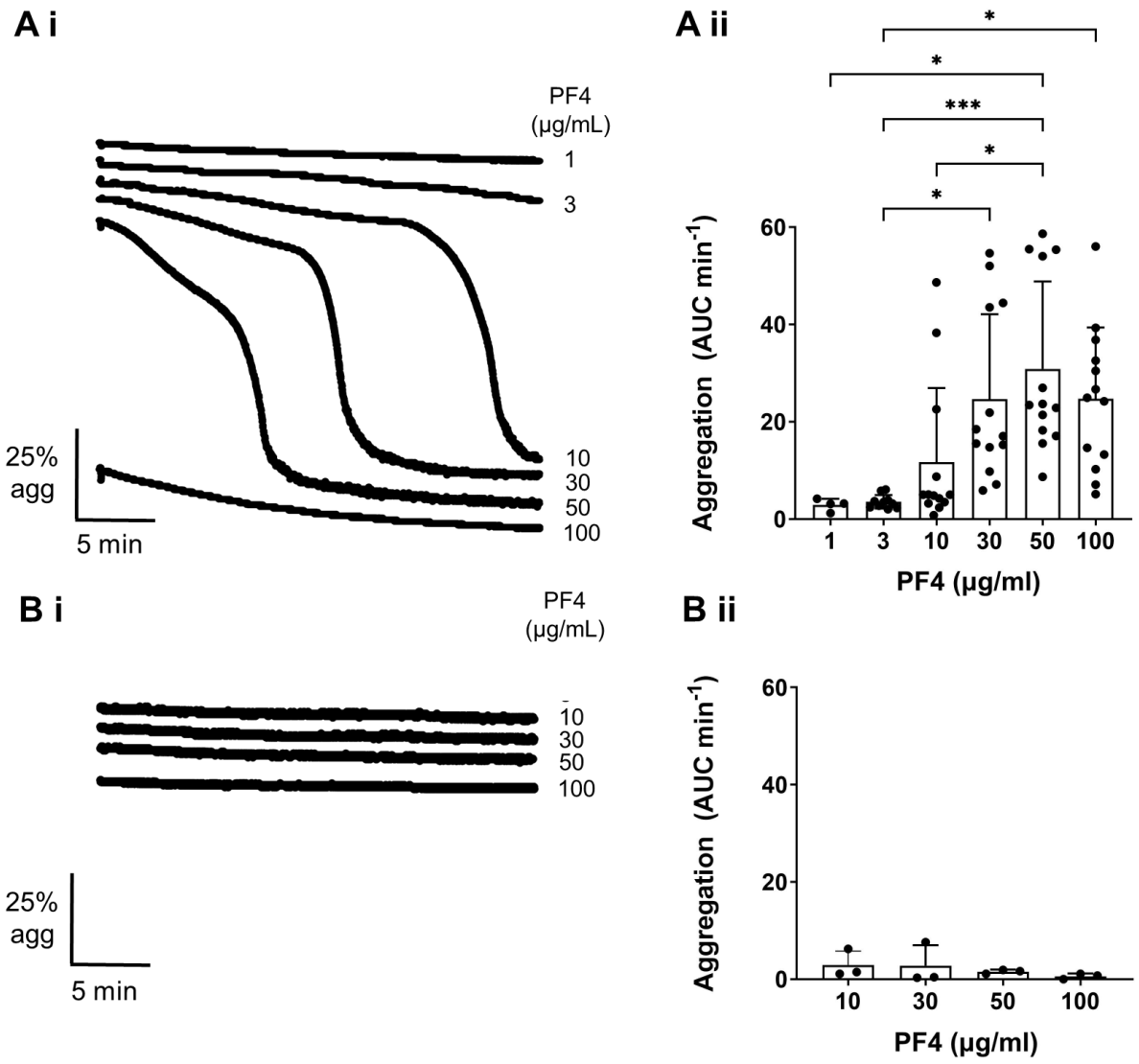

Figure 3.2. PF4 induces dose-dependent platelet aggregation in washed platelets but not in platelet rich plasma.

Adapted from (Buka et al., 2024). (A) Dose response to PF4 in washed platelets was assessed by LTA. Pre-warmed platelets (2×10^8/mL) at 37 °C were stirred at 1200 rpm for 1 min before addition of PF4 (1-100 µg/mL). (Ai) Representative aggregation traces, (Aii) Quantification of aggregation (area under curve per minute [AUC min^{-1}] for 30 min, n=4-13). Statistical testing of differences by Friedman test. (B) As for A but platelet rich plasma used instead of washed platelets and n=3 for Bii. *P < .05, ***P<.001.

Pre-treatment of platelets for 10 min with the integrin $\alpha_{IIb}\beta_3$ inhibitor, eptifibatide 9 µM, abrogated aggregation to PF4 50 µg/mL in five responders. As integrin $\alpha_{IIb}\beta_3$ is the key receptor that mediates platelet aggregation, this demonstrates that the observed response was indeed aggregation (Figure 3.3).

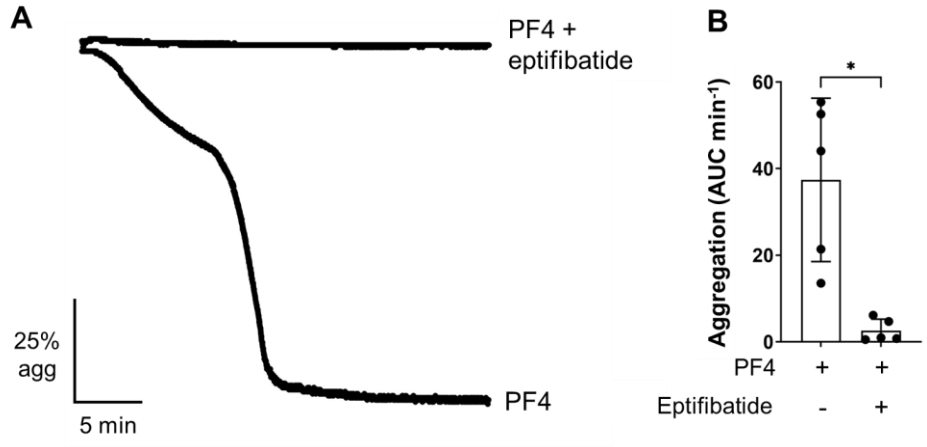

Figure 3.3. Platelet response to PF4 is integrin dependent.

Unmodified from (Buka et al., 2024). Platelet activation was assessed by LTA. Pre-warmed platelets (2×10^8/mL) at 37 °C were pre-incubated with eptifibatide 9 µM or vehicle control (PBS) for 5 min then stirred at 1200 rpm for 1 min before addition of PF4 (50 µg/mL). (A) Representative aggregation traces, (B) Quantification of aggregation (area under curve per minute [AUC min^{-1}] for 30 min, n=5). Statistical testing of differences by paired t-test. *P < .05.

To check that the observed effects were not due to impurities or contamination of PF4, three formulations were analysed by SDS-PAGE and Coomassie blue staining (Figure 3.4A). Compared to PF4 sourced from Prof. Doug Cines (University of Pennsylvania, USA), the formulation used in the initial functional experiments (Chromatec Gmbh, Greifswald, Germany), shows improved purity (Figure 3.4Ai). PF4 from collaborators in Liverpool, which was isolated from healthy volunteers, was of insufficient quality (Figure 3.4Ai) and required a four-fold increase in the amount loaded onto the gel for similar band intensity, but with additional impurities (Figure 3.4Aii). To compare ChromaTec and Doug Cines formulations further, functional activity was assessed. Both formulations led to platelet α-granule release, as measured by flow cytometry for platelet surface P-selectin expression in a dose-dependent

manner with the ChromaTec formulation slightly more potent. Collagen-related peptide (CRP) was used as a positive control (Figure 3.4B). Both PF4 formulations led to platelet aggregation but again, the ChromaTec formulation appeared to be more potent (Figure 3.4C); in one donor (Figure 3.4ii, open triangles) the strong aggregation seen with ChromaTec PF4 was not recapitulated with Doug Cines PF4. As PF4 was readily available from Chromatec on an on-going basis, all future work was conducted with this reagent. Furthermore, the bell-shaped dose-response curve seen in LTA was not apparent in flow cytometry, with responses increasing in all three donors from 50 to 100 µg/mL PF4.

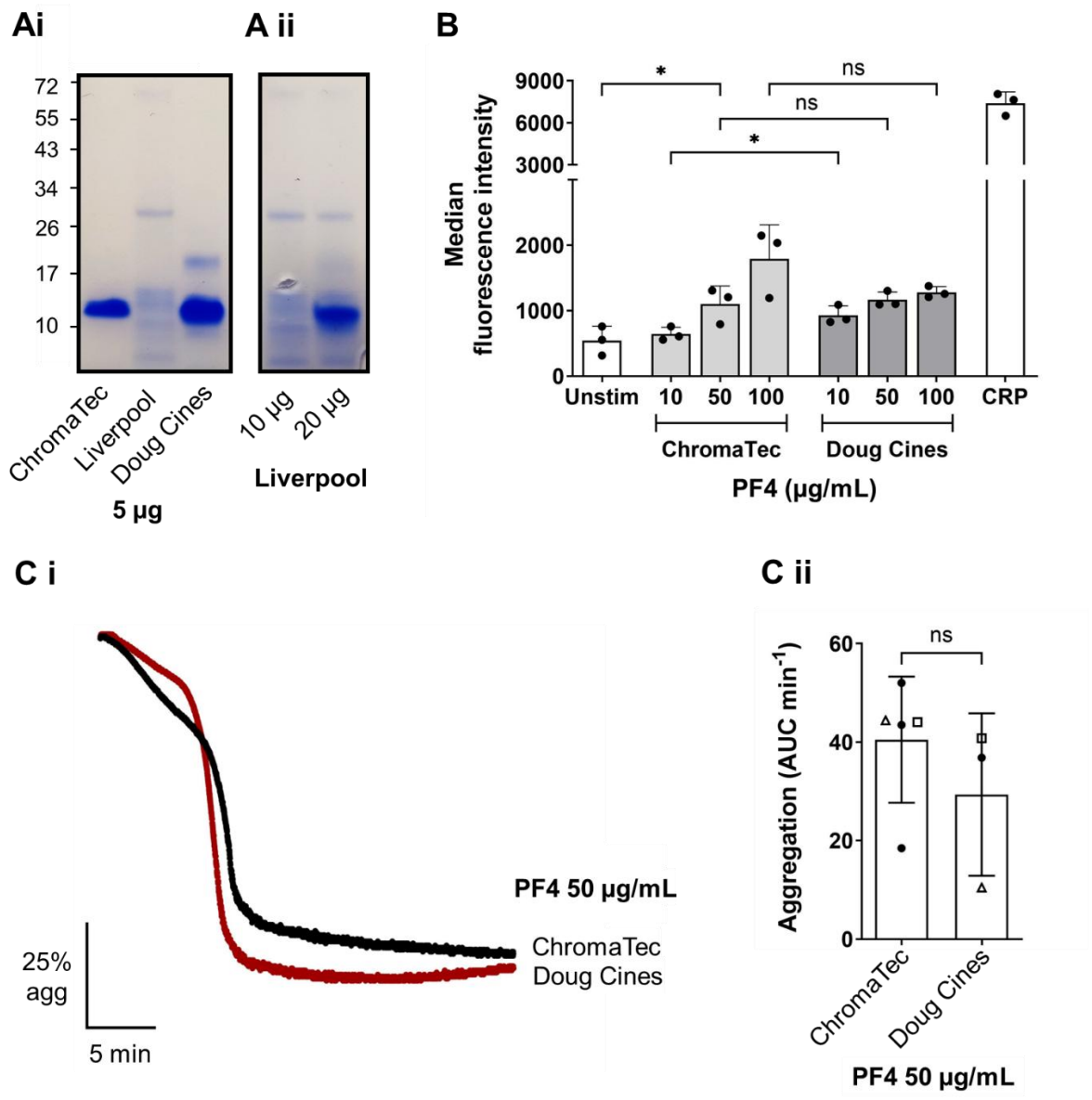

Figure 3.4. Comparison of composition and activity of formulations of PF4.

(A) Three formulations of PF4, ChromaTec, Liverpool, and Doug Cines, were separated by SDS-PAGE and stained with Coomassie blue. (A i) 5 µg of each formulation loaded. (A ii) 10 and 20 µg of Liverpool PF4 loaded. (B) Platelets (2×10^8/mL) were incubated at RT with either ChromaTec or Doug Cines PF4 (10, 50, or 100 µg/mL), or CRP 1 µg/mL as a positive control, before being stained with anti-P-selectin antibody and analysed by flow cytometry. Quantification by median fluorescence intensity. Statistical testing of differences by one-way ANOVA. (C) Pre-warmed platelets (2×10^8/mL) at 37 °C were stirred at 1200 rpm for 1 min before addition of either ChromaTec or Doug Cines PF4 (50 µg/mL). (Ci) Representative aggregation traces (donor represented by open squares in Cii), (Cii) Quantification of aggregation (area under curve per minute [AUC min^{-1}] for 30 min, n=3-5), open square represents donor with comparable response to Chromatec and Doug Cines PF4, open triangle represents donor with high response to Chromatec but low response to Doug Cines PF4. Other donors represented by closed black circles (and are all different donors). Statistical testing of differences by t-test. *P < .05, ns = not significant.

3.3.3. PF4 binds c-Mpl and activates JAK2

To investigate the mechanism of platelet activation to PF4, platelets were first stimulated with PF4 50 µg/mL, lysed at increasing time points, and western blotted for pan-phosphotyrosine (4G10). Results of this time-course analysis (which was done in only one healthy platelet donor) show that phosphorylated bands at ~95 kDa appear after 180 s, peaking at 600 s (Figure 3.5). 600 s was therefore chosen as the stirring time for future experiments investigating phosphorylation-dependent signalling.

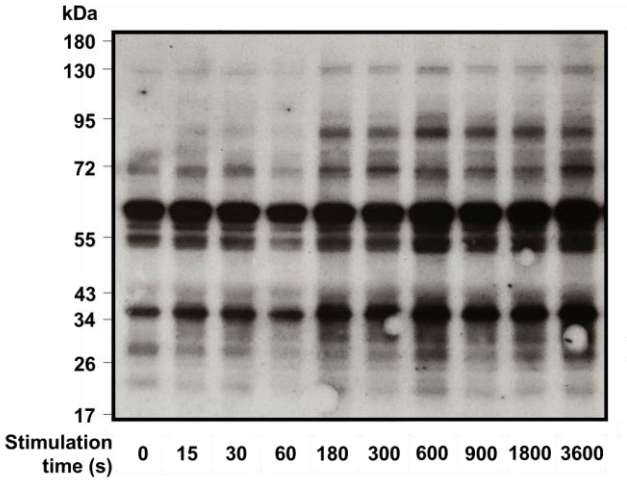

Figure 3.5. PF4 induces phosphorylated bands at 95 kDa after 180 s, peaking at 600 s.

Protein phosphorylation to PF4 was assessed by western blot for panphosphotyrosine. Washed platelets (4×10^8/mL) were pre-incubated with eptifibatide (9 µM) for 10 min, warmed to 37°C then stirred at 1200 rpm before addition of PF4 50 µg/mL. After 0 to 3600 s, platelets were lysed. Protein was separated by sodium dodecyl sulfate (SDS) gel electrophoresis, transferred to a polyvinylidene fluoride membrane, and analysed for phosphotyrosine (4G10).

To investigate the signalling mechanism further, following electrophoresis, a small region of SDS-polyacrilamide gel electrophoresis (PAGE) gels at 95 kDa containing lysates from PF4-stimulated platelets taken from two donors were sent for phosphoproteomic analysis by mass spectrometry. The analysis detected 586 and 646 proteins for platelet donor 1 and 2 respectively. Of these, two and five proteins respectively were unique, tyrosine-phosphorylated proteins and are shown in Table 3.1. The original mass spectrometry data are deposited to the PRoteomics IDEntifications Database (PRIDE) and are available via www.ProteomeXchange.org (identifier PXD043558).

Table 3.1. Tyrosine phosphorylated proteins identified in mass spectrometry of proteins at 95 kDa as separated by SDS-PAGE.

Samples from two healthy responders to PF4 were sent for mass spectrometry which identified seven tyrosine-phosphorylated proteins. Signal transducer and activator of transcription 5a and 5b, (STAT5a and STAT5b) were identified as the most likely proteins to be involved in signalling downstream of PF4-induced platelet activation.

Protein	Molecular weight of whole protein (kDa)	Tyrosine phosphorylation site
Donor 1		
Ectonucleoside triphosphate diphosphohydrolase 5	48	Y65
Solute carrier family 2, facilitated glucose transporter member 3	54	Y141
Donor 2		
Armadillo repeat-containing X-linked protein 2	66	Y417
Homeobox protein engrailed-1	40	Y378
Protein kinase C delta type	77	Y514
Signal transducer and activator of transcription 5a	92	Y699
Signal transducer and activator of transcription 5b	90	Y694

The identification of signal transducer and activator of transcription 5A (STAT5a) and 5B (STAT5b) was of particular interest as these proteins are activated downstream of Janus kinase (JAK proteins) and it was thus hypothesised that PF4 may signal through a JAK-dependent mechanism (Figure 3.6).

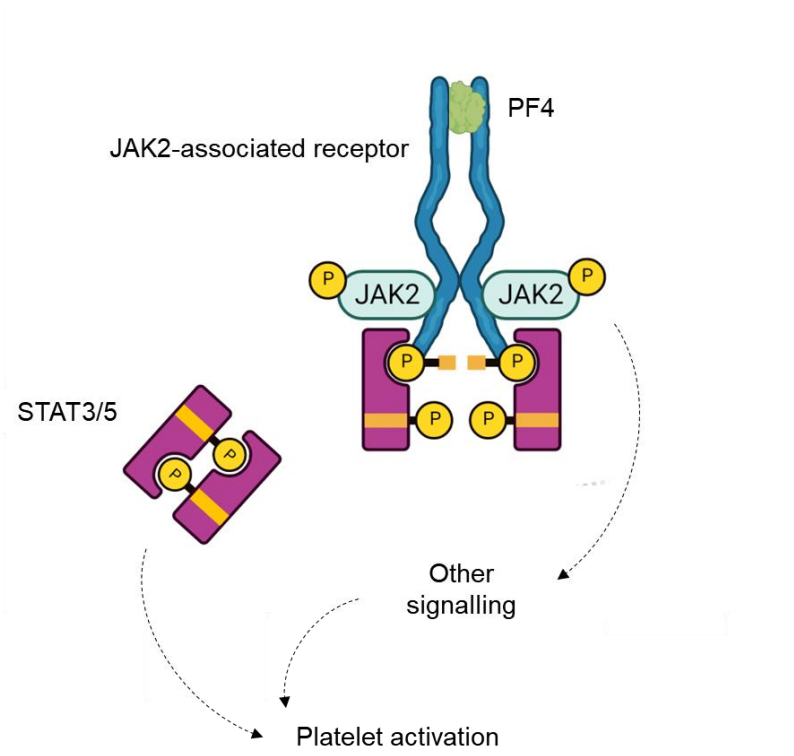

Figure 3.6. Hypothesised JAK2-dependent signalling mechanism for activation of platelets by PF4.

STAT5a and STAT5b are two highly homologous proteins but STAT5b has an additional six amino acid sequence at position 687 (Maurer et al., 2019). Thus, identical peptides are detected by mass spectrometry for STAT5a phosphorylated at Y694 and for STAT5b at Y699. Protein kinase C delta type (PKCδ) may also be of interest as it is activated downstream of diacylglycerol but has been reported to be activated by a range of agonists including the protease-activated receptor (PAR) 4 agonist, AYPGKF, the PAR1 agonist, SFLLRN and the GPVI agonist, convulxin (Bhavanasi et al., 2010). The JAK/STAT pathway was therefore focused on as it was considered most likely to lead to the identification of a receptor.

To confirm the findings of mass spectrometry, washed platelets were stimulated with increasing concentrations of PF4 for 600 s, lysed, western blotted, and stained for pan-phosphotyrosine, phosphorylated STAT5a, and phosphorylated STAT5b (pSTAT5a/b), the latter two using an antibody that recognises the same phosphorylated sequence in STAT5a and STAT5b. As STAT3, a closely related protein to STAT5, has also been reported to play a

role in platelet activation (Zhou et al., 2013; Vassilev et al., 2002), western blots were also probed for phosphorylated STAT3 (pSTAT3). Figure 3.7Ai shows results of protein phosphorylation in response to increasing concentrations of PF4. Bands at 95 kDa appear at 3 µg/mL PF4 but intensify at 10 µg/mL which is reflected in the staining for pSTAT3 and pSTAT5 (Figure 3.7Aii). As STAT3 and STAT5a/b phosphorylation are dependent on Janus kinase 2 (JAK2) in megakaryocytes (Drachman et al., 1999; Hitchcock et al., 2021), JAK2 was next immunoprecipitated and western blotted using pan-phosphotyrosine antibody 4G10, again showing dose-dependent increase in band intensity (Figure 3.7Aiii and Figure 3.7B).

As previously mentioned, in platelets, there are three receptors that have major signalling through JAK: the TPO receptor, c-Mpl, insulin-like growth factor receptor 1 (IGFR1), and the IL-6 receptor subunit glycoprotein 130 (GP130) (Burkhart et al., 2012; Huang et al., 2021). It was hypothesised that one of these receptors would be the PF4 receptor and that the most likely candidate was c-Mpl which is expressed at ~1,600 copies per platelet (Burkhart et al., 2012; Huang et al., 2021). Western blots were therefore stained for phosphorylated c-Mpl (p-c-Mpl) which was found to be present, again, with band intensity increasing concentration of PF4 (Figure 3.7Aiv and Figure 3.7B). For all four proteins, STAT3, STAT5, JAK2 and c-Mpl, phosphorylation was detectable at PF4 10 µg/mL and peaked at 50 µg/mL (Figure 3.7B) which was consistent with the functional LTA data. Spleen tyrosine kinase (Syk) was used as a relevant loading control due to its role in platelet signalling and quantitative data were normalised to the band intensity of the loading control.

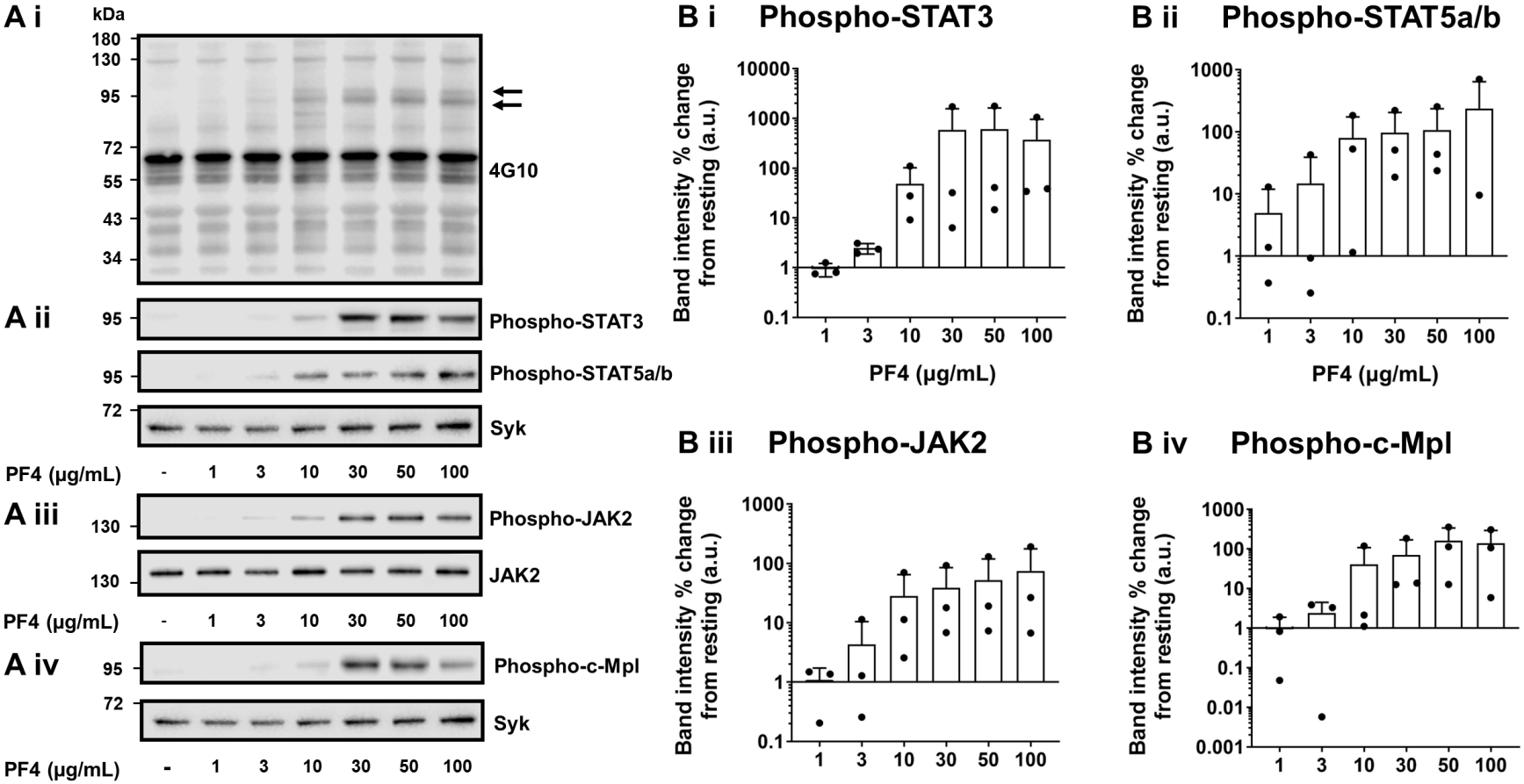
A i
kDa
180
130
95
72
55
43
34
4G10
A ii
95
Phospho-STAT3
95
Phospho-STAT5a/b
72
Syk
PF4 (µg/mL)
- 1 3 10 30 50 100
A iii
130
Phospho-JAK2
130
JAK2
PF4 (µg/mL)
- 1 3 10 30 50 100
A iv
95
Phospho-c-Mpl
72
Syk
PF4 (µg/mL)
- 1 3 10 30 50 100
B i Phospho-STAT3
Band intensity % change from resting (a.u.)
10000
1000
100
10
1
0.1
1 3 10 30 50 100
PF4 (µg/mL)
B ii Phospho-STAT5a/b
Band intensity % change from resting (a.u.)
1000
100
10
1
0.1
1 3 10 30 50 100
PF4 (µg/mL)
B iii Phospho-JAK2
Band intensity % change from resting (a.u.)
1000
100
10
1
0.1
1 3 10 30 50 100
B iv Phospho-c-Mpl
Band intensity % change from resting (a.u.)
1000
100
10
1
0.1
0.01
0.001
1 3 10 30 50 100

Figure 3.7. PF4 activates platelets through the c-Mpl-JAK2-STAT3/5 pathway.

Adapted from (Buka et al., 2024). Western blot analysis of platelet lysates showing dose-dependent phosphorylation of STAT3, STAT5a/b, JAK2, and c-Mpl by PF4. Platelets (4×10^8/mL) were pre-incubated with eptifibatide (9 µM) for 10 min, warmed to 37°C then stirred at 1200 rpm before addition of PF4 (1 to 100 µg/mL). Platelets were lysed after 10 min and protein was separated by SDS-PAGE. Protein was transferred to a polyvinylidene fluoride membrane, and stained for phospho-STAT3, phospho-STAT5, and phospho-c-Mpl. For JAK2, samples were immunoprecipitated prior to western blotting and staining for pan-phosphotyrosine (4G10). (Ai) Representative western blot of whole platelet lysate using 4G10; (Aii) Representative western blots using antibodies to phospho-STAT3 and phospho-STAT5a/b; (Aiii) Representative western blot using 4G10 after immunoprecipitation for JAK2; (Aiv) Representative western blot using an antibody to phospho-c-Mpl. Membranes were stripped and reprobed for Syk as a loading control. (B) Quantification of pixel lane intensities for phosphorylation of the four proteins as indicated, presented as % change from resting and normalised for loading controls. Statistical analysis by one-way ANOVA with no significance of difference observed.

To further investigate the interaction between PF4 and c-Mpl, surface plasmon resonance (SPR) experiments were undertaken by Dr Eleyna Slater, University of Birmingham. With c-Mpl bound to the chip and PF4 flowed over the surface, SPR showed a direct interaction between PF4 and c-Mpl with a dissociation constant (K_D) of 744 nM (5.8 µg/mL) (Figure 3.8A). This contrasted with a K_D for the interaction between TPO and c-Mpl of 3.5 nM (201 ng/mL; based on mass spectrometry analysis of mature, glycosylated protein (Hoffman et al., 1996)) (Figure 3.8B). Both exhibit a high on-rate but as stated above, TPO interacts at a much lower molar concentration than PF4. Both show a high off-rate, although dissociation of PF4 appears faster than for TPO. Furthermore, the interaction of PF4 with c-Mpl is over two orders of magnitude weaker than that of PF4 with heparin. The sensorgrams and K_D for TPO are similar to those that have been previously reported (Tsutsumi et al., 2023), validating the findings with PF4.

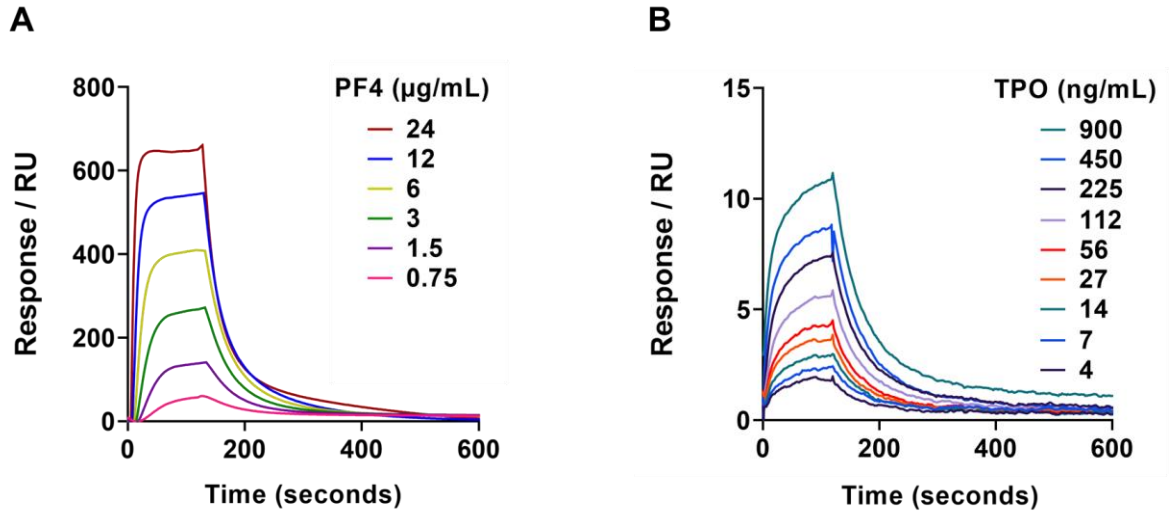

Figure 3.8. Surface plasmon resonance showing direct interaction of PF4 TPO receptor c-Mpl and compared with TPO.

(A) Surface plasmon resonance (SPR) showing binding of PF4 to c-Mpl. c-Mpl was conjugated onto the chip and PF4 flowed over. (B) c-Mpl was conjugated onto the chip and TPO flowed over. Sensorgrams are double reference subtracted, and at least two replicates were injected per cycle with experimental replicates of n=3. RU: response units.

3.3.4. Healthy donor platelet responses to PF4 and TPO show inter- and intra-donor variability

Given that TPO has also been reported to potentiate platelet activation to agonists such as collagen and thrombin (Pasquet et al., 2000; Moore et al., 2019), the effect of TPO alone on washed platelet aggregation was assessed. As for PF4, TPO induced dose-dependent aggregation beginning at 30 ng/mL (0.8 nM) and peaking at 50-100 ng/mL (1.4 – 2.8 nM) (Figure 3.9A). 100 ng/mL was the maximum concentration used as this is the level at which functional proliferative responses to TPO plateau (Proteintech, n.d.). and is, in any case far higher than TPO levels reach in blood (Lupia et al., 2009, 2022; Makar et al., 2013).

Similar to aggregation to PF4, aggregation to TPO occurred in a biphasic manner with a slow first wave followed by a rapid second phase (Figure 3.9A). Next, aggregation responses to PF4 and TPO were compared and it was observed that aggregation responses to PF4 and TPO in individual donors were not correlated (Figure 3.9B); donors who were high responders to PF4 (responding at 10 µg/mL) were not necessarily responders to TPO and vice-versa.

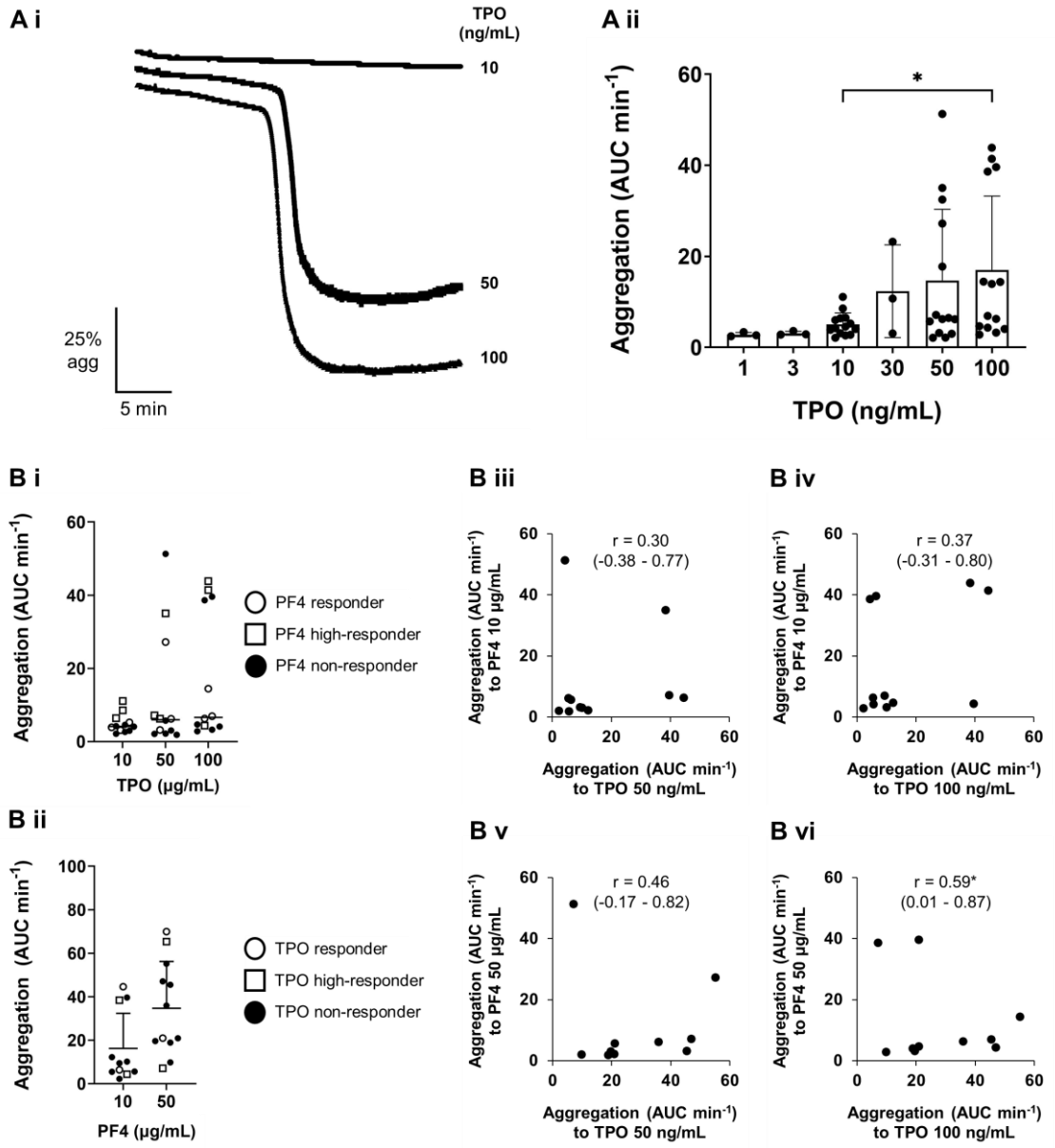

Figure 3.9. Healthy donor platelet aggregation to TPO is not correlated with aggregation to PF4.

(A) TPO induces platelet aggregation in a dose-dependent manner. Pre-warmed platelets (2×10^8/mL) at 37°C were stirred at 1200 rpm for 1 min before addition of TPO (10 to 100 ng/mL). (Ai) Representative aggregation traces (Aii) Quantification of aggregation (area under curve per minute [AUC min^{-1}] for 30 min, n=3-14). Statistical testing of differences by Friedman test. (B) Correlation of aggregation responses to PF4 and TPO. (Bi) Quantification of aggregation responses (AUC min^{-1} for 30 min, n=11) to increasing concentration of TPO (10 to 100 ng/mL) according to responder status to PF4. PF4 responders are those who had >50% aggregation to 50 µg/mL and to 10 µg/mL. (Bii) As for Bi but results displayed as responses to increasing concentration of PF4 according to responder status to TPO. TPO responders are those who had >50% aggregation to 100 ng/mL and TPO high responders to 50 ng/mL. (Biii) Quantification of aggregation responses (AUC min^{-1} for 30 min, n=11) to PF4 10 µg/mL (y-axis) plotted against response to TPO 50 ng/mL (x-axis). (Biv) As for Biii but TPO 100 ng/mL on y-axis. (Bv) As for Biii but PF4 50 µg/mL on y-axis. (Bvi) As for Bv but TPO 100 ng/mL on x-axis. Statistical testing of correlation by Spearman's rank correlation coefficient. *P < .05.

3.3.5. Inhibitors of c-Mpl and JAK2 block platelet aggregation to PF4

Only one reagent to block the c-Mpl receptor, a polyclonal goat anti-human IgG (Thermo Fisher Scientific, Waltham, USA), was available commercially. Product literature showed an ND50 ("neutralising dose 50", concentration of antibody required to inhibit 50% of the target activity) of 0.5-2.5 µg/mL to block proliferation of a megakaryocytic leukaemia cell line to TPO 10 ng/mL (Thermo Fisher Scientific, n.d.). Thus, 10 µg/mL was chosen as an initial concentration to assess blockade. Figure 3.10A shows that although the antibody did, in some donors, block platelet aggregation responses to PF4 50 µg/mL and TPO 100 ng/mL, this blockade was not consistent and in one donor each for PF4 and TPO, the antibody in fact enhanced aggregation (red and blue circles). The antibody also did not reduce phosphorylation of c-Mpl, STAT3, or STAT5a/b in response to PF4 50 µg/mL or TPO 100 ng/mL (Figure 3.10B)

Given the evidence of enhancement of activation, the concentration of anti-c-Mpl antibody was not escalated. Instead, the effect of the antibody at 10 µg/mL concentration was assessed against PF4 10 µg/mL in responsive donors which resulted in consistent abrogation of both the first and second waves of aggregation (Figure 3.10C).

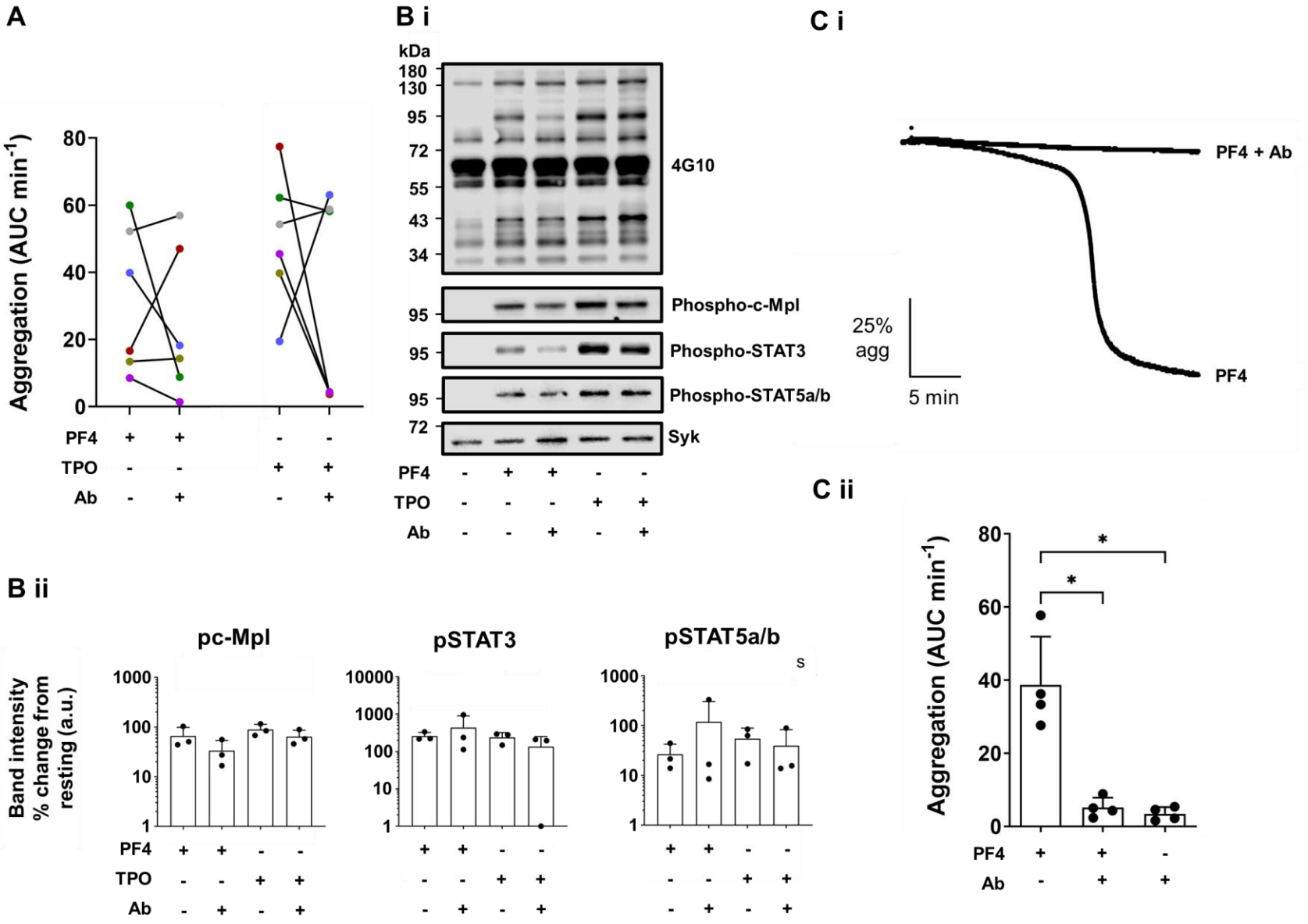
A
Aggregation (AUC min-1)
80
60
40
20
0
PF4 + + - -
TPO - - + +
Ab - + - +
B i
kDa
180
130
95
72
55
43
34
4G10
95
Phospho-c-Mpl
95
Phospho-STAT3
95
Phospho-STAT5a/b
72
Syk
PF4 - + + - -
TPO - - - + +
Ab - - + - +
C i
PF4 + Ab
25% agg
5 min
PF4
C ii
Aggregation (AUC min-1)
80
60
40
20
0
*
*
PF4 + + -
Ab - + +
B ii
Band intensity % change from resting (a.u.)
pc-Mpl
pSTAT3
pSTAT5a/b
1000
100
10
1
10000
1000
100
10
1
1000
100
10
1
PF4 + + - -
TPO - - + +
Ab - + - +

Figure 3.10. Anti-c-Mpl antibody does not consistently block platelet aggregation or phosphorylation of STAT3 or STAT5a/b to higher concentrations of TPO or PF4, but does block aggregation to a lower concentration of PF4.

(A) Platelet aggregation to high dose PF4 and TPO is not blocked by anti-c-Mpl antibody. Pre-warmed platelets (2×10^8/mL) at 37°C were incubated with anti-c-Mpl antibody 10 µg/mL or vehicle control (PBS) for 5 min, then stirred at 1200 rpm for 1 min before addition of PF4 50 µg/mL or TPO 100 ng/mL. Quantification of aggregation (area under curve per minute [AUC min-1] for 30 min, n=6, colours represent individual donors). Statistical testing of differences by Friedman test. (B) Anti-c-Mpl antibody does not block STAT3, STAT5, or c-Mpl phosphorylation to PF4 or TPO. Washed platelets (4×10^8/mL) were pre-incubated with eptifibatide (9 µM) for 10 min, warmed to 37°C then stirred at 1200 rpm before addition of PF4 50 µg/mL or TPO 100 ng/mL. After 600 s, platelets were lysed. Protein was separated by SDS-PAGE, transferred to a polyvinylidene fluoride membrane, and analysed for pan-phosphotyrosine (4G10), phospho-c-Mpl (pc-Mpl) phospho-STAT3 (pSTAT3), phospho-STAT5a/b (pSTAT5a/b), and Syk (loading control). (Bi) Representative western blots. (Bii) Quantification of pixel lane intensities for phosphorylation of pc-Mpl, pSTAT3 and pSTAT5a/b measured as fold change relative to resting (n=3). Values are normalized for loading controls. Statistical analysis by one-way ANOVA. (C) Anti-c-Mpl antibody blocks platelet aggregation to low-concentration PF4. As for A but PF4 10 µg/mL added instead of 50 µg/mL, n=4. Statistical testing of difference by one-way ANOVA. *P < .05.

Next, the effect of JAK2 inhibition using the JAK1 and JAK2 inhibitor, ruxolitinib was investigated. Ruxolitinib is a widely used, effective therapeutic agent for myeloproliferative disorders and graft-versus host disease and has an IC50 (inhibitory concentration 50%) of 3.3 nM and 2.8 nM for JAK1 and JAK2 respectively (Quintás-Cardama et al., 2010). Ruxolitinib was selected over other inhibitors as although it is not specific for JAK2, it is more specific for JAK proteins than other JAK2 inhibitors. For example, although fedratinib is 30 times more potent at inhibiting JAK2 than JAK1 (IC50 3 nM versus 105 nM), is it reported to have more non-JAK inhibiting activity (Zhou et al., 2014a). To define a concentration of ruxolitinib that could specifically block JAK2 signalling in platelets whilst limiting any off-target effects, platelets were activated with low dose thrombin (0.4 U/mL) and the effect of increasing concentration of ruxolitinib was assessed. Ruxolitinib was observed to inhibit thrombin-mediated platelet activation at concentrations ≥ 300 nM but 100 nM had no effect (Figure 3.11A). Ruxolitinib 10 µM has previously been shown to have an inhibitory effect on platelet aggregation to the activation of GPVI by collagen (Parra-Izquierdo et al., 2022), but 100 nM had no effect on the activation induced by low concentrations of CRP (Figure 3.11B).

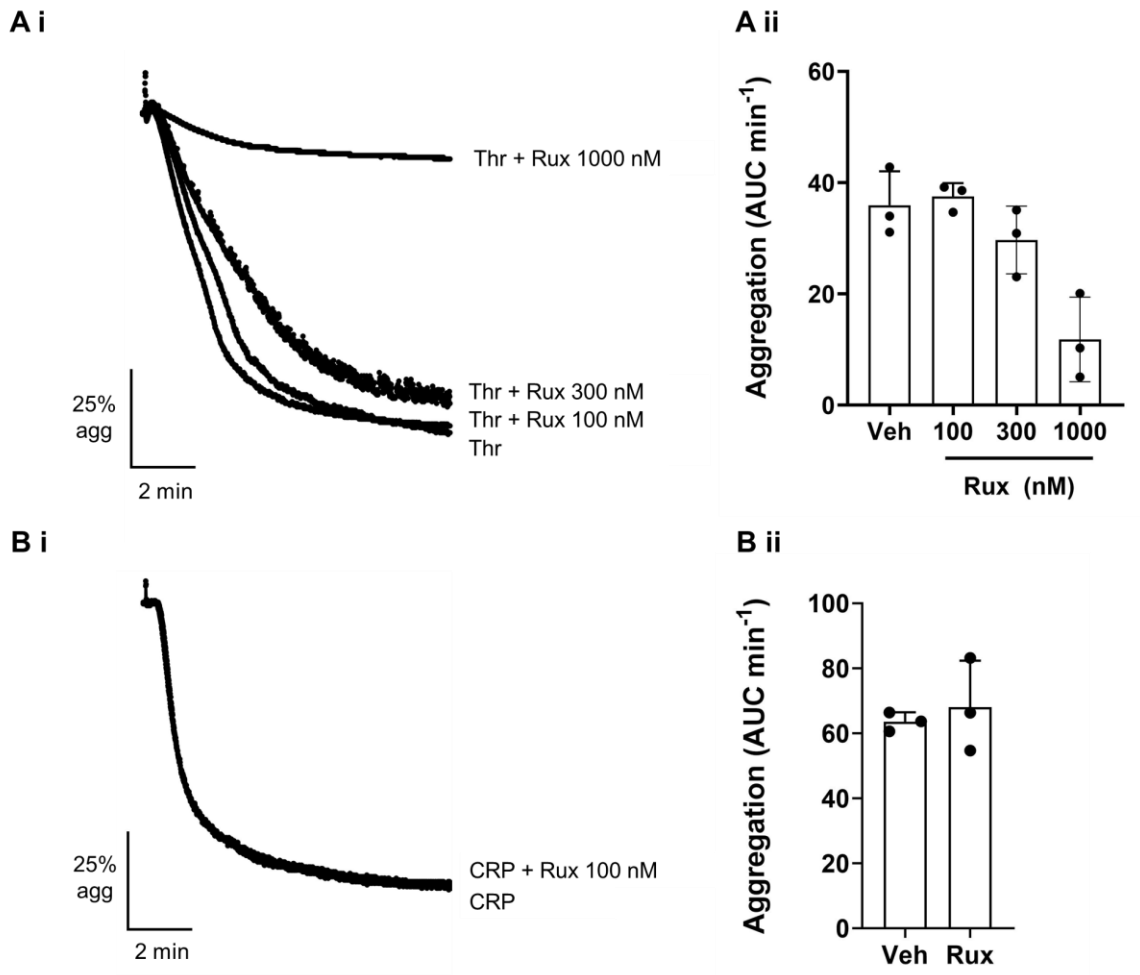

Figure 3.11. Ruxolitinib 100 nM has no effect on platelet aggregation to thrombin or CRP.

Adapted from (Buka et al., 2024). (A) The effect of ruxolitinib on platelet activation by PF4 was assessed by LTA. Pre-warmed platelets (2×10^8/mL) at 37°C were incubated with ruxolitinib 100-1000 nM (Rux) or vehicle control (DMSO 0.01%) for 5 min, then stirred at 1200 rpm for 1 min before addition of thrombin 0.4 U/mL (Thr). (Ai) Representative aggregation traces. (Aii) Quantification of aggregation (area under curve per minute [AUC min^{-1}] for 10 min, n=3). Statistical testing of differences by one-way ANOVA. (B) As for A but after platelets pre-incubated with Rux 100 nM only and CRP 1 µg/mL added. Statistical testing of difference by paired t-test.

Ruxolitinib 100 nM, but not lower concentrations, consistently blocked aggregation to PF4 50 µg/mL (Figure 3.12A) and this was also shown to block aggregation to TPO 100 ng/mL (Figure 3.12B). This led to blockade of both the first and second waves of aggregation (Figure 3.12Ai) Furthermore, ruxolitinib blocked STAT3 and STAT5a/b phosphorylation to PF4 in a concentration-dependent manner, maximal at 100 nM which was mirrored in the blockade of phosphorylation in response to TPO 100 ng/mL (Figure 3.12C).

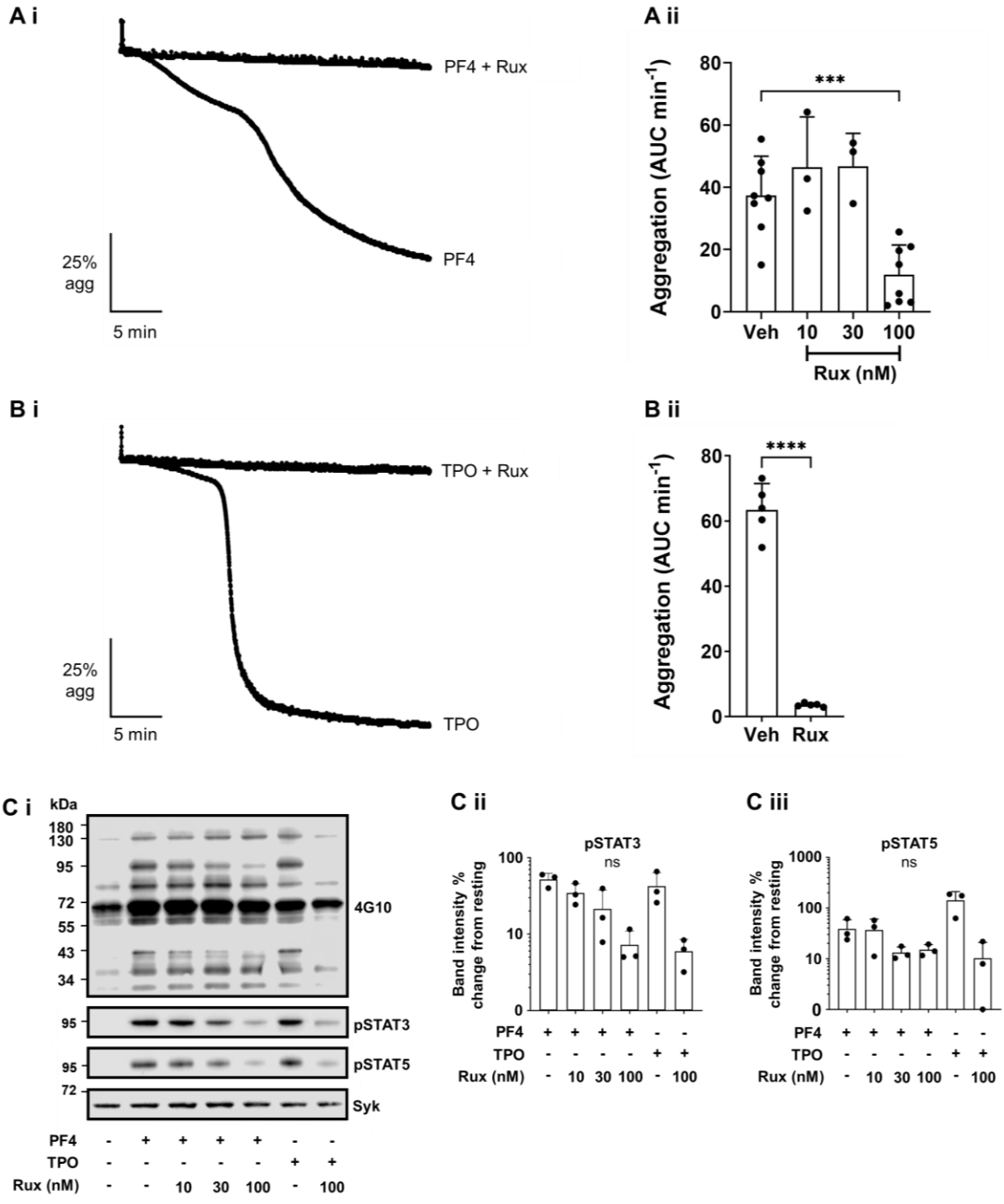

Figure 3.12. Ruxolitinib blocks PF4- and TPO-mediated platelet aggregation and phosphorylation of STAT3 and STAT5.

(A) Platelet aggregation to PF4 50 µg/mL is blocked by ruxolitinib 100 nM. Pre-warmed platelets (2×10^8/mL) at 37°C were incubated with ruxolitinib 10-100 nM (Rux) or vehicle control (DMSO 0.01%) for 5 min, then stirred at 1200 rpm for 1 min before addition of PF4 50 µg/mL. (Ai) Representative aggregation traces (Aii) Quantification of aggregation (area under curve per minute [AUC min^{-1}] for 30 min, n=3-8). Statistical testing of differences by one-way ANOVA. (B) As for A but only Rux 100 nM used and TPO 100 ng/mL added instead of PF4, n=5. Statistical testing of difference by paired t-test. (C) Phosphorylation of STAT3 and STAT5 is reduced by Rux. Platelets ($4x10^8$/mL) were pre-incubated with eptifibatide (9 µM) for 10 min,

Rux 10-100 nM for 5 min, warmed to 37°C, then stirred at 1200 rpm before addition of PF4 50 µg/mL or TPO 100 ng/mL. After 600 s, platelets were lysed. Protein was separated by SDS-PAGE, transferred to a polyvinylidene fluoride membrane, and analysed for pan-phosphotyrosine (4G10), phospho-STAT3 (pSTAT3), phospho-STAT5a/b (pSTAT5a/b), and Syk (loading control). (Bi) Representative western blots. (Bii) Quantification of pixel lane intensities for phosphorylation pSTAT3 and pSTAT5a/b measured as fold change relative to resting (n=3). Values are normalised for loading controls. Statistical analysis by one-way ANOVA. ***P < .001, ****P < .0001

As a later aim of this thesis is to assess the role of PF4-mediated platelet activation in VITT and HIT, the effect of inhibitors of ITAM signalling on PF4 were tested. As described in section 1.5.1, ITAM receptors include the collagen receptor GPVI and FcγRIIA. Two well-established inhibitors of ITAM signalling were used: the SRC family kinase inhibitor, dasatinib (1 µM) and the Syk inhibitor, PRT-060318 (10 µM). These concentrations abrogate platelet aggregation to the GPVI agonist CRP (Figure 3.13A) but not to PF4 (Figure 3.13B).

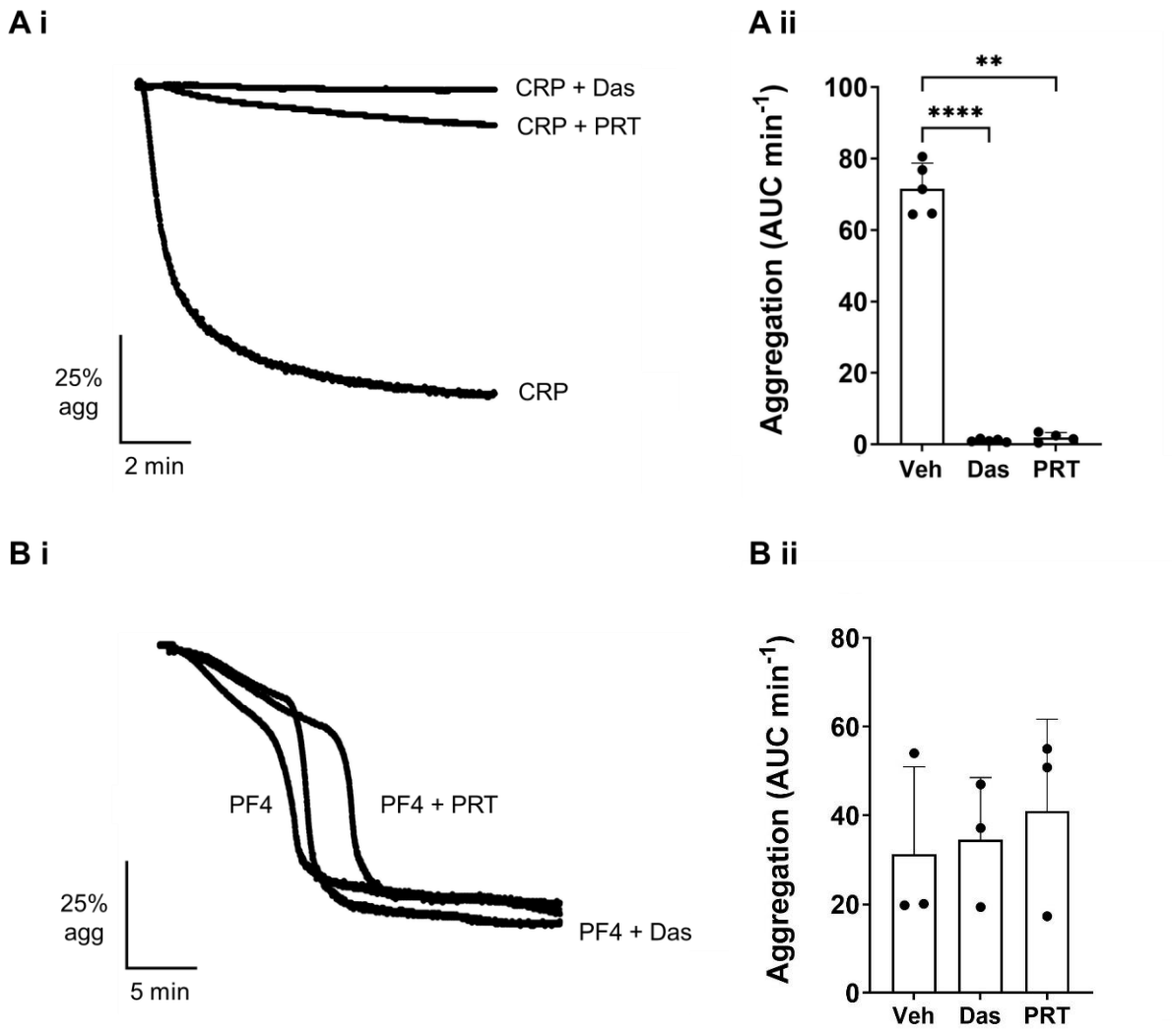

Figure 3.13. Inhibitors of Syk and Src at concentrations that block CRP have no effect on platelet aggregation to PF4.

Unmodified from (Buka et al., 2024). (A) The effect of inhibitors on PF4-mediated platelet activation were assessed by LTA. Pre-warmed platelets (2×10^8/mL) at 37°C were incubated with dasatinib 1 µM (Das), PRT-060318 10 µM (PRT), or vehicle control (DMSO 0.01%) (Veh) for 5 min, then stirred at 1200 rpm for 1 min before addition of CRP 1 µg/mL. (Ai) Representative aggregation traces. (Aii) Quantification of aggregation (area under curve per minute [AUC min^{-1}] for 10 min, n=4-5). Statistical testing of differences by one-way ANOVA. (B) As for A but PF4 50 µg/mL added instead of CRP and aggregation measured for 30 min (n=3). **P < .01, ****P < .0001.

It was previously reported that PF4 potentiates platelet aggregation responses to subthreshold doses of thrombin, arachidonic acid, and ADP (Capitanio et al., 1985). Furthermore, as TPO also potentiates responses to thrombin as well as collagen (Moore et al., 2019; Pasquet et al., 2000), it was hypothesised that PF4 would also potentiate platelet responses to stimulation through an ITAM receptor. This is of course of interest in the context of HIT and VITT. Aggregation to subthreshold concentration CRP (which activates platelets through GPVI) was indeed potentiated by PF4 10 µg/mL and this was blocked by ruxolitinib 100 nM A). As expected, the previously described enhancing effect, of TPO (Pasquet et al., 2000) was also confirmed to occur with TPO 10 ng/mL and this was also blocked with ruxolitinib (Figure 3.14B). The anti-c-Mpl antibody had some effect on aggregation, in some donors blocking completely (Figure 3.14Ci), but did not significantly block the potentiation of CRP by PF4 (Figure 3.14Cii).

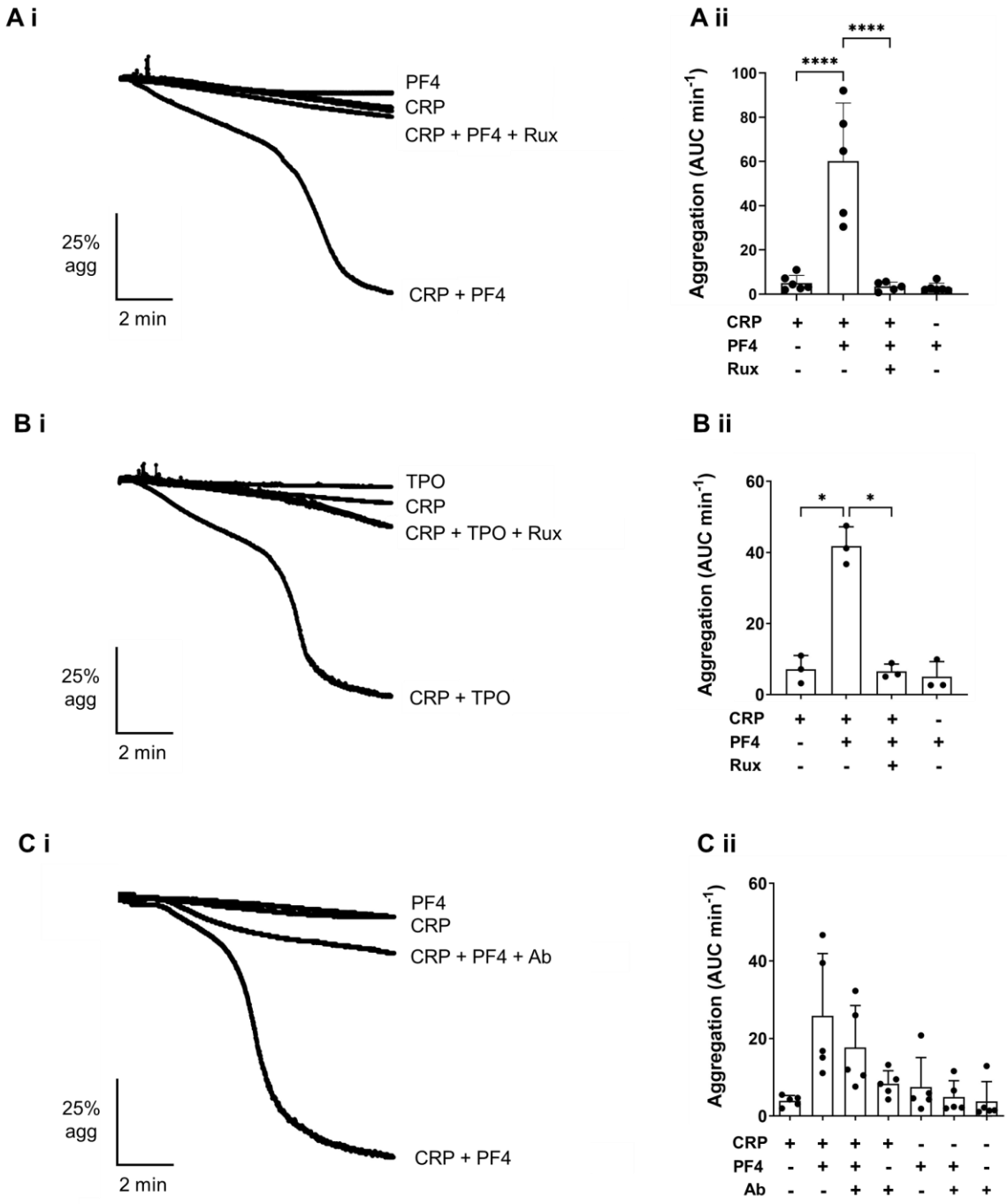

Figure 3.14. Ruxolitinib blocks PF4 and TPO-mediated potentiation of platelet aggregation to subthreshold concentration of CRP.

Adapted from (Buka et al., 2024). (A) Platelet activation was assessed by LTA. Pre-warmed platelets (2×10^8/mL) at 37°C were incubated with ruxolitinib 100 nM (Rux) for 5 min, PF4 for 5 min, then stirred at 1200 rpm for 1 min before addition of CRP 0.03 µg/mL. (Ai) Representative aggregation traces. (Aii) Quantification of aggregation (area under curve per minute [AUC min^{-1}] for 10 min, n=5). Statistical testing of differences by one-way ANOVA. (B) As for A but TPO 10 ng/mL added instead of PF4. (C) As for A but anti-c-Mpl antibody 10 µg/mL (Ab) added instead of Rux. *P < .05, ****P < .0001

3.3.6. Inhibitors of PI3K, STAT3/5 and mTOR have variable effects on platelet aggregation to PF4 and TPO

The following sections further investigate the signalling pathways downstream of PF4 and TPO-induced platelet activation. The possible signalling pathways investigated in the following experiments are summarised in Figure 3.15 along with the targets of the various inhibitors that are used.

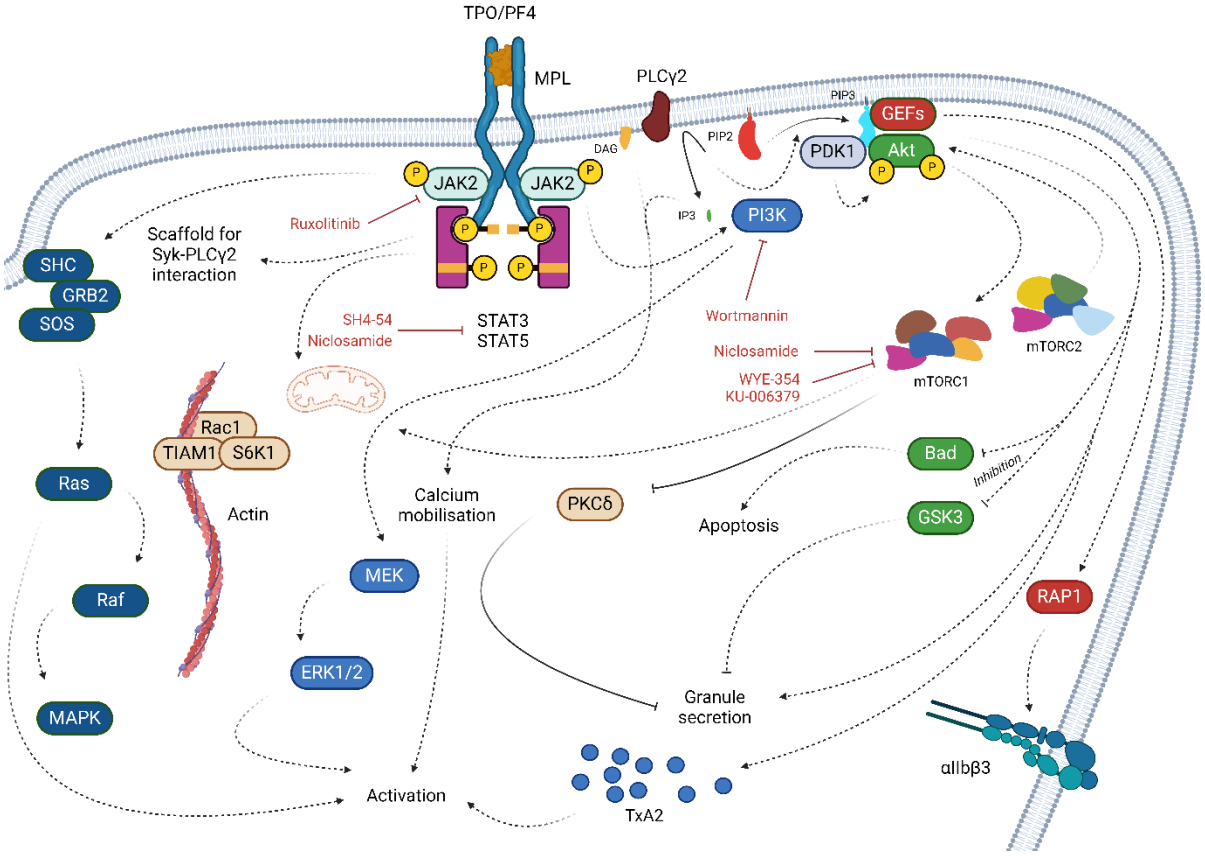

Figure 3.15. Receptors, signalling molecules, pathways, and inhibitors that may be involved in signalling downstream of PF4- and TPO-c-Mpl binding.

Bad: Bcl-2-associated agonist of cell death; ERK1/2: extracellular signal-regulated kinases 1 and 2; GSK3: glycogen synthase kinase 3; GRB2: growth factor receptor-bound protein 2; JAK2: Janus kinase 2; MAPK: mitogen-activated protein kinase; MEK: mitogen-activated protein kinase kinase; mTORC1/2: mammalian target of rapamycin complex 1/2 PDK1: phosphoinositide-dependent kinase 1; PF4: platelet factor 4; PI3K: phosphoinositide 3-kinase; PKCδ: protein kinase C delta; PLCγ2: phosphatidylinositol-4,5-bisphosphate phosphodiesterase gamma-2; Rac1: ras-related C3 botulinum toxin substrate 1; Raf: rapidly accelerated fibrosarcoma kinase; Rap1: ras-related protein 1; Ras: rat sarcoma virus oncogene; SHC: Src homology 2 domain containing protein; S6K1: ribosomal protein S6 kinase beta-1; SOS: son of sevenless; STAT3/5: signal transducer and activator of transcription 3/5; Tiam1: T-cell lymphoma invasion and metastasis 1; TPO: thrombopoietin TxA2: thromboxane A2.

STAT3 and STAT5 are transcription factors that mediate the downstream effects of c-Mpl stimulation by TPO in megakaryocytes by dimerising and translocating to the nucleus where they act to drive megakaryocytic transcriptional programming (Bacon et al., 1995; Hitchcock et al., 2021). Thus, as transcription factors, one may hypothesise that they do not have a role in platelet activation and that their observed phosphorylation downstream of c-Mpl and JAK2 is merely a bystander effect. However, STAT3 has been shown to regulate collagen-induced platelet activation where it serves as a so-called protein scaffold to facilitate the catalytic interaction between Syk and PLCγ2 (Zhou et al., 2013). Still, as PF4-mediated platelet activation does not appear to involve Syk (as shown by lack of blocking activity by PRT-060318), the question remains as to whether STAT3 and or STAT5a/b may have an additional role. Secondly, there is also evidence that after TPO-mediated activation, STAT3 can bind to the regulatory D-loop of mitochondrial DNA in platelets (Vassilev et al., 2002) demonstrating an additional possible mechanism.

3.3.6.1. Inhibitors of STAT3 and STAT5

The LTA experiments in this section were performed by final year BMedSc student, Mitchell Hall, under my supervision.

Four inhibitors of STAT3 and/or STAT5 were selected based on reported selectivity and potency (Schust et al., 2006; Müller et al., 2008; Yin et al., 2023; Ren et al., 2010) (Table 3.2, page 130). High concentrations of Stattic 10 µM (a selective STAT3 inhibitor) and “STAT5 inhibitor” 100 µM (a selective STAT5 inhibitor) did not block aggregation to PF4 50 µg/mL (Figure 3.16A). The combined STAT3 and STAT5 inhibitor SH4-54 blocked at 10 µM (Figure 3.16B) and niclosamide, a STAT3 inhibitor, blocked at 1 µM. Both SH4-54 and niclosamide inhibited the second wave of aggregation but not the first (Figure 3.16Bi and Figure 3.16Ci).

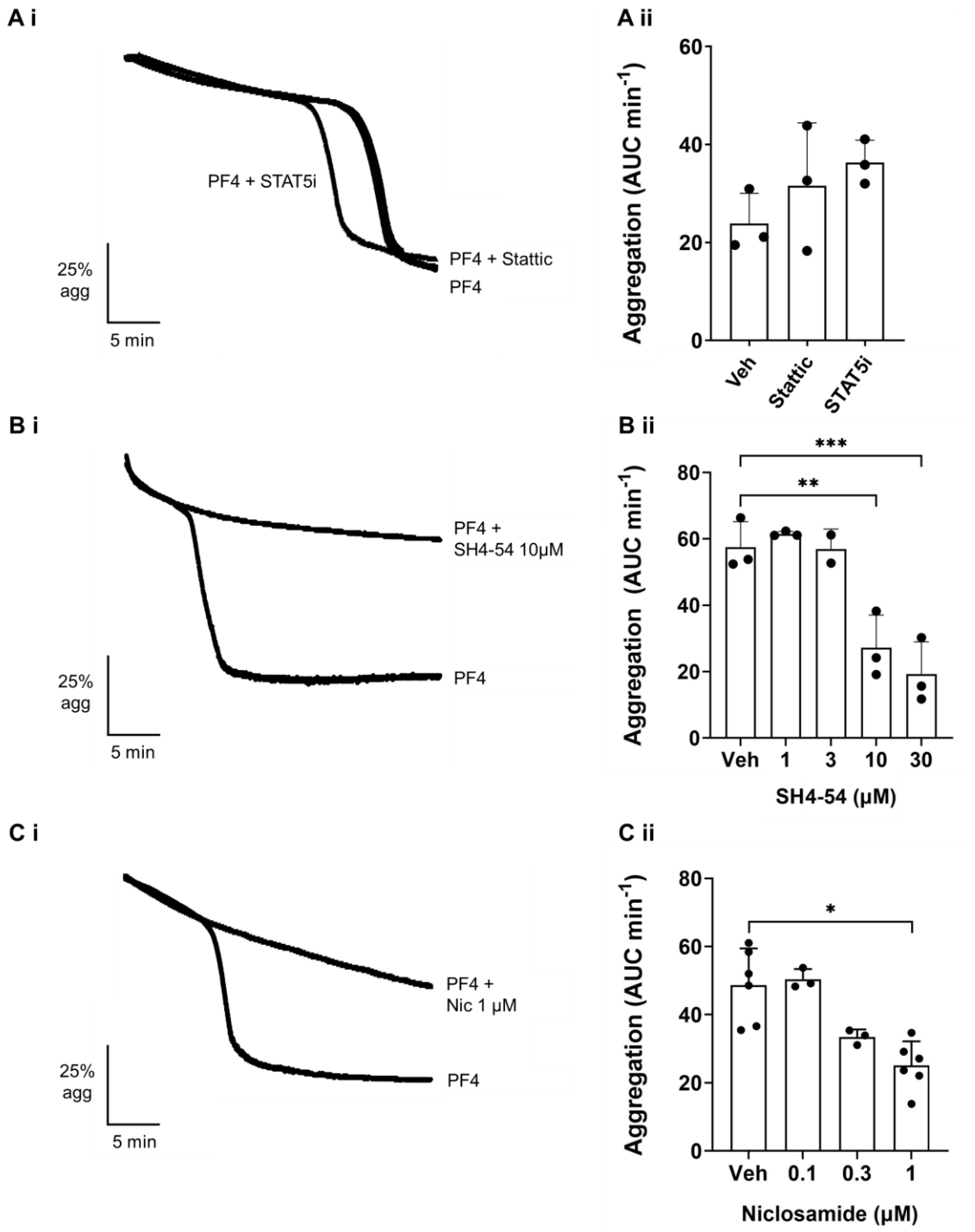

Figure 3.16. Effect of STAT3 and STAT5a/b inhibitors on PF4-induced platelet aggregation.

(A) Pre-warmed platelets (2×10^8/mL) at 37°C were incubated with stattic 10 μM, STAT5 inhibitor 100 μM (STAT5i) or vehicle control (DMSO 0.01%) (Veh) for 5 min, then stirred at 1200 rpm for 1 min before addition of PF4 50 μg/mL. (Ai) Representative aggregation traces. (Aii) Quantification of aggregation (area under curve per minute [AUC min^{-1}] for 30 min, n=3). Statistical testing of differences by one-way ANOVA. (B) As for A but SH4-54 1-30 μM used instead of stattic or STAT5i. (C) As for B but niclosamide 0.1-1 μM (Nic) used instead of SH4-54 and n=3-6. *P < .05, **P < .01, ***P < .001.

3.3.6.2. Inhibition of mammalian target of rapamycin (mTOR)

As niclosamide was the only inhibitor to block PF4-mediated aggregation at a low concentration (≤1 μM), the mechanism was investigated further. As well as inhibiting STAT3, niclosamide is also reported to be an inhibitor of mammalian target of rapamycin (mTOR). mTOR is a kinase that forms two different complexes, mTORC1 and mTORC2 which are distinguished by unique associated proteins, Raptor and Rictor (Kim et al., 2017). Both complexes are present in platelets and roles in platelet activation, spreading, and the maintenance of stable platelet aggregate formation under flow have been described (Aslan et al., 2011). Two inhibitors of mTOR, KU-0063794 and WYE-354 were selected as unlike the clinically used drug, rapamycin, which only blocks the activity of mTORC1, they inhibit both mTORC1 and mTORC2 (García-Martínez et al., 2009; Yu et al., 2009). Further, in a previous study, both inhibited aggregation in apyrase-treated platelets at 10 μM concentration (Aslan et al., 2011; Yu et al., 2009).

Neither WYE-354 nor KU-0063794 significantly blocked platelet aggregation to PF4, although there was some evidence of a dose-dependent effect of WYE-354 peaking at 10 μM but then rebounding at 30 μM (Figure 3.17Aii). KU-0063794 did appear to have some effect in one donor which peaked at 30 μM (Figure 3.17Bi) but no consistent blockade was seen (Figure 3.17Bii)

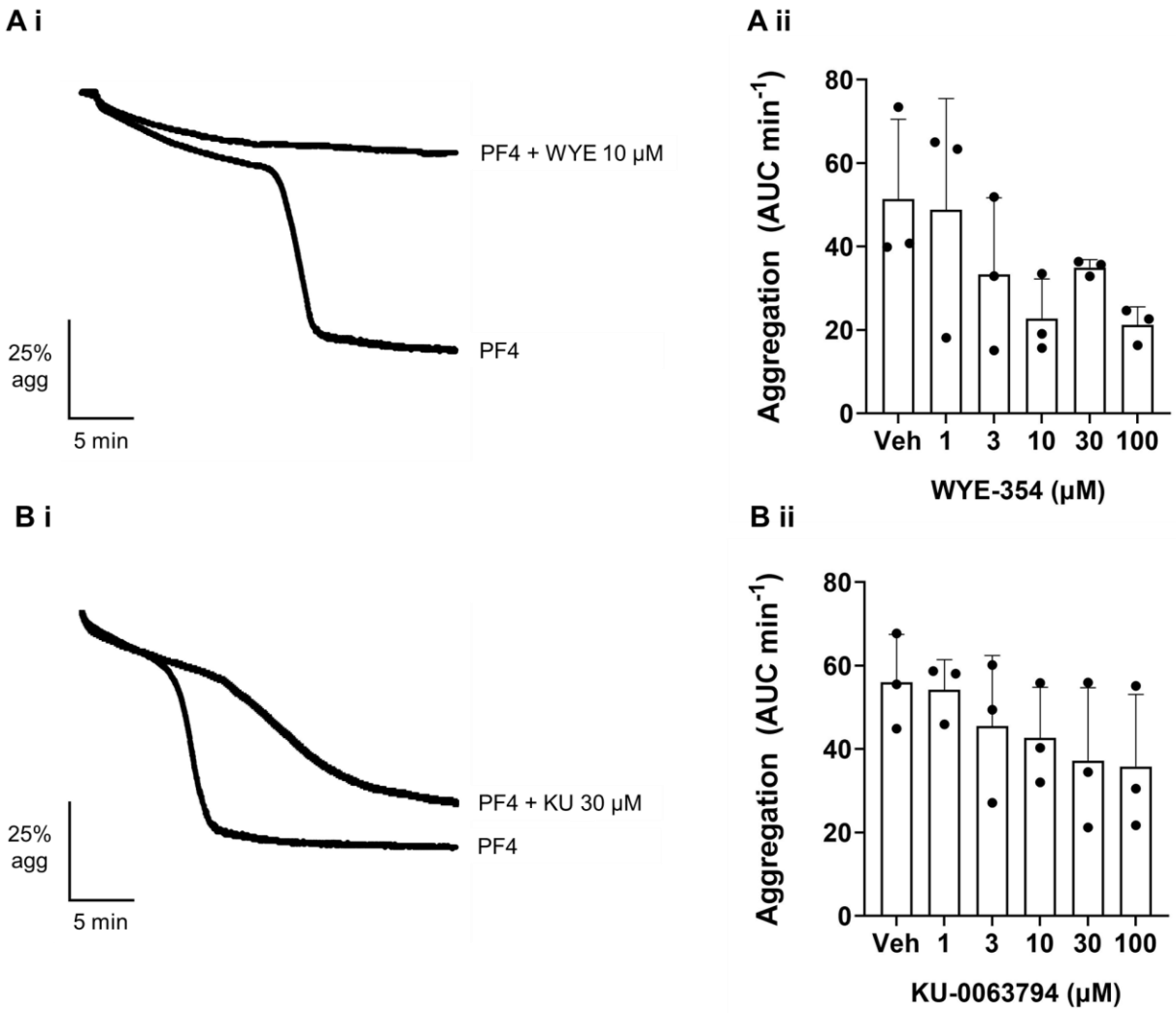

Figure 3.17. Effects of mTOR inhibitors on PF4-induced platelet aggregation.

(A) Pre-warmed platelets (2×10^8/mL) at 37°C were incubated with WYE-354 1-100 µM (WYE) or vehicle control (DMSO 0.01%) (Veh) for 5 min, then stirred at 1200 rpm for 1 min before addition of PF4 50 µg/mL. (Ai) Representative aggregation traces. (Aii) Quantification of aggregation (area under curve per minute [AUC min^{-1}] for 30 min, n=3). Statistical testing of differences by one-way ANOVA. (B) As for A but KU-0063794 1-100 µM used instead of WYE.

Next, the effects of niclosamide, SH4-54, WYE-354 and KU-0063794 on TPO-mediated aggregation were assessed. The concentrations selected were those that had been observed to have an effect on PF4-mediated aggregation. Figure 3.18A shows that only niclosamide blocked TPO-mediated aggregation although there were some reductions in aggregation due to a delayed second phase observed with the other inhibitors, particularly WYE-354. However, if these are true effects the relatively high concentrations of ≥10 µM may indicate off-target

activity. However, all four inhibitors had no effect on CRP-mediated aggregation (Figure 3.18B).

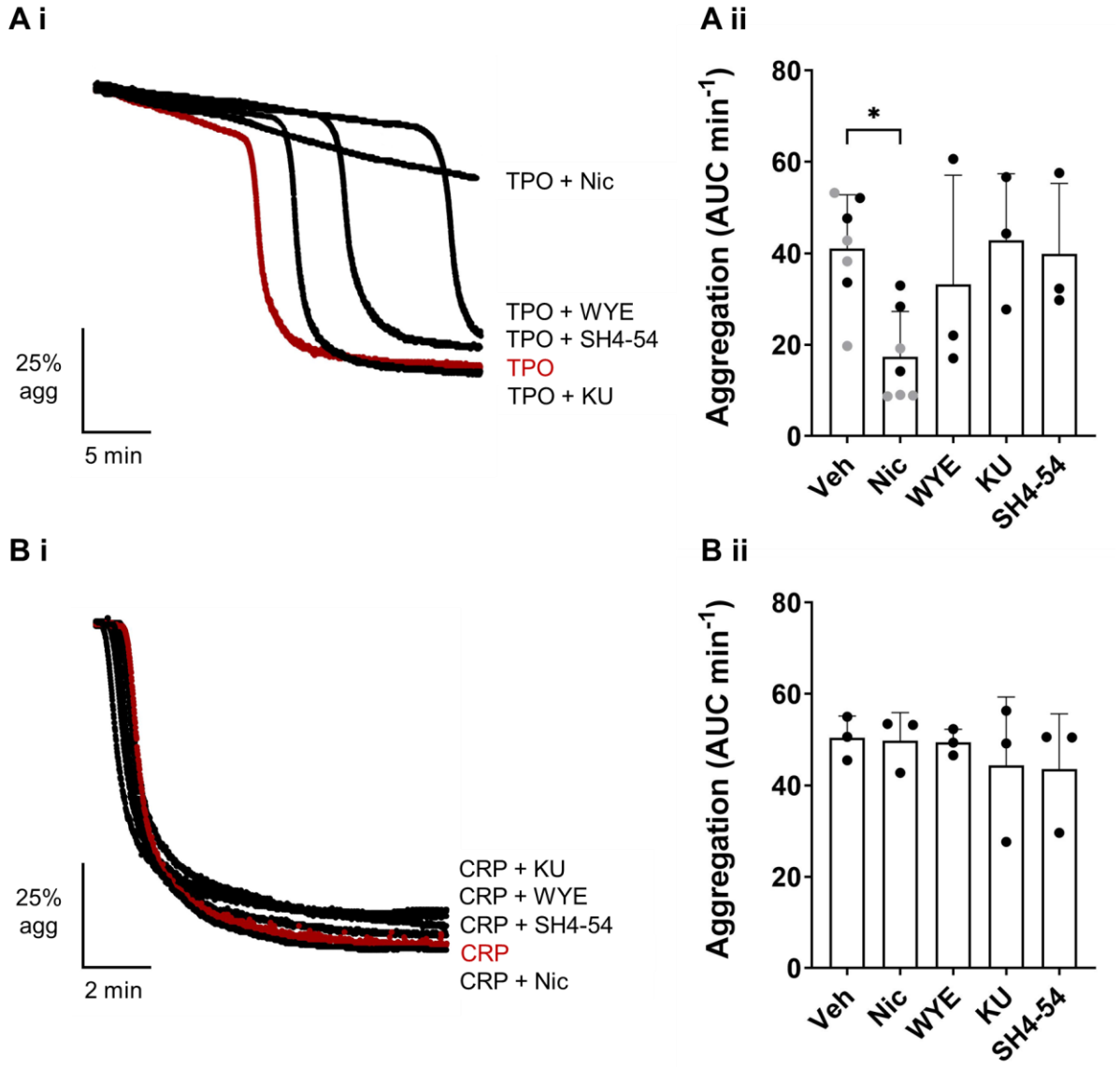

Figure 3.18. Effects of STAT3, STAT5, and mTOR inhibitors on TPO- and CRP-mediated platelet aggregation.

(A) Pre-warmed platelets (2×10^8/mL) at 37°C were incubated with niclosamide 1 µM (Nic), WYE-354 10 µM (WYE), or KU-0063794 30 µM (KU), SH4-54 10 µM, or vehicle control (DMSO 0.01%) (Veh) for 5 min, then stirred at 1200 rpm for 1 min before addition of TPO 100 ng/mL. (Ai) Representative aggregation traces. (Aii) Quantification of aggregation (area under curve per minute [AUC min^{-1}] for 30 min, n=3-7), grey circles represent additional donors for Nic. Statistical testing of differences by one-way ANOVA. (B) As for A but CRP 1 µg/mL added instead of TPO and aggregation measured for 10 min, n=3.

Finally, the role of the PI3K pathway was investigated as it has previously been shown to be essential in mediating the priming effect of TPO on platelets (Moore et al., 2019). PI3Ks are a family of enzymes that phosphorylate phosphoinositide lipids on the intracellular surface of the plasma membrane. In platelets, class I PI3Ks phosphorylate phosphatidylinositol 4,5-bisphosphate (PIP2) to produce phosphatidylinositol 3,4,5-trisphosphate (PIP3). AKT (protein kinase B) then binds to PIP3 and is phosphorylated by phosphoinositide-dependent kinase 1 (PDK1) and mTORC2 (Figure 3.15). As such, the effect of the pan-PI3K inhibitor, wortmannin, on platelet aggregation to PF4 was assessed. Wortmannin 100 nM, which is an established inhibitor concentration in platelets (Moore et al., 2019) blocked both the first and second wave of aggregation (Figure 3.19).

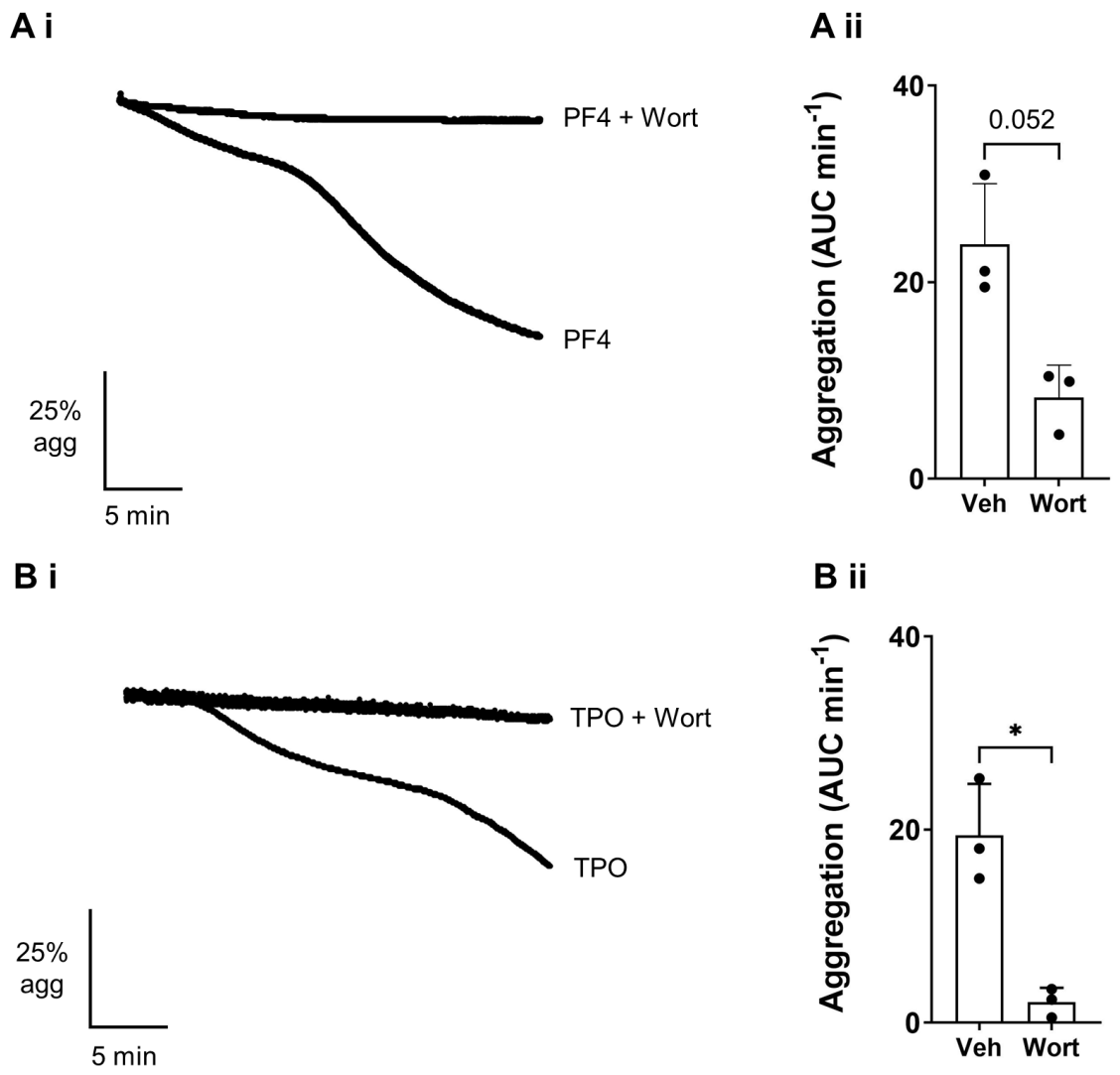

Figure 3.19. Wortmannin blocks platelet aggregation to PF4 and TPO.

(A) Pre-warmed platelets (2×10^8/mL) at 37°C were incubated wortmannin 100 nM (Wort), or vehicle control (DMSO 0.01%) (Veh) for 5 min, then stirred at 1200 rpm for 1 min before addition of PF4 50 µg/mL. (Ai) Representative aggregation traces. (Aii) Quantification of aggregation (area under curve per minute [AUC min^{-1}] for 30 min, n=3). Statistical testing of difference by paired t-test. (B) As for A but TPO 100 ng/mL added instead of PF4. *P < .05.

3.3.7. Inhibitors of PI3K, STAT3/5 and mTOR have variable effects on P-selectin expression and integrin $\alpha_{IIb}\beta_3$ activation in response to PF4 and TPO stimulation

To further investigate the effect of these inhibitors on platelet activation to PF4 and TPO, flow cytometry experiments were performed. After pre-incubation with concentrations of inhibitors that blocked platelet aggregation in the above experiments (or where there was a trend towards blockade), washed platelets were stimulated with PF4 50 µg/mL and TPO 100 ng/mL for 45 min before being analysed by flow cytometry for P-selectin and activated integrin $\alpha_{IIb}\beta_3$. 45 min was chosen as a time point to ensure maximal and stable expression of these p-selectin thus minimising variability. Figure 3.20 shows change in percentage positive cells relative to vehicle control although statistical analyses were performed on the raw percentage positive data. For each activation marker, for both PF4 and TPO, the results in Figure 3.20 are displayed separately for ruxolitinib, wortmannin, and niclosamide compared to the other inhibitors. This is because seven donors were used for these inhibitors (which significantly blocked aggregation at concentrations ≤ 1 µg/mL) compared to three for the other inhibitors and as the data did not pass normality testing for all the conditions, a non-parametric test of significance of difference was required, which cannot handle missing data.

For PF4, in some donors, there were notable, but not statistically significant reductions in P-selectin expression with ruxolitinib and wortmannin although the magnitude of reduction with wortmannin was greater than that for ruxolitinib (Figure 3.20Ai). Additionally, WYE-354 appeared to reduce P-selectin expression in 2/3 donors (Figure 3.20Aii). Dasatinib did however significantly reduce P-selectin expression to PF4. Similar findings were observed with flow cytometry for integrin $\alpha_{IIb}\beta_3$ activation and the reduction with wortmannin was statistically significant (Figure 3.20Bi). Surprisingly, although niclosamide reduced integrin $\alpha_{IIb}\beta_3$ activation (Figure 3.20Bi), consistent with the aggregometry data, it appeared to enhance P-selectin expression (Figure 3.20Ai). With TPO 100 ng/mL, the magnitude of P-selectin expression was lower than that for PF4 50 µg/mL but even so, the effects of the inhibitors mirrored those for PF4 (Figure 3.20C and Figure 3.20D). Wortmannin significantly reduced P-

selectin expression and both wortmannin and ruxolitinib significantly reduced integrin $\alpha_{IIb}\beta_3$ activation (Figure 3.20Ci and Figure 3.20Cii). Once again, niclosamide enhanced P-selectin expression (Figure 3.20Ci) but reduced integrin $\alpha_{IIb}\beta_3$ activation (Figure 3.20Di). Thus, although ruxolitinib completely abrogates platelet aggregation to PF4, the above experiments show only an incomplete (and statistically non-significant) effect on α-granule release and integrin activation. The effect of wortmannin is similarly non-significant (although more pronounced) for p-selectin expression but is significant for integrin activation. This perhaps suggests an additional mechanism of PF4-induced α-granule release.

PF4: P-selectin

A i

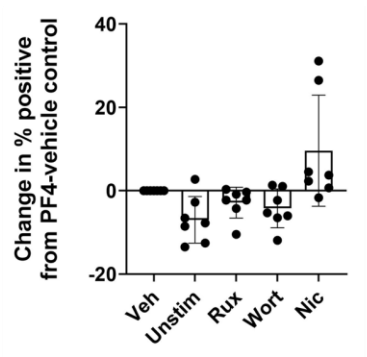

A ii

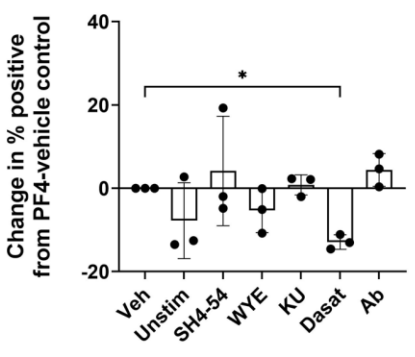

PF4: activated integrin $\alpha_{IIb}\beta_3$

B i

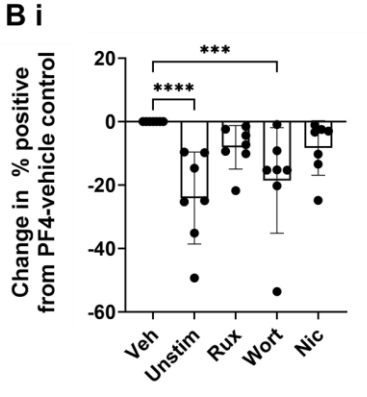

B ii

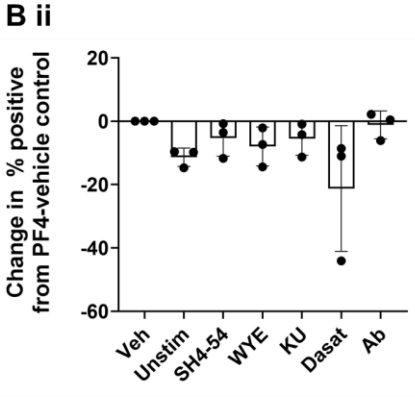

TPO: P-selectin

C i

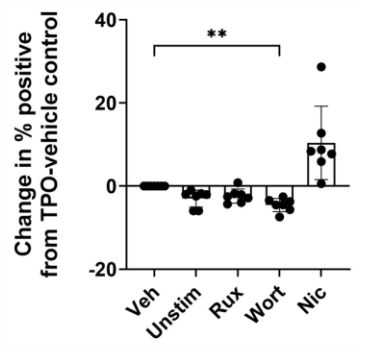

C ii

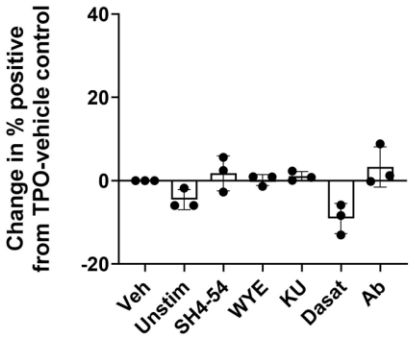

TPO: activated integrin $\alpha_{IIb}\beta_3$

D i

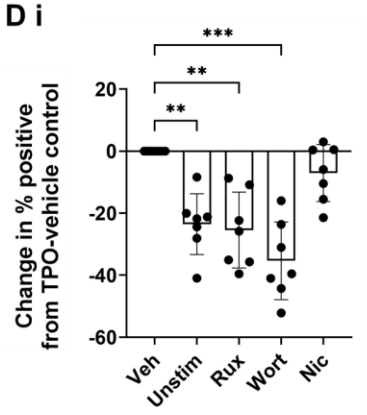

D ii

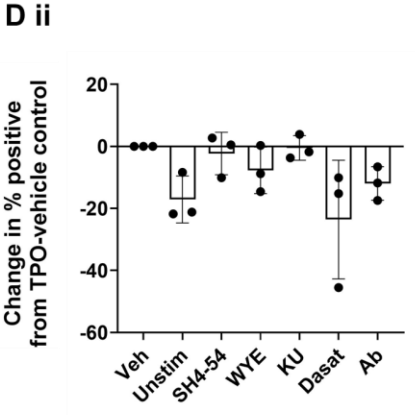

Figure 3.20. Effect of inhibitors on PF4 and TPO-mediated P-selectin expression and integrin $\alpha_{IIb}\beta_3$ activation as measured by flow cytometry.

50 µL platelets (2×10^8/mL) were incubated with ruxolitinib 100 nM (Rux), wortmannin 100 nM (Wort), niclosamide 1 µM (Nic), SH4-54 10 µM, WYE-354 10 µM (WYE), KU-0063794 10 µM (KU) dasatinib 1 µM (Dasat), anti-c-mpl antibody 10 µg/mL (Ab) or vehicle control (DMSO 0.01%) (Veh) for 5 min. Platelets were then stimulated with PF4 50 µg/mL or TPO 100 ng/mL for 45 min at RT after which 50 µL PBS containing anti-P-selectin antibody and PAC-1 antibody (for activated integrin $\alpha_{IIb}\beta_3$), or isotype controls were added for 20 min at RT. 200 µL PBS was then added and platelets analysed by flow cytometry. Percentage positive cells were calculated according to the relevant isotype control and data transformed to show change in percentage positive cells from PF4 + vehicle or TPO + vehicle controls. (A) PF4-induced P-selectin expression. (A i) Effect of Rux, Wort, and Nic (n=7). Statistical testing of difference by Friedman test. (B i) Effect of SH4-54, WYE, KU, Dasat, and Ab (n=3). Statistical testing of difference by one-way ANOVA. (B) As for A, but platelets stained for activated integrin $\alpha_{IIb}\beta_3$. (C) As for A but platelets stimulated with TPO. (D) As for B but platelets stained for activated integrin $\alpha_{IIb}\beta_3$.

3.3.8. Ruxolitinib, wortmannin, dasatinib, and anti-c-Mpl antibody but not niclosamide, block platelet spreading on PF4

The previous data has shown PF4's effect on two facets of platelet activation, namely the ability to induce aggregation, integrin activation, and α-granule release. Cytoskeletal reorganisation, as measured by microscopy for platelet spreading is another component of platelet activation and the ability of PF4 to induce this has not been investigated. First, a dose response using coverslips coated with PF4 10, 50, and 100 µg/mL was performed in three donors who were previously known to have responded to PF4 50 µg/mL in LTA. This showed that at 10 µg/mL, there was platelet adherence in all 3 donors and spreading in 2 donors. In contrast to LTA and flow cytometry, the spreading response was maximal at 10 µg/mL (Figure 3.21A) which is explained as reagents in coating solution settle and concentrate onto a surface. This reflects the expected biology of PF4 where it binds to cellular surfaces, concentrating it at the site of receptor interactions. Compared to collagen, which was used as a positive control, fewer platelets adhered and spread on PF4-coated coverslips, and of those that did, spreading was less pronounced and maximal at 10 µg/mL. Platelets did not spread on coverslips coated with TPO 10, 50, or 100 ng/mL (Figure 3.21B). A possible reason for platelet spreading on PF4 and not TPO is that PF4 would be expected to bind to platelet surface GAGs through charge interactions, thus aiding recruitment of platelets. Of course, platelets may not be spreading *on* PF4 but may be becoming activated by PF4 and then spreading.

Pre-treatment of platelets with ruxolitinib, wortmannin, dasatinib, and the anti-c-Mpl antibody reduced platelet spreading on PF4 10 µg/mL although these differences were not statistically significant (Figure 3.22B). In two donors, niclosamide enhanced spreading, similar to the effects on P-selectin expression. Again, collagen was used as a positive control.

The results of the effects of the various inhibitors on platelet aggregation, P-selectin expression, integrin $\alpha_{IIb}\beta_3$ activation and spreading are summarised in Table 3.2.

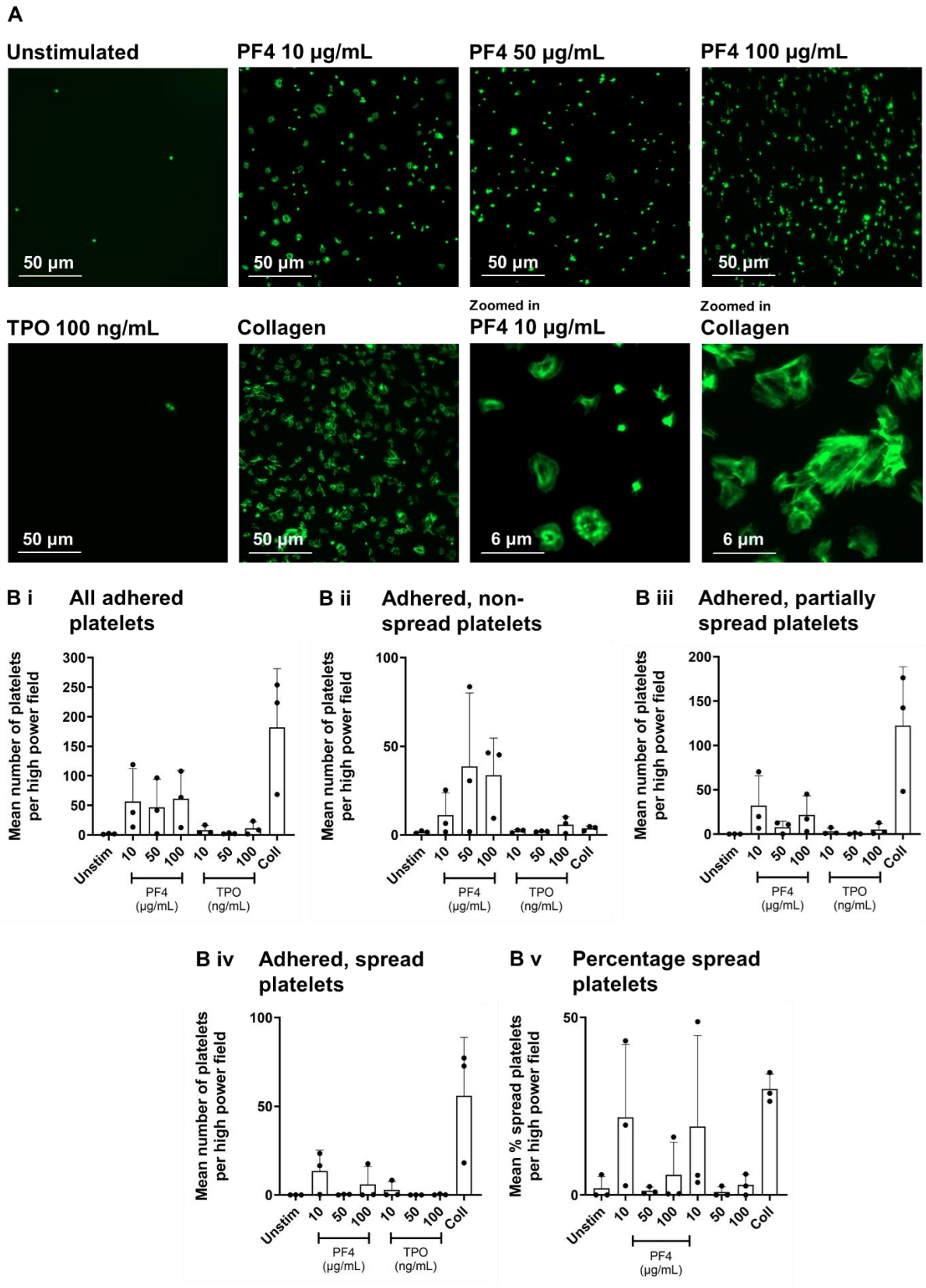
A
Unstimulated
PF4 10 µg/mL
PF4 50 µg/mL
PF4 100 µg/mL
50 µm
TPO 100 ng/mL
Collagen
Zoomed in
PF4 10 µg/mL
Zoomed in
Collagen
6 µm
B i
All adhered platelets
B ii
Adhered, non-spread platelets
B iii
Adhered, partially spread platelets
Mean number of platelets per high power field
Unstim
Coll
PF4 (µg/mL)
TPO (ng/mL)
B iv
Adhered, spread platelets
B v
Percentage spread platelets
Mean % spread platelets per high power field

Figure 3.21. Platelets spread on PF4-coated glass coverslips.

Glass coverslips in wells of a 24-well plate were coated with PF4 10-100 µg/mL, TPO 10-100 ng/mL, or collagen 50 µg/mL (Coll). Platelets (2×10^7/mL) were added and incubated for 45 min at 37°C after which they were washed with PBS, fixed, stained with FITC-conjugated phalloidin, and imaged by epifluorescent microscopy. Number of adhered, partially spread, and fully spread platelets were counted. (A) Representative images of platelet spreading on PF4 10-100 µg/mL, TPO 100 ng/mL, or Coll (B) Quantification of (Bi) adhered, (Bii) non-spread, (Biii) partially spread, (Biv) spread, and (Bv) percentage spread platelets (of all adhered platelets).

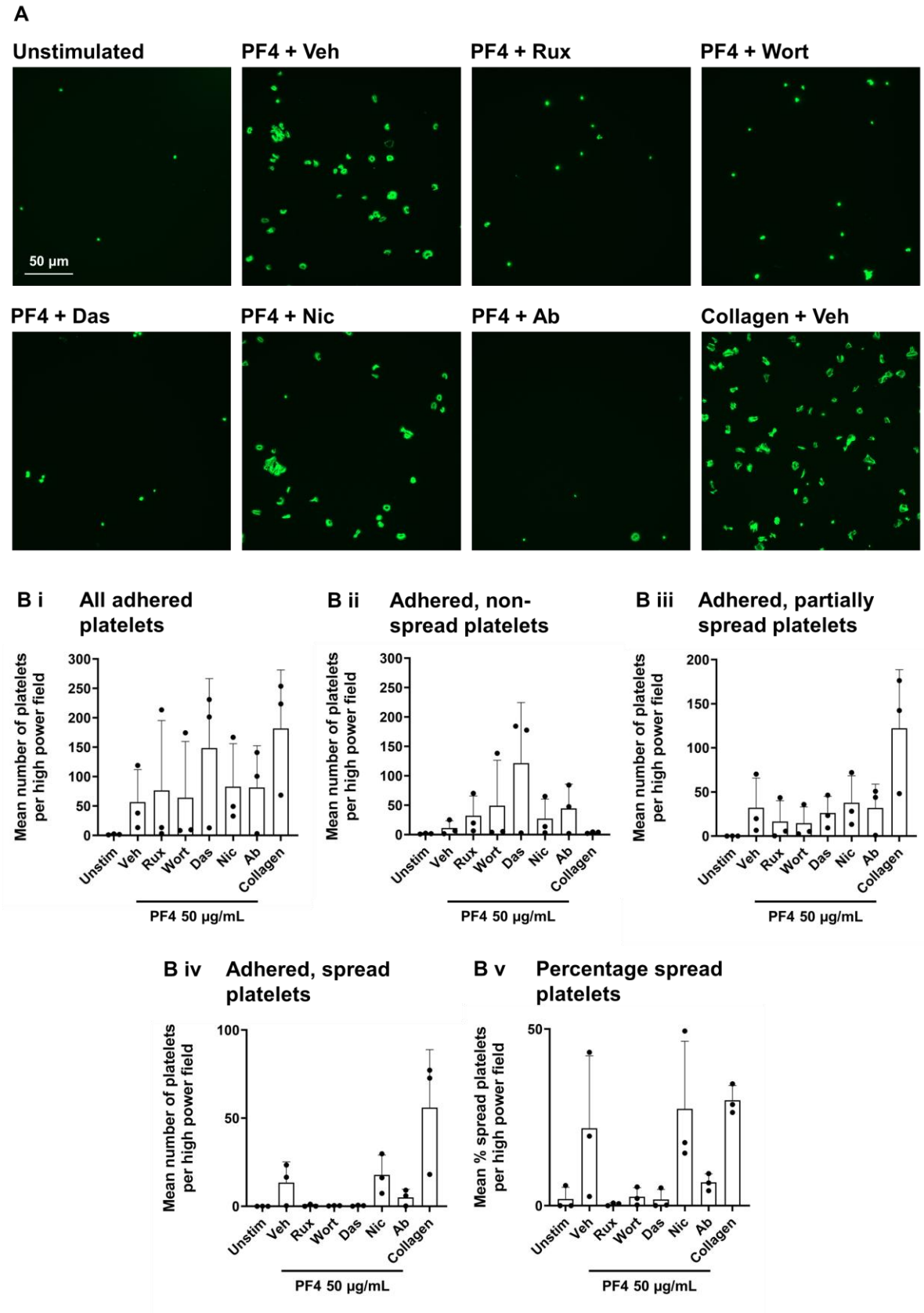
A
Unstimulated
PF4 + Veh
PF4 + Rux
PF4 + Wort
50 µm
PF4 + Das
PF4 + Nic
PF4 + Ab
Collagen + Veh
B i
All adhered platelets
B ii
Adhered, non-spread platelets
B iii
Adhered, partially spread platelets
Mean number of platelets per high power field
Unstim
Veh
Rux
Wort
Das
Nic
Ab
Collagen
PF4 50 µg/mL
B iv
Adhered, spread platelets
B v
Percentage spread platelets
Mean % spread platelets per high power field

Figure 3.22. Effects of inhibitors on platelet spreading on PF4-coated glass coverslips.

Glass coverslips in wells of a 24-well plate were coated with PF4 10 µg/mL or collagen 50 µg/mL) as a positive control. Platelets (2×10^7/mL) were incubated for 5 min with ruxolitinib 100 nM (Rux), wortmannin 100 nM (Wort), dasatinib 1 µM (Das), niclosamide 1 µM (Nic), anti-c-mpl antibody 10 µg/mL (Ab) or vehicle control (Veh, DMSO 0.01%). Then, platelets were added to the wells and incubated for 45 min at 37°C after which they were washed with PBS, fixed, stained with FITC-conjugated phalloidin, and imaged by epifluorescent microscopy. Number of adhered, partially spread, and fully spread platelets were counted. (A) Representative images of platelet spreading on PF4 with inhibitors as labelled or collagen. (B) Quantification of (Bi) adhered, (Bii) non-spread, (Biii) partially spread, (Biv) spread, and (Bv) percentage spread platelets (of all adhered platelets) as mean numbers of 20 high powered (x63) fields. Statistical testing of differences by one-way ANOVA. N=3 healthy donors.

Table 3.2. Effects of inhibitors of JAK2, PI3K, STAT3/5, mTOR, Src and anti-c-Mpl antibody on aggregation, P-selectin and activated αIIbβ3-integrin expression, and platelet spreading.

↓ significant inhibition, ↘ non-significant reduction suggestive of inhibition, ↔ no effect, ↗ non-significant increase suggestive of enhancement, ↑ significant enhancement. *Blocks PF4 10 µg/mL at antibody concentration of 10 µg/mL. ND: not done. ATP: adenosine triphosphate c-Mpl: cellular myeloproliferative leukemia protein, JAK1: Janus kinase 1, JAK2: Janus kinase 2, mTOR: mechanistic target of rapamycin, mTORC1: mechanistic target of rapamycin complex 1, mTORC2: mechanistic target of rapamycin complex 2, PF4: platelet factor 4, PI3K: phosphoinositide 3-kinase, SH2: src homology 2, STAT3: signal transducer and activator of transcription 3, STAT5: signal transducer and activator of transcription 5, TPO: thrombopoietin.

Inhibitor	Target	Mechanism of action	Inhibitor concentration	Aggregation		P-selectin expression		Activated integrin $\alpha_{IIb}\beta_3$		Spreading	
				PF4	TPO	PF4	TPO	PF4	TPO	PF4	TPO
c-Mpl antibody	c-Mpl	Polyclonal antibody (Thermo Fisher Scientific, n.d.)	10 µg/mL	↓*	↘	↔	↔	↔	↓	↘	NA
Dasatinib	Src	Blocks ATP binding site, thus kinase activity (Olivieri A and Manzione L, 2007)	1 µM	↔	NA	↓	↓	↘	↘	↘	NA
KU-0063794	mTOR	Blocks kinase activity of mTORC1 and mTORC2, suppressing Akt activation (García-Martínez et al., 2009)	30 µM	↔	↔	↔	↔	↔	↔	NA	NA
Niclosamide	STAT3 mTOR	Inhibits phosphorylation and nuclear translocation, independent of SH2 domain (Ren et al., 2010) Acidification of cytoplasm leading to selective mTORC1 inhibition (Fonseca et al., 2012)	1 µM	↓	↓	↗	↑	↘	↘	↑	NA
Ruxolitinib	JAK1 JAK2	Blocks ATP binding site, thus kinase activity (Zhou et al., 2014b)	100 nM	↓	↓	↘	↘	↘	↓	↘	NA
SH4-54	STAT3 STAT5	Targets SH2 domain, inhibiting activation and dimerisation (Ali et al., 2016)	10 µM	↓	↔	↔	↔	↔	↔	NA	NA
STAT5 inhibitor	STAT5	Targets SH2 domain, inhibiting activation and dimerisation (Müller et al., 2008)	100 µM	↔	NA	NA	NA	NA	NA	NA	NA

Stattic	STAT3	Targets SH2 domain, inhibiting activation, dimerisation, and nuclear translocation (Schust et al., 2006)	10 µM	↔	NA	NA	NA	NA	NA	NA	NA
Wortmannin	PI3K	Blocks ATP binding site, thus kinase activity (Wymann et al., 1996)	100 nM	↓	↓	↘	↓	↘	↓	↘	NA
WYE-354	mTOR	Blocks ATP-binding site thus kinase activity of mTORC1 and mTORC2 (Yu et al., 2009)	10 µM	↘	↔	↔	↔	↔	↔	NA	NA

.

3.3.9. PF4 partially blocks TPO binding to c-Mpl

PF4 is a known inhibitor of megakaryopoiesis, and a previous study reported that the effected is mediated through binding to LRP1 on megakaryocytes (Lambert et al., 2009). However, this protein is only expressed briefly in the latter stages of megakaryocyte differentiation (Lambert et al., 2009) and a signalling mechanism by which PF4 mediates its effects through the receptor has not been described. As it is now known that PF4 binds to c-Mpl, the key receptor through which TPO drives megakaryopoiesis, a clear question is whether PF4 can interfere with TPO binding to its receptor. The question is further complicated by the fact that both are agonists of c-Mpl in platelets.

First, the effect of combining TPO and PF4 were assessed using LTA. As expected, there was a small, non-significant additive effect leading to enhancement of platelet aggregation when platelets were pre-incubated with PF4 10 µg/mL prior to stimulation with TPO ng/mL (Figure 3.23A). A competitive binding ELISA was then performed; c-Mpl was bound to the plate and incubated with increasing concentrations of PF4 before addition of TPO. Figure 3.23B shows that TPO-c-Mpl binding was decreased with PF4 plateauing at 1 µg/mL producing a reduction to ~50% TPO binding. The binding ELISA experiments were performed by Dr Samantha Montague.

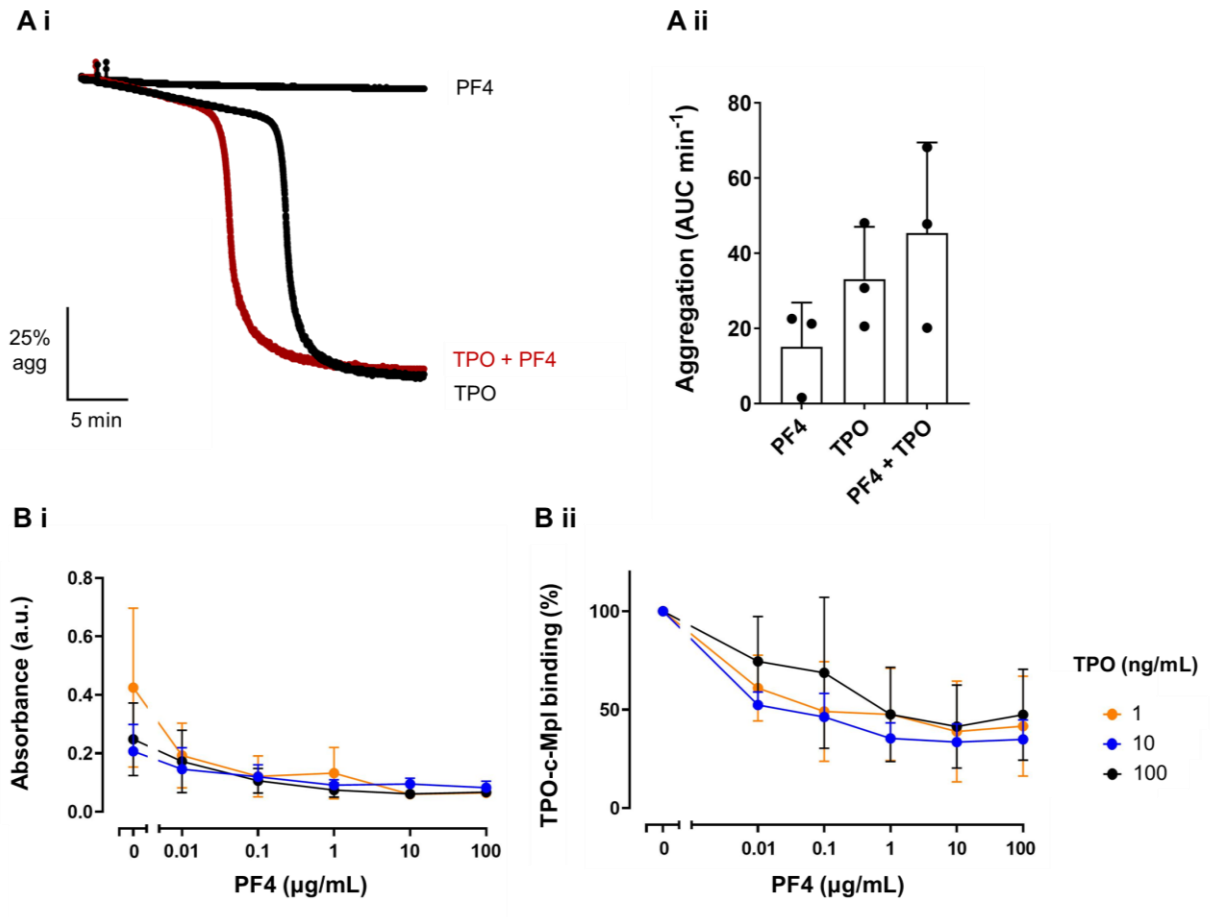

Figure 3.23. PF4 does not block TPO-induced platelet aggregation but partially blocks TPO binding in competitive binding ELISA.

Part B appears as a standalone figure in (Buka et al., 2024). (A) Pre-warmed platelets (2×10^8mL) at 37°C were incubated with PF4 10 µg/mL for 5 min or vehicle control (PBS) before stirring for 1 min followed by addition of TPO 100 ng/mL. (Ai) Representative aggregation traces; (Aii) Quantification of aggregation. (Aii) Quantification of aggregation (area under curve per minute [AUC min^{-1}] for 30 min, n=3). Statistical testing of difference by one-way ANOVA. (B) Competitive binding ELISA. Recombinant c-Mpl was coated onto an ELISA plate then incubated with increasing concentrations of PF4 (0.01 – 100 µg/mL) or vehicle control (PBS). Wells were then incubated with TPO (1, 10, or 100 ng/mL) followed by washing and then detection using an anti-TPO antibody and anti-rabbit secondary HRP. (Bi) Absorbance (a.u.) read at 450 nm; (Bii) % change in TPO-c-Mpl binding (n=3).

Finally, AlphaFold (Jumper et al., 2021) modelling of the binding of PF4 to c-Mpl was performed. The cryo-electron microscopy (EM) structure of TPO binding to dimeric c-Mpl was published in 2023 (Tsutsumi et al., 2023) and this structure (PDB: 8G04) was used to inform the modelling of PF4-c-Mpl. Figure 3.24A shows the cryo-EM structure of c-Mpl and TPO. The AlphaFold predicted structure of PF4 with dimeric c-Mpl (Figure 3.24B) is unlikely to be correct as PF4 is not folded correctly and appears to straddle the binding pocket of c-Mpl with its α-helices on the outside and the β-pleated sheets facing towards c-Mpl. Iterations where the PF4 tetramer was entered into AlphaFold as one molecule (rather than the monomer and telling AlphaFold that there should be four copies), did not change the outcome. Next, therefore, a predicted structure of PF4 binding to one c-Mpl monomer was generated and aligned to the known structure of the TPO-c-Mpl dimer complex but just showing one monomer (Figure 3.24C). In Figure 3.24D, the second c-Mpl monomer is overlaid showing impossible overlap between PF4 and the second monomer, indicating that this predicted structure is also not correct. Next, a predicted structure of a PF4 dimer binding to c-Mpl (Figure 3.24F) which showed high similarity to the AlphaFold predicted structure of c-Mpl-TPO (Figure 3.24E) was overlaid with the cryo-EM structure of c-Mpl-TPO (Figure 3.24A). The PF4 dimer was then replaced with the known crystal structure of PF4 (PDB: 1RHP (Zhang et al., 1994)) by aligning to the dimer (Figure 3.24G). This final model demonstrates PF4 protruding from the binding pocket and is somewhat consistent with the observation of blockade of TPO binding by PF4. Ultimately, formal structural and functional studies in megakaryocytes will be required to further investigate whether PF4 blocking of TPO binding to c-Mpl leads to functional effects in these cells.

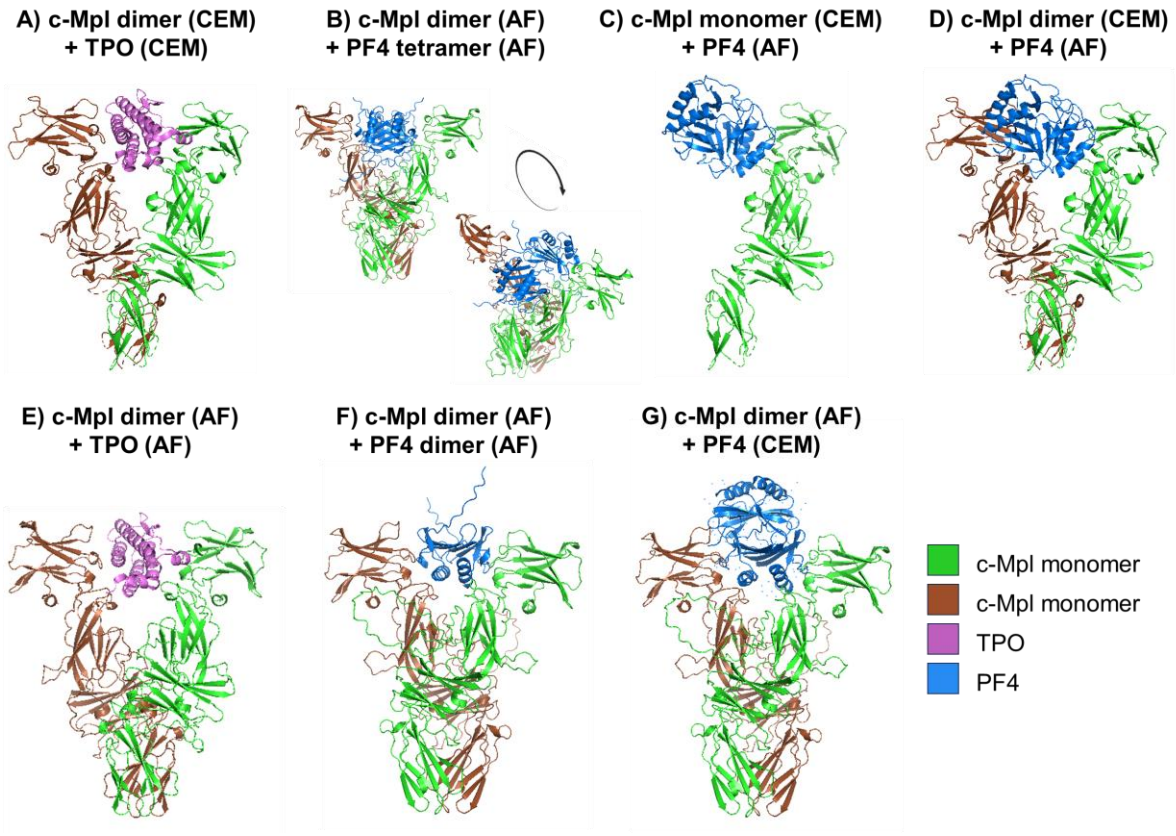

Figure 3.24. PF4 is not predicted to bind to c-Mpl in the same manner as TPO.

Cryo-electron microscopy (CEM) and AlphaFold (AF) predicted structures of PF4 (blue) or TPO (magenta) binding to c-Mpl (green and brown representing two monomers forming a dimer). (A) CEM structure of TPO binding to dimeric c-Mpl (PDB: 8G04). (B) A predicted binding of PF4 tetramer to c-Mpl dimer. (C) AF predicted binding of PF4 tetramer to one c-Mpl monomer aligned to CEM c-Mpl structure (inter-chain predicted template modelling score [ipTM]: 0.21, predicted template modelling score [pTM]: 0.5). (D) As for C but aligned to CE c-Mpl dimeric structure. (E) AF predicted structure of TPO binding to dimeric c-Mpl (ipTM 0.57, pTM 0.56). (F) AF predicted structure of PF4 dimer binding to and dimerising c-Mpl dimer (ipTM 0.49l pTM 0.6). (G) As for F but with PF4 dimer substituted for crystal structure of PF4 (PDB: 1RHP) aligned to the AF predicted structure of the PF4 dimer in F.

3.4. Discussion

The key findings in this chapter are:

1. PF4 induces platelet aggregation which is mediated through binding to c-Mpl and signalling through JAK2.
2. PF4-mediated platelet aggregation can be blocked by a c-Mpl blocking antibody, and inhibitors of JAK2, and PI3K.

3.4.1. PF4 activates platelets

These results show that PF4 can stimulate platelet aggregation across a concentration range of 10-100 µg/mL (1.28-12.8 µM), with a peak at 50 µg/mL. It does so through the TPO receptor, c-Mpl, with a K_D for this interaction of 744 nM - 200 times weaker than TPO.

The established function of c-Mpl on platelets is to act as a sink for TPO and negatively regulate platelet production (Hitchcock et al., 2021). TPO is produced constitutively in the liver and is the key hormone driving megakaryopoiesis and platelet production in the bone marrow (Hitchcock and Kaushansky, 2014). With more platelets in circulation, more TPO can be taken up by platelets, thus preventing it exerting effects in the bone marrow, and decreasing platelet production to maintain a steady state platelet count. However, it has been known for 30 years that TPO (≥5 ng/mL) potentiates platelet activation to low-dose agonists including thrombin, collagen, and ADP (Ezumi et al., 1995, 1999; Pasquet et al., 2000; Moore et al., 2019) with this priming occurring by signalling through PI3K (Moore et al., 2019). There are also reports that TPO at high doses (≥100 ng/mL) can induce platelet aggregation alone (Hitchcock and Kaushansky, 2014) but the above experiments show aggregation to TPO alone at concentrations as low as 30 ng/mL. This increased sensitivity may be due to the purity of the recombinant formulation that we have used and/or the washed platelet preparation technique. Nevertheless, these are still very high concentrations of TPO when viewed in the context of plasma levels of ~50 pg/mL (Makar et al., 2013). Even in severe disease states such as sepsis,

burns, and COVID-19, plasma TPO levels reach only as high as 400 pg/mL (Lupia et al., 2009, 2022), an order of magnitude lower than the at least 5 ng/mL required to prime platelets. Still, Lupia et al. showed that plasma from patients with unstable angina and COVID-19 had raised TPO levels, and that this plasma could enhance platelet aggregation to ADP and epinephrine in PRP even though levels of TPO in these samples were only 50-400 pg/mL (Lupia et al., 2006, 2022). Addition of soluble c-Mpl (in the form of a "TPOR-Fc chimera") blocked this enhancing effect leading to the conclusion that this was TPO-dependent. In fact, the observations in this chapter may provide an explanation for the paradox of such low plasma TPO levels resulting in priming that has not otherwise been shown at such low concentrations; unmeasured PF4 may be contributing to the platelet priming in these conditions. Given the blood concentrations of TPO, the physiological relevance of TPO-induced platelet priming is questionable and PF4-induced platelet priming is more plausible.

The data in this chapter show that PF4 can induce JAK/STAT phosphorylation at concentrations ≥3 µg/mL (0.38 µM) with functional effects seen at 10 µg/mL (1.28 µM). PF4 is present in plasma at low concentration but is greatly elevated in serum, reflecting its controlled release from platelets upon activation (Chesterman et al., 1978). Exactly how much PF4 is present in blood is a matter of debate as studies give wildly different values – from between 1 and 20,000 ng/mL in serum (Table 3.3); these different measurements clearly cannot all represent the truth. Mass spectrometry has shown that there are ~500,000 copies of PF4 per platelet (Burkhart et al., 2012; Huang et al., 2021), which, using a typical platelet count of 250 x 10^9/L works out as 1.6 µg per millilitre of whole blood (Figure 3.25). Thus, it is plausible that with a high availability of PF4 at sites of platelet activation and PF4 release, local concentrations would reach and exceed 10 µg/mL. PF4 had no effect on aggregation in PRP which likely indicates binding of PF4 to abundant, negatively charged plasma proteins such as abumin. This calls into question the physiological relevance of this chapter's observations but again, at sites of thrombus formation, the initial platelet plug will limit the entry of plasma components into the local area. The bell-shaped nature of the dose response curve, which

peaks at 50 µg/mL and is slightly reduced at 100 µg/mL may also reflect a negative feedback mechanism whereby extensive platelet activation results in very high local concentrations of PF4. It has been previously suggested that as PF4 binds to the negatively charged GAGs on the platelet surface, at optimal concentrations, it will neutralise repellent negative charge between cells perhaps enhancing interaction and aggregation. However, at higher concentrations, excess positive charge may lead to repulsion (Kowalska et al., 2010). It is also likely that just as TPO dimerises c-Mpl (Tsutsumi et al., 2023), then PF4 also does so. Thus, at higher concentrations PF4 may saturate c-Mpl monomers, preventing dimerisation.

Mass of 1 molecule of PF4 in g:

Molecular mass of one PF4 molecule = 7.8 kDa

1 kDa in g = 1.66×10^{-21} g

$7.8 \text{ kDa} \times 1.66 \times 10^{-21}$ g/kDa = ***1.3×10^{-20} g***

PF4 molecules per mL of whole blood:

PF4 molecules per platelet: 500,000

Platelets per mL of whole blood: 250,000,000

500,000 x 250,000,000 = ***125×10^{12}***

Mass of PF4 per mL of whole blood

Mass of one PF4 molecule x molecules per mL of whole blood

1.3×10^{-20} g x 125×10^{12} molecules/mL = ***162.5×10^{-8} g/mL***

$162.5 / 1 \times 10^{6}$ = ***1.625 µg/mL***

Figure 3.25. Calculation of amount of PF4 per mL of whole blood based on mass spectrometry data.

Table 3.3. PF4 levels in plasma and serum is highly variable across different publications.

Anticoagulant for plasma samples is reported where available. *Range of values given as study describes levels after different blood preparation protocols. CPB: cardiopulmonary bypass; SD: standard deviation; EDTA: ethylenediaminetetraacetic acid; SSc: systemic sclerosis; ND; not done; SLE: systemic lupus erythematosus, AS: ankylosing spondylitis; ELISA: enzyme-linked immunosorbent assay; UC: ulcerative colitis; CD: Crohn's disease; ECMO: extracorporeal membranous oxygenation; RT: room temperature; VITT vaccine-induced immune thrombosis and thrombocytopenia.

Subjects	Plasma	Serum	Technique	Reference
Healthy **CPB**	Median 7.4 ng/mL (range 4-24) 1079-1560 ng/mL (n=2)	8140 ng/mL (SD 1922)	Radioimmunoassay in EDTA-theophylline-PGE_1	(Chesterman et al., 1978)
Healthy (African American) **Healthy (White)**	ND	18098 ng/mL (SD ±10796) 20285 ng/mL (SD ±19480)	Single-plex assay kit (Meso Scale Discovery)	(Bhatnagar et al., 2012)
Healthy **SSc** **SLE** **AS** **Liver fibrosis**	0.09 ng/mL (SD ±0.08) 25.7 ng/mL (SD ±2.6) 1.3 ng/mL (SD ±1.0) 1.4 ng/mL (SD ±1.1 1.7 ng/mL (SD ±1.3)		ELISA (R&D Systems)	(van Bon et al., 2014)
Healthy **SSc**	ND	1.4 ng/mL (IQR 0.2-2.7) 4.8 ng/mL (IQR 1.8-10.8)	Fluorescence-based immunoassay (Merck Millipore)	(Valentini et al., 2017)
Healthy **Sjögren's**	ND	1.0 ng/mL (0.02-11.8) 1.8 ng/mL (0.02 14.4)	Fluorescence-based immunoassay (Merck Millipore)	(Vettori et al., 2016)
Healthy	Mean EDTA: 79 ng/mL (SD 66) Mean Heparin: 292 ng/mL (SD 227)	8965 ng/mL (SD 2144)	ELISA (R&D Systems)	(R&D Systems, 2016)
Healthy	On ice: 12-39 ng/mL (SD ± 11/35)* RT: 35-262 ng/mL (SD ±22-199)*	On ice 72 ng/mL (SD ±43) Room temp: 130 ng/mL (SD ±69)	ELISA (American Diagnostica Inc)	(Kong et al., 2017)
Healthy **UC (active)** **CD (active)**	ND	20 mg/mL 26 mg/mL 34 mg/mL	ELISA (R&D Systems)	(Ye et al., 2017)

Healthy **ECMO**	Med 0.03 µg/mL (range 0.01-0.13) Med 0.21 µg/mL (range 0.09-0.25)	ND	ELISA (Thermo-Fisher)	(Mazzeffi et al., 2021)
Healthy **VITT (diagnosis)** **VITT (follow-up)**	ND	14 ng/mL (SD 10-16.5) 7 ng/mL (SD 4-10) 16 ng/mL (SD 15-18)	ELISA (Invitrogen)	(Montague et al., 2022)

3.4.2. PF4 and mechanisms of platelet activation

The data in this chapter show that PF4 mediates platelet aggregation by binding c-Mpl and signalling through JAK2 and PI3K. This is shown by surface plasmon resonance, receptor blockade, and the blocking effect of various inhibitors of downstream sigalling. The mechanism is broadly consistent with the mechanism by which TPO exerts its effects in megakaryocytes and platelets (Ezumi et al., 1995; Hitchcock et al., 2021). However, the data show that responsiveness of healthy donor platelets to PF4 and TPO do not correlate; high responders to PF4 are not necessarily high responders to TPO and vice-versa. Also, the shape of the aggregation curves with TPO and PF4 are subtly different whereby the initial slope with PF4 is steeper than that for TPO. The effects of inhibitors of JAK2, PI3K, STAT3, STAT5, and mTOR on PF4 and TPO are broadly similar, but these studies are challenging to interpret as some of these inhibitors are poorly characterised and off-target effects are likely.

In the above studies, STAT3 and STAT5 are prominent as identification of phosphorylated STAT5 was the first step in identifying c-Mpl as the PF4 receptor. In megakaryocytes, these proteins translocate to the nucleus and drive transcription but as platelets do not have a nucleus, it was also hypothesised that they could also have a functional role. In this chapter, four inhibitors of STAT3 and/or STAT5 were used, SH4-54, Stattic, STAT5 inhibitor, and niclosamide. All work by blocking the SH2 domain, which is essential for STAT phosphorylation, activation and dimerisation but whilst SH4-54 is active against both STAT3 and STAT5, Stattic is specific for STAT3 and STAT5 inhibitor for STAT5. Interestingly, only SH4-54 was found to have an effect, blocking PF4- but not TPO-mediated aggregation albeit at a high concentration of 10 μM. Given that the reported effective concentration in cell cytotoxicity assays is ~ 0.1-1 μM (Selleckchem, n.d.), off-target effects are likely at this concentration and cannot be discounted. Still, Zhou et al. have previously shown that STAT3 can act as a scaffold protein facilitating the interaction of Syk and PLCγ2 downstream of GPVI (Zhou et al., 2013). However, the above data demonstrate that the Syk inhibitor PRT-060318 does not block platelet aggregation to PF4, so it is unlikely that this mechanism is prominent.

Vassilev et al. showed a second possible mechanism is through translocation and binding to the regulatory region of mitochondrial DNA thus affecting mitochondrial transcription and function (Vassilev et al., 2002). So, there is evidence that STAT3 does have non-transcriptional, functional roles in platelets, and it is plausible that it plays a supporting role in activation.

The effect of niclosamide was also investigated as this is a STAT3 inhibitor and this was found to significantly inhibit both PF4- and TPO-mediated aggregation at the lower concentration of 1 μM. Niclosamide is reported to inhibit STAT3 by inhibition of phosphorylation and nuclear translocation independent of the SH2 domain (Ren et al., 2010). As an effect was seen with niclosamide and not with stattic, it was hypothesised that the inhibitory effect of niclosamide on mTOR may be the mechanism by which it blocks PF4- and TPO-mediated aggregation. Niclosamide is reported to selectively inhibit mTORC1 (compared to mTORC2) by inhibiting proton flux leading to cytoplasmic acidification which in platelets may be associated with a reduction in activation of Akt, a downstream effector of PI3K (Fonseca et al., 2012). A second generation mTOR inhibitor, WYE-354, that inhibits both mTORC1 and mTORC2 did cause a non-significant, yet noticeable reduction in PF4- but not TPO-mediated platelet aggregation. A second, similar inhibitor, KU-0063794 had no effect on either although in a previous study, WYE-354 did show greater potency than KU-0063794 in blocking collagen-mediated aggregation in apyrase-treated platelets (Aslan et al., 2011). Apyrase degrades ADP thus preventing ADP-mediated secondary platelet activation and was used in the previously referenced study to eliminate effects of inhibitors on secondary platelet activation. In the present study, this was not done as the steeper part of the aggregation curve in PF4-activated platelets is likely due to secondary activation.

The data are therefore inconclusive. Ruxolitinib and wortmannin convincingly block platelet aggregation to PF4 and TPO but ruxolitinib and wortmannin show incomplete blockade of P-selectin expression and non-significant blockade of spreading. Evidently, JAK2 and PI3K are

important in mediating aggregation but additional mechanisms that bring about α-granule release are possible.

The data do not clearly demonstrate a key role for STAT3, STAT5, or mTOR in mediating platelet aggregation downstream of c-Mpl. The significant effect of niclosamide in blocking aggregation is intriguing but it is not possible to rule out effects on other processes not involving STAT3 or mTOR. It is also intriguing that although niclosamide blocked aggregation to PF4 and TPO, it significantly enhanced α-granule secretion and platelet spreading on PF4. A possible mechanism for this could be that the inhibition of mTORC1 leads to reduced activation of PKCδ, which inhibits granule secretion and filopodial formation (Pula et al., 2006). Tyrosine phosphorylated PKCδ was, incidentally, detected in its phosphorylated form in the mass spectrometry analysis described in section 3.3.3. Further investigation using inhibitors of PKCδ as well as other pathways downstream of JAK2 such as the MAPK pathway is needed to further understand these processes. However, the complex network of activating and inhibitory signals, and feedback loops make this a challenging task, one that is perhaps better suited to proteomics-based methods. An approach using the high throughput technique of phospho-flow cytometry may also be more fruitful.

3.4.3. Blockade of c-Mpl-TPO interaction by PF4

The mechanisms by which TPO exerts its effects in in megakaryocytes are well described (Hitchcock et al., 2021). It was anticipated that in platelets, the signalling pathways triggered by PF4 would be similar, if not identical to those triggered by TPO. However, although PF4 and TPO are both agonists of platelets, PF4 has the opposite effect to TPO in megakaryocytes, inhibiting megakaryocyte differentiation and platelet production (Xi et al., 1996) which has been attributed to an interaction with low density lipoprotein receptor-related protein 1 (LRP1). However, as mentioned previously, this receptor is expressed only transiently, late in megakaryopoiesis (Lambert et al., 2009). Furthermore, secretion of PF4 from megakaryocytes has been shown to maintain haematopoietic stem cell (HSC) quiescence through unknown mechanisms (Bruns et al., 2014). As HSCs express c-Mpl, binding to this receptor is a possible mechanism.

A simple mechanism by which PF4 could inhibit TPO-induced differentiation and proliferation of megakaryocytes is through directly blocking TPO's binding with c-Mpl. In the binding ELISA PF4 reduced, but did not eliminate, TPO binding to c-Mpl. The AlphaFold modelling is interesting as it is consistent with the hypothesis that PF4 would block TPO-binding, but it is inconclusive and further, in-depth structural studies are needed.

Erhardt et al. reported that whilst TPO leads to phosphorylation of AKT and STAT1, STAT3, and STAT5, the TPO receptor agonist eltrombopag does not induce AKT phosphorylation nor prime platelet responses to low-dose agonists (Erhardt et al., 2009). Notably, Akt is a downstream effector of PI3K and is essential for platelet priming by TPO (Moore et al., 2019). In their paper describing the crystal structure of TPO dimerising c-Mpl, Tsutusmi et al. contributed important explanations about the relationship between c-Mpl agonist structure, induction of differential signalling, and corresponding functional effects (Tsutsumi et al., 2023). They reported that TPO has a low- and a high-affinity binding site for c-Mpl and bridges two monomers to form a dimer by binding to one using its low-affinity site, and the other using its

high affinity site. Substitutions of basic amino acids in the low-affinity site altered dimerisation and downstream signalling, and they were able to demonstrate decoupling of the two phenotypic outputs of TPO binding to c-Mpl: megakaryopoiesis and platelet production *versus* HSC proliferation. They showed that these mutations in TPO were associated with subtle changes in signalling patterns, which varied with increasing concentrations (0-100 ng/mL) and over time (0-240 min). This study sets a precedent that different ligands of the same c-Mpl receptor can induce different downstream signalling and functional effects in megakaryocytes. One possible mechanism could be that compared to TPO, PF4 may differentially stimulate the activation of the E3 ubiquitin ligase c-Cbl, which is known to be activated as a product of c-Mpl activation (Saur et al., 2010). Of course, this does not discount the interaction with LRP1 and the possibility of the existence of other, as yet unidentified receptors and pathways.

4. The role of PF4 and heparin in the activation of platelets in anti-PF4 immunothrombotic syndromes

4.1. Introduction

4.1.1. Mechanisms of thrombosis in anti-PF4 immunothrombotic syndromes

As discussed previously, in anti-PF4 immunothrombotic syndromes, immune complexes activate platelets by binding to FcγRIIA (Kelton et al., 1988). Platelet activation results in granule release, shape change, and aggregation which promotes thrombus formation. α-granule release results in the translocation of P-selectin to the platelet surface facilitating interplay with monocytes and neutrophils to form leukocyte-platelet aggregates (Khairy et al., 2001, 2004). Direct activation of neutrophils and monocytes, also through Fc receptors, further contributes to the pathophysiology through release of inflammatory mediators, neutrophil extracellular trap (NET) formation (NETosis) (Perdomo et al., 2019; Leung et al., 2022), and activation of the coagulation cascade through tissue factor expression (Perdomo et al., 2019; Leung et al., 2022) (Kasthuri et al., 2012). Further complexity is added by the interaction of PF4 with many negatively charged molecules other than heparin including cell surface GAGs (Okayama et al., 1986; Loscalzo et al., 1985; Visentin et al., 1994; Rauova et al., 2006), polyphosphates (Cines et al., 2016), vWF (Nazy et al., 2020), fibrin (Carr et al., 1987), and DNA in NETs (Gollomp et al., 2020; Ngo et al., 2023).

The data presented in Chapter 3 showing that PF4 can bind to c-Mpl and activate platelets (Buka et al., 2024), coupled with the knowledge that heparin activates platelets through PEAR1 (Kardeby et al., 2023), raises the question of whether these mechanisms are relevant in anti-PF4 immunothrombotic syndromes. Free heparin and PF4, as well as heparin and PF4 bound in immune complexes could contribute to platelet activation. As such, immune complexes could in fact not only be multivalent ligands of FcγRIIA; the binding of c-Mpl and

PEAR1 may also contribute by increasing the avidity of the entire complexes in addition to direct activation through induction of signalling.

It was therefore hypothesised that PF4-mediated platelet activation could play a role in the pathophysiology of the anti-PF4 immunothrombotic syndromes. Secondly, it was hypothesised that in HIT, heparin, may also contribute to platelet activation. These hypotheses are summarised in Figure 4.1.

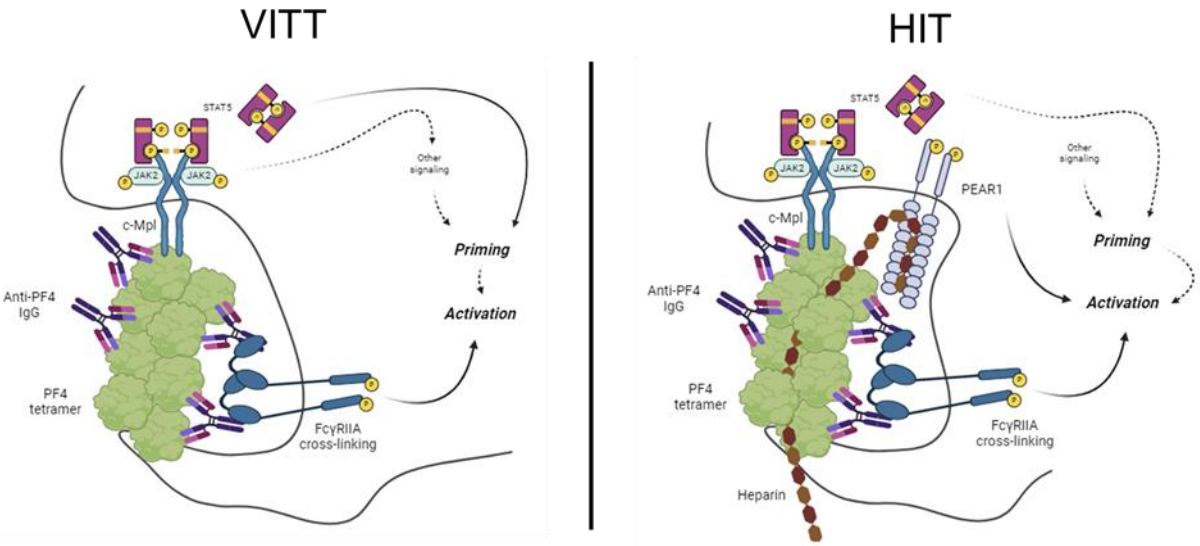

Figure 4.1. Hypothesised additional mechanisms of platelet activation in VITT and HIT.

c-Mpl: c-myeloproliferative leukaemia protein; FcγRIIA: Fc gamma receptor IIA; HIT: heparin-induced thrombocytopenia; IgG: immunoglobulin; JAK2: Janus kinase 2; P: phosphorylation; PF4: platelet factor 4; STAT: signal transducer of activation; VITT: vaccine-induced immune thrombocytopenia with thrombosis.

4.2. Results

4.2.1. VITT: Patient details

Patients with VITT were recruited from University Hospitals Birmingham by Dr Pip Nicolson. In total, 12 patients were recruited, and plasma and sera were saved from presentation and follow-up visits. However, this was a scare resource and by the time that the present studies took place, many of these samples, particularly diagnostic samples, had been used. Thus, the following experiments make use of samples from three patients whose presentation is summarised in Table 4.1. This study leverages the extensive, longitudinal characterisation of the patient samples by Dr Samantha Montague, University of Birminhgam. The full case histories of these patients are published (Montague et al., 2022) and the identifying numbers of these patients in that publication are denoted in parentheses in the first column of the table.

Table 4.1. Basic demographics and presenting characteristics of patients with VITT whose material is used in this chapter.

*Numbers of patients in (Montague et al., 2022). CVST: cerebral venous sinus thrombosis; ELISA: enzyme linked immunosorbent assay; F: female; M: male; OD: optical density.

Patient (*)	Age	Sex	Presentation days post-vaccination	Presentation platelet count ($\times 10^9$/L)	Site of thrombosis	Sample – days post-vaccination	Anti-PF4 ELISA optical density (OD)	
							Diagnosis	Sample
1 (P4)	43	F	14	11	CVST	15	0.92	1.66
2 (P2)	21	M	10	113	Ischaemic stroke	221	2.58	1.41
3 (P6)	47	F	20	78	CVST	109	2.37	1.34

4.2.2. Testing of isolated VITT IgG

Patient 1 underwent plasma exchange and as such, several litres of plasma were collected and stored. This enabled isolation of IgG from plasma, which was performed by Dr Luis Moran, Dr Samantha Montague, and Dr Margaret Goodall, University of Birmingham. Dr Samantha Montague first characterised the reagent and established optimal concentrations for platelet activation in LTA. This reagent, termed ‘VITT IgG’ was tested for its platelet activating potential by LTA. VITT IgG did not cause platelet activation alone, but when combined with PF4, rapid, strong activation was observed (Figure 4.2). Consistent with the known phenomenon of

significant inter-donor variability in responses to HIT sera (Warkentin et al., 1992), not all healthy donor platelets responded robustly to VITT IgG with PF4. In this section, any donors that did not reach >50% aggregation to VITT IgG or sera in the presence of PF4 within 30 min were deemed to be low-responders and were excluded. The Src inhibitor, dasatinib, and the Syk inhibitor, PRT-060318, are both known to block FcγRIIA-mediated platelet activation in VITT and HIT (Smith et al., 2021; Reilly et al., 2011), and PRT-060318 has also shown efficacy in an animal model of HIT (Reilly et al., 2011). Figure 4.2A shows that aggregation to VITT IgG + PF4 is blocked by dasatinib 1 µM and PRT-060318 10 µM. As expected, aggregation to VITT IgG was also blocked by the mouse anti-human FcγRIIA monoclonal antibody IV.3 10 µg/mL, a well-established inhibitor of *in vitro* FcγRIIA activation at this concentration (Arman et al., 2014; Smith et al., 2021; Lee et al., 2024). Together, these results demonstrate that VITT IgG activates platelets in a PF4-dependent manner through FcγRIIA.

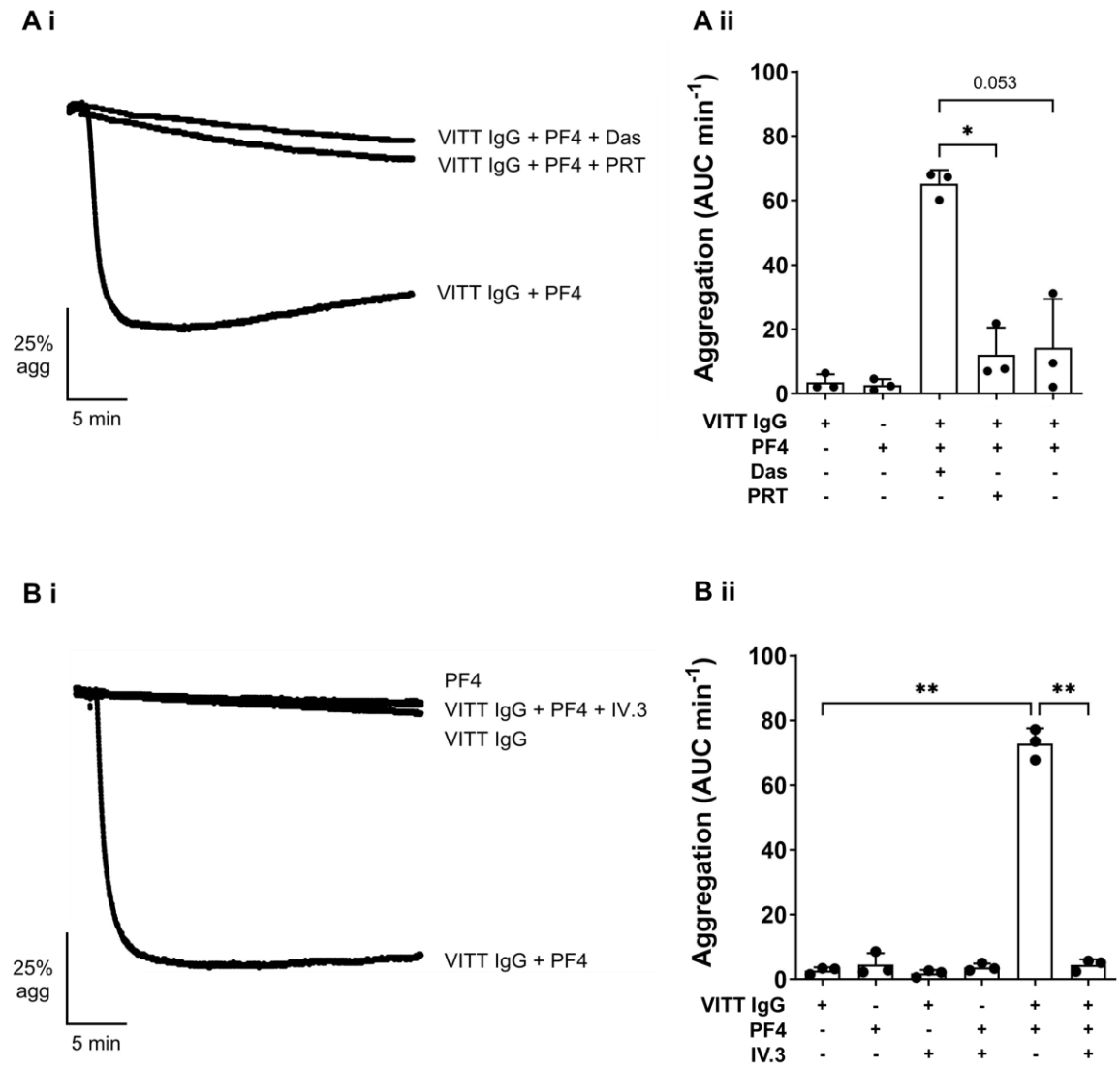

Figure 4.2. Isolated IgG from a patient with VITT (VITT IgG) activates platelets in a PF4-dependent manner through FcγRIIA.

(A) Inhibitors of Syk and Src block platelet aggregation to VITT IgG and PF4. Pre-warmed platelets (2×10^8/mL) at 37°C were incubated with dasatinib 1 µM (Das), PRT-060318 10 µM (PRT) or vehicle control (DMSO 0.01%) for 5 min, then PF4 10 µg/mL for 5 min, then stirred at 1200 rpm for 1 min before addition of VITT IgG (100 µg/mL). (Ai) Representative aggregation traces. (Aii) Quantification of aggregation (area under curve per minute [AUC min^{-1}] for 30 min, n=3). Statistical testing of difference by one-way ANOVA. (B) As for A but IV.3 10 µg/mL or vehicle control (PBS) added instead of Das or PRT. *P< .05, **P < .01.

4.2.3. Blockade of the PF4-c-Mpl-JAK2 pathway reduces platelet activation to VITT IgG

In Chapter 3 it was shown that ruxolitinib 100 nM does not affect platelet aggregation to collagen-related peptide (CRP) 1 µg/mL. In the context of VITT, this is important as the signalling downstream of GPVI is shared by FcγRIIA. Nevertheless, the effects of ruxolitinib 100 nM on FcγRIIA-mediated platelet aggregation were assessed. Ruxolitinib had no effect on platelet aggregation to stimulation of FcγRIIA by crosslinked IV.3 (IV.3 + anti-mouse IgG) nor a VITT-like monoclonal antibody, 1E12 (Vayne et al., 2024) (Figure 4.3). The experiments with 1E12 were carried out by Dr Samantha Montague.

Ruxolitinib 100 nM was then used in combination with VITT IgG and PF4 to assess the contribution of the PF4-c-Mpl-JAK2 pathway to aggregation with these reagents. As before, VITT IgG had no effect on its own, but in the presence of PF4 strong aggregation was observed (Figure 4.4). However, there was donor variability, with some weaker responses, and donors where >50% aggregation did not occur within 30 min were excluded. When platelets were pre-incubated with ruxolitinib, aggregation was significantly reduced (Figure 4.4Aii) typically through reduction in the maximum amplitude of aggregation rather than speed of aggregation (Figure 4.4Ai). A similar reduction was seen with the anti-c-Mpl antibody in platelets from some healthy donors although the effect was not as pronounced as that seen with ruxolitinib and the reduction was not statistically significant (Figure 4.4B). Several of the replicate experiments investigating the effect of c-Mpl antibody on aggregation to VITT IgG with PF4 were performed by Dr Samantha Montague.

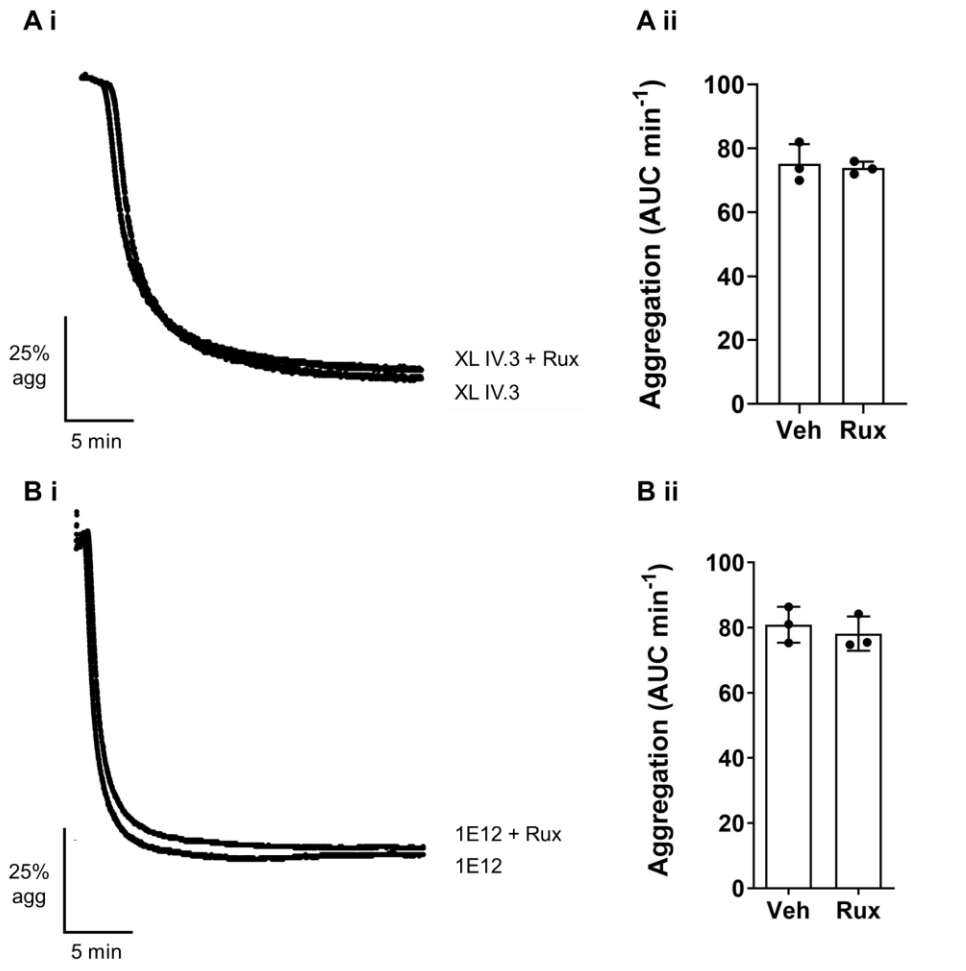

Figure 4.3. Ruxolitinib does not inhibit platelet aggregation to agonists of FcγRIIA.

(A) Ruxolitinib does not inhibit platelet aggregation to crosslinked IV.3. (A) Pre-warmed platelets (2×10^8/mL) at 37°C were incubated with ruxolitinib 100 nM (Rux), or vehicle control (DMSO 0.01%) (Veh) for 5 min, then IV.3 1 µg/mL for 5 min, then stirred at 1200 rpm for 1 min before addition of goat anti-mouse IgG (30 µg/mL). (Ai) Representative aggregation traces. (Aii) Quantification of aggregation (area under curve per minute [AUC min^{-1}] for 30 min, n=3). Statistical testing of difference by one-way ANOVA. (B) As for A but no IV.3 added and 1E12 10 µg/mL added instead of goat anti-mouse IgG. Statistical testing of difference by paired t-test.

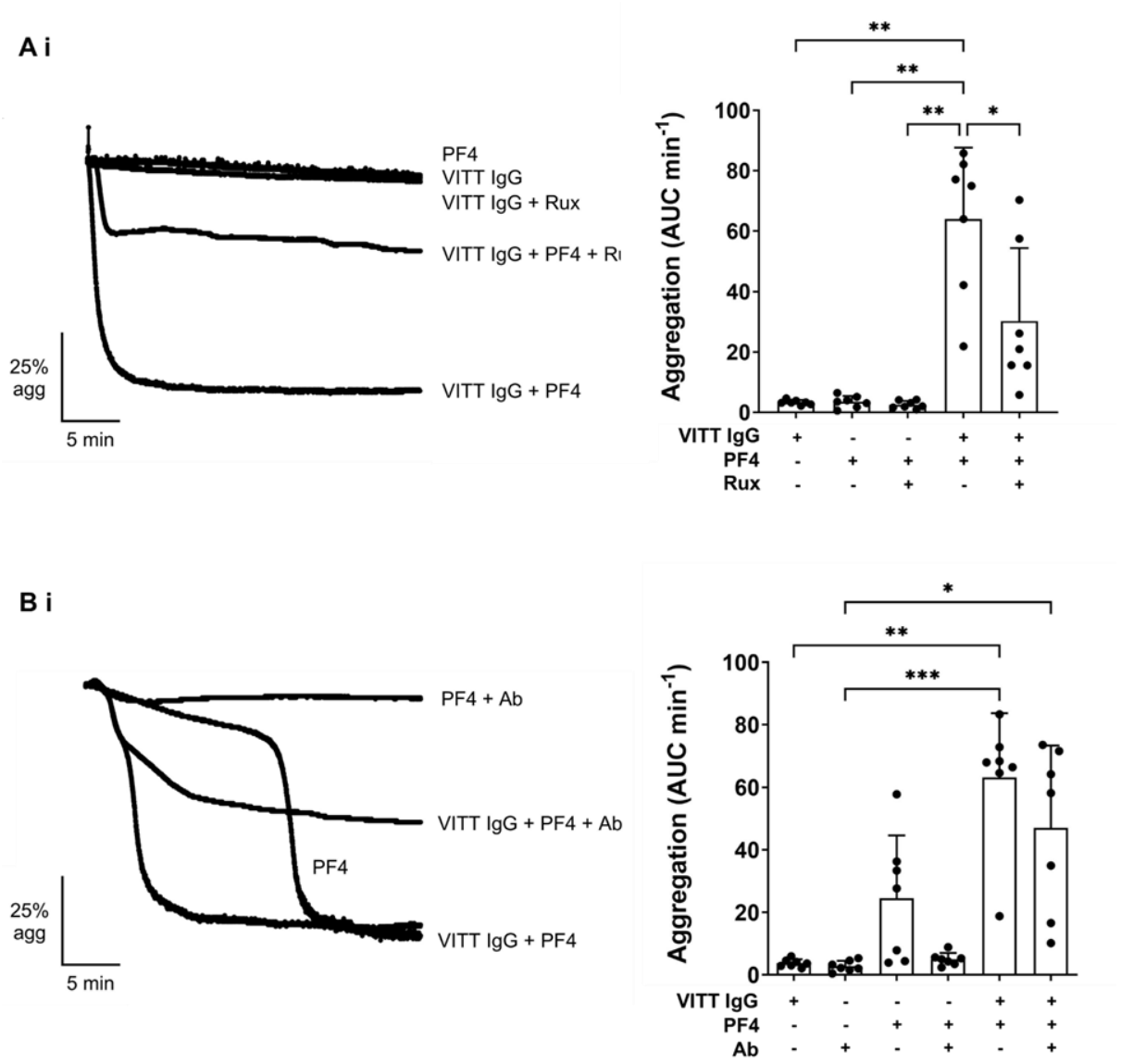

Figure 4.4. Blockade of the c-Mpl-JAK2 pathway reduces platelet aggregation to VITT IgG with PF4.

Adapted from (Buka et al., 2024). (A) Ruxolitinib reduces platelet aggregation to VITT IgG with PF4. Pre-warmed platelets (2×10^8/mL) at 37°C were incubated ruxolitinib 100 nM (Rux), or vehicle control (DMSO 0.01%) (Veh) for 5 min, then PF4 10 µg/mL or vehicle control (PBS) for 5 min, then stirred at 1200 rpm for 1 min before addition of VITT IgG (100 µg/mL). (Ai) Representative aggregation traces. (Aii) Quantification of aggregation (area under curve per minute [AUC min^{-1}] for 30 min, n=7). Statistical testing of differences by one-way ANOVA. (B) As for A but anti-c-Mpl antibody (10 µg/mL) or vehicle control (PBS) used instead of Rux. Statistical testing of differences by Friedman test. *P < .05, **P < .01, ***P < .001.

Next, the experiments were repeated with sera from two other patients with VITT. These two sera were selected as they had been previously characterised as moderately activating at the specific time points used (Montague et al., 2022). Serum from patient 2 (P2) was from 221 days post-vaccination and patient 3 (P3) was from 109 days post-vaccination. At this time the ELISA OD for both samples remained above 1.3, well above the positive cut-off for the test of 0.4 (clinical details and OD values shown in Table 4.1). These two sera and time points were also chosen because there was plentiful volume of stored sample.

To account for healthy donor variation in responses to VITT sera, for each healthy donor, a dose response to serum alone was first conducted (between 0.67% and 3% final volume of serum in the aggregation cuvette) to determine a volume of serum that resulted in an initial aggregation trace of ~45° that could be both enhanced with PF4 and potentially blocked with ruxolitinib. There were no donors that did not respond to at least 3% serum. With P2 serum, ruxolitinib reduced aggregation to serum alone as well as aggregation to serum in the presence of PF4 10 µg/mL (Figure 4.5A). With P3 serum, a significant reduction in aggregation was only observed where exogenous PF4 had been added (Figure 4.5B).

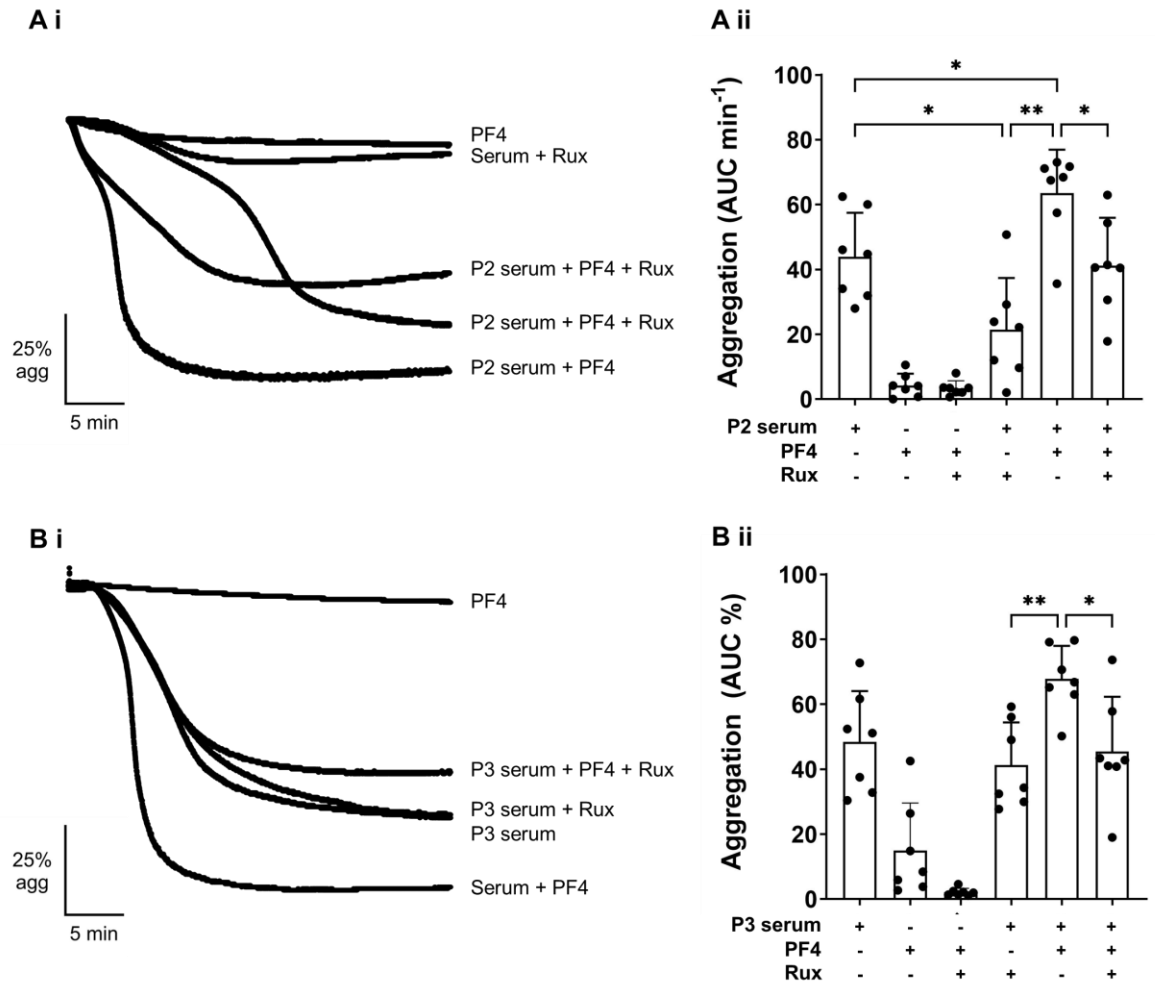

Figure 4.5. JAK2 inhibition reduces platelet aggregation to VITT sera.

Adapted from (Buka et al., 2024). (A) Pre-warmed platelets (2×10^8/mL) at 37°C were incubated ruxolitinib 100 nM (Rux), or vehicle control (DMSO 0.01%) (Veh) for 5 min, then PF4 10 µg/mL or vehicle control (PBS) for 5 min, then stirred at 1200 rpm for 1 min before addition of P2 VITT serum. Serum was added at between 0.67% to 3% final concentration depending on an initial dose-response for each individual platelet donor (see text). (Ai) Representative aggregation traces. (Aii) Quantification of aggregation (area under curve per minute [AUC min^{-1}] for 30 min, n=7). Statistical testing of differences by one-way ANOVA. (B) As for A but P3 serum added instead P2 serum. *P < .05, **P < .01.

The canonical understanding of how PF4 enhances platelet activation to HIT and VITT sera is through enhancement of immune complex formation. However, these data raise the question of the relative contribution by exogenous PF4 of signalling through c-Mpl and increased immune complex formation to the enhancement of platelet activation in diagnostic assays. To this end, the effect of TPO 10 ng/mL (a low dose that does not activate platelets alone) instead of PF4 in the LTA assays described above, was investigated. The addition of TPO to isolated VITT IgG had no effect, whilst in the same donors, VITT IgG with PF4 led to robust aggregation (Figure 4.6A). The same experiment was repeated using P3 serum and although this was only repeated in three donors due to low serum availability, TPO was observed to enhance aggregation to serum which was non-significantly reduced with ruxolitinib (Figure 4.6B).

Together these experiments show that in serum, there is adequate PF4 present for immune complex formation and that activation is enhanced by c-Mpl activation. Further experiments could be done with combinations of low concentration PF4, TPO and VITT IgG to investigate the relative contributions of enhancement of immune complex formation, signalling through c-Mpl, and signalling through FcγRIIA.

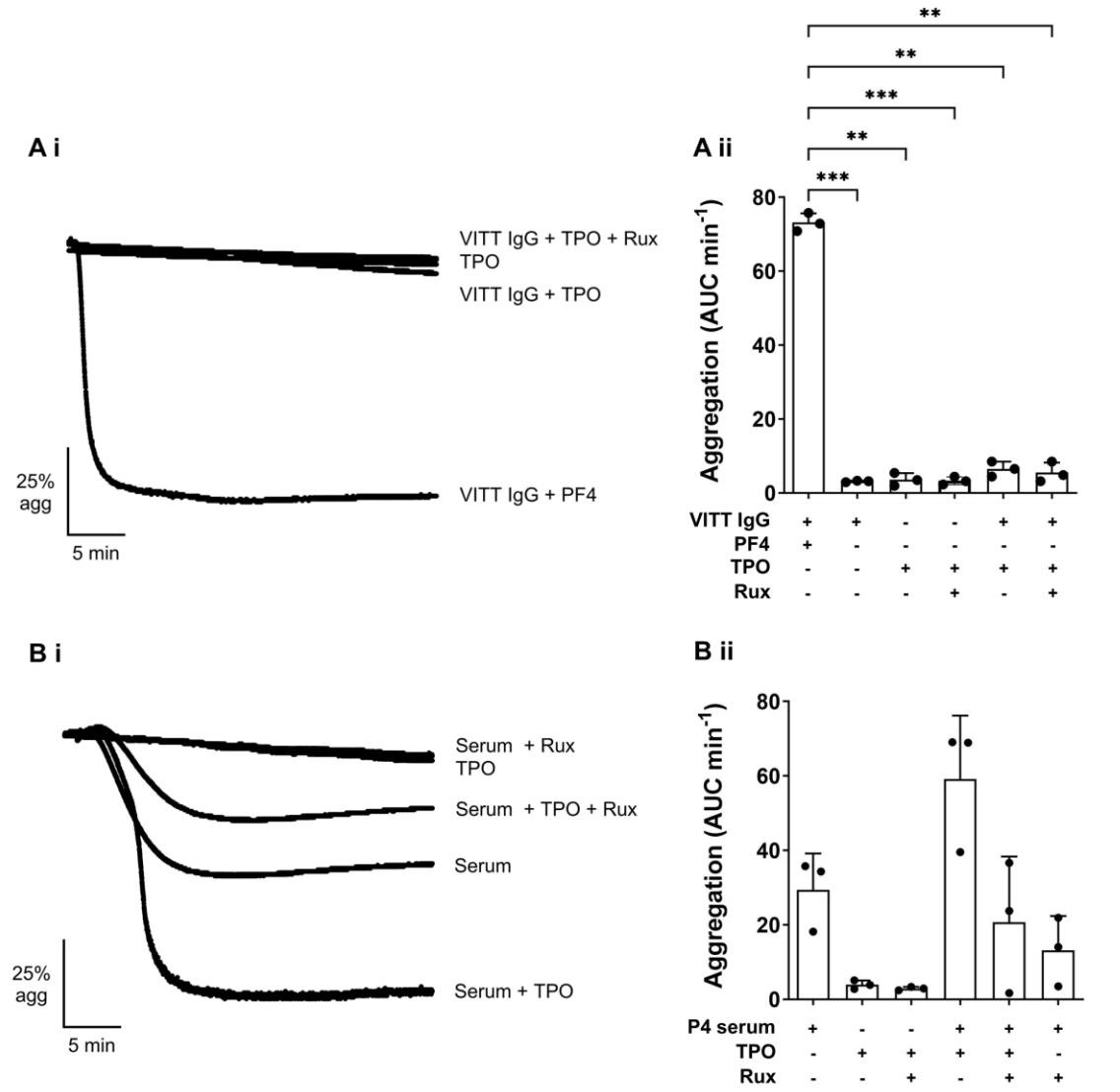

Figure 4.6. TPO does not facilitate aggregation to VITT IgG but does enhance platelet aggregation to VITT serum which is reduced with ruxolitinib.

(A) Pre-warmed platelets (2×10^8/mL) at 37°C were incubated ruxolitinib 100 nM (Rux), or vehicle control (DMSO 0.01%) (Veh) for 5 min, then TPO 10 ng/mL or vehicle control (PBS) for 5 min, then stirred at 1200 rpm for 1 min before addition of VITT IgG. (Ai) Representative aggregation traces. (Aii) Quantification of aggregation (area under curve per minute [AUC min^{-1}] for 30 min, n=3). Statistical testing of differences by one-way ANOVA. (B) As for A but P2 serum added instead of VITT IgG. Serum was added at between 1.5 to 3% final concentration depending on an initial dose-response for each individual platelet donor (see text). **P < .01. ***P < .001.

There are four possible mechanisms by which PF4 contributes to platelet activation in the above experiments. As shown by the data in this section, exogenous PF4 enhances activation through contribution to immune complex formation (no activation seen with VITT IgG alone nor VITT IgG with TPO), and through signalling (activation partially blocked with ruxolitinib and TPO enhances aggregation to VITT sera). It is probable that free PF4, binding to c-Mpl leads to potentiation of activation but also possible that PF4 within the immune complex can activate c-Mpl, as shown in Figure 4.1. The additional interaction of PF4 with c-Mpl is also expected to increase the avidity of the entire immune complex to the platelet surface and therefore enhance the interaction of Fc regions of anti-PF4 antibodies with FcγRIIA. A fourth possible mechanism is binding of PF4 to platelet surface GAGs, neutralising negative charge, and enhancing platelet apposition.

To explore this further, a pilot experiment was performed whereby platelets activated by PF4, and/or VITT IgG and/or the VITT-like monoclonal antibody 1E12 were lysed and examined for tyrosine phosphorylation by Western blot. The results of this experiment are shown in Figure 4.7. As expected, with PF4 10 µg/mL and 50 µg/mL, phosphorylated bands were visible at ~95 kDa (indicated by arrows) consistent with STAT3, STAT5 and c-Mpl phosphorylation. With the addition of VITT IgG, the bands intensified with donor 1 but reduced in intensity with donors 2 and 3. These bands also reduced in intensity with control IgG with all three donors. VITT IgG with PF4 did not generate clear phosphorylated bands at between 40 and 50 kDa which is where FcγRIIA is expected (Cell Signalling Technology, n.d.) but the bands visible in platelets activated with 1E12, indicating weaker FcγRIIA stimulation with VITT IgG compared to 1E12. Further, 1E12 did not require exogenous PF4 to lead to this phosphorylation, which is consistent with earlier findings and published reports (Vayne et al., 2021b), presumably relying on its high affinity to efficiently form immune complexes with the small amount of PF4 that is available. Further investigation of the possible mechanisms requires more extensive analysis of phosphorylation including c-Mpl and FcγRIIA the latter of which requires immunoprecipitation.

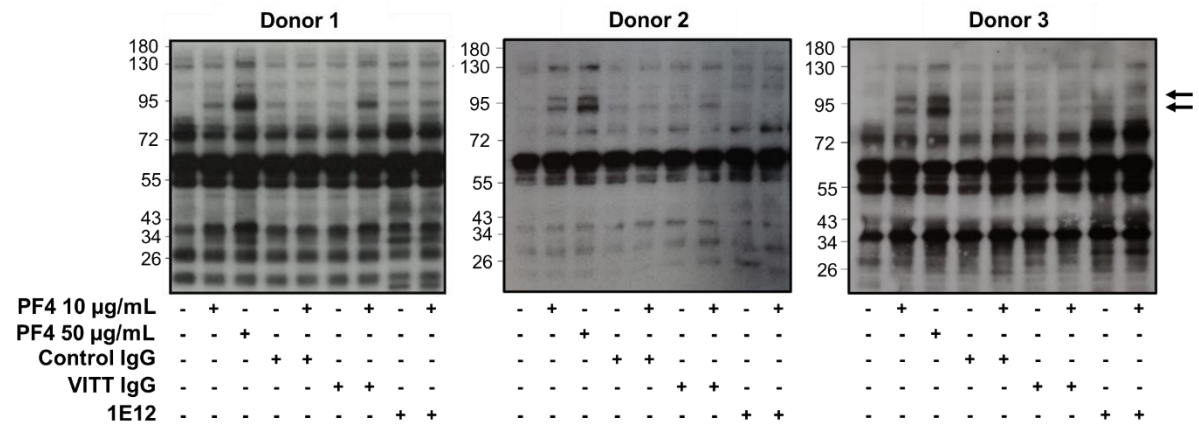

Figure 4.7. Platelet phosphorylation in response to PF4 and VITT IgG.

Washed platelets (4×10^8/mL) from three healthy donors were pre-incubated with eptifibatide for 10 minutes (9 µM) and warmed at 37°C for 5 minutes. Platelets were pre-incubated with PF4 10 or 50 µg/mL or vehicle (PBS). Platelets were then stirred at 1200 rpm for one minute after which control IgG (100 µg/mL), VITT IgG (100 µg/mL), 1E12 (10 µg/mL) or vehicle control (PBS) was added. After 10 min, platelets were lysed. Protein was separated by sodium dodecyl sulfate (SDS) gel electrophoresis, transferred to a polyvinylidene fluoride membrane, and analysed for pan-phosphotyrosine (4G10). Arrows mark bands of interest at 95 kDa likely associated with phosphorylation of STAT3, STAT5a/b and c-Mpl.

4.2.4. Ruxolitinib does not affect platelet aggregation to HIT-like monoclonal antibody, KKO with PF4.

As HIT is very similar in pathophysiology to VITT, it was hypothesised that platelet activation by PF4 may also play a role in HIT. To investigate this further, a commercially available, mouse-derived HIT-like anti-PF4/heparin antibody, KKO 10 µg/mL (133 nM), was used (Arepally et al., 2000). 10 µg/mL was previously established as the minimum concentration that induces aggregation in washed platelets in the presence of PF4 (Samantha Montague, unpublished). As expected, KKO did not induce platelet aggregation alone but stimulated strong aggregation when combined with PF4 10 µg/mL (Figure 4.8A). The combination of KKO and PF4 in the presence and absence of heparin has previously been shown (as expected) to act through FcγRIIA and to be blocked by IV.3 (Nevzorova et al., 2019; Arepally et al., 2000).

Ruxolitinib 100 nM had no effect on aggregation to KKO with PF4 (Figure 4.8A). Although KKO does behave like a HIT-like antibody, it is of the IgG2b subclass which is not present in humans (Bruhns and Jönsson, 2015). Thus, a second monoclonal antibody, 5B9 (Kizlik-Masson et al., 2017), was acquired from collaborators (Jerôme Rollin and Yves Gruel, Université de Tours, France) and the experiments repeated. As for KKO, 5B9 with PF4 in the presence and absence of heparin has also been shown to be blocked by IV.3 (Kizlik-Masson et al., 2017). 5B9 20 µg/mL (67 nM) alone had no effect on platelet aggregation but the addition of PF4 led to strong aggregation (Figure 4.8B). 20 µg/mL was used as this is the minimum concentration required to result in aggregation in the presence of PF4 (Kizlik-Masson et al., 2017). Again, ruxolitinib had no clear effect on aggregation to 5B9 with PF4 (Figure 4.8B).

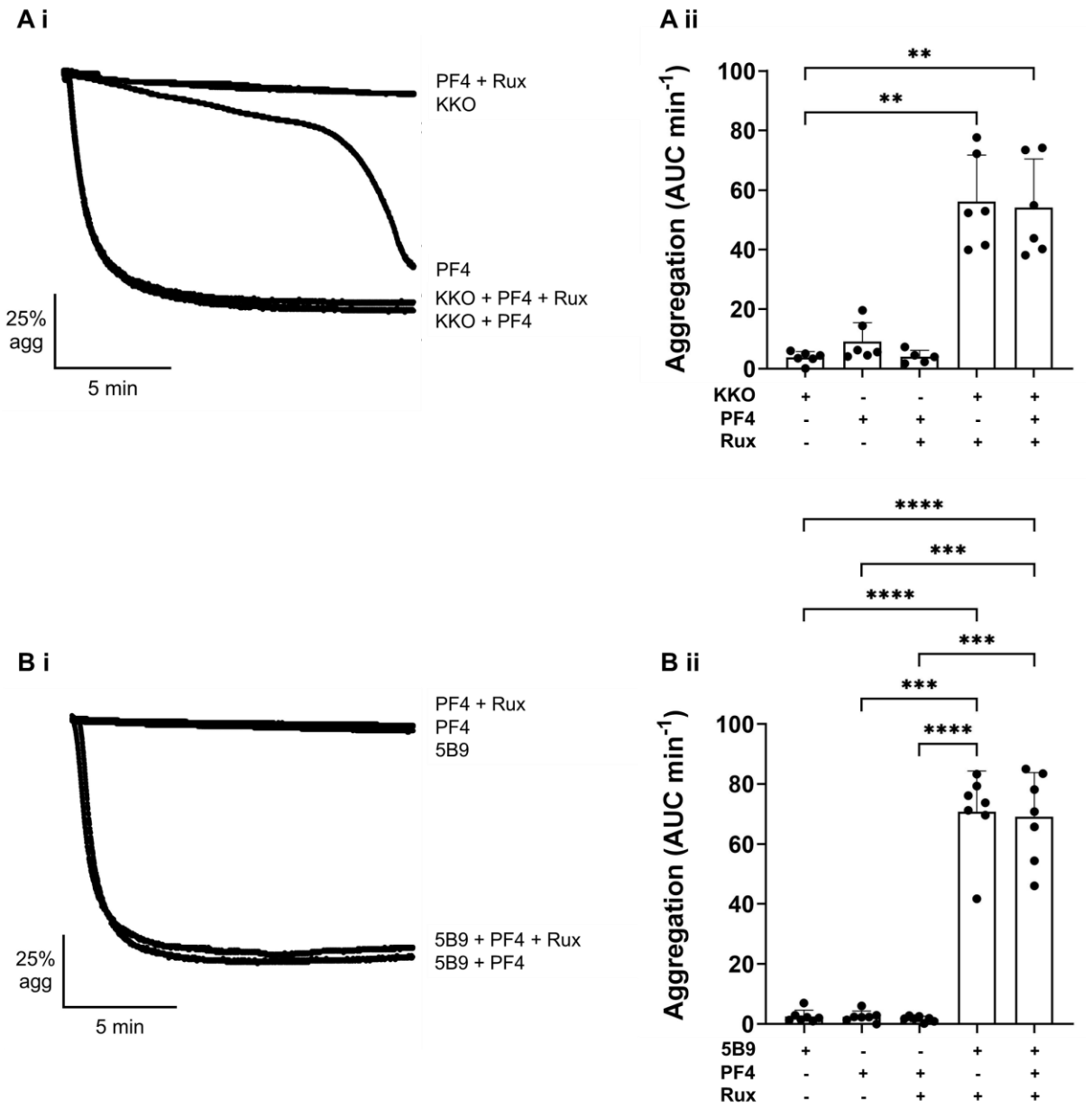

Figure 4.8. Ruxolitinib does not inhibit platelet aggregation to the HIT-like monoclonal antibodies KKO or 5B9 with PF4.

(A) Pre-warmed platelets (2×10^8/mL) at 37°C were incubated with ruxolitinib 100 nM (Rux), or vehicle control (DMSO 0.01%) for 5 min, PF4 10 µg/mL or vehicle control (PBS) for 5 min, then stirred at 1200 rpm for 1 min before addition of KKO 10 µg/mL. (Ai) Representative aggregation traces. (Aii) Quantification of aggregation (area under curve per minute [AUC min^{-1}] for 15 min, n=6). (B) As for A but 5B9 20 µg/mL added instead of KKO, n=7. Statistical testing of differences by one-way ANOVA. **P < .01, ***P < .001 ****P <0.0001.

4.2.5. Characterisation of platelet aggregation by HIT sera

The above experiments are limited as in the presence of PF4, these monoclonal antibodies produce very strong aggregation. As HIT is characterised by polyclonal rather than monoclonal antibodies, sera from patients with HIT was next evaluated. As samples from patients with HIT had not been previously collected and stored locally, we explored other options for acquisition of sera from patients who had been tested for HIT. In England, clinical grade, functional diagnostic testing for HIT only takes place in the NHSBT laboratory in Bristol and it was arranged that 11 samples that had been collected from patients in local hospitals could be transferred back to Birmingham via the University of Birmingham Human Bioresource Centre. These sera are labelled 1 to 11 in descending order of anti-PF4/heparin ELISA optical density measurement which is expected to generally correlate with platelet activation in functional studies (Table 4.2) (Warkentin et al., 2008b). Clinical details were not available for these patients.

Table 4.2. Sera from 11 patients with HIT.

Samples were acquired from National Health Service Blood and Transplant (NHSBT) and are ordered in descending order of anti-PF4/heparin ELISA optical density measurement.

Patient	Optical density
1	3.4
2	3.2
3	3.1
4	3.1
5	2.8
6	2.6
7	2.3
8	1.2
9	0.9
10	0.7
11	0.6

The sera were screened for their platelet activating activity by LTA using platelets from four healthy donors. These donors were randomly selected; whether they were '*responsive'* donors to HIT reagents was unknown prior to this screening. Figure 4.9 shows the results of this screening whereby platelets were stimulated with either serum alone, serum with PF4 10

µg/mL, serum with heparin 0.5 IU/mL, or serum with PF4 and heparin. As expected, platelet activation was generally strongest for sera with the higher ELISA OD values apart from serum 1 which was only weakly activating Figure 4.9.

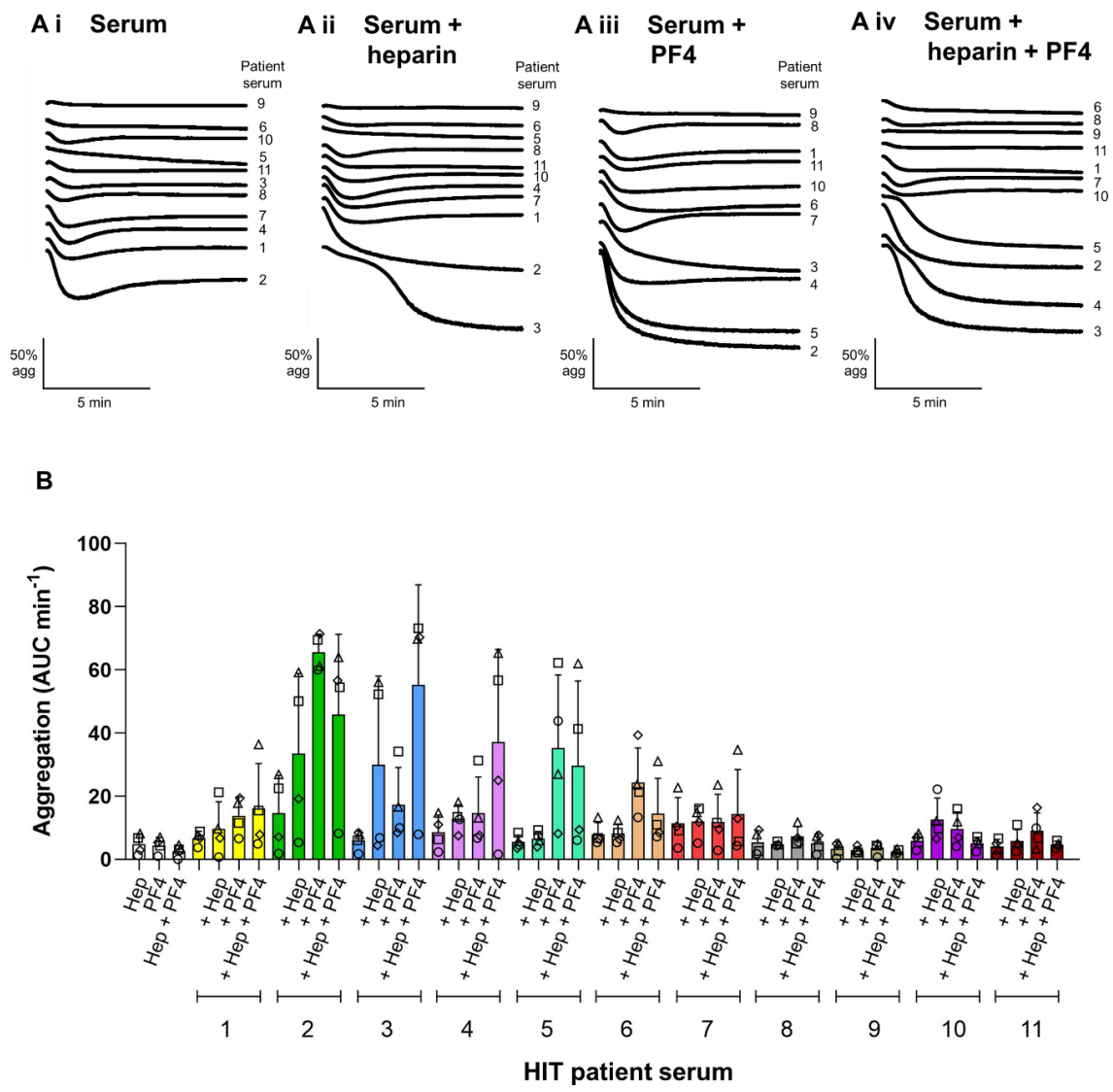

Figure 4.9. Characterisation of platelet aggregation responses to 11 serum samples from patients with HIT.

Platelet aggregation was assessed by LTA. Pre-warmed platelets (2×10^8/mL) at 37°C were incubated with heparin 0.5 IU/mL (Hep) or vehicle control (PBS) for 5 min then PF4 10 µg/mL or vehicle control (PBS) for 5 min. Platelets were then stirred at 1200 rpm for an additional minute before addition of serum (3.3% final concentration). The first three columns on the left (unfilled bars), Hep, PF4, and Hep + PF4 controls, were run without the addition of serum. The first, unlabelled column for each patient sample is serum alone, and in subsequent columns, serum was added in the presence of Hep, PF4, or Hep + PF4. (A) Representative aggregation traces for one donor (open squares in B). Quantification of aggregation (area under curve per minute [AUC min^{-1}]) for 10 min. Responses for individual donors are denoted by consistent shapes (e.g. open squares), n=4.

4.2.6. Ruxolitinib has occasional effects on platelet aggregation to HIT sera

Only serum 2, in the presence of PF4, led to strong aggregation in all four donors but there were moderate responses in at least one donor to serum 3, 4, 5, 6, and 7 in the presence of PF4 or PF4 + heparin (Figure 4.9). As it was the strongest activating serum, serum 2 was first used to further investigate the role of PF4 in platelet activation in HIT. To conserve serum, the final concentration of serum was decreased to 1% which still produced strong aggregation in the presence of PF4 (Figure 4.10). In most donors, ruxolitinib, had no effect (Figure 4.10Ai and Aiii) apart from in one donor where there was a substantial reduction in aggregation (Figure 4.10Aii and Aiii open squares). The next strongest activating serum was serum 3 although with PF4 alone, serum 5 appeared to be stronger. However, as there was insufficient volume of serum 5 to carry out extensive replicates, the effects of ruxolitinib on serum 3 were instead investigated. However, as serum 3 with PF4 alone was not strongly activating, the effect of ruxolitinib on serum with PF4 *and* heparin was investigated. Again, ruxolitinib had an occasional inhibitory effect (Figure 4.10B), reducing aggregation to serum + PF4 in one donor (Figure 4.10Bi and Biii open diamonds), and to serum + PF4 + heparin in two donors (Figure 4.10Bii and Biii open circles). After these initial investigations, samples from a patient diagnosed with HIT locally were acquired. This patient had a clinical history consistent with classical HIT and an ELISA OD of 3.3 measured in the clinical laboratory. Serum from this patient (hereby referred to as patient 12) was found to be strongly activating and in some donors, there was evidence of heparin-independent activation. Ruxolitinib had no effect on aggregation to this serum in the presence of PF4 (Figure 4.10C).

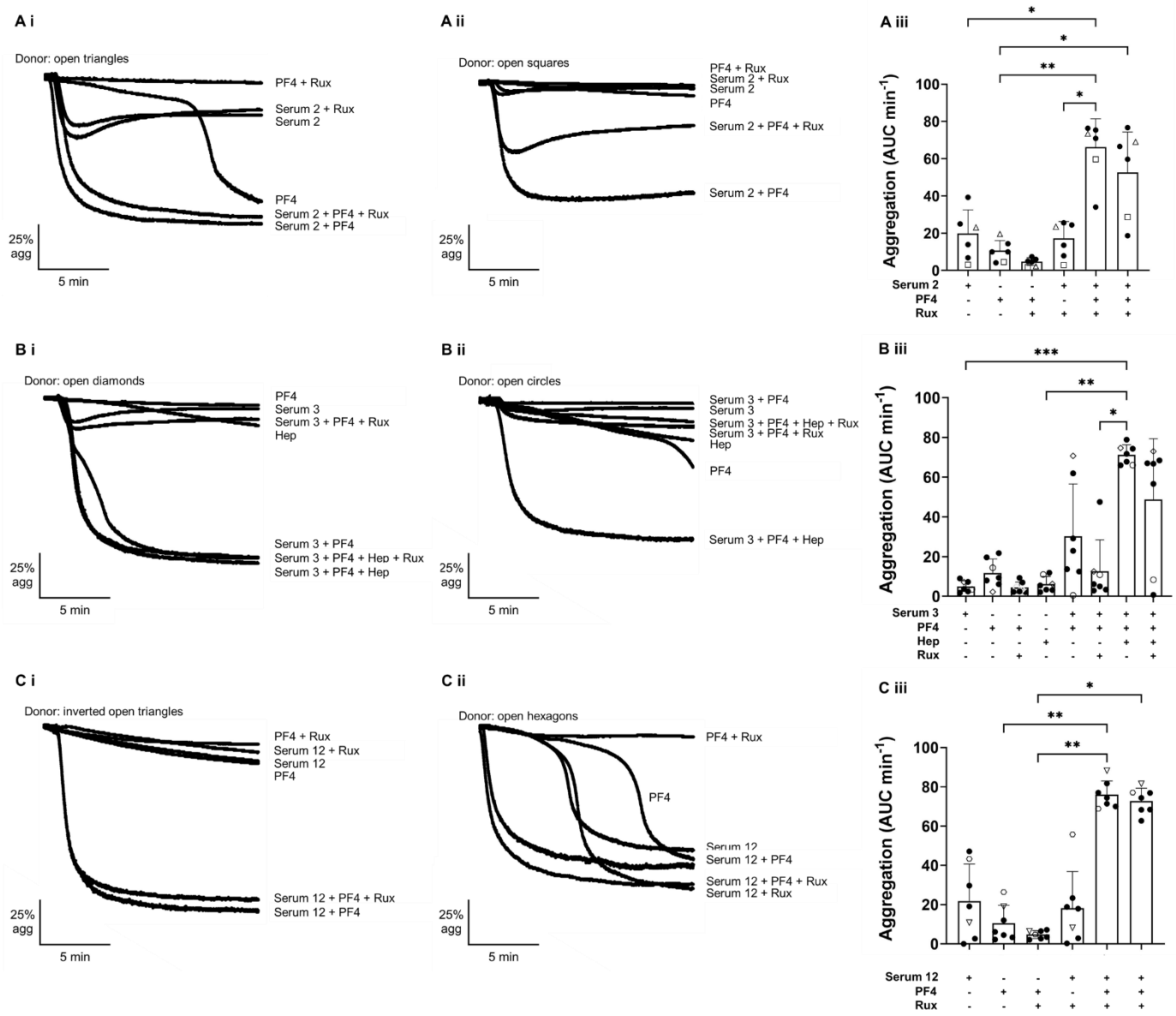
A i
Donor: open triangles
PF4 + Rux
Serum 2 + Rux
Serum 2
PF4
Serum 2 + PF4 + Rux
Serum 2 + PF4
25% agg
5 min
A ii
Donor: open squares
PF4 + Rux
Serum 2 + Rux
Serum 2
PF4
Serum 2 + PF4 + Rux
Serum 2 + PF4
25% agg
5 min
A iii
Aggregation (AUC min-1)
Serum 2
PF4
Rux
B i
Donor: open diamonds
PF4
Serum 3
Serum 3 + PF4 + Rux
Hep
Serum 3 + PF4
Serum 3 + PF4 + Hep + Rux
Serum 3 + PF4 + Hep
25% agg
5 min
B ii
Donor: open circles
Serum 3 + PF4
Serum 3
Serum 3 + PF4 + Hep + Rux
Serum 3 + PF4 + Rux
Hep
PF4
Serum 3 + PF4 + Hep
25% agg
5 min
B iii
Aggregation (AUC min-1)
Serum 3
PF4
Hep
Rux
C i
Donor: inverted open triangles
PF4 + Rux
Serum 12 + Rux
Serum 12
PF4
Serum 12 + PF4 + Rux
Serum 12 + PF4
25% agg
5 min
C ii
Donor: open hexagons
PF4 + Rux
PF4
Serum 12 + PF4
Serum 12 + PF4 + Rux
Serum 12 + Rux
25% agg
5 min
C iii
Aggregation (AUC min-1)
Serum 12
PF4
Rux

Figure 4.10. The effect of ruxolitinib on platelet aggregation to HIT sera.

Platelet aggregation was assessed by LTA. (A) Pre-warmed platelets (2×10^8/mL) at 37°C were incubated with ruxolitinib 100 nM (Rux) or vehicle control (DMSO 0.01%) for 5 min, then PF4 or vehicle control (PBS) for 5 min, then PF4 10 µg/mL or vehicle control (PBS) for 5 min. Platelets were then stirred at 1200 rpm for an additional minute before addition of serum (1% final concentration). (Ai and Aii) Representative aggregation traces for two donors (Ai: open triangles in Aiii; Aii: open squares in Aiii). (Aiii) Quantification of aggregation (area under curve per minute [AUC min^{-1}]) for 15 min (n=4). Responses for individual donors are denoted by consistent shapes (e.g. open squares). (B) As for A but platelets also pre-incubated with heparin 0.5 IU/mL or vehicle control (PBS) for 5 min after incubation with PF4 or vehicle control, and serum 3 used instead of serum 2. (C) As for A but serum 12 used instead of serum 2). Statistical testing of differences by one-way ANOVA (A) and Friedman test (B) and (C). *P < .05, **P < .01, ***P < .001.

4.2.7. Inhibition of heparin-PEAR1 interaction reduces platelet aggregation to HIT antibodies and sera

Clearly, a key component of immune complexes in HIT is heparin. Heparin is formed of heavily sulphated repeating disaccharide units and is known to activate platelets directly through interaction with PEAR1 (Kardeby et al., 2023). Thus, it was hypothesised that this interaction may also have a role in platelet activation in HIT.

In order to study the additive effect of heparin, it was necessary to identify a way to block only the heparin-PEAR1 component whilst having no effect on FcγRIIA-mediated activation. The ligation of PEAR1 by heparin induces signalling through PI3K p110β isoform which can be blocked by the inhibitor TGX-221 (Kardeby et al., 2023). However, PI3Kβ also mediates platelet activation via FcγRIIA and TGX-221 was observed to abrogate platelet aggregation to crosslinked IV.3 (Figure 4.11). Moreover, this would also be expected to have an effect on activation of c-Mpl by PF4 as the pan-PI3K inhibitor wortmannin blocks activation to PF4, and TPO-induced platelet potentiation has been previously reported to be mediated by PI3Kβ (Moore et al., 2019).

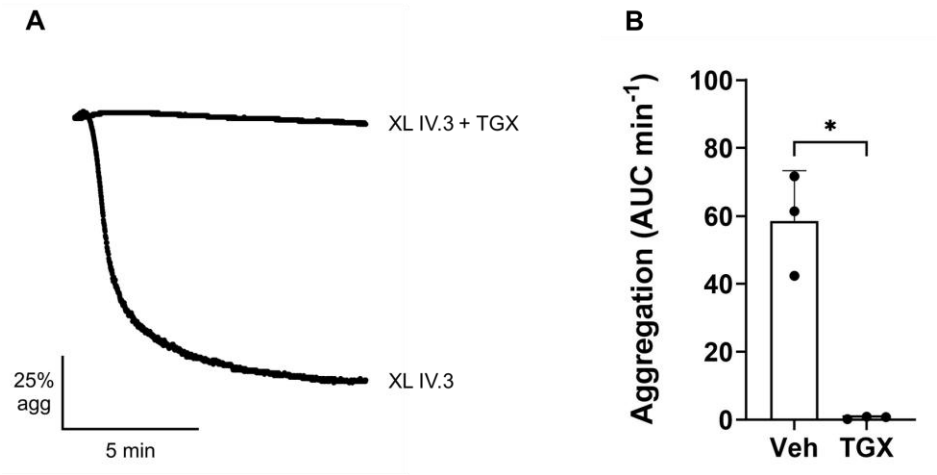

Figure 4.11. Inhibition of PI3Kβ with TGX-221 blocks platelet aggregation to an agonist of FcγRIIA.

Pre-warmed platelets (2×10^8/mL) at 37°C were pre-incubated with TGX-221 500 nM (TGX), or vehicle control (DMSO 0.01%) (Veh) for 5 min, then IV.3 1 µg/mL for 5 min, then stirred at 1200 rpm for 1 min before addition of goat anti-mouse IgG (30 µg/mL). (A) Representative aggregation traces. (B) Quantification of aggregation (area under curve per minute [AUC min^{-1}] for 10 min, n=3). Statistical testing of difference by paired t-test. *P < .05.

Raising antibodies against the whole PEAR1 receptor would be expected to be an inadequately targeted reagent as PEAR1 is also activated by platelet-platelet contact through its small, extracellular EMI domain (Kauskot et al., 2012). Thus, the Birmingham platelet group has developed a nanobody (Nb138) which was raised against the heparin binding 13th EGF-like domain of PEAR1. This was previously shown to block activation of platelets to a heparin-sulfate proteoglycan molecule (Martin et al., 2024; Kardeby et al., 2023) and was therefore used in the following experiments. The nanobody was produced in-house by Dr Eleyna Slater, Dr Rachel Lamerton, University of Birmingham and visiting medical student Hugo Lagonotte (Université de Tours, France).

On its own, heparin (0.5 IU/mL) induces aggregation, which is characterised by a slow initial phase, then in some donors, a more rapid, second phase leading to >50% aggregation (Figure 4.12A). This is consistent with the pattern of aggregation that has been previously described (Kardeby et al., 2023). Nb138 did not induce platelet aggregation on its own and reduced aggregation to heparin at low nanomolar concentration, with significant blockade at 100 nM

(Figure 4.12A). Nb138 had no effect on platelet aggregation to cross-linked IV.3 demonstrating, as expected, no effect on platelet activation through FcγRIIA (Figure 4.12B). Previously, Nb138 was also shown to have no effect on platelet aggregation to collagen and reduced Akt phosphorylation downstream of heparin-induced PEAR1 activation (Kardeby et al., 2023). Further evidence that Nb138 specifically binds PEAR1 is detailed in a previous manuscript showing strong binding of monovalent Nb138 to PEAR1 by surface plasmon resonance (K_D 14.2 nM) (Martin et al., 2024).

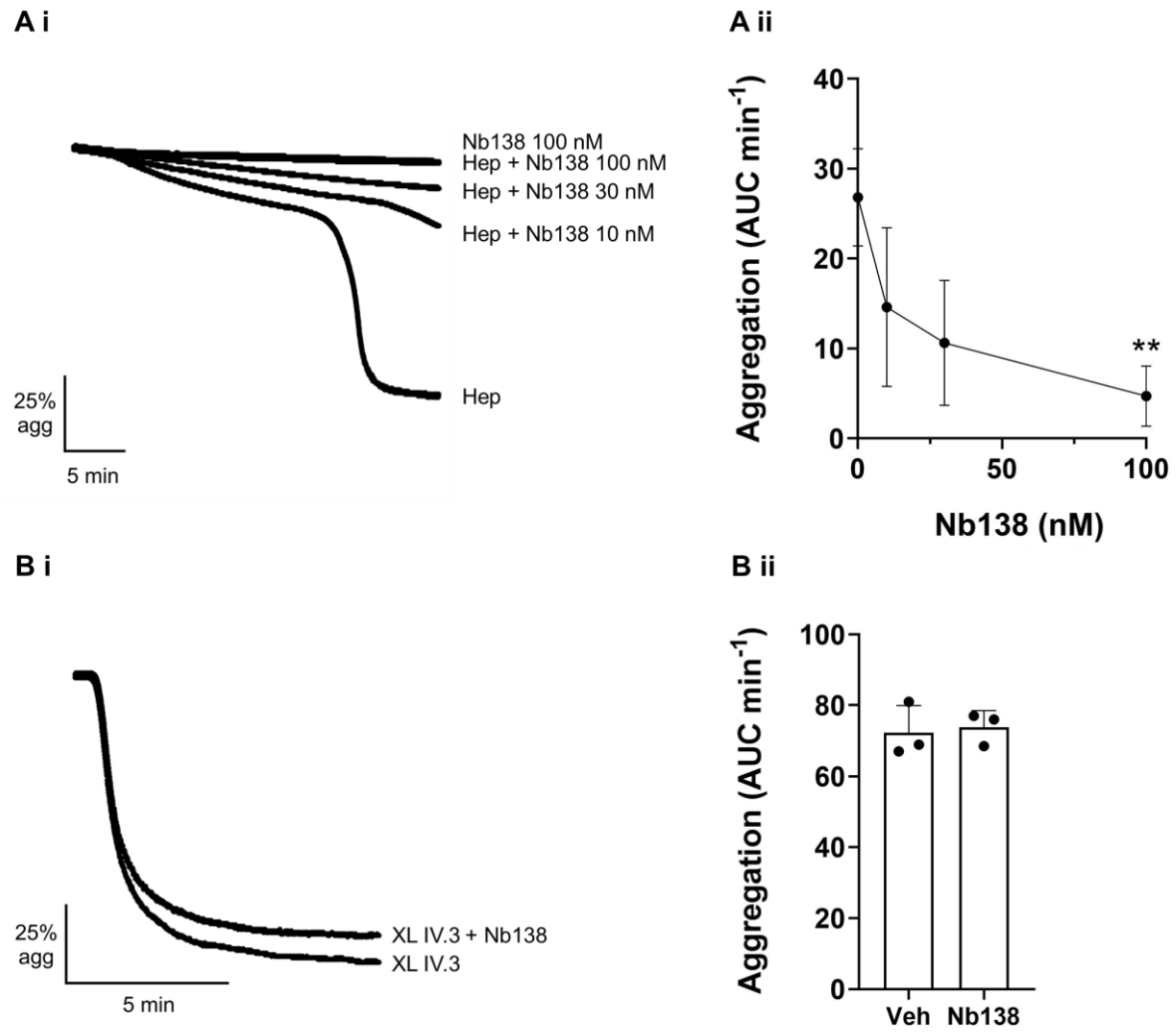

Figure 4.12. PEAR1 inhibitory nanobody 138 blocks heparin-induced aggregation but not FcγRIIA mediated aggregation by crosslinked IV.3.

(A) Pre-warmed platelets (2×10^8/mL) at 37°C were incubated with nanobody 138 100 nM (Nb138), or vehicle control (PBS) (Veh) for 5 min, then stirred at 1200 rpm for 1 min before addition of heparin 0.5 IU/mL. (Ai) Representative aggregation traces. (Aii) Quantification of aggregation (area under curve per minute [AUC min^{-1}] for 30 min, n=3). Statistical testing of difference by one-way ANOVA. (B) As for A but after pre-incubation with nanobody, platelets were incubated with IV.3 1 µg/mL for 5 min, then stirred at 1200 rpm for 1 min before addition of goat anti-mouse IgG (30 µg/mL) (crosslinked IV.3 [XL IV.3]). Aggregation measured for 10 min. Statistical testing of difference by paired t-test. **P < .01.

Thus, experiments were conducted using healthy donors' platelets, Nb138, heparin, 5B9, and patient sera to investigate the role of the heparin-PEAR1 interaction in platelet activation in HIT. Given the well described variation in healthy donors' platelet responses to HIT sera (Warkentin et al., 1992), only donors where the combination of 5B9 or serum with heparin 0.5 IU/mL resulted in >50% aggregation within 30 min were included (each donor assessed separately for each unique agonist – 5B9, and various sera). The other HIT-like monoclonal antibody (mAb), KKO, does not activate platelets in the presence of heparin, without exogenous PF4, and so was not used for these experiments.

In the following experiments, quantification of aggregation is shown in Figure 4.13. Given the marked variability in responses of donor platelets in these experiments, aggregation traces for all 7 donors are shown separately in Figure 4.14. As previously described, 5B9 alone does not stimulate platelet aggregation but does so when combined with heparin (Figure 4.13Ai and Figure 4.14A). Unlike with 5B9 and PF4, aggregation to 5B9 in the presence of heparin is often delayed by several minutes (Figure 4.13Ai and Figure 4.14A). Pre-incubation of platelets with Nb138 led to a non-significant reduction in aggregation as measured by AUC min^{-1} (Figure 4.13Ai). In the seven donors, Nb138 blocked aggregation completely in two, delayed aggregation by > 20 min in one and delayed by 2-4 min in three. Aggregation in one donor was unaffected. To better quantify the delay in aggregation, time to 50% aggregation was calculated and results are shown in Figure 4.13Aii which shows a significant delay in time to 50% aggregation. Next, serum 3 was used instead of 5B9 with similar results. Pre-incubation of platelets with Nb138 led to a block of aggregation in four donors and delay of about 5 min in the remaining three (Figure 4.13B and Figure 4.14B). With serum 12, Nb138 did not block aggregation in any donors but did significantly delay aggregation, with a delay of over 2 min observed in 6 of 7 donors (Figure 4.13C and Figure 4.14C). Notably, there was no effect of Nb138 in the 3 donors where serum 12 alone resulted in aggregation over 50% (Figure 4.13Cii).

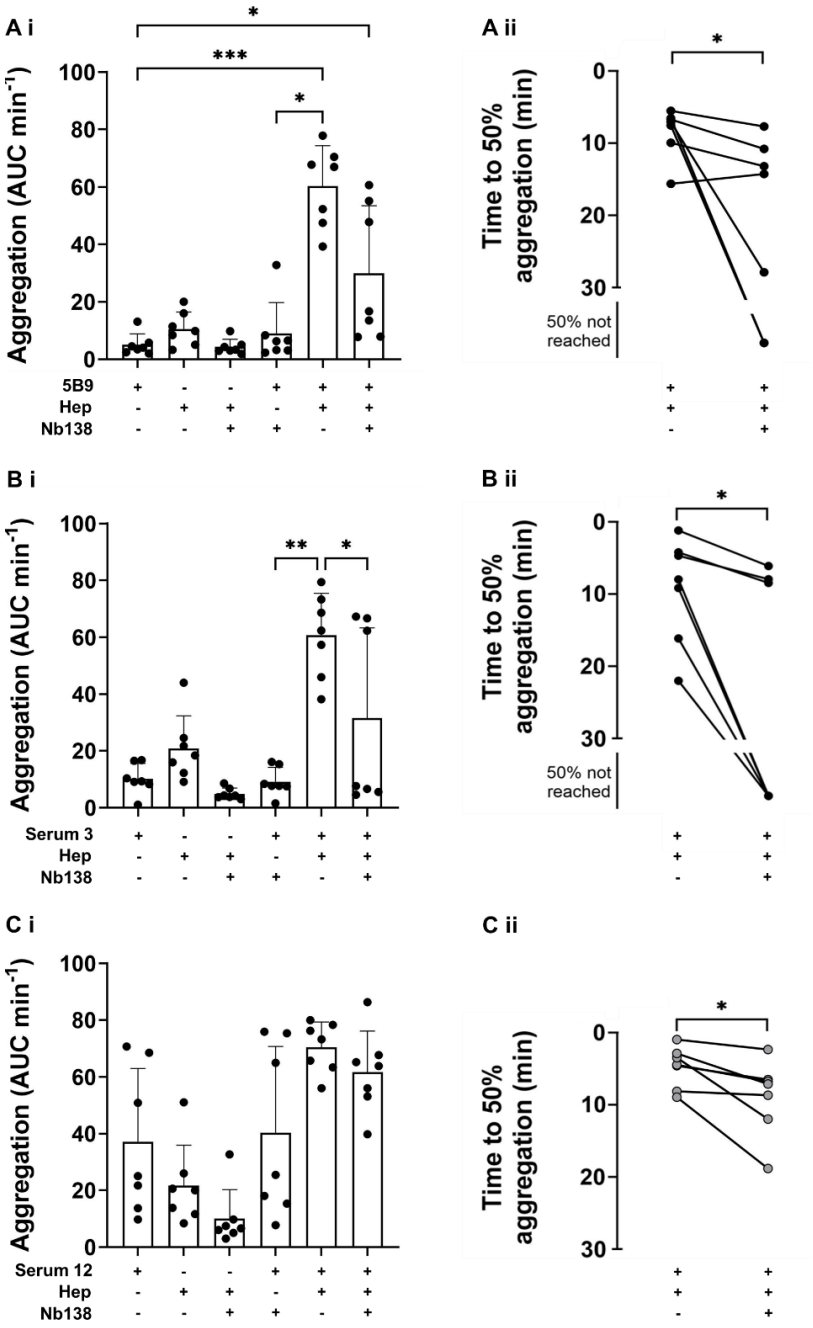

Figure 4.13. Blockade of the PEAR1-heparin interaction with nanobody 138 reduces platelet aggregation to a HIT-like mAb and HIT sera.

(A) Pre-warmed platelets (2×10^8/mL) at 37°C were incubated with nanobody 138 100 nM (Nb138), or vehicle control (PBS) for 5 min, heparin 0.5 IU/mL (Hep) or vehicle control (PBS) for 5 min, then stirred at 1200 rpm for 1 min before addition of 5B9 20 µg/mL. (Ai) Quantification of aggregation (area under curve per minute [AUC min^{-1}] for 30 min, n=7). Statistical testing of differences by Friedman test. (Aii) Quantification of speed of aggregation as measured by time to 50% aggregation in min showing change in responses for individual donors as joined circles. Statistical testing of difference by paired t-test. (B) As for A but serum 3 (3.3% final concentration) used instead of 5B9. (C) As for B but serum 12 (1%) final concentration used instead of serum 3. For C, points are shown in filled grey circles to show separation as points are closely overlaid. *P < .05, **P < .01, ***P < .001.

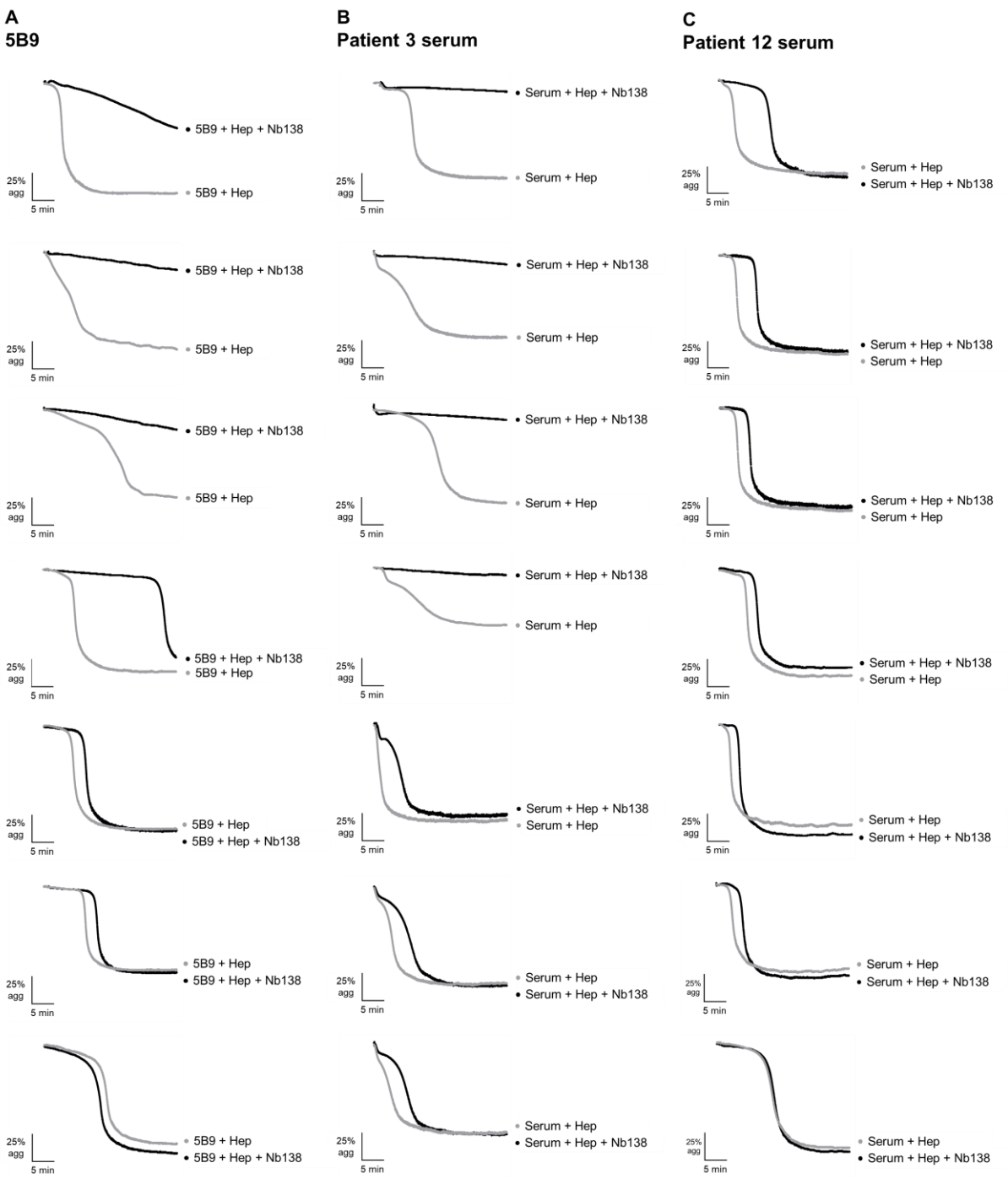

Figure 4.14. Aggregation traces showing that nanobody 138 blocks or delays aggregation to HIT-like mAb and HIT sera.

As for Figure 4.13 but showing aggregation traces for 5B9 or sera with heparin (Hep) (grey traces) compared to the platelets pre-incubated with nanobody 138 (Nb138) (black traces) for all donors. Aggregation measured over 30 min. N=7 for each agonist.

4.2.8. Inhibition of heparin-PEAR1 interaction reduces platelet activation in a flow-cytometry based HIT assay

Whilst LTA is a recognised diagnostic test for HIT, it is not as sensitive as other methods (Arachchillage et al., 2023). As discussed in Chapter 1, the gold standard functional assay is the serotonin release assay (SRA) but has technical challenges and is not established in England (Arachchillage et al., 2023). Flow-cytometry based assays do however have similar sensitivity and specificity as the SRA (Tardy-Poncet et al., 2021) and as such, this approach is used by the UK reference laboratory for diagnosis of HIT (National Health Service Blood and Transplant, 2023). The effect of Nb138 on platelet activation in a flow cytometry-based assay was therefore investigated. The assay was based on the volumes of methods of the commercially available HITAlert assay (IQ Products, n.d.). In the in-house assay, P-selectin expression was used as a marker of α-granule release and thus platelet activation. The assay was however modified to use reduced volumes of sera to conserve this resource and used washed platelets instead of PRP to increase the sensitivity given the reduced volume of serum. The heparin concentration used in the following assays, 0.5 IU/mL, is the same as that used in the HITAlert assay, mirrors the concentration used in LTA above, and is consistent with the ranges used and recommended by others (Vayne et al., 2020; Arachchillage et al., 2023). An hour incubation at RT under gentle agitation was also used to reflect the protocol of the HITAlert assay.

First, Nb138 100 nM was shown to have no activating effect on platelets consistent with the observations in LTA. Heparin 0.5 IU/mL stimulated P-selectin expression which was significantly reduced by Nb138 (Figure 4.15).

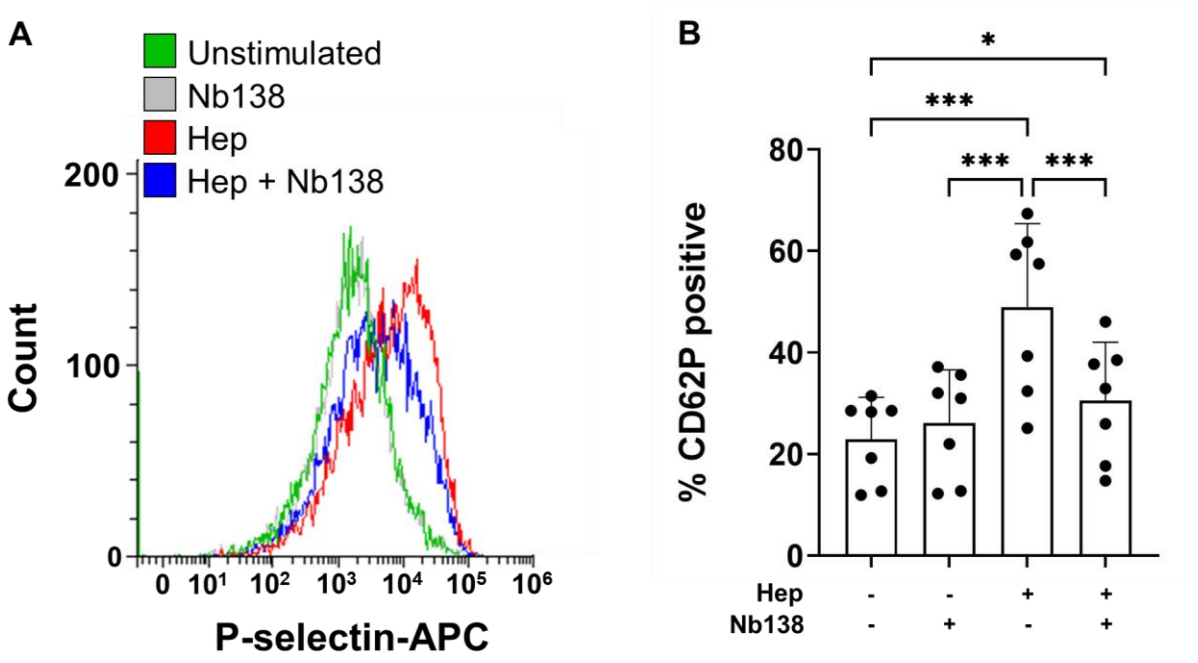

Figure 4.15. Nanobody 138 reduces P-selectin expression in response to heparin.

Platelets (1×10^8/mL) were gently agitated at RT for an hour with Nanobody 138 100 nM (Nb138) or vehicle control (PBS) and/or heparin 0.5 IU/mL (Hep) or vehicle control (PBS), then stained with APC-anti-P selectin antibody and analysed by flow cytometry. (A) Representative histogram. (B) Quantitation of P-selectin expression by percentage positive cells relative to isotype control. Statistical testing of differences by one-way ANOVA. *P < .05, ***P < .001.

To investigate the effect of Nb138 on platelet activation in the HIT flow cytometry assay, platelet donors were excluded if they did not have a greater than two-fold change from baseline in median fluorescence intensity with 5B9 or sera in the presence of heparin. In contrast to LTA where 5B9 alone was never observed to cause any aggregation (Figure 4.13), stimulation with 5B9 alone led to a small but significant increase in P-selectin expression (mean increase from unstimulated: 15 percentage points, Figure 4.16A). This was markedly increased with the addition of heparin (mean increase from unstimulated: 40 percentage points) and the increased activation was significantly reduced by Nb138 (mean decrease from 5B9 + heparin: 15 percentage points, Figure 4.16A). Similar findings were observed with serum 3 which, without additional heparin, led to a mean increase of 21 percentage points from unstimulated (Figure 4.16B). Serum with heparin resulted in a mean 30 percentage points increase from unstimulated and there was a 12 percentage points mean reduction in this with Nb138 (Figure 4.16B). With serum 12, there was a mean 33 percentage points increase from unstimulated, a mean 45 percentage points increase with serum + heparin, and a mean 18 percentage points reduction from serum + heparin with the addition of Nb138 although this reduction was not statistically significant (Figure 4.16C).

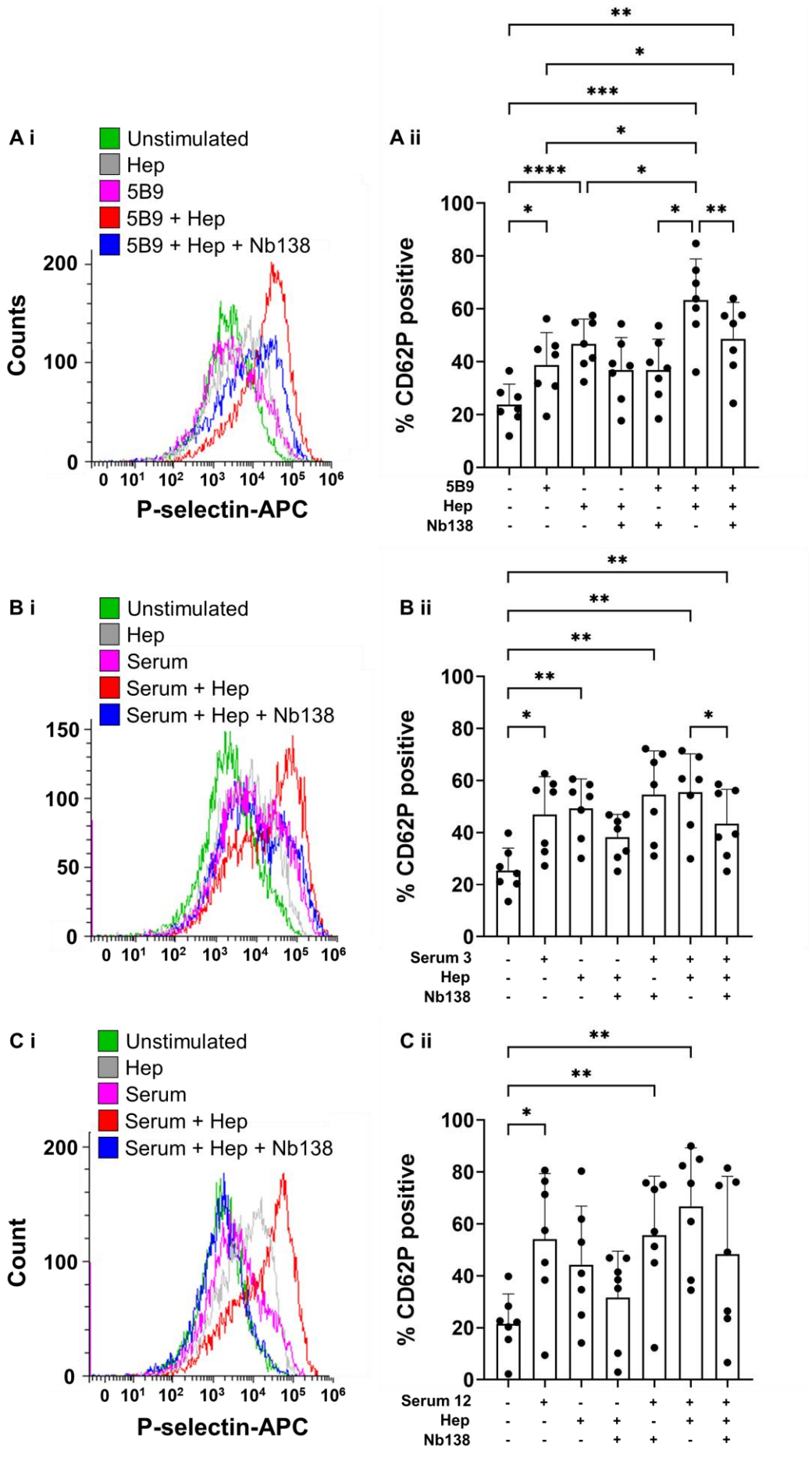
A i
Unstimulated
Hep
5B9
5B9 + Hep
5B9 + Hep + Nb138
Counts
P-selectin-APC
A ii
% CD62P positive
5B9
Hep
Nb138
B i
Unstimulated
Hep
Serum
Serum + Hep
Serum + Hep + Nb138
B ii
% CD62P positive
Serum 3
Hep
Nb138
C i
Unstimulated
Hep
Serum
Serum + Hep
Serum + Hep + Nb138
Count
P-selectin-APC
C ii
% CD62P positive
Serum 12
Hep
Nb138

Figure 4.16. Nanobody 138 reduces P-selectin expression in response to HIT-like mAb and HIT sera in the presence of heparin.

Platelets (1×10^8/mL) were gently agitated at RT for 1 hour with nanobody 138 100 nM (Nb138) or vehicle control (PBS) and/or heparin 0.5 IU/mL (Hep) or vehicle control (PBS) and/or 5B9 20 µg/mL or vehicle control PBS, then stained with APC-anti-P selectin antibody and analysed by flow cytometry. (Ai) Representative histograms showing difference between unstimulated control, 5B9 + Hep and 5B9 + Hep + Nb138. (Aii) Quantification of activation by percentage of cells positive for P-selectin relative to isotype control. Statistical testing of differences by one-way ANOVA. (B) As for A but using serum 3 (3.3% final concentration) instead of 5B9. (C) As for B but using serum 12 (1%) final concentration instead of serum 3. *P < .05, **P < .01, ***P < .001, ****P < .0001.

The above findings demonstrate a role for heparin-induced activation of platelets via PEAR1 in diagnostic HIT assays. As inhibitors of FcγRIIA and downstream signalling are proposed as therapies for HIT (Müller et al., 2024) this additional mechanism of platelet activation may need to be accounted for when developing and deploying novel therapies. The mouse anti-human FcγRIIA antibody IV.3 is well-described to block FcγRIIA-mediated aggregation at 10 µg/mL concentration (Arman et al., 2014; Smith et al., 2021; Lee et al., 2024) but as this would not be expected to block the heparin component of the activation, blockade of PEAR1 might also be required for maximal inhibition. This was further investigated by both LTA and flow cytometry using the assays and reagents (5B9, serum 3, serum 12 and heparin) described above.

With 5B9 and 0.5 IU/mL heparin, IV.3 led to a reduction in aggregation but only with the addition of Nb138 was this reduction significant (Figure 4.17Aii). The additional effect was most marked in three donors, one of which is shown as a representative aggregation trace in Figure 4.17Ai. This finding was mirrored when platelet activation was measured by flow cytometry (Figure 4.17Aiii). With IV.3 alone, there was a mean reduction of 11 percentage points from 5B9 with heparin but with the addition of Nb138, there was a significant reduction (mean reduction 26 percentage points). With serum 3, there was no significant additional effect of nanobody, although in one donor there was a marked effect in LTA (Figure 4.17Bi). With serum 12, there was again no significant effect in LTA but in flow cytometry, only IV.3 with Nb138 (not IV.3 alone) showed a significant reduction from serum with heparin (mean

reduction 40 percentage points). These data suggest that in some circumstances, blockade of FcγRIIA is insufficient to fully inhibit platelet activation, an observation that may have translational implications that are discussed later.

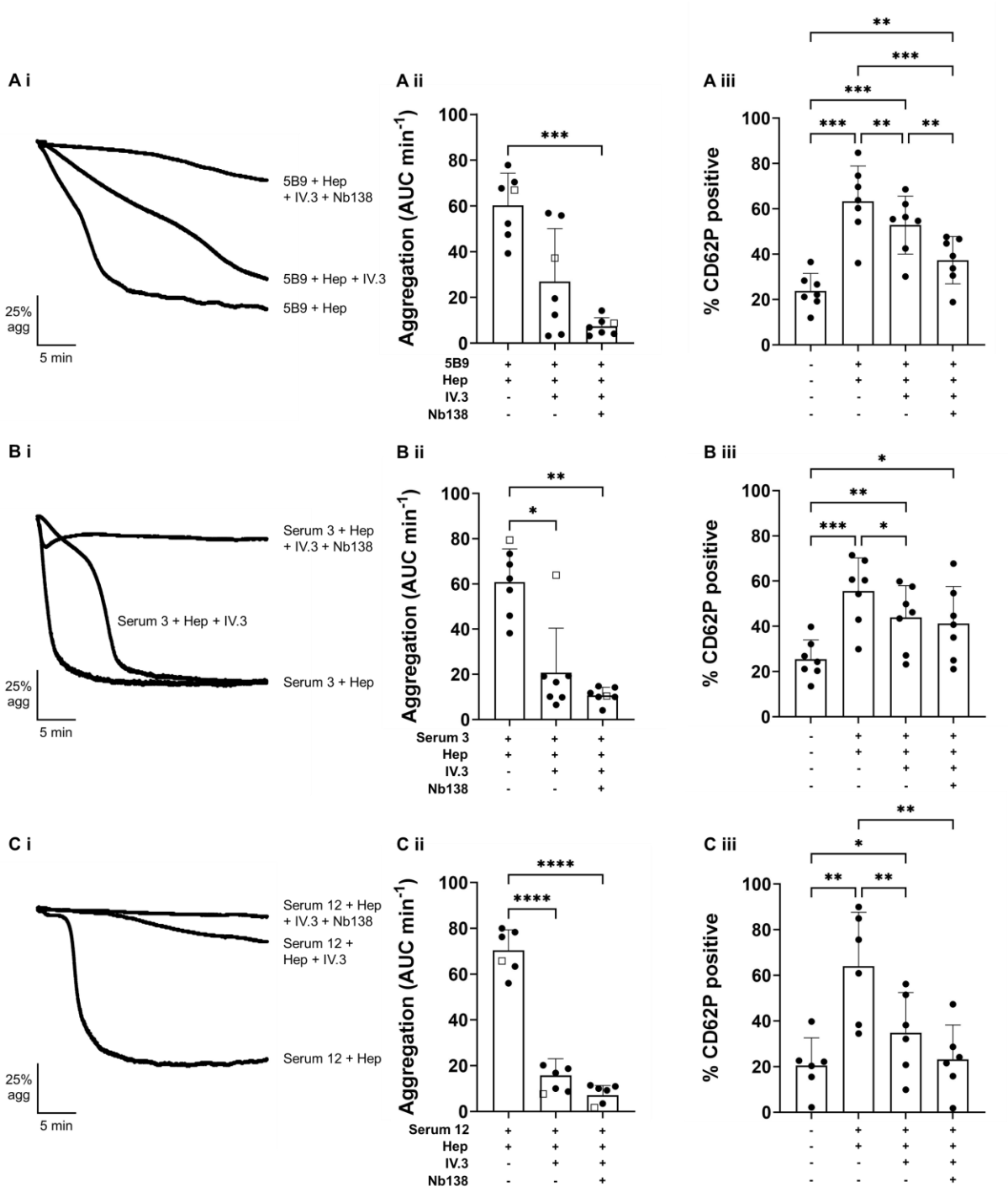

Figure 4.17. Maximal blockade of platelet activation to some HIT reagents requires both inhibition of FcγRIIA and PEAR1.

(Ai-ii) Pre-warmed platelets (2×10^8/mL) at 37°C were incubated with IV.3 10 µg/mL or vehicle control (PBS) and nanobody 138 100 nM (Nb138) or vehicle control (PBS) for 5 min, heparin 0.5 IU/mL (Hep) for 5 min, then stirred at 1200 rpm for 1 min before addition of 5B9 20 µg/mL. (Ai) Representative aggregation trace for donor denoted by open squares in Aii. (Aii) Quantification of aggregation (area under curve per minute [AUC min^{-1}] for 30 min, n=7). Statistical testing of differences by one-way ANOVA. (Aiii) Platelets (1×10^8/mL) were gently agitated at RT for 60 min with IV.3 10 µg/mL or vehicle control (PBS), nanobody 138 100 nM (Nb138) or vehicle control (PBS) heparin 0.5 IU/mL (Hep) or vehicle control (PBS) and 5B9

20 µg/mL or vehicle control (PBS), then stained with APC-anti-P selectin antibody and analysed by flow cytometry. Quantification of activation by percentage of cells positive for P-selectin according to comparison with isotype control. Statistical testing of differences by one-way ANOVA. (B) As for A but serum 3 (3.3% final concentration) used instead of 5B9. (C) As for B but serum 12 (1%) final concentration used instead of serum 3 and n=6. *P < .05, **P < .01, ***P < .001, ****P < .0001.

4.3. Discussion

The key findings in this chapter are:

1. The PF4-c-Mpl interaction contributes to platelet activation in VITT and can be blocked by JAK2 inhibition.
2. Blockade of PF4-c-Mpl interaction does not significantly reduce platelet activation in HIT.
3. The heparin-PEAR1 interaction contributes to platelet activation in HIT and can be blocked by an inhibitory PEAR1 nanobody.

The activation of platelets by HIT sera has been known to occur through FcγRIIA since 1988 (Kelton et al., 1988) and although several other mechanisms of thrombosis including activation of neutrophils and monocytes, NETosis, and prevention of vWF cleavage have been identified, until now, no other direct mechanism of platelet activation by immune complexes has been demonstrated. Although platelets are vital in the pathophysiology of HIT and VITT, leukocyte activation and NETosis is a key driver of thromboinflammation (Arepally and Padmanabhan, 2021; Gollomp et al., 2018). Nevertheless, the demonstration of platelet activation is crucial in diagnostic assays of HIT and VITT, and as such the findings in this chapter could at least be considered as variables in these assays and may contribute to the well-described phenomenon of significant variability in healthy donors' platelet responses to FcγRIIA agonists (Warkentin et al., 1992).

4.3.1. PF4-c-Mpl interaction contributes to platelet activation in VITT

The data in the first section of this chapter demonstrate that the signalling role of PF4 through c-Mpl can contribute to platelet activation. However, these experiments were carefully designed to increase the likelihood of finding an effect. The sera that were used were selected as they were moderately activating (Montague et al., 2022) and the experiments were further refined by using a bespoke concentration of serum for each healthy donor such that weak-

moderate aggregation could be induced and that both enhancement by PF4 and blockade by ruxolitinib could be observed.

Although care was taken to use the lowest possible concentration of ruxolitinib, high concentrations of JAK2 inhibitors have been previously shown to impact collagen-mediated platelet activation (Parra-Izquierdo et al., 2022). Thus, an effect of ruxolitinib on the signalling downstream of FcγRIIA remains a possibility. Ruxolitinib at 100 nM had no effect on aggregation to crosslinked IV.3 but this is a powerful stimulus that could feasibly overcome any weak inhibitory effect. The polyclonal anti-c-Mpl antibody recapitulated the effect of ruxolitinib on aggregation to VITT IgG with PF4 but due to the scarcity of VITT sera, the effects of this on sera was not tested.

Nevertheless, the findings may have physiological relevance as the potentiating effect of PF4 could extend the effective window of concentration through which VITT antibodies can cause platelet activation. As antibody levels rise in the early stages of the disease, this could bring forward in time the occurrence of platelet activation and extend the window as levels recede. Still, isolated VITT IgG, in the presence of PF4, results in rapid, strong aggregation and ruxolitinib reduces aggregation. However, although it induces robust functional responses, the isolated VITT IgG is probably still a much weaker FcγRIIA agonist than crosslinked IV.3 and the VITT-like monoclonal antibody 1E12. 1E12 stimulates platelets without additional PF4 presumably as its high affinity (Vayne et al., 2021a) enables significant complex formation with the low level of PF4 bound to the surface of platelets. Subsequent work performed in the group which is as yet unpublished, has shown that PF4 potentiates platelet activation to lower concentrations of 1E12, but this is not blocked by ruxolitinib. Although it is possible that another unknown mechanism is involved, a reasonable interpretation is that as long as there is enough PF4 and 1E12 to form sufficient immune complexes, the activation occurs solely through FcγRIIA with this reagent. Supporting this, 1E12 induces clear phosphorylation of bands at ~45 kDa consistent with FcγRIIA phosphorylation (Figure 4.7), whilst this is not visible with lysates from platelets stimulated with VITT IgG and PF4. Of course, immunoprecipitation

of FcγRIIA and western blotting for tyrosine phosphorylation would be needed to confirm these findings. Another possible reason for the weaker effect of isolated VITT IgG is that the presence of other bystander immunoglobulins could bind to and block FcγRIIA. Isolation of anti-PF4 antibodies from patients with VITT is an approach that should be considered for further investigations, although the use of a whole IgG fraction better reflects pathophysiological reality.

4.3.2. Involvement of PF4 and heparin in platelet activation in heparin-induced thrombocytopenia

The findings discussed above were next applied to HIT where it was hypothesised that PF4 would similarly contribute to platelet activation. Although there was no consistent effect of ruxolitinib, there was a noticeable effect in occasional donors across all three HIT sera that were used. The use of LTA in these experiments has both strengths and limitations. On one hand it provides granular information on the timing, and thus strength, of response – and therefore differentiates well between activating sera. But, on the other hand, it is poorly sensitive – strongly activating sera are required to produce aggregation, particularly in HIT without the presence of additional PF4. The flow cytometry-based assay that was used with Nb138 for the investigation of the role of heparin could have been deployed here but this was not explored due to the lack of convincing signal of an effect of ruxolitinib in the LTA assays. Another limitation is the use of ruxolitinib as the inhibitor as this does not inhibit any possible enhancement of avidity that is imparted by the PF4-c-Mpl interaction. To disrupt this, blockade of the c-Mpl receptor is required but this was not pursued due to the shortcomings in the available c-Mpl blocking antibody. Again, this could be a focus of future studies.

Immune complexes in HIT obviously differ from VITT as they contain heparin and as such, there is an additional interaction to consider. Heparin is known to activate platelets through PEAR1 (Kardeby et al., 2023) a platelet ITAM receptor, against which the laboratory has previously generated nanobodies (Martin et al., 2024). Nanobodies are versatile tools that can be linked to produce multivalent ligands that activate platelets but monovalent nanobodies are

extremely useful as specific inhibitors of receptors (Martin et al., 2024). In the above studies, monovalent Nb138 was used to investigate the role of the heparin-PEAR1 interaction in platelet activation in HIT. Although PEAR1 and c-Mpl are present in platelets at similar amounts (1,600 to 1,800 copies per platelet), only two agonists of c-Mpl are known. TPO and PF4 – and both induce slow aggregation and, whilst heparin-induced platelet aggregation curve is similar in shape to that of PF4 and TPO, other agonists of PEAR1 such as fucoidan are capable of inducing rapid and strong aggregation (Kardeby et al., 2019). Furthermore, PEAR1 has been reported to become tyrosine phosphorylated on platelet contact and is thus a platelet aggregate-stabilising receptor (Nanda et al., 2005; Kauskot et al., 2012). Finally, as heparin is a long, flexible ligand, it may have more chance of interacting with PEAR1 whilst bound in an immune complex than PF4 would do with c-Mpl. For these reasons, the heparin-PEAR1 interaction could be considered more likely than PF4-c-Mpl to play a role in activation.

The data demonstrate that heparin may well be an underappreciated variable in functional, diagnostic HIT assays and this may also contribute to the variation in donor platelet responses in these assays. In two distinct assays, there was a clear effect, most marked with the HIT-like monoclonal antibody, 5B9, whereby pre-incubation of platelets with Nb138 reduces platelet activation. This was also shown with two HIT sera, one of which exhibits heparin-independent activity. The results in LTA are most illuminating. Unlike the effect of inhibiting the PF4-c-Mpl interaction which never completely blocked, but limited the amplitude of aggregation, blockade of PEAR1 seems to either completely block aggregation or delay its onset. This is a curious finding indicating that the mechanisms by which PF4 and heparin potentiate activation are different with combinations of the aforementioned mechanisms at play.

There are however several limitations to the findings. Firstly, these experiments have all been conducted in washed platelets whilst diagnostic assays including the HITAlert flow-cytometry based assay use PRP. Further, only P-selectin was used as a readout for activation; other markers such as annexin-V binding for PS exposure are also used clinically and effects on

this could be assessed. It was recently reported that imaging flow cytometry could also be used in the diagnosis of HIT with high sensitivity and specificity (Carré et al., 2024) and it would be interesting to investigate the effects of blocking the various pathways on platelet morphology. The reason for the use of washed platelets in the present study was to increase the sensitivity of the assays, increasing the likelihood of seeing reasonable platelet activation that could then be inhibited with Nb138. This enhanced sensitivity also means that less serum could be used – these were extensive experiments using a finite amount of strongly activating patient sera and thus the experiments were optimised to conserve this precious resource. The use of washed platelets also better standardises the assays and importantly the gold-standard diagnostic SRA also uses washed platelets. It would therefore be interesting to assess the effect of Nb138 in the SRA and HIPA as well as in assays such as flow cytometry and LTA using PRP. One may anticipate that performing the same experiments with PRP may quench the effect of heparin and is a line of investigation that could be pursued. A further limitation of the experiments is that a single concentration of “low-dose” heparin of 0.5 IU/mL is used which is on the upper limit of the recommended concentration range for HIT assays (Arachchillage et al., 2023). This is also higher than the 0.1 to 0.3 IU/mL range used in the SRA (Warkentin et al., 2015) but remains consistent with the concentration used in the HITAlert, flow-cytometry based assay (IQ Products, n.d.). It is unknown whether using lower concentrations of heparin would negate the findings. However, rather than there being a simple linear dose relationship between heparin and platelet activation in HIT, the variability in the construction and stoichiometry of HIT immune complexes means that the highest heparin concentration may not in fact be strongest. Indeed, activation to 5B9 is reported to be maximal with heparin 0.1 IU/mL (Kizlik-Masson et al., 2017) and repeating the experiments at a range of heparin concentrations would be beneficial. However, the scarcity of reagents meant the experiments had to be rationalised. Nonetheless, 0.5 IU/mL is within the target therapeutic range of 0.3 to 0.7 IU/mL (Olson et al., 1998) suggesting that the findings may have pathophysiological relevance.

Finally, it was shown that blockade of aggregation by IV.3 is not always enough to maximally inhibit platelet activation in HIT. This may be of translational significance, as it suggests that in the early stages of the disease, when heparin is present, any treatment aimed at stopping platelet activation would also need to block heparin-induced platelet activation via PEAR1. A limitation to these experiments is that only one concentration of IV.3 is used and the effect of increasing the concentration was not assessed, but this is an established concentration used *in vitro* (Padmanabhan et al., 2015; Smith et al., 2021) and is far in excess of doses that have been used *in vivo* (Leung et al., 2024). Further assessment of healthy donors' platelet PEAR1 surface expression and activating responses to a range of PEAR1 stimuli would also be beneficial to ascertain whether there is any correlation between levels and responsiveness to agonists of FcγRIIA.

4.3.3. Mechanisms of contribution by PF4 and heparin to platelet activation

Further work could focus further on the mechanisms by which PF4 and heparin have their effects in HIT and/or VITT. Both may contribute to activation in several ways.

1. Addition of exogenous PF4 and/or heparin contributes to enhanced immune complex formation.
2. Free PF4 binds to and signals through c-Mpl and free heparin binds to and signals through PEAR1 leading to platelet activation, or potentiation of activation through FcγRIIA.
3. PF4 and/or heparin contained in immune complexes activate c-Mpl and PEAR1 respectively.
4. Immune complex-bound PF4 and/or heparin binding to c-Mpl and PEAR1 respectively enhance the avidity of the entire complexes, enhancing platelet activation through FcγRIIA.
5. As previously suggested, PF4 may neutralise repellent negative charge endowed by platelet surface GAGs enabling closer approximation of platelets (Kowalska et al., 2010).

Given that without PF4, VITT IgG could not induce platelet aggregation and that TPO enhanced aggregation to VITT sera but not VITT IgG, the first mechanism is clearly important. Similarly, in HIT, as addition of high concentration heparin classically blocks platelet activation, adding heparin in the right ratio clearly enhances immune complex formation.

The observations that PF4 alone and heparin alone in the concentrations used to enhance activation to HIT and VITT agonists, activate platelets in some donors and lead to phosphorylation of downstream signalling pathways (Kardeby et al., 2023; Buka et al., 2024) suggest that the second mechanism also plays a role, although it is plausible that the additional PF4 and heparin could all be incorporated into immune complexes. However, the observations that PF4 10 µg/mL also potentiates platelet aggregation to low dose CRP provides additional evidence of this mechanism. The ability of PF4 to enhance activation of FcγRIIA by other agonists such as nanobodies, crosslinked IV.3 or anti-CD9 antibody was not explored in this thesis.

The data in this chapter do not provide evidence to specifically support or refute mechanisms 3 or 4 but both are plausible and logical. The additional interactions of PF4 and heparin with their receptors, in addition to the interaction of PF4 with platelet surface GAGs would be expected to enhance the avidity of the entire immune complex binding to platelets. Clearly, as ruxolitinib reduces aggregation, this is not the sole mechanism, but it may contribute. Unfortunately, it is not currently possible to selectively block the downstream signalling of heparin-PEAR1, as TGX-221, which inhibits PI3K p110β, also blocks FcγRIIA-induced activation.

The results of a pilot experiment where lysates from platelets stimulated with VITT IgG and PF4 were Western blotted and stained for phosphotyrosine were shown in Figure 4.7. In the first donor, there was a suggestion of enhancement of bands at 95 kDa (consistent with STAT3, STAT5, and c-Mpl phosphorylation) with the addition of VITT IgG to PF4 but this was not seen in lysates from two additional donors. This suggests that c-Mpl signalling may be strengthened by the immune complex-FcγRIIA interaction, but further work is needed. To

pursue this further, it would be necessary to optimise experimental conditions and stain for phosphorylated c-Mpl, STAT3, STAT5, as well as phosphorylation of immunoprecipitated JAK2 and FcγRIIA in multiple donors. Another option would be to investigate using phospho-flow cytometry either in platelets or transfected cells, which would have the advantage of being higher throughput with the option to have readouts at multiple time points.

There is precedent for activation of multiple receptors by multivalent immune complexes although this area is not well explored. In antiphospholipid syndrome, autoantibodies dimerise β2-Glycoprotein I (β2-GPI, also known as apolipoprotein H [APOH]), a plasma protein. These dimers have been shown to activate platelets through glycoprotein Ibα and apolipoprotein E receptor 2 - two distinct pathways, both of which are required for platelet activation (Urbanus et al., 2008). Coll et al. showed in a conference abstract that anti-β2-GPI antibodies can also activate platelets through FcγRIIA suggesting three possible mechanisms of platelet activation from one immune complex (Coll et al., 2017). This is consistent with another report showing that anti-prothrombin antibodies, another class of antibodies involved in antiphospholipid syndrome, also activate platelets through FcγRIIA (Chayoua et al., 2021).

Further experiments would also require the development of better tools, particularly an inhibitor of c-Mpl tailored to block PF4 binding, as the polyclonal anti-c-Mpl antibody that was used in the above experiments is not well characterised, does not effectively block higher doses of PF4 or TPO, and occasionally appeared to contribute to platelet activation. Nanobodies could be raised against c-Mpl and tested for inhibitory activity against PF4 and TPO. Additionally, multivalent nanobody constructs could be developed as has been done previously for FcγRIIA and PEAR1 to assess for activating potential. More intriguingly, multivalent constructs consisting of nanobodies against two or three receptors could be developed. It is already known that whilst a trivalent FcγRIIA nanobody (three monomers connected by a linker) did not activate platelets, the tetravalent nanobody did (Martin et al., 2024). It would be intriguing to investigate whether a monovalent PEAR1 nanobody linked to

monovalent, divalent, or trivalent FcγRIIA nanobody could activate platelets. Downstream signalling could also be assessed and these nanobodies could also be useful imaging tools.

In conclusion, the data in this chapter demonstrate further complexity in the pathophysiology of the anti-PF4 immunothrombotic syndromes. Synergistic platelet activating effects through c-Mpl and PEAR1 seem to have relevance for diagnostic assays but may also be physiologically relevant mechanisms that should be considered when developing novel therapies.

5. Endothelial activation in HIT and VITT

5.1. Introduction

5.1.1. VITT and cerebral venous sinus thrombosis

When patients began to present with VITT, the frequent occurrence of thrombosis in the cerebral veins was striking (Pavord et al., 2021). In the general population, CVST is rare, occurring at an incidence of 3 to 15 per million people per year (Capecchi et al., 2018). Although most cases are idiopathic, hormonal exposure in oral contraceptives, hormone replacement therapy or pregnancy increases the risk (Bousser and Crassard, 2012). However, in VITT, half of all patients had CVST and in two thirds, this was complicated by secondary haemorrhage with the presence of CVST corresponding with over a doubling of mortality risk (Pavord et al., 2021). In contrast, CVST has been reported to occur in only 1.6% of patients with HIT despite the similar pathophysiology (Aguiar de Sousa et al., 2022).

Since the recognition of VITT, only one manuscript has presented data that has shown pathophysiological differences between patients with VITT and CVST compared to those without CVST. Huynh et al. showed that of 39 patients with VITT, 17 required exogenous PF4 to achieve platelet activation *in vitro* (termed *PF4-dependent*) and 22 had reactivity without additional PF4 (termed *PF4-independent*) (Huynh et al., 2023). The study found that CVST occurred in 11 of 22 patients with PF4-independent antibodies and in only 1 patient with PF4-dependent antibodies. The authors further showed that patients with PF4-independent antibodies had, in addition to VITT antibodies that bound to the heparin-binding site of PF4, additional antibodies that were typical of HIT and bound the poles of PF4. These patients also had significantly stronger binding to PF4 indicative of a higher antibody titre but also suggesting that targeting two sites on PF4 may contribute to stronger binding (Huynh et al., 2023). The term PF4-independent is misleading as these antibodies do require PF4 to work, it is just that *additional* PF4 is not required to be added to the assay to achieve platelet activation. This is presumably because the antibodies can efficiently make use of the little PF4

that is already present within the assay – in the patient serum, and on the surface of donor platelets. As shown previously (Vayne et al., 2021a) and in Chapter 4, the anti-PF4 VITT-like monoclonal antibody, 1E12, can also activate washed platelets in the absence of serum or exogenous PF4 suggesting that residual PF4 on the platelet surface is sufficient.

However, this data only explores why *some* patients with VITT develop CVST, not why CVST is common in VITT but rare in HIT. Thus, the mechanism that links the presence of these PF4-independent antibodies, anti-PF4 antibody epitopes, and CVST is still a mystery. It has been proposed that antibodies against both PF4 epitopes could lead to the formation of larger immune complexes or immune complexes that incorporate more IgG – which can crosslink more Fc receptors (Huynh et al., 2023). Again though, it is unclear how this translates to CVST. Moreover, antibodies targeting two regions on PF4 are seen in autoimmune HIT which is associated with higher rates of thrombosis, but CVST is still uncommon (Warkentin, 2023a), although more reports are required to confirm this.

One further clue stems from observations made by Stegner et al. who treated mice with a monovalent anti-CLEC2 F(ab), *INU1-fab* (Stegner et al., 2022). Although this did not cause platelet activation *in vitro*, when INU1-fab was infused into mice it led to a rapid onset thrombosis, within minutes, specifically affecting the cerebral veins and accompanied by thrombocytopenia. This was in contrast to bivalent INU1 antibody which produced platelet activation *in vitro* and platelet consumption *in vivo* but no such cerebral venous thrombosis. Heparin had a very limited effect on this phenotype but platelet depletion, knockout of CLEC2, and blockade of platelet aggregation by inhibition of integrin $\alpha_{IIb}\beta_3$ prevented cerebral venous thrombosis and death. In anti integrin $\alpha_{IIb}\beta_3$-treated mice, INU1-fab was still detectable at the platelet surface. The authors suggested that these findings indicated that INU1-fab may alter the conformation of CLEC-2 causing it to interact with an unknown ligand in the cerebral veins, and that this process is dependent on integrin $\alpha_{IIb}\beta_3$ to facilitate this interaction. It is difficult to apply these observations directly to VITT, but the findings do show how a platelet-driven

thrombotic process can specifically affect the cerebral veins demonstrating that there is something unique about this anatomic location.

Given the above data, it was hypothesised that characteristics of the cerebral venous endothelium would hold the key for elucidating the mechanisms of CVST in VITT.

5.1.2. Endothelium

The endothelium is a monolayer, consisting of specialised, adaptable endothelial cells that cover all intravascular surfaces in the body. It performs an abundance of critical functions including the maintenance of vascular integrity and control of movement of molecules, regulation of vascular tone, control of haemostasis and thrombosis, control of inflammation, attraction and migration of immune cells, and angiogenesis, among others (Trimm and Red-Horse, 2023). The phenotype of endothelial cells is highly variable with clear differences in gene expression between venous and arterial endothelial cells, and further differences depending on the exact anatomical location. A key influence on endothelial phenotype is shear stress. For example, at arterial shear, shear-induced Notch signalling leads to upregulation of Connexin37 and then p27-induced cell cycle arrest leading to the expression of genes that lead to arterial specification of the cells (Fang et al., 2017). Recently, high-throughput, single-cell omics has revealed the rich diversity of vascular endothelial cells and defined specific marker genes for human organ-specific subtypes (Kalucka et al., 2020; Garcia et al., 2022; Winkler et al., 2022). These have been elegantly summarised previously (Trimm and Red-Horse, 2023) and for the cerebral vein, the markers include atypical chemokine receptor 1 (ACKR1), interleukin 1 receptor type 1 (IL1R1), teashirt zinc finger homeobox 2 (TSHZ2), prostaglandin D2 synthase (PTGDS), periostin (POSTN), and deoxyribonuclease I (DNASE1) (Trimm and Red-Horse, 2023).

In venous thrombosis, stagnation of blood flow is a key initiating event. This is clinically apparent in the massive increase in the risk of venous thrombosis in individuals with acute immobility. Normal blood flow stimulates the constitutive production of a range of

antithrombotic factors including PGI_2, nitric oxide, and thrombomodulin which inhibit platelets and thrombin generation thus preventing unsolicited thrombosis and regulating physiological clot formation (Wang et al., 2018; Rayes and Brill, 2024). Perturbation of blood flow culminates in endothelial activation characterised by release of Wiebel-Palladi bodies that contain vWF, and upregulation of adhesion molecules leading to capture and activation of platelets and leukocytes resulting in activation of the clotting cascade and ultimately fibrin deposition (Rayes and Brill, 2024).

5.1.2.1. Endothelial activation in anti-PF4 immunothrombotic syndromes

Although venous thrombosis and endothelial activation caused by perturbed flow is relatively well understood, this is clearly not the mechanism of thrombosis in HIT and VITT (nor in unprovoked venous thrombosis). FcγRIIA is not expressed on endothelial cells (apart from dermal microvascular cells) (Gröger et al., 1996) and no study has shown direct endothelial activation by anti-PF4/heparin antibodies. However, Herbert et al. showed that, in the presence of platelets, sera from patients with HIT led to *in vitro* expression of intercellular adhesion molecule 1 (ICAM-1), vascular cell adhesion molecule 1 (ICAM-1) and tissue factor, amongst other markers (Herbert et al., 1998).

Endothelial cells express GAGs, predominantly heparan sulfate to which PF4 can bind and form antigenic complexes that can be recognised by anti-PF4/heparin antibodies (Visentin et al., 1994). In an endothelialised microfluidic model of HIT, Hayes et al. showed that PF4 released from platelets binds to endothelial cells adjacent to photochemical induced, injured endothelium (Hayes et al., 2017). Furthermore, PF4 binds to vWF and forms antigenic complexes that can be recognised by anti-PF4/heparin antibodies contributing to thrombus propagation at these sites (Johnston et al., 2020). PF4 and anti-PF4/heparin antibodies also prevent cleavage of vWF by ADAMTS13, further compounding the prothrombotic state (Nazy et al., 2020).

Patients with VITT have been shown to have elevated vWF activity (De Michele et al., 2022) and increased levels of soluble ICAM-1 and E-selectin in peripheral blood (Abrams et al., 2024). Treatment of human umbilical vein endothelial cells (HUVECS) with VITT patient sera or plasma mixed with recalcified whole blood in a microfluidic system at venous shear, led to P-selectin and tissue factor expression, the latter of which was increased by additional PF4 (Dupuy et al., 2022). These data do provide evidence that, as expected, the endothelium is inflamed in VITT, but the sequence of events is unclear. Moreover, differences between HIT and VITT have not been studied.

Although there is conflicting data, PF4 is not generally considered to be directly chemotactic (Petersen et al., 1996; Clark-Lewis et al., 1993; Pervushina et al., 2004; Graca et al., 2023), which is consistent with it being an ELR-negative chemokine. However, using an *in vivo* cellular migration model, Gray et al showed that PF4, injected into an air pouch on the dorsal aspect of mice led to the recruitment of a broad range of cells including neutrophils, monocytes, eosinophils, dendritic cells, T cells, and natural killer cells (Gray et al., 2023). These results suggest that PF4 itself may play a role in promoting thromboinflammation at the endothelial surface besides its role as a nidus for immune complex formation. It was thus hypothesised that anti-PF4 antibodies might enhance recruitment and retention of PF4 itself and thus enhance PF4-mediated inflammatory effects at the endothelial surface.

The aims of this chapter were therefore to:

1. Visualise PF4 at the endothelial cell surface.
2. Investigate whether VITT sera and antibodies can directly activate endothelial cells.
3. Investigate differences between VITT and HIT sera-induced endothelial activation and platelet recruitment.

5.2. Results

5.2.1. PF4 can be imaged binding to endothelial cells

Although PF4 is known to bind to endothelial cells, this has not previously been directly imaged. As such, it is not clear whether this binding is uniform or localised. A further aim was to, in addition to assessing endothelial activation, determine whether VITT and HIT reagents differentially led to increased PF4 deposition at the endothelial surface.

First, two fluorophore-conjugated anti-PF4 antibodies (Alexa Fluor 488 and Alexa Fluor 647) were tested on platelets that had spread on collagen 50 µg/mL to determine which should be used in further experiments. Both antibodies stained PF4 which was observed concentrated in the interior of the cell (Figure 5.1). However, as the intention was to stain surface PF4 on endothelial cells, and PF4 is clearly present in lower amounts on surfaces, peripheral staining of platelets was examined to differentiate the two antibodies. Peripheral staining was more clearly visible with the Alexa Fluor 488 antibody, suggestive of PF4 on the platelet surface. As such, this antibody was used in future experiments. This experiment was only performed once.

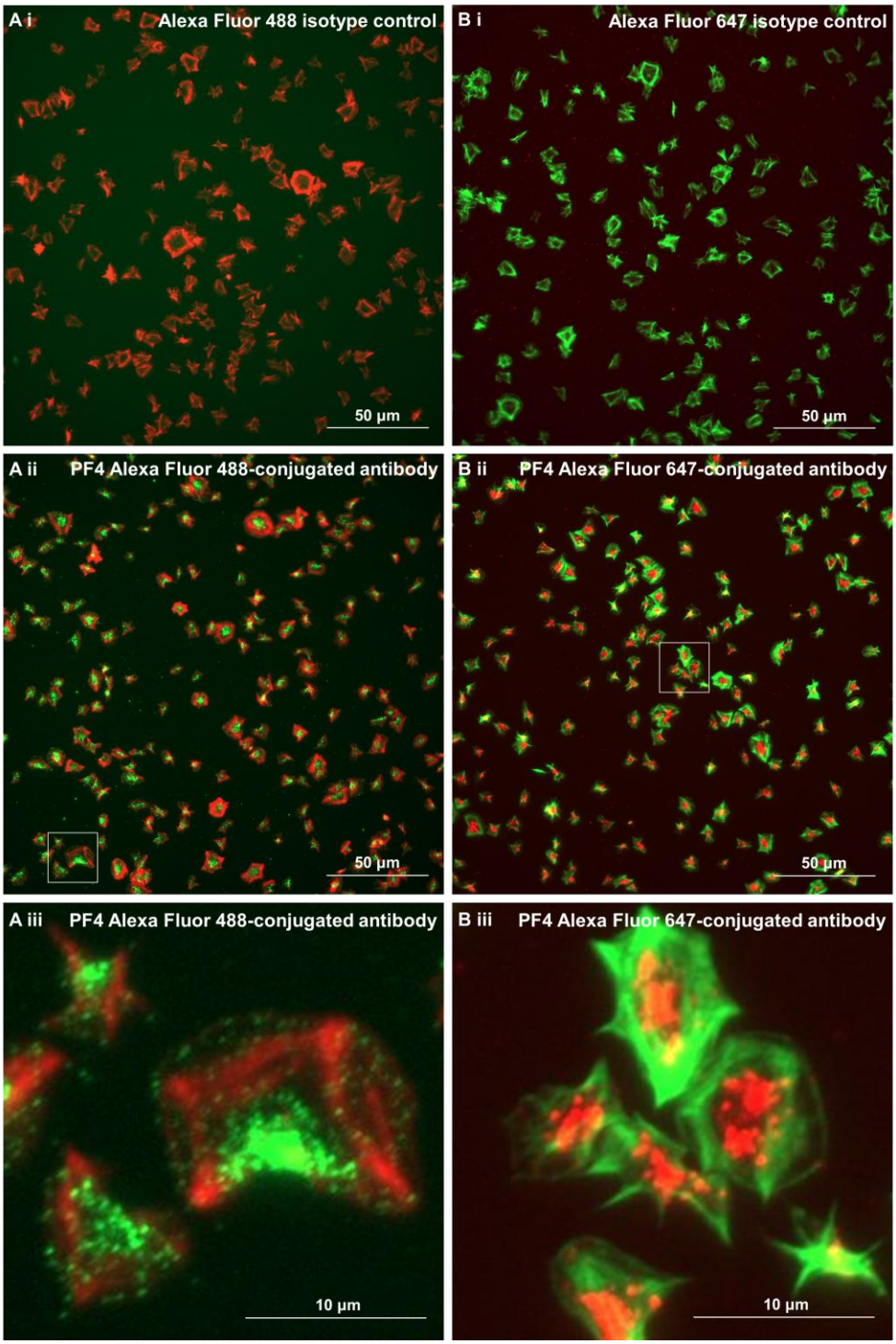

Figure 5.1. Anti-PF4 monoclonal antibody conjugated to Alexa Fluor 488 visualises PF4 better than when conjugated to Alexa Fluor 647

Washed platelets (2×10^7/mL) were added to coverslips coated with fibrinogen (100 µg/mL) and incubated at 37°C for 30 min to adhere and spread. Platelets were then fixed and permeabilised, then stained with (A) Anti-PF4-Alexa Fluor 488 (1:100) or isotype control and phalloidin-Alexa Fluor 647 (1:50) or (B) Anti-PF4-Alexa Fluor 647 (1:100) or isotype control and phalloidin-Alexa Fluor 488 (1:750). Top panel: isotype controls, middle panel: anti-PF4 antibodies, bottom panel: magnified images of area contained within white boxes in middle panel. Scale as indicated.

Next, human dermal microvascular endothelial cells (HDMECs), that were cultured by Dr Jenefa Begum, University of Birmingham, were incubated with PF4 10 or 50 µg/mL for 45 min then imaged. However, no PF4 could be visualised after three replicate experiments. The methods were scrutinised, and it was determined that the likely cause for this was that PF4 was being added to endothelial cells in media containing serum. Thus, the experiments were repeated in serum-free media showing that a dose-dependent increase in PF4 deposition could be detected by imaging (Figure 5.2).

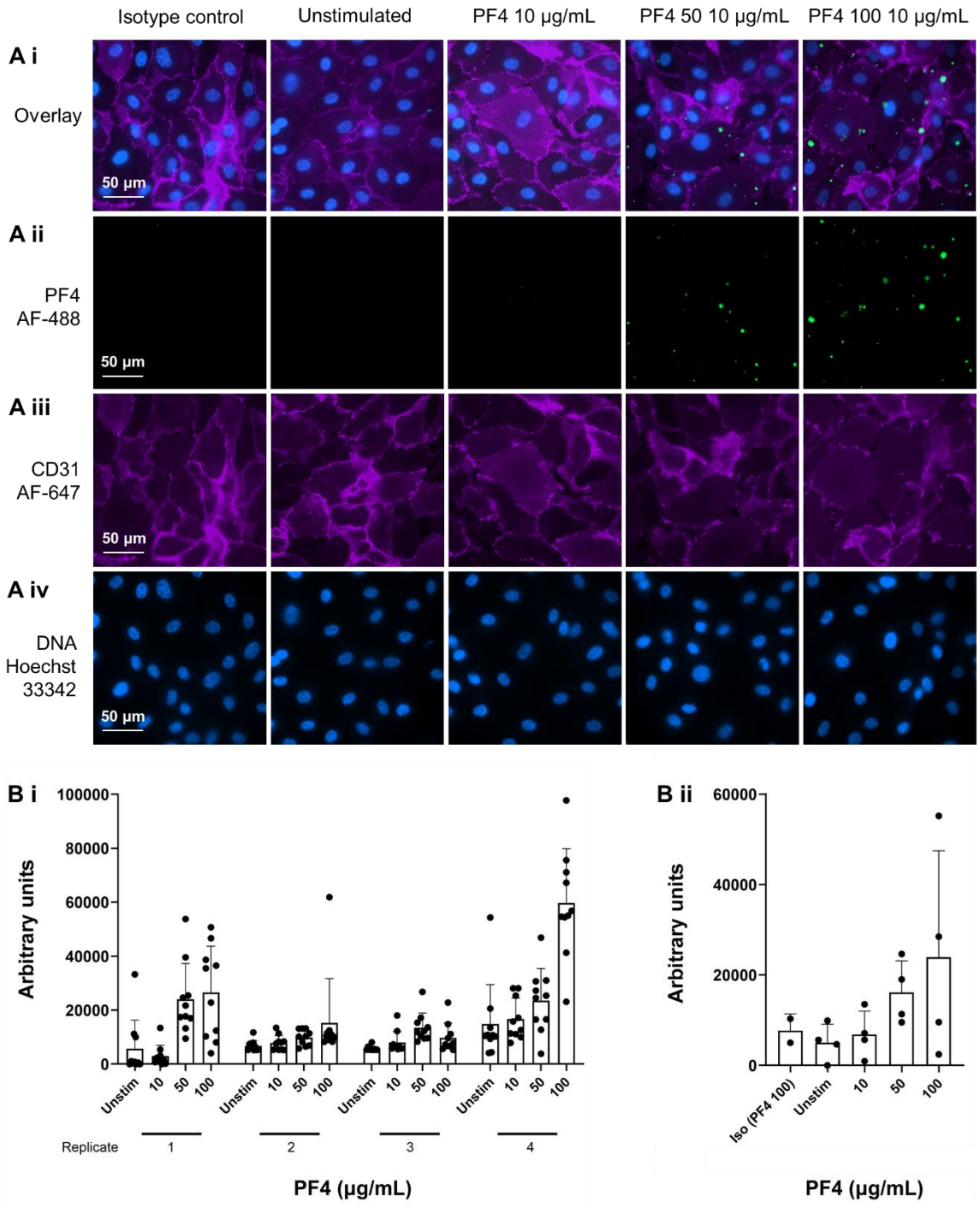

Figure 5.2. Uneven PF4 deposition detected on endothelial cells.

Human dermal microvascular endothelial cells were cultured until >90% confluent and then incubated for 30 min with PF4 10-100 µg/mL or vehicle control (PBS) in serum-free media. Cells were stained using Alexa Fluor (AF)-488-anti-PF4 or isotype control, AF-647-anti-CD31 antibodies and DNA stain, Hoechst 33342 and imaged using epi-fluorescent microscopy. (A) Representative images. (B) Quantitation of PF4 staining based on 10 fields of view at ×63 magnification from distinct areas of the dish. (Bi) Results of four replicate experiments with each filled black circle corresponding to one field of view. (Bii) Mean values for each of the four experimental replicates. Statistical testing of difference by one way ANOVA. Unstim: unstimulated.

5.2.2. PF4 does not recruit platelets to endothelial cells

As discussed above, PF4 has been shown to induce migration of a wide range of immune cells but it is not known whether PF4 is able to recruit platelets to the endothelial surface. To investigate further, HDMECs were incubated with PF4 for three hours in serum free media followed by incubation with washed platelets for 30 min. Three hours was chosen as it is the minimum time required for synthesis and expression of adhesion molecules but kept short to limit the time that cells are starved of serum. The intention was that, if PF4 were observed to recruit platelets, then it would be possible to stain for both PF4 and platelets to ascertain whether PF4 directly facilitates platelet binding or whether this is due to an indirect mechanism. The exploratory conditions of low dose heparin (0.5 IU/mL) and heparin with low dose PF4 (10 µg/mL) were also included. Heparin was included here as endothelial cells express PEAR1 (Nanda et al., 2005) but the effect of an interaction between heparin and PEAR1 on endothelial cells is unknown. As shown in Figure 5.3, no discernible effect of PF4, nor heparin, nor the combination of PF4 with heparin was demonstrated.

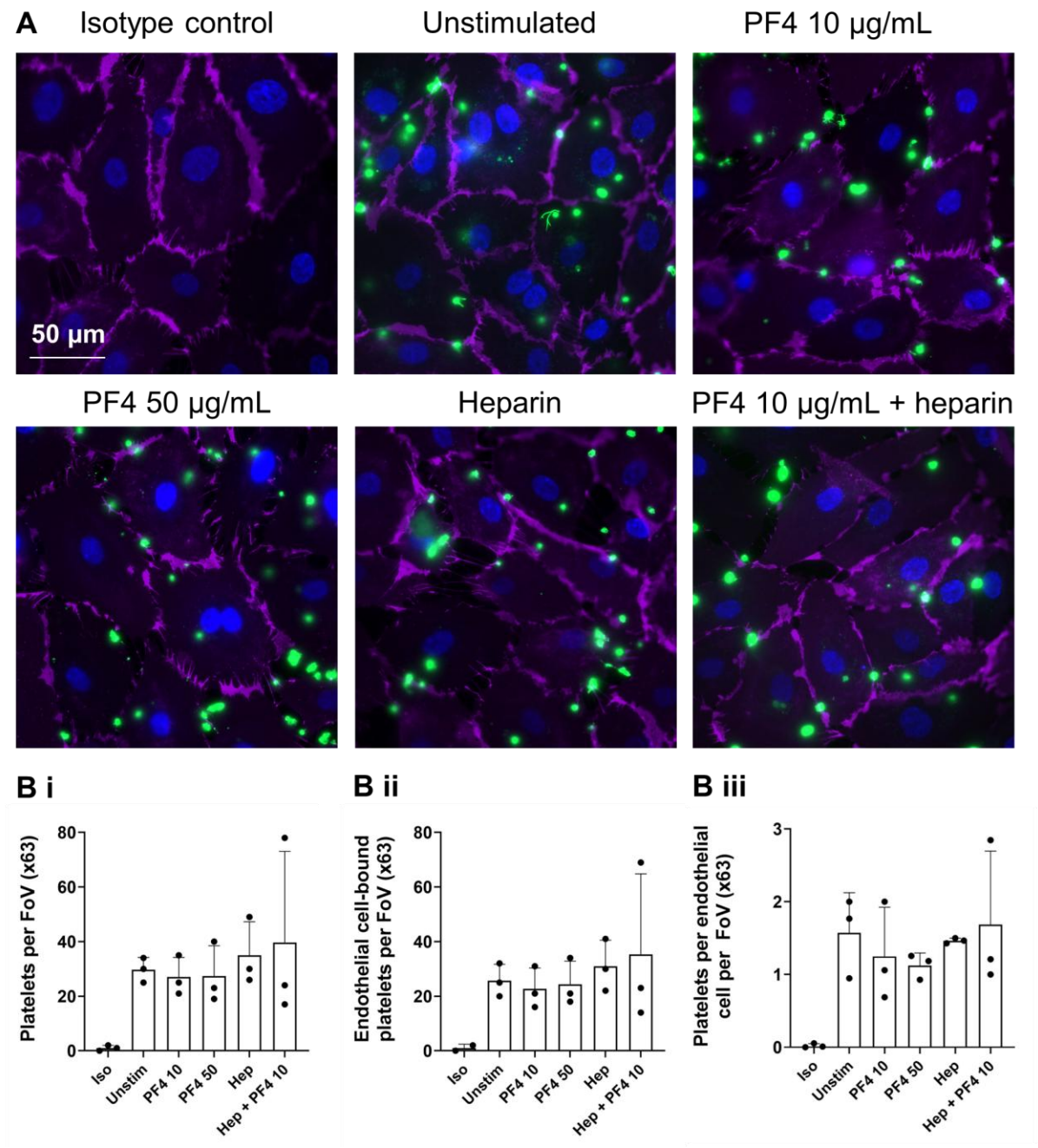

Figure 5.3. PF4 does not recruit platelets to endothelial cells.

Human dermal microvascular endothelial cells were cultured until >90% confluent and then incubated for three hours with PF4 10 or 50 µg/mL, heparin 0.5 IU/mL (Hep), PF4 + Hep, or vehicle control (PBS) in serum-free media. Cells were stained using Alexa Fluor 647-anti-CD31 antibody which stains endothelial cell surfaces, DNA stain Hoechst 33342, and FITC-anti-CD41 antibody which stains platelet surfaces, and imaged using epifluorescent microscopy. (A) Representative images. (B) Quantitation of platelet staining based on 10 fields of view (FoV) at ×63 magnification from distinct areas of the dish. (Bi) Mean platelets per FoV; (Bii) Mean endothelial cell-bound platelets per FoV; (Biii) Mean platelets per endothelial cell per FoV. Unstim: unstimulated.

5.2.3. VITT and HIT antibodies do not directly activate endothelial cells

As HMDECs are unusual in their expression of FcγRIIA, HUVECs were used for the remaining experiments. To study endothelial cell inflammation, rather than using epifluorescent microscopy, a more sensitive, quantitative technique using flow cytometry was used. These techniques have been optimised and protocolised by Dr Julie Rayes and her team, University of Birmingham. In short, cultured HUVECs were transferred to low-serum media (Opti-MEM) and incubated for four hours with VITT serum (P3 in Chapter 4, day +54 from presentation), HIT serum (P12 in Chapter 4, day +1 from presentation), isolated VITT IgG (P1 in Chapter 4, day +1 from presentation), or the HIT-like mAb KKO, in various combinations with PF4 and/or heparin. Endothelial cell activation was assessed by flow cytometry for ICAM-1, VCAM-1, P-selectin, and tissue factor. It was further hypothesised that these reagents may contribute to increased binding of PF4 to the endothelial cells and thus, PF4 was also stained for.

Figure 5.4 (for clarity set across two pages) shows that TNFα results in detectable ICAM-1, VCAM-1, and P-selectin expression. However, there was no clear, consistent effect of any sera, or antibodies, with or without heparin or PF4. This was consistent with previous observations that HIT sera do not directly activate endothelial cells without platelets (Herbert et al., 1998). There was similarly no enhanced binding of PF4 to either TNFα-treated endothelium or endothelium that had been incubated with VITT or HIT reagents. However, the anti-PF4 staining had a high background.

A Representative image of confluent HuVECs

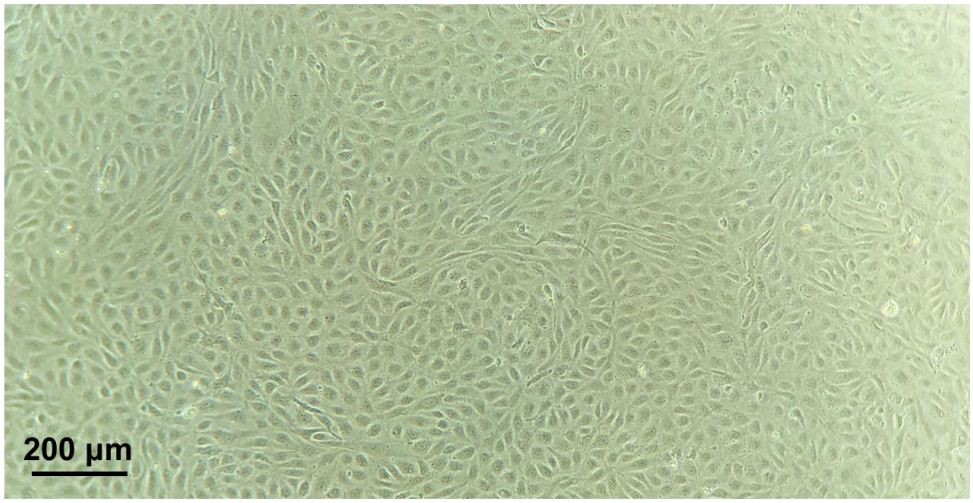

B ICAM-1

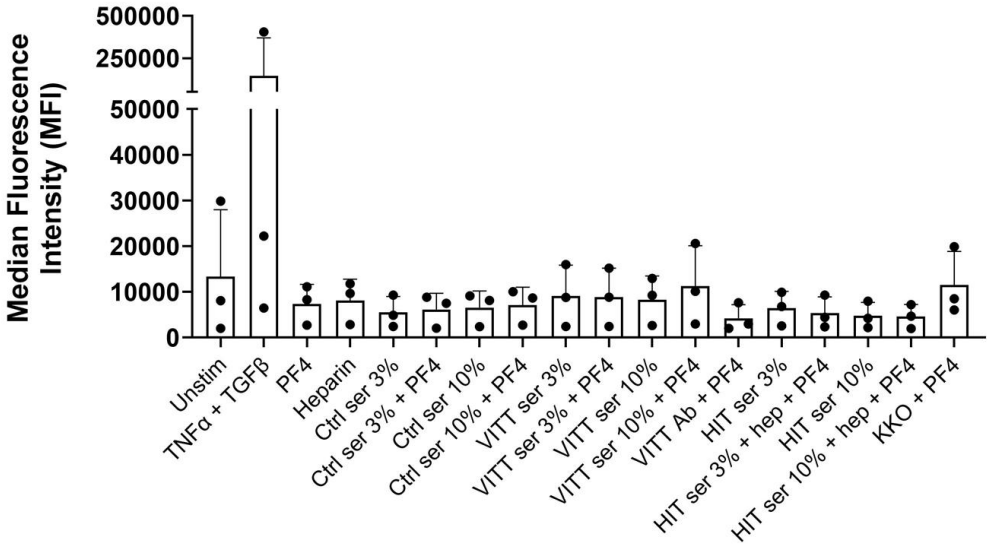

C VCAM-1

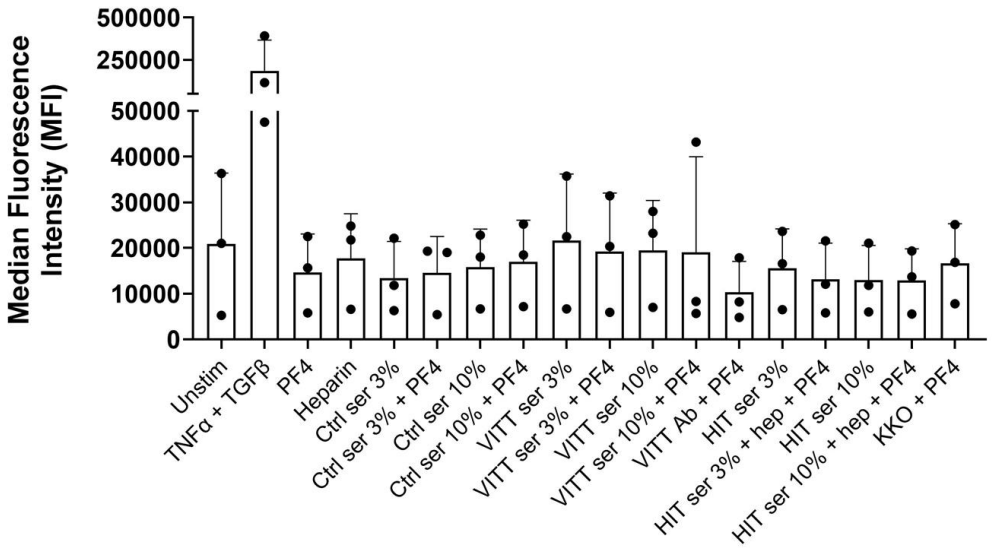

D P-selectin

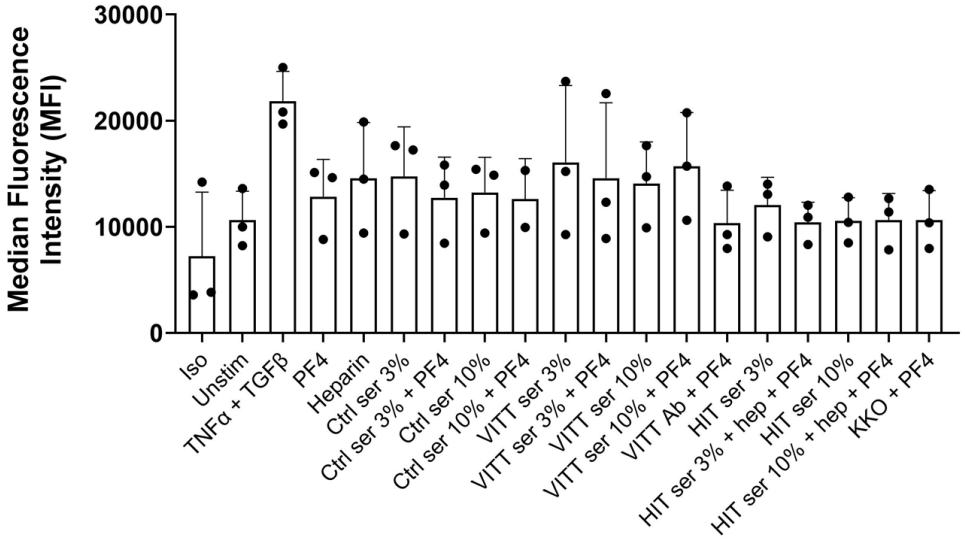

E Tissue factor

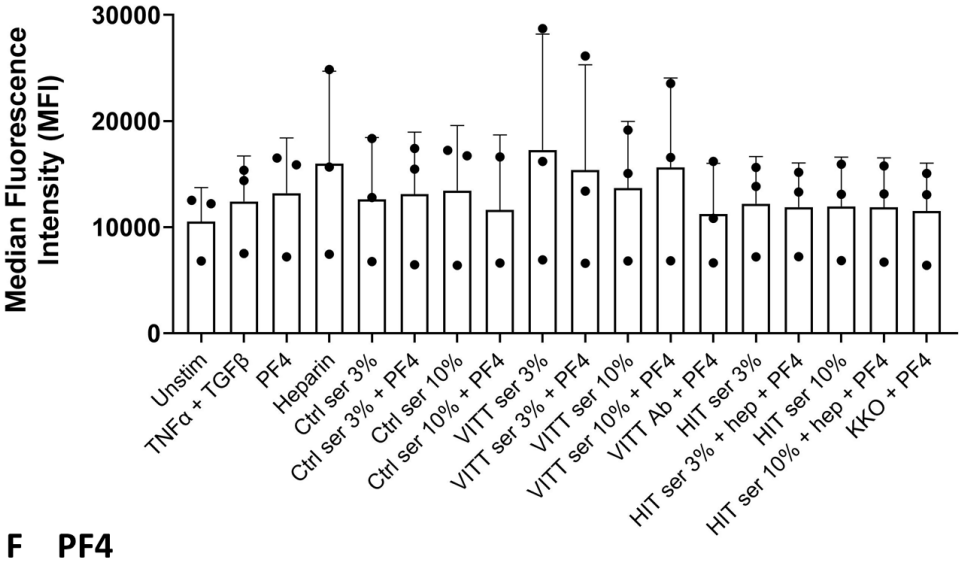

F PF4

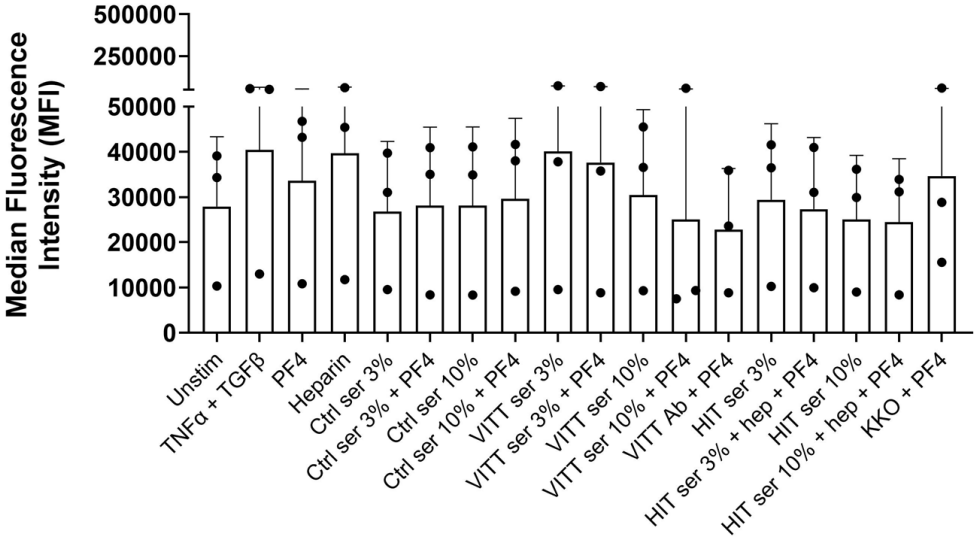

Figure 5.4. VITT and HIT sera and antibodies do not directly activate endothelial cells as measured by ICAM-1, VCAM-1, tissue factor, or P-selectin expression.

Human umbilical vein endothelial cells (HUVECs) were cultured until >90% confluent and then incubated for four hours with PF4 10 µg/mL, heparin 0.5 IU/mL (Hep), control serum (Ctrl ser), VITT serum (VITT ser), HIT serum (HIT ser) 3% or 10%, KKO 20 µg/mL, all ± PF4 10 µg/mL ± Hep 0.5 IU/mL. After four hours, cells were detached using trypsin 0.04% / EDTA 0.03%, pelleted, resuspended, blocked, and stained for 20 min on ice with FITC-ICAM-1, PE-Cy5-VCAM-1, APC-Cy7-P-selectin, PE-tissue factor, and AF-647-PF4 antibodies, or isotype controls, and analysed by flow cytometry using a CytoFLEX LX flow cytometer (Beckman Coulter, Indianapolis, USA). (A) Representative image of confluent HUVECs at the time of experiments (×10 magnification). (B-F) Quantification of median fluorescence intensity for (A) ICAM-1, (B) VCAM-1, (C) tissue factor, (D) P-selectin, and (E) PF4. Values are normalised for isotype controls where the cells in the isotype well had been treated with PF4 10 µg/mL and appropriate compensation settings applied.

5.2.4. Assessment of recruitment of platelets to endothelial cells by VITT and HIT reagents by flow cytometry.

As platelets are reported to be important for inducing endothelial inflammation in response to HIT sera (Herbert et al., 1998), the ability of platelets to be recruited to endothelium in the presence of HIT and VITT reagents was assessed. Anti-PF4 immunothrombotic syndromes are characterised by a proinflammatory state with a milieu of circulating cytokines and NETs. In prior studies in HIT, this situation has been reflected in the use of low dose TNFα to pre-activate the endothelial cells (Witzemann et al., 2023). Thus, in the following experiment, HUVECs were primed with TNFα 1 ng/mL for three hours followed by addition of washed platelets and HIT or VITT reagents for 45 min after which cells were washed, detached, fixed, stained, and analysed by flow cytometry. The VITT patient serum was from VITT patient 3 at the same time point as used in Chapter 4 (patient details in Table 4.1 - patient presented with CVST) and the HIT patient serum was from HIT patient 12 (also Chapter 4) who did not have CVST. A further diagnostic serum sample from a patient who presented with a spontaneous anti-PF4 disorder was also tested. This patient presented with portal vein thrombosis and ischaemic stroke, and thrombocytopenia. ELISA OD was >3.0 and functional assays showed FcγRIIA-dependent platelet activation but with hallmarks of both HIT and VITT. Further details of this patient and extensive laboratory work-up are published elsewhere .

First, endothelial cells were gated on by forward and side scatter (Figure 5.5Ai) and gating confirmed by staining for CD31 (Figure 5.5Aii and Aiii). Next, endothelial cells were gated on positivity for CD41 indicating bound platelets (Figure 5.5Aiv). Figure 5.5B shows the results of four repeat experiments using washed platelets from four different healthy donors. Although there was evidence of increased platelet attachment compared to endothelial cells that had only been treated with low dose TNFα, there was no clear pattern or condition where this was markedly heightened. This likely reflects platelet donor variation in response to HIT and VITT reagents, the small sample size, and the small number of HIT and VITT reagents used, all compounded by a technically challenging assay with multiple steps. As such, although there are interesting and important questions that should be addressed in future, no further

experiments in this sub-project were performed due to the limited volumes of patient samples that were available and other associated costs.

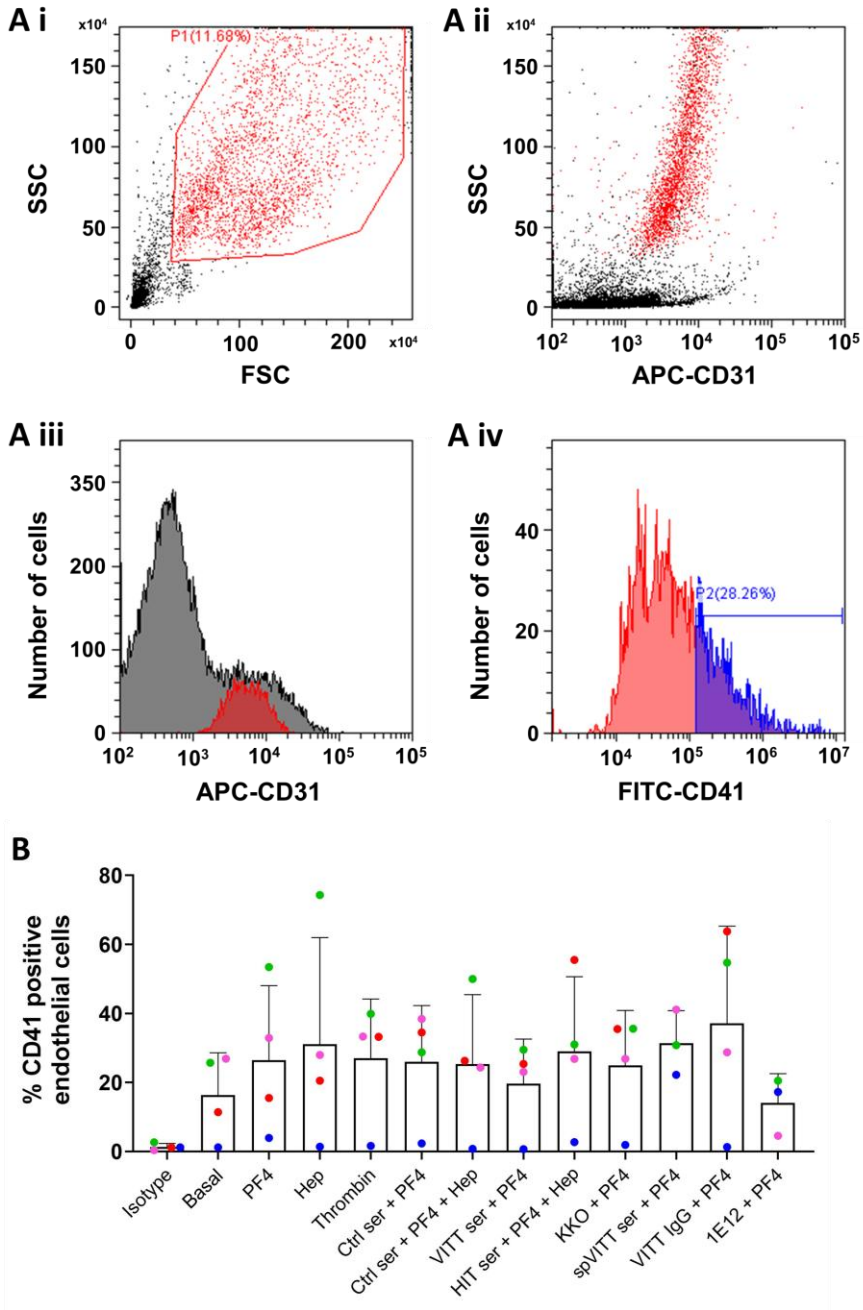

Figure 5.5. VITT and HIT reagents do not lead to platelet recruitment to endothelial cells.

HUVECs were cultured in 24 well plates to ≥90% confluence then washed and recovered in Opti-MEM low serum media containing TNFα 1 ng/mL and incubated for three hours at 37°C. Cells were then washed and platelets (1×10^8/mL final concentration) were added in the presence of serum from a healthy control (Ctrl), a patient with VITT (VITT ser), a patient with HIT (HIT ser) or a patient with spontaneous VITT (spVITT) (3% final concentration), KKO 20 µg/mL, VITT IgG 100 µg/mL, or 1E12 for 45 min. Cells were then washed, detached, fixed, and stained with FITC-CD41 antibody and analysed by flow cytometry. (A) Gating strategy: (Ai) Endothelial cells identified by forward and side scatter; (Aii) Cells identified by gating on forward and side scatter were confirmed as CD31 positive; (Aiii) Cells gated in Ai are CD31 positive; (Aiv) Proportion of endothelial cells positive for CD41 were assessed according to isotype control (not shown). (B) Quantification of % endothelial cells with bound platelets assessed by positivity for CD41.

5.3. Discussion

The key findings in this chapter are:

1. PF4 binds to endothelial cells in an uneven, patchy manner.
2. PF4 does not recruit washed platelets to endothelial cells.
3. VITT and HIT reagents do not directly activate endothelial cells, nor is there evidence of platelet recruitment in leukocyte-free conditions.

5.3.1. PF4 binds to endothelial cells in a patchy manner

PF4 is well-described to bind to GAGs (Lord et al., 2017; Stringer and Gallagher, 1997; Handin and Cohen, 1976; Loscalzo et al., 1985) and by logical extension, GAGs on the surface of endothelial cells (Rybak et al., 1989; Sachais et al., 2004; Dai et al., 2018). However, to my knowledge, this binding has not been visualised. The present study clearly demonstrates the binding of PF4 to endothelial cells in a concentration-dependent manner. At the resolution displayed in Figure 5.2, the staining is patchy rather than diffuse and is characterised by numerous clumps of intense fluorescence. This may be artefactual but may reflect geographically heterogeneous display of GAGs or GAG sulfation on the surface of endothelial cells. It would be interesting to evaluate the binding of PF4 to endothelial cells from other anatomical locations.

5.3.2. VITT and HIT antibodies do not directly activate endothelial cells

The direct effect of HIT sera on endothelial cells has been described in the literature where no effect was observed. However, this was only one study, the direct effects of VITT sera have not been described, and possible differential effects of HIT and VITT have never been investigated. As such, HUVECs were treated with HIT and VITT sera, the monoclonal HIT-like antibody, KKO, and isolated VITT IgG, in the presence or absence of PF4 (and heparin in the case of HIT reagents). Although TNFα activated the endothelial cells as measured by ICAM-1, VCAM-1 and P-selectin expression, no clear effect was seen with the HIT and VITT

reagents. The very limited mechanistic evidence for the aetiology of CVST described in section 5.1.1, is suggestive of a platelet-driven process and as such, the ability of VITT and HIT reagents to drive platelet attachment and therefore thrombosis formation at the endothelial surface, was next assessed. The experiment was inconclusive with evidence of platelet attachment to endothelial cells but the responses to the different reagents were highly variable and not significantly increased above baseline.

5.2.3. Limitations of these experiments

These pilot experiments are very limited in their scope and potential to show differences between baseline, HIT, and VITT reagents. The next logical experiment to perform would be to look at endothelial markers of activation in the presence of platelets and HIT and VITT reagents to try and recapitulate findings from an earlier study (Herbert et al., 1998). One could then add other blood components in a stepwise manner to investigate the relative contribution of different cell types, an interplay which is known to influence thrombosis in HIT (Dai et al., 2018).

Throughout the course of these experiments, it became clear that to truly establish differences between HIT and VITT, one would need many more patient samples, tested on many more donor platelets. These experiments would also need some degree of standardisation of these reagents, for example only using diagnostic specimens, and/or isolating anti-PF4 antibodies from plasma and using the same concentrations. Another key limitation is the use of HUVECs which, while an established tool in endothelial cell biology, are different to cerebral vein endothelial cells. Furthermore, cerebral vein endothelial cells are not commercially available and therefore one has to question the validity of this approach to addressing the question of CVST in VITT. Another consideration is that whilst flow cytometry is sensitive for changes in expression of selected markers of inflammation, it is limited in its scope. Measuring ICAM-1, VCAM-1, P-selectin and tissue factor expression will detect large scale differences in inflammation but possible differences between HIT and VITT may be subtle. Omics

approaches including RNA sequencing may be more likely to yield results but again would require a drastic increase in sample size and replicate experiments.

Another important limitation is the lack of flow in these models. For simplicity, the experiments were begun in static conditions in order to become familiar with the techniques but ideally flow at venous shear rates should be incorporated. Consideration should also be given to culturing the endothelial cells under venous shear as flow alters their phenotype (Dessalles et al., 2021). There are countless options to account for factors such as topography, curvature, stiffness, flow velocity, flow dynamics, and pressure. A further limitation of many flow models is that they do not generate occlusive thrombi as seen in CVST in VITT which could be overcome by parallel arm models (Berry et al., 2021).

So, there are countless options for developing models of CVST but a lack of basic knowledge about the cerebral veins is hampering progress. We lack key information such as quantification of cerebral vein flow rates and understanding of the composition of blood flow exiting the brain. We also lack key tools to facilitate these studies including access to primary cerebral vein endothelial cells.

Thus, one may conclude that this line of investigation is highly unlikely to elucidate mechanisms of CVST in VITT. The approach is hampered by the rarity of sufficient quantities of samples from patients with VITT and HIT and is perhaps destined to fail due to the sheer number of possible variables at play. These include, but are not limited to, characteristics of anti-PF4 antibodies, amount of anti-PF4 antibodies, characteristics and responsiveness of donor/patient platelets, timing of patient sample acquisition, endothelial cell characteristics including anatomical derivation, endothelial pre-activation, presence of flow and flow rate, presence of other triggers including ChAdOx1, and techniques used to measure endothelial cell activation.

Perhaps a fruitful path forward would be to use transgenic mice expressing human FcγRIIA, human PF4, and knocked out mouse PF4 (Reilly et al., 2001). This would allow sequential

hypothesis testing. For example, as suggested by Huynh et al. (2023), exposure of these mice to combinations of antibodies targeting different epitopes on PF4 may produce CVST in some mice.

6. General discussion

6.1. Summary of results

This study has investigated the nature and mechanism of platelet activation by PF4 and its role in the pathogenesis of VITT and HIT. The studies of ancillary pathways of platelet activation in VITT and then HIT were extended to evaluate the role of heparin on platelet activation in HIT. Finally, pilot studies to investigate differential effects of VITT and HIT reagents on endothelial cells were performed.

The key findings in this thesis are:

1. PF4 activates platelets through the TPO receptor, c-Mpl with associated signalling through JAK2.
2. PF4 contributes to platelet activation in VITT.
3. Heparin contributes to platelet activation in HIT.

6.2. Platelet factor 4

Over the last 70 years, research on PF4 has shown it to have multiple, disparate biological roles across a 1000-fold concentration range seemingly allow it to fine tune biological processes in context-dependent ways. This is represented in Figure 6.1 which shows the strength of interactions of PF4 and functional effects across the concentration range. The majority of these effects are dependent on charge-mediated binding to GAGs with the exception of some of its anti-angiogenic properties (Table 1.2).

The amino acid sequences of PF4 across example species in orders of mammals for which data is available are shown in Figure 6.2. There is marked variation in N-terminal sequences, but the ELR negative status is maintained in a variety of ways. Further, the maintenance of positive charge over tens of millions of years of mammalian evolution (Goswami et al., 2022) particularly at the C-terminus is striking. Across the entire molecule, where substitutions in positively charged amino acids occur, these are usually conservative e.g. lysine to arginine or

are shifted as denoted in orange for tiger (*Panthera tigris*) and horse (*Equus ferus*). In the latter scenario, presumably either a positively charged residue was lost then re-evolved adjacent, or a positive charged residue was gained followed by an adjacent loss. As discussed previously, the physiological role of anti-PF4/heparin antibodies has been proposed as a mechanism by which the immune system can recognise negative charge. Mice with polymicrobial sepsis and no heparin exposure have been shown to generate anti-PF4/heparin antibodies demonstrating that this is an evolutionarily conserved immune mechanism (Krauel et al., 2011). However, as mentioned earlier, only primates have FcγRIIA, and therefore, only primates have an Fc receptor on their platelets (Lejeune et al., 2019). As such, although mice can generate anti-PF4/heparin antibodies, they do not develop HIT (Trist et al., 2014; Hogarth et al., 2014). At some point in primate evolution, the acquisition of FcγRIIA by platelets would likely have provided a selective advantage in response to infection. Although the anti-PF4 response is clearly physiological, HIT is an unfortunate consequence of this whereby the normal physiology is perturbed by the infusion of more negatively charge than would ever be seen in nature. The spontaneous HIT- and VITT-like syndromes are further examples of the evolutionary trade-off between this innovative response to infection balanced against the risks of directing a powerful immune response against a self-protein.

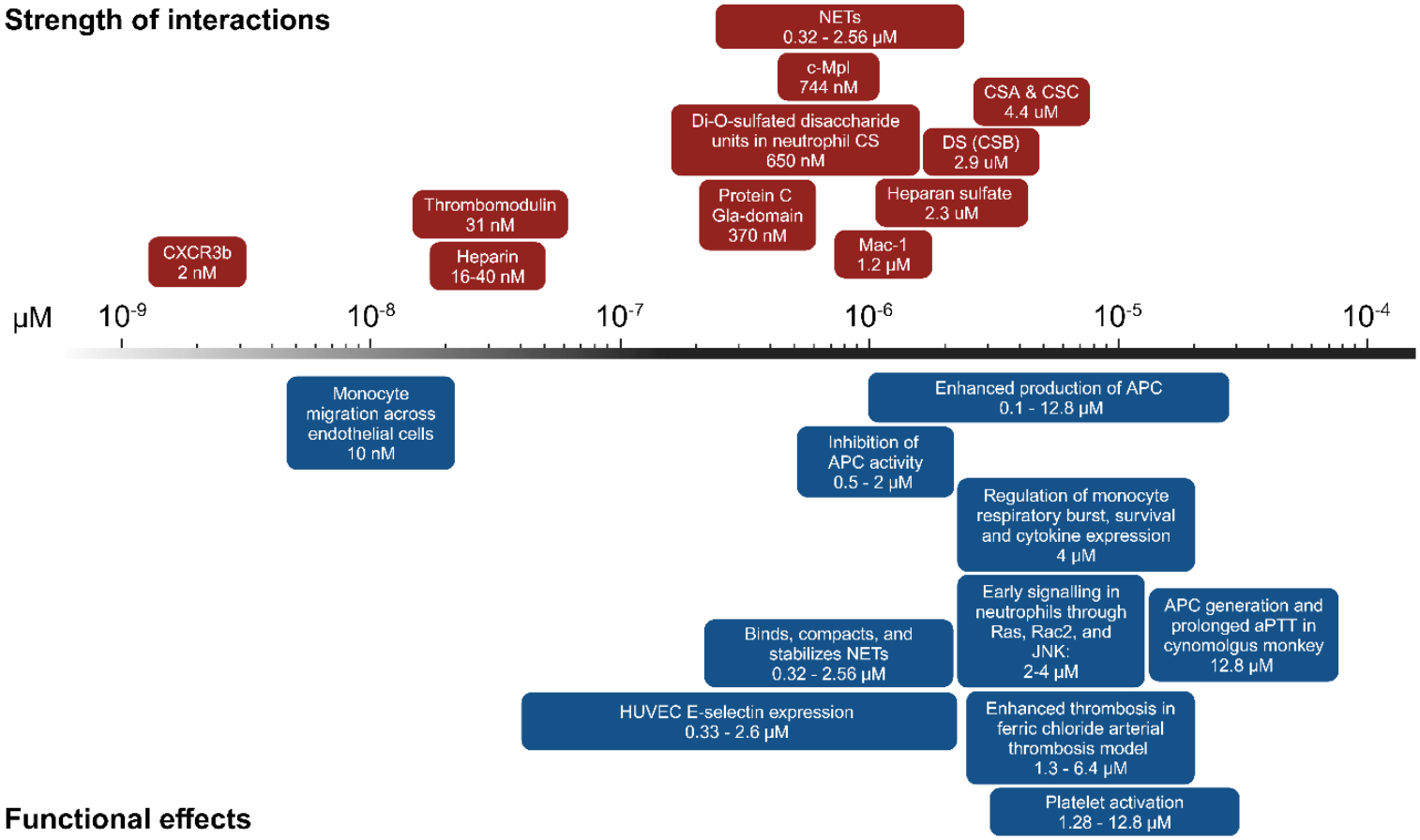

Figure 6.1. PF4 has interactions and functions across a four-log concentration range - from 2 nM to 12.8 µM.

Above the line (red) are measurements of PF4's interactions with other molecules including GAGs and receptors. Below the line (blue) are concentrations inducing PF4's observed functional effects. CXCR3b: CXC motif chemokine receptor 3b; NETs: neutrophil extracellular traps; CS: chondroitin sulfate; CSA: chondroitin sulfate A; CSB: chondroitin sulfate B; CSC: chondroitin sulfate C; DS: dermatan sulfate; APC: activated protein C; HUVEC: human umbilical vein endothelial cells; JNK: c-Jun N-terminal kinase; aPTT: activated partial thromboplastin time. Created with Biorender.com.

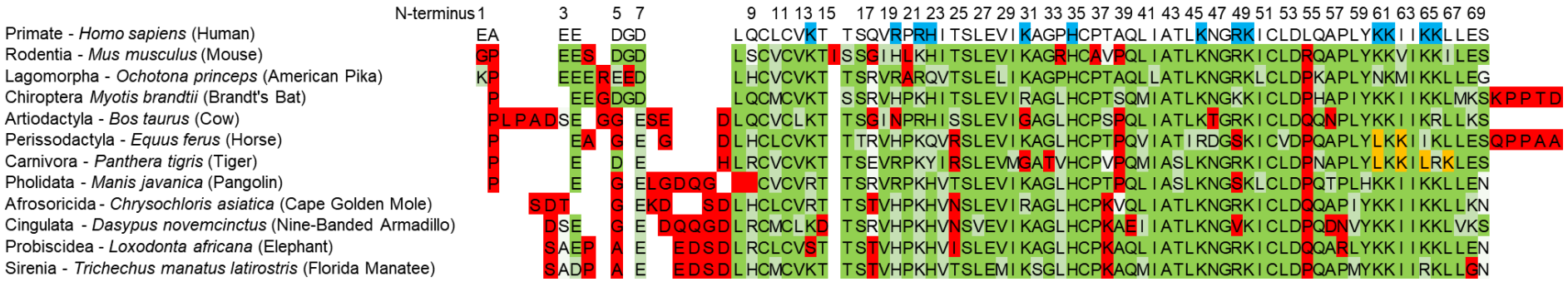

Figure 6.2. Amino acid sequences of PF4 in species representative of all orders of mammals for which data is available.

The amino acid sequence of human PF4 is given in the top row with positively charged residues highlighted in blue. One representative species per mammalian order is listed in order of evolutionary distance from humans (closest topmost). In rows other than for human PF4, amino acids that are unchanced are highlighted in dark green, resides where there are conservative or semi-conservative substitutions are highlighted in lighter green and light green respectively. Residues with non-conservative substitutions or where there are insertions are highlighted in red. Amber highlighted residues show where positively charged residues have been conserved but are shifted by one amino acid.

6.2.1. PF4 and TPO

Chemokines are in general, promiscuous molecules, binding and signalling through numerous receptors (Hughes and Nibbs, 2018). However, PF4 also interacts with receptors that are seemingly unrelated to immune function such as LRP1 (Lambert et al., 2009), the red cell Duffy antigen (McMorran et al., 2012), and now c-Mpl. From the data presented, c-Mpl appears to be the principal receptor that mediates platelet activation to PF4 although this is not known definitively. The anti-c-Mpl blocking antibody that was used is a poorly characterised reagent designed to inhibit TPO-induced megakaryocyte proliferation rather than PF4-induced platelet activation; it is plausible that other JAK2-associated receptors could be involved. Furthermore, PF4 may also bind to other platelet receptors, particularly where there is heavy glycosylation.

The “low” 5-10 ng/mL concentration of TPO that primes platelets is at least 10-fold higher than the upper limit of reported plasma levels in disease states such as infection, burns, and aplastic anaemia (Lupia et al., 2009, 2022; Zhao et al., 2018; Makar et al., 2013). However, PF4 seems to activate platelets at physiologically relevant concentrations. The data therefore show that both PF4 and TPO activate platelets through c-Mpl but only PF4 does so at physiologically relevant concentrations. Thus, the previously observed priming effect of TPO (Moore et al., 2019) may be a smoking gun for the more physiologically relevant effect of PF4 which occurs through a similar mechanism.

The data does however generate a contradiction. Whilst TPO is well-described to promote haematopoietic stem cell maintenance, megakaryocyte differentiation, and platelet production, and PF4 and TPO both activate platelets, PF4 has an opposite effect in the bone marrow where it inhibits megakaryocyte colony formation, limits platelet production, maintains haematopoietic stem cells in a quiescent state, and prevents haematopoietic stem cell ageing (Lambert et al., 2009; Bruns et al., 2014; Zhang et al., 2024). The effects on megakaryocytes have been reported to occur through LRP1 but other mechanisms are possible particularly as LRP1 is only expressed at a late stage of megakaryocyte differentiation. PF4 may block TPO-

induced signalling through c-Mpl but the mechanism by which an agonist could do this is unclear. Further work on megakaryocytes and high throughput evaluation of signalling downstream of c-Mpl is required.

6.3. Novel mechanisms of platelet activation in VITT and HIT

The understanding of how thrombosis occurs in anti-PF4 immunothrombotic syndromes has now advanced far beyond a simple recognition of platelet activation by PF4-containing immune complexes through FcγRIIA. As discussed in section 4.1.1, PF4 binds to many other negatively charged molecules than heparin which can be recognised by anti-PF4/heparin antibodies and there is complex interplay between numerous cell types leading to thromboinflammation. Although there is less data, these processes must be different in VITT compared to HIT given that antibodies bind to the heparin binding site and would thus be expected to displace negatively charged polyanions. Nevertheless, the core process is platelet activation - thrombosis in both VITT and HIT is a platelet-initiated process which does not occur without the presence of FcγRIIA.

The data in this thesis demonstrate two further mechanisms by which platelets may be activated in these disorders. First, PF4 can activate platelets via c-Mpl, and second, heparin can activate platelets through PEAR1. Although the data do not prove physiological relvance of these observations, the concentrations of reagents used in these assays reflect those found *in vivo*. The findings may have some relevance for the study of the high degree of inter-individual variation that is seen in the platelets of healthy individuals. This variation has long been recognised (Warkentin et al., 1992) and is a limitation of functional diagnostic platelet assays for HIT and VITT, but its biological underpinning is not understood. Polymorphisms in FcγRIIA have been demonstrated to increase susceptibility to thrombosis in HIT (Rollin et al., 2015) but have not been correlated with FcγRIIA ligand reactivity *in vitro*. The present study raises questions about whether heparin-PEAR1 and possibly PF4-c-Mpl interactions may modulate donor platelet responsiveness.

Finally, the data may have some therapeutic relevance. Novel treatment strategies including therapies that target signalling downstream of FcγRIIA are attractive options. The Bruton tyrosin kinase inhibitor, ibrutinib has good evidence of *in vitro* efficacy in blocking platelet

activation in both HIT and VITT (Goldmann et al., 2019; Smith et al., 2021) and has been successfully used to treat a patient with a chronic anti-PF4 immunothrombotic disorder (Lindhoff-Last et al., 2023). Given the data in this thesis, a drug that can block signalling through FcγRIIA, PEAR1, and c-Mpl, such as a PI3K inhibitor could be an attractive option. Alternatively, combination therapy blocking all three pathways could be considered but the contribution of the PEAR1 and c-Mpl pathways *in vivo* is probably minor. However, all potential treatments require careful pre-clinical evaluation. HIT and VITT are thromboinflammatory disorders and whilst platelets are clearly required at the onset, activation of leukocytes, release of inflammatory mediators, and endothelial inflammation are key drivers in pathogenesis (Arepally and Padmanabhan, 2021). Thus, these therapies require testing in more complex *in vitro* assays and *in vivo*. Additionally, there may be limiting toxicities particularly with PI3K inhibitors (Hanlon and Brander, 2020). Emerging therapies for HIT and VITT have been recently reviewed (Müller et al., 2024). Ultimately, novel therapies should if at all possible be evaluated in clinical trials. Although HIT is relatively rare, moderately sized prospective studies have been performed including single arm studies of the direct thrombin inhibitors, argatroban (Lewis et al., 2001, 2003), lepirudin (Greinacher et al., 2000), and a small, randomised study of danaparoid versus dextran 70 (Chong et al., 2001). Another, larger, randomised trial studied patients with suspected HIT and compared argatroban with desirudin (Boyce et al., 2011). These publications demonstrate that running trials in HIT is feasible and given the on-going high mortality and high complication rate, there is much scope for improvement. Intervention at an early stage with targeted therapy that does not increase the risk of bleeding and otherwise has a good safety profile would be very attractive. Future trials focusing on this larger group of patients with intervention delivered as soon as HIT is suspected, or even prophylactically to high risk receipients of heparin may have a good chance of leading to improved outcomes.

Even without the development of novel treatments, there is still much room for improvement in the diagnosis, management, and outcomes of patients with HIT and suspected HIT. HIT is

relatively rare, poorly understood by non-specialists, and difficult to diagnose. The 4Ts score has good negative predictive value, but it suffers from underuse and inter-observer variability (Crowther 2014). Other scoring systems are available but are not widely used (Cuker et al., 2010; Nilius et al., 2022). Testing is also fraught with difficulties in access and interpretation, again adding to diagnostic delays. Finally, treatment consisting of switching thrombocytopenic patients to unfamiliar non-heparin anticoagulants at intensive doses in patients who are already often critically ill and who may require invasive procedures, is associated with harm. Pishko et al. reported a 36% incidence of major bleeding in patients with HIT, but this was even higher at 44% in patients with suspected HIT treated with anticoagulation who were subsequently found not to have HIT (Pishko et al., 2019). Thus, although novel therapeutic options should be evaluated, there are several systems issues that could be addressed to speed up identification and diagnosis or rule-out of HIT. For example, simple measures to reduce unnecessary heparin use have been shown to reduce the incidence of HIT (McGowan et al., 2016). Technology such as artificial intelligence-powered systems to flag and test patients may improve results (Zon et al., 2024) but given the patchwork of electronic health records used throughout the world, these will often need local innovation to implement. Artificial intelligence may also be able to improve the diagnosis of the rare presentations of spontaneous anti-PF4 immunothrombotic syndromes, prompting general clinicians to consider these diagnoses and of course other rare diseases such as thrombotic thrombocytopenic purpura early in the disease course.

6.4. The conundrum of CVST in VITT

As discussed previously, the only data showing biological differences between patients with VITT who did or did not have CVST is that those with CVST have additional detectable anti-PF4 antibodies that target regions of PF4 away from the heparin binding site. The key observation that facilitates critical thinking about this problem is the low incidence of CVST in HIT. This means that factors that are the same between the two disorders, such as blood flow

velocity, or lack of valves and muscular walls in the CVS are unlikely to (fully) explain the phenomenon.

An important difference is the triggers of these disorders. Adenovirus can rarely affect the central nervous system (Schwartz et al., 2019), ChAdOx1 was associated with increased incidence of post-vaccination headache than the mRNA vaccine, BNT162b2 (Menni et al., 2021), and there have been reports of VITT presenting as headache before the onset of any thrombosis (Salih et al., 2021). In VITT, it is plausible that adenoviral particles or even one or more of the other hundreds of (mostly human) proteins that contaminate the vaccine product could exert some effect on the cerebral veins or even the brain leading to local inflammation, priming the cerebral veins for thrombosis.

Perhaps a more compelling line of thought is to consider the anti-PF4 antibody epitopes. In VITT, antibodies target the heparin-binding region of PF4 (Huynh et al., 2021) and addition of heparin at low-doses that would enhance platelet activation to HIT antibodies, has the effect of disrupting immune complex formation and preventing platelet activation (Warkentin and Greinacher, 2022). This implies that these antibodies need to displace cellular surface GAGs in order to bind PF4 and form immune complexes. This in turn suggests that surfaces may not be as important in VITT as they may be in HIT. However, Huynh et al. showed that in addition to VITT-like antibodies, patients with CVST had HIT-like antibodies (Huynh et al., 2023). The authors proposed that more than one binding site could result in larger immune complexes, or at least complexes that contain more immunoglobulin molecules which could therefore activate platelets and leukocytes more strongly. The fact that the CVS is indeed a rare site for thrombosis suggests that intense thrombotic drive is required to overcome its protective barriers. The observations of Huynh et al. may imply that there is the opportunity for immune complex formation in suspension *as well as* at surfaces, which could give the required prothrombotic force.

6.5. Final conclusions

VITT emerged suddenly as a completely unexpected, rare, idiosyncratic side effect of adenoviral vector vaccination against COVID-19. For the individuals affected, it was a catastrophic, life-threatening event either leading to death or causing substantial morbidity, disability, loss of earnings, and loss of quality of life. However, the emergence of VITT has accelerated understanding of immunothrombosis and the work contained in this thesis is a small contribution to the field. It is now clear that VITT is part of a spectrum of anti-PF4 immunothrombotic disorders and future work to interrogate how subtle differences in pathophysiology manifest as thrombosis at different sites will offer further insights into human health and disease.

References

Abrams, S.T., Du, M., Shaw, R.J., et al. (2024) Damage-associated cellular markers in the clinical and pathogenic profile of vaccine-induced immune thrombotic thrombocytopenia. *J Thromb Haemost*, 22 (4): 1145–1153. doi:10.1016/j.jtha.2023.12.008.

Affandi, A.J., Carvalheiro, T., Ottria, A., et al. (2022) CXCL4 drives fibrosis by promoting several key cellular and molecular processes. *Cell Rep*, 38 (1). doi:10.1016/j.celrep.2021.110189.

Affandi, A.J., Silva-Cardoso, S.C., Garcia, S., et al. (2018) CXCL4 is a novel inducer of human Th17 cells and correlates with IL-17 and IL-22 in psoriatic arthritis. *Eur J Immunol*, 48 (3): 522–531. doi:10.1002/eji.201747195.

Agbani, E.O. and Poole, A.W. (2017) Procoagulant platelets: Generation, function, and therapeutic targeting in thrombosis. *Blood*, 130 (20): 2171–2179. doi:10.1182/blood-2017-05-787259.

de Agostini, A.I., Watkins, S.C., Slayter, H.S., et al. (1990) Localization of anticoagulantly active heparan sulfate proteoglycans in vascular endothelium: antithrombin binding on cultured endothelial cells and perfused rat aorta. *J Cell Biol*, 111 (3): 1293–1304. doi:10.1083/jcb.111.3.1293.

Aguayo, E., Sanaiha, Y., Seo, Y.-J., et al. (2018) Heparin-induced thrombocytopenia in cardiac surgery: Incidence, costs, and duration of stay. *Surgery*, 164 (6): 1377–1381. doi:10.1016/j.surg.2018.07.013.

Aguiar de Sousa, D., Romoli, M., Sánchez Van Kammen, M., et al. (2022) Cerebral Venous Thrombosis in Patients With Heparin-Induced Thrombocytopenia a Systematic Review. *Stroke*, 53 (6): 1892–1903. doi:10.1161/STROKEAHA.121.036824.

Ah Kioon, D.M., Tripodo, C., Fernandez, D., et al. (2018) Plasmacytoid dendritic cells promote systemic sclerosis with a key role for TLR8. *Sci Transl Med*, 10 (423): eaam8458.

Ali, A.M., Gómez-Biagi, R.F., Rosa, D.A., et al. (2016) Disarming an Electrophilic Warhead: Retaining Potency in Tyrosine Kinase Inhibitor (TKI)-Resistant CML Lines While Circumventing Pharmacokinetic Liabilities. *ChemMedChem*, 11 (8): 850–861. doi:10.1002/cmdc.201600021.

Amelot, A.A., Tagzirt, M., Ducouret, G., et al. (2007) Platelet factor 4 (CXCL4) seals blood clots by altering the structure of fibrin. *J Biol Chem*, 282 (1): 710–720. doi:10.1074/jbc.M606650200.

Amirkhosravi, A., Boulaftali, Y., Robles-Carrillo, L., et al. (2014) CalDAG-GEFI deficiency protects mice from FcγRIIa-mediated thrombotic thrombocytopenia induced by CD40L and β2GPI immune complexes. *J Thromb Haemost*, 12 (12): 2113–2119. doi:10.1111/jth.12748.

Ansari, N., Najafi, S., Shahrabi, S., et al. (2021) PEAR1 polymorphisms as a prognostic factor in hemostasis and cardiovascular diseases. *J Thromb Thrombolysis*, 51 (1): 89–95. doi:10.1007/s11239-020-02149-w.

Antczak, A.J., Vieth, J.A., Singh, N., et al. (2011) Internalization of IgG-coated targets results in activation and secretion of soluble CD40 ligand and RANTES by human platelets. *Clin Vaccine Immunol*, 18 (2): 210–216. doi:10.1128/CVI.00296-10.

Antithrombotic Trialists' Collaboration (2002) Collaborative meta-analysis of randomised trials of antiplatelet therapy for prevention of death, myocardial infarction, and stroke in high risk patients. *BMJ*, 324 (7329): 71–86. doi:10.1136/bmj.324.7329.71.

Arachchillage, D.J., Thachil, J., Anderson, J.A.M., et al. (2023) Diagnosis and management of heparin-induced thrombocytopenia: Third edition. *Br J Haematol*, 204 (2): 459–475. doi:10.1111/bjh.19180.

Arepally, G., McKenzie, S.E., Jiang, X.-M., et al. (1997) FcγRIIA H/R131 Polymorphism, Subclass-Specific IgG Anti-Heparin/Platelet Factor 4 Antibodies and Clinical Course in

Patients With Heparin-Induced Thrombocytopenia and Thrombosis. *Blood*, 89 (2): 370–375. doi:10.1182/blood.V89.2.370.

Arepally, G.M. and Hursting, M.J. (2008) Platelet factor 4/heparin antibody (IgG/M/A) in healthy subjects: a literature analysis of commercial immunoassay results. *J Thromb Thrombolysis*, 26 (1): 55–61. doi:10.1007/s11239-008-0217-y.

Arepally, G.M., Kamei, S., Park, K.S., et al. (2000) Characterization of a murine monoclonal antibody that mimics heparin-induced thrombocytopenia antibodies. *Blood*, 95 (5): 1533–40.

Arepally, G.M. and Padmanabhan, A. (2021) Heparin-Induced Thrombocytopenia: A Focus on Thrombosis. *Arterioscler Thromb Vasc Biol*, 41 (1): 141–152. doi:10.1161/ATVBAHA.120.315445.

Arman, M. and Krauel, K. (2015) Human platelet IgG Fc receptor FcγRIIA in immunity and thrombosis. *J Thromb Haemost*, 13 (6): 893–908. doi:10.1111/jth.12905.

Arman, M., Krauel, K., Tilley, D.O., et al. (2014) Amplification of bacteria-induced platelet activation is triggered by FcγRIIA, integrin αIIbβ3, and platelet factor 4. *Blood*, 123: 3166–3174. doi:10.1182/blood-2013.

Aslan, J.E., Tormoen, G.W., Loren, C.P., et al. (2011) S6K1 and mTOR regulate Rac1-driven platelet activation and aggregation. *Blood*, 118 (11): 3129–36. doi:10.1182/blood-2011-02-331579.

Babur, Ö., Melrose, A.R., Cunliffe, J.M., et al. (2020) Phosphoproteomic quantitation and causal analysis reveal pathways in GPVI/ITAM-mediated platelet activation programs. *Blood*, 136 (20): 2346–2358. doi:10.1182/BLOOD.2020005496.

Bacon, C.M., Tortolani, P.J., Shimosaka, A., et al. (1995) Thrombopoietin (TPO) induces tyrosine phosphorylation and activation of STAT5 and STAT3. *FEBS Lett*, 370 (1–2): 63–8. doi:10.1016/0014-5793(95)00796-c.

Baker, A.T., Boyd, R.J., Sarkar, D., et al. (2021) ChAdOx1 interacts with CAR and PF4 with implications for thrombosis with thrombocytopenia syndrome. *Sci Adv*, 7 (49): 1–15. doi:10.1126/sciadv.abl8213.

Barber, A.J., Käser-Glanzmann, R., Jakábová, M., et al. (1972) Characterization of a chondroitin 4-sulfate proteoglycan carrier for heparin neutralizing activity (platelet factor 4) released from human blood platelets. *Biochim Biophys Acta*, 286 (2): 312–329. doi:10.1016/0304-4165(72)90267-X.

Barbui, T., Finazzi, G. and Falanga, A. (2013) Myeloproliferative neoplasms and thrombosis. *Blood*, 122 (13): 2176–2184. doi:10.1182/blood-2013-03-460154.

Bennett, P., Celik, F., Winstanley, J., et al. (2023a) Living with vaccine-induced immune thrombocytopenia and thrombosis: a qualitative study. *BMJ Open*, 13 (7): e072658. doi:10.1136/bmjopen-2023-072658.

Bennett, P., Celik, F., Winstanley, J., et al. (2023b) Qualitative study of the consequences of vaccine-induced immune thrombocytopenia and thrombosis: the experiences of family members. *BMJ Open*, 13 (12): e080363. doi:10.1136/bmjopen-2023-080363.

Beppler, J., Koehler-Santos, P., Pasqualim, G., et al. (2016) Fc Gamma Receptor IIA (CD32A) R131 Polymorphism as a Marker of Genetic Susceptibility to Sepsis. *Inflammation*, 39 (2): 518–525. doi:10.1007/s10753-015-0275-1.

Berlacher, M.D., Vieth, J.A., Heflin, B.C., et al. (2013) FcγRIIa Ligation Induces Platelet Hypersensitivity to Thrombotic Stimuli. *Am J Pathol*, 182 (1): 244–254. doi:10.1016/j.ajpath.2012.09.005.

Berry, J., Peaudecerf, F.J., Masters, N.A., et al. (2021) An “occlusive thrombosis-on-a-chip” microfluidic device for investigating the effect of anti-thrombotic drugs. *Lab Chip*, 21 (21): 4104–4117. doi:10.1039/D1LC00347J.

Bhatnagar, P., Lu, X., Evans, M.K., et al. (2012) Genetic variants in platelet factor 4 modulate inflammatory and platelet activation biomarkers. *Circ Cardiovasc Genet*, 5 (4): 412–21. doi:10.1161/CIRCGENETICS.111.961813.

Bhavanasi, D., Kim, S., Goldfinger, L.E., et al. (2010) Protein Kinase C Delta Mediates the Activation of Protein Kinase D In Platelets. *Blood*, 116 (21): 2021–2021. doi:10.1182/blood.V116.21.2021.2021.

Boersma, H.H., Kietselaer, B.L.J.H., Stolk, L.M.L., et al. (2005) Past, present, and future of annexin A5: from protein discovery to clinical applications. *J Nucl Med*, 46 (12): 2035–50.

Boilard, E., Paré, G., Rousseau, M., et al. (2014) Influenza virus H1N1 activates platelets through FcγRIIA signaling and thrombin generation. *Blood*, 123 (18): 2854–2863. doi:10.1182/blood-2013-07-515536.

van Bon, L., Affandi, A.J., Broen, J., et al. (2014) Proteome-wide Analysis and CXCL4 as a Biomarker in Systemic Sclerosis. *N Engl J Med*, 370 (5): 433–443. doi:10.1056/nejmoa1114576.

Bournazos, S., Gupta, A. and Ravetch, J. V. (2020) The role of IgG Fc receptors in antibody-dependent enhancement. *Nat Rev Immunol*, 20 (10): 633–643. doi:10.1038/s41577-020-00410-0.

Bousser, M.-G. and Crassard, I. (2012) Cerebral venous thrombosis, pregnancy and oral contraceptives. *Thromb Res*, 130: S19–S22. doi:10.1016/j.thromres.2012.08.264.

Boyce, S.W., Bandyk, D.F., Bartholomew, J.R., et al. (2011) A Randomized, Open-Label Pilot Study Comparing Desirudin and Argatroban in Patients With Suspected Heparin-Induced Thrombocytopenia With or Without Thrombosis: PREVENT-HIT Study. *Am J Ther*, 18 (1): 14–22. doi:10.1097/MJT.0b013e3181f65503.

Brodard, J., Alberio, L., Angelillo-Scherrer, A., et al. (2020) Accuracy of heparin-induced platelet aggregation test for the diagnosis of heparin-induced thrombocytopenia. *Thromb Res*, 185: 27–30. doi:10.1016/j.thromres.2019.11.004.

Bruhns, P., Iannascoli, B., England, P., et al. (2009) Specificity and affinity of human Fcγ receptors and their polymorphic variants for human IgG subclasses. *Blood*, 113 (16): 3716–3725. doi:10.1182/blood-2008-09-179754.

Bruhns, P. and Jönsson, F. (2015) Mouse and human FcR effector functions. *Immunol Rev*, 268 (1): 25–51. doi:10.1111/imr.12350.

Bruns, I., Daniel Lucas, Pinho, S., et al. (2014) Megakaryocytes regulate hematopoietic stem cell quiescence via Cxcl4 secretion. *Nat Med*, 20 (11): 1315–1320. doi:doi:10.1038/nm.3707.

Buka, R.J., Montague, S.J., Moran, L.A., et al. (2024) PF4 activates the c-Mpl-Jak2 pathway in platelets. *Blood*, 143 (1): 64–69. doi:10.1182/blood.2023020872.

Buka, R.J. and Pavord, S. (2024) Anti-platelet factor 4 immunothrombotic syndromes. *Br J Haematol*, 205 (4): 1291–1295. doi:10.1111/bjh.19663.

Burkhart, J.M., Vaudel, M., Gambaryan, S., et al. (2012) The first comprehensive and quantitative analysis of human platelet protein composition allows the comparative analysis of structural and functional pathways. *Blood*, 120 (15): 73–82. doi:10.1182/blood-2012-04-416594.

Cai, Z., Yarovoi, S. V, Zhu, Z., et al. (2015) Atomic description of the immune complex involved in heparin-induced thrombocytopenia. *Nat Comm*, 6: 8277. doi:10.1038/ncomms9277.

Capecchi, M., Abbattista, M. and Martinelli, I. (2018) Cerebral venous sinus thrombosis. *J Thromb Haemost*, 16 (10): 1918–1931. doi:10.1111/jth.14210.

Capitanio, A.M., Niewiarowski, S., Rucinski, B., et al. (1985) Interaction of platelet factor 4 with human platelets. *Biochim Biophys Acta*, 839 (2): 161–173. doi:10.1016/0304-4165(85)90033-9.

Carlsson, L.E., Santoso, S., Baurichter, G., et al. (1998) Heparin-Induced Thrombocytopenia: New Insights Into the Impact of the FcγRIIa-R-H131 Polymorphism. *Blood*, 92 (5): 1526–1531. doi:10.1182/blood.V92.5.1526.

Carminita, E., Becker, I.C. and Italiano, J.E. (2024) What It Takes To Be a Platelet: Evolving Concepts in Platelet Production. *Circ Res*, 135 (4): 540–549. doi:10.1161/CIRCRESAHA.124.323579.

Carr, M.E., White, G.C. and Gabriel, D.A. (1987) Platelet factor 4 enhances fibrin fiber polymerization. *Thromb Res*, 45 (5): 539–43. doi:10.1016/0049-3848(87)90316-1.

Carré, J., Demont, Y., Mouton, C., et al. (2024) Imaging flow cytometry as a novel approach for the diagnosis of heparin-induced thrombocytopenia. *Br J Haematol*. doi:10.1111/bjh.19945.

Casanova, J.L., Holland, S.M. and Notarangelo, L.D. (2012) Inborn Errors of Human JAKs and STATs. *Immunity*, 36 (4): 515–528. doi:10.1016/j.immuni.2012.03.016.

Cattaneo, M., Cerletti, C., Harrison, P., et al. (2013) Recommendations for the standardization of light transmission aggregometry: A consensus of the working party from the platelet physiology subcommittee of SSC/ISTH. *J Thromb Haemost*, 11 (6): 1183–1189. doi:10.1111/jth.12231.

Cell Signalling Technology (n.d.) *FcγRIIA (E3K8U) Rabbit mAb #60432*. Available at: https://www.cellsignal.com/products/primary-antibodies/fcgriia-e3k8u-rabbit-mab/60432 (Accessed: 28 January 2025).

Chayoua, W., Nicolson, P.L.R., Meijers, J.C.M., et al. (2021) Antiprothrombin antibodies induce platelet activation: A possible explanation for anti-FXa therapy failure in patients with antiphospholipid syndrome? *J Thromb Haemost*, 19 (7): 1776–1782. doi:10.1111/jth.15320.

Chesterman, C.N., McGready, J.R., Doyle, D.J., et al. (1978) Plasma Levels of Platelet Factor 4 Measured by Radioimmunoassay. *Br J Haematol*, 40 (3): 489–500. doi:10.1111/j.1365-2141.1978.tb05819.x.

Chong, B.H., Gallus, A.S., Cade, J.F., et al. (2001) Prospective randomised open-label comparison of danaparoid with dextran 70 in the treatment of heparin-induced thrombocytopaenia with thrombosis: a clinical outcome study. *Thromb Haemost*, 86 (5): 1170–5.

Cines, D.B. and Greinacher, A. (2021) Vaccine-induced immune thrombotic thrombocytopenia. *Blood*, 141 (14): 1659–1665.

Cines, D.B., Yarovoi, S. V., Zaitsev, S. V., et al. (2016) Polyphosphate/platelet factor 4 complexes can mediate heparin-independent platelet activation in heparin-induced thrombocytopenia. *Blood Adv*, 1 (1): 62–74. doi:10.1182/bloodadvances.2016000877.

Clark-Lewis, I., Dewald, B., Geiser, T., et al. (1993) Platelet factor 4 binds to interleukin 8 receptors and activates neutrophils when its N terminus is modified with Glu-Leu-Arg. *Proc Natl Acad Sci U S A*, 90 (8): 3574–3577. doi:10.1073/pnas.90.8.3574.

Coll, E., Brodie M, Robles-Carrillo L, et al. (2017) “Platelet Activation by Antiphospholipid Antibodies through the IgG Receptor FcγRIIa: Possible Role in Thrombosis Associated with Antiphospholipid Syndrome? [Poster presentation].” In *Res Pract Haemost Thromb*. 2017. pp. 1099–1100. doi:10.1002/rth2.12012.

Conley, C.L., Hartmann, R.C. and Lalley, J.S. (1948) The Relationship of Heparin Activity to Platelet Concentration. *Experimental Biology and Medicine*, 69 (2): 284–287. doi:10.3181/00379727-69-16693.

Cook, J.J., Niewiarowski, S., Yan, Z., et al. (1992) Platelet factor 4 efficiently reverses heparin anticoagulation in the rat without adverse effects of heparin-protamine complexes. *Circulation*, 85 (3): 1102–9. doi:10.1161/01.cir.85.3.1102.

Cowan, S.W., Bakshi, E.N., Machin, K.J., et al. (1986) Binding of heparin to human platelet factor 4. *Biochem J*, 234 (2): 485–8. doi:10.1042/bj2340485.

Crijns, H., Vanheule, V. and Proost, P. (2020) Targeting Chemokine-Glycosaminoglycan Interactions to Inhibit Inflammation. *Front Immunol*, 11 (43). doi:10.3389/fimmu.2020.00483.

Cross, N.C.P., Godfrey, A.L., Cargo, C., et al. (2021) The use of genetic tests to diagnose and manage patients with myeloproliferative and myeloproliferative/myelodysplastic neoplasms, and related disorders. *Br J Haematol*. doi:10.1111/bjh.17766.

Cuker, A. (2014) Clinical and laboratory diagnosis of heparin-induced thrombocytopenia: an integrated approach. *Semin Thromb Hemost*, 40 (1): 106–14. doi:10.1055/s-0033-1363461.

Cuker, A., Arepally, G., Crowther, M., et al. (2010) The HIT Expert Probability (HEP) Score: a novel pre-test probability model for heparin-induced thrombocytopenia based on broad expert opinion. *J Thromb Haemost*, 8 (12): 2642–2650. doi:10.1111/j.1538-7836.2010.04059.x.

Cuker, A., Arepally, G.M., Chong, B.H., et al. (2018) American Society of Hematology 2018 guidelines for management of venous thromboembolism: Heparin-induced thrombocytopenia. *Blood Adv*, 2 (22): 3360–3392. doi:10.1182/bloodadvances.2018024489.

Cuker, A., Gimotty, P.A., Crowther, M.A., et al. (2012) Predictive value of the 4Ts scoring system for heparin-induced thrombocytopenia: a systematic review and meta-analysis. *Blood*, 120 (20): 4160–4167. doi:10.1182/blood-2012-07-443051.

Dai, J., Madeeva, D., Hayes, V., et al. (2018) Dynamic intercellular redistribution of HIT antigen modulates heparin-induced thrombocytopenia. *Blood*, 132 (7): 727–734. doi:10.1182/blood-2018-02-830737.

Dawood, B.B., Wilde, J. and Watson, S.P. (2007) Reference curves for aggregation and ATP secretion to aid diagnose of platelet-based bleeding disorders: Effect of inhibition of ADP and thromboxane A2 pathways. *Platelets*, 18 (5): 329–345. doi:10.1080/09537100601024111.

Dehmer, G.J., Fisher, M., Tate, D.A., et al. (1995) Reversal of heparin anticoagulation by recombinant platelet factor 4 in humans. *Circulation*, 91 (8): 2188–94. doi:10.1161/01.cir.91.8.2188.

Dessalles, C.A., Leclech, C., Castagnino, A., et al. (2021) Integration of substrate- and flow-derived stresses in endothelial cell mechanobiology. *Commun Biol*, 4 (1): 764. doi:10.1038/s42003-021-02285-w.

Deuel, T.F., Keim, P.S., Farmer, M., et al. (1977) Amino acid sequence of human platelet factor 4. *Proc Natl Acad Sci U S A.*, 74 (6): 2256–2258. doi:10.1073/pnas.74.6.2256.

Deutsch, E., Wawersich, E. and Franke, G. (1957) Occurrence of antiheparin factor in thrombocytes & tissues. I. Antiheparin activity of thrombocytes. *Thrombosis et diathesis haemorrhagica*, 1 (3–4): 397–412.

DeVries, M.E., Kelvin, A.A., Xu, L., et al. (2006) Defining the Origins and Evolution of the Chemokine/Chemokine Receptor System. *J Immunol*, 176 (1): 401–415. doi:10.4049/jimmunol.176.1.401.

Dhakal, B., Kreuziger, L.B., Rein, L., et al. (2018) Disease burden, complication rates, and health-care costs of heparin-induced thrombocytopenia in the USA: a population-based study. *Lancet Haematol*, 5 (5): e220–e231. doi:10.1016/S2352-3026(18)30046-2.

Dickhout, A., Tullemans, B.M.E., Heemskerk, J.W.M., et al. (2021) Galectin-1 and platelet factor 4 (CXCL4) induce complementary platelet responses in vitro. *PLoS ONE*, 16 (1): 1–18. doi:10.1371/journal.pone.0244736.

Dimopoulou, D., Mentesidou, L., Dettoraki, A., et al. (2024) A cluster of pediatric VITT-like cases with thrombosis and thrombocytopenia following respiratory infections-Case series. *Res Pract Thromb Haemost*, 8 (7): 102589. doi:10.1016/j.rpth.2024.102589.

Drachman, J.G., Millett, K.M. and Kaushansky, K. (1999) Thrombopoietin signal transduction requires functional JAK2, not TYK2. *J Biol Chem*, 274 (19): 13480–13484. doi:10.1074/jbc.274.19.13480.

Dubrac, A., Quemener, C., Lacazette, E., et al. (2010) Functional divergence between 2 chemokines is conferred by single amino acid change. *Blood*, 116 (22): 4703–4711. doi:10.1182/blood-2010-03-274852.

Dudek, A.Z., Nesmelova, I., Mayo, K., et al. (2003) Platelet factor 4 promotes adhesion of hematopoietic progenitor cells and binds IL-8: Novel mechanisms for modulation of hematopoiesis. *Blood*, 101 (12): 4687–4694. doi:10.1182/blood-2002-08-2363.

Dudek, A.Z., Pennell, C.A., Decker, T.D., et al. (1997) Platelet factor 4 binds to glycanated forms of thrombomodulin and to Protein C. A potential mechanism for enhancing generation of activated protein C. *J Biol Chem*, 272 (50): 31785–31792. doi:10.1074/jbc.272.50.31785.

Duffau, P., Seneschal, J., Nicco, C., et al. (2010) Platelet CD154 Potentiates Interferon-α Secretion by Plasmacytoid Dendritic Cells in Systemic Lupus Erythematosus. *Sci Trans Med*, 2 (47): 47ra63. doi:10.1126/scitranslmed.3001001.

Duits, A.J., Bootsma, H., Derksen, R.H.W.M., et al. (1995) Skewed distribution of IgG Fc receptor IIa (CD32) polymorphism is associated with renal disease in systemic lupus erythematosus patients. *Arthritis Rheum*, 38 (12): 1832–1836. doi:10.1002/art.1780381217.

Dupuy, A., Liu, X., Tieng, J., et al. (2022) Endothelial Cell Activation Enhances Thromboinflammation in Vitt. *Blood*, 140 (Supplement 1): 1656–1657. doi:10.1182/blood-2022-168441.

Eaton, N., Subramaniam, S., Schulte, M.L., et al. (2021) Bleeding diathesis in mice lacking JAK2 in platelets. *Blood Adv*, 5 (15): 2969–2981. doi:10.1182/BLOODADVANCES.2020003032.

Eisman, R., Surey, S., Ramachandran, B., et al. (1990) Structural and functional comparison of the genes for human platelet factor 4 and PF4(alt). *Blood*, 76 (2): 336–344. doi:10.1182/blood.v76.2.336.336.

Endeman, H., Cornips, M.C.A., Grutters, J.C., et al. (2009) The Fcγ Receptor IIA-R/R131 Genotype Is Associated with Severe Sepsis in Community-Acquired Pneumonia. *Clin Vaccine Immunol*, 16 (7): 1087–1090. doi:10.1128/CVI.00037-09.

Erhardt, J.A., Erickson-Miller, C.L., Aivado, M., et al. (2009) Comparative analyses of the small molecule thrombopoietin receptor agonist eltrombopag and thrombopoietin on in vitro platelet function. *Exp Hematol*, 37 (9): 1030–1037. doi:10.1016/j.exphem.2009.06.011.

Eslin, D.E., Zhang, C., Samuels, K.J., et al. (2004) Transgenic mice studies demonstrate a role for platelet factor 4 in thrombosis: Dissociation between anticoagulant and antithrombotic effect of heparin. *Blood*, 104 (10): 3173–3180. doi:10.1182/blood-2003-11-3994.

Etheridge, S.L., Roh, M.E., Cosgrove, M.E., et al. (2014) JAK2V617F-positive endothelial cells contribute to clotting abnormalities in myeloproliferative neoplasms. *Proc Nat Acad Sci U S A*, 111 (6): 2295–2300. doi:10.1073/pnas.1312148111.

Everett, B.M., Yeh, R., Foo, S.Y., et al. (2007) Prevalence of Heparin/Platelet Factor 4 Antibodies Before and After Cardiac Surgery. *Ann Thorac Surg*, 83 (2): 592–597. doi:10.1016/j.athoracsur.2006.09.040.

Ezumi, Y., Nishida, E., Uchiyama, T., et al. (1999) Thrombopoietin potentiates agonist-stimulated activation of p38 mitogen-activated protein kinase in human platelets. *Biochem Biophys Res Commun*, 261 (1): 58–63. doi:10.1006/bbrc.1999.0979.

Ezumi, Y., Takayama, H. and Okuma, M. (1995) Thrombopoietin, c-Mpl ligand, induces tyrosine phosphorylation of Tyk2, JAK2, and STAT3, and enhances agonists-induced aggregation in platelets in vitro. *FEBS Letters*, 374: 48–52.

Falet, H.E., Rivadeneyra, L. and Hoffmeister, K.M. (2022) Clinical impact of glycans in platelet and megakaryocyte biology. *Blood*, 132 (22): 3255–3263.

Falsey, A.R., Sobieszczyk, M.E., Hirsch, I., et al. (2021) Phase 3 Safety and Efficacy of AZD1222 (ChAdOx1 nCoV-19) Covid-19 Vaccine. *N Engl J Med*, 385 (25): 2348–2360. doi:10.1056/NEJMoa2105290.

Fang, J.S., Coon, B.G., Gillis, N., et al. (2017) Shear-induced Notch-Cx37-p27 axis arrests endothelial cell cycle to enable arterial specification. *Nat Commun*, 8 (1). doi:10.1038/s41467-017-01742-7.

Fielder, P., Gurney, A., Stefanich, E., et al. (1996) Regulation of thrombopoietin levels by c-mpl-mediated binding to platelets. *Blood*, 87 (6): 2154–2161. doi:10.1182/blood.V87.6.2154.bloodjournal8762154.

Fiore, M.M. and Kakkar, V. V (2003) Platelet factor 4 neutralizes heparan sulfate-enhanced antithrombin inactivation of factor Xa by preventing interaction(s) of enzyme with polysaccharide. *Biochem Biophys Res Commun*, 7: 311.

Fleischer, J., Grage-Griebenow, E., Kasper, B., et al. (2002) Platelet Factor 4 Inhibits Proliferation and Cytokine Release of Activated Human T Cells. *J Immunol*, 169 (2): 770–777. doi:10.4049/jimmunol.169.2.770.

Fonseca, B.D., Diering, G.H., Bidinosti, M.A., et al. (2012) Structure-Activity Analysis of Niclosamide Reveals Potential Role for Cytoplasmic pH in Control of Mammalian Target of Rapamycin Complex 1 (mTORC1) Signaling. *J Biol Chem*, 287 (21): 17530–17545. doi:10.1074/jbc.M112.359638.

Forsberg, E., Pejler, G., Ringvall, M., et al. (1999) Abnormal mast cells in mice deficient in a heparin-synthesizing enzyme. *Nature*, 400: 773–776.

Fox, J.M., Kausar, F., Day, A., et al. (2018) CXCL4/Platelet Factor 4 is an agonist of CCR1 and drives human monocyte migration. *Sci Rep*, 8 (1): 1–15. doi:10.1038/s41598-018-27710-9.

Gao, C., Boylan, B., Bougie, D., et al. (2009) Eptifibatide-induced thrombocytopenia and thrombosis in humans require FcγRIIa and the integrin β3 cytoplasmic domain. *J Clin Invest*, 119 (3): 504–511. doi:10.1172/JCI36745.

Gao, C., Boylan, B., Fang, J., et al. (2011) Heparin promotes platelet responsiveness by potentiating αIIbβ3-mediated outside-in signaling. *Blood*, 117 (18): 4946–4952. doi:10.1182/blood-2010-09-307751.

Garcia, F.J., Sun, N., Lee, H., et al. (2022) Single-cell dissection of the human brain vasculature. *Nature*, 603 (7903): 893–899. doi:10.1038/s41586-022-04521-7.

García-Martínez, J.M., Moran, J., Clarke, R.G., et al. (2009) Ku-0063794 is a specific inhibitor of the mammalian target of rapamycin (mTOR). *Biochem J*, 421 (1): 29–42. doi:10.1042/BJ20090489.

Gardiner, E.E., Karunakaran, D., Arthur, J.F., et al. (2008) Dual ITAM-mediated proteolytic pathways for irreversible inactivation of platelet receptors: de-ITAM-izing FcγRIIa. *Blood*, 111 (1): 165–174. doi:10.1182/blood-2007-04-086983.

Gengrinovitch, S., Greenberg, S.M., Cohen, T., et al. (1995) Platelet factor-4 inhibits the mitogenic activity of VEGF121 and VEGF165 using several concurrent mechanisms. *J Biol Chem*, 270 (25): 15059–15065. doi:10.1074/jbc.270.25.15059.

Gentilini, G., Kirschbaum, N.E., Augustine, J.A., et al. (1999) Inhibition of human umbilical vein endothelial cell proliferation by the CXC chemokine, platelet factor 4 (PF4), is

associated with impaired downregulation of p21(Cip1/WAF1). *Blood*, 93 (1): 25–33. doi:10.1182/blood.v93.1.25.

Gewirtz, A., Calabretta, B., Rucinski, B., et al. (1989) Inhibition of human megakaryocytopoiesis in vitro by platelet factor 4 (PF4) and a synthetic COOH-terminal PF4 peptide. *J Clin Invest*, 83 (5): 1477–1486. doi:10.1172/JCI114041.

Gleissner, C.A., Von Hundelshausen, P. and Ley, K. (2008) Platelet chemokines in vascular disease. *Arterioscler Thromb Vasc Biol*, 28 (11): 1920–1927. doi:10.1161/ATVBAHA.108.169417.

Gleissner, C.A., Shaked, I., Erbel, C., et al. (2010a) CXCL4 downregulates the atheroprotective hemoglobin receptor CD163 in human macrophages. *Circ Res*, 106 (1): 203–211. doi:10.1161/CIRCRESAHA.109.199505.

Gleissner, C.A., Shaked, I., Little, K.M., et al. (2010b) CXC Chemokine Ligand 4 Induces a Unique Transcriptome in Monocyte-Derived Macrophages. *J Immunol*, 184 (9): 4810–4818. doi:10.4049/jimmunol.0901368.

Gleitz, H.L.F.E., Dugourd, A.L.J.F., Leimkühler, N.B., et al. (2020) Increased CXCL4 expression in hematopoietic cells links inflammation and progression of bone marrow fibrosis in MPN. *Blood*, 136 (18): 2051–2064. doi:10.1182/BLOOD.2019004095.

Goldmann, L., Duan, R., Kragh, T., et al. (2019) Oral Bruton tyrosine kinase inhibitors block activation of the platelet Fc receptor CD32a (FcγRIIA): a new option in HIT? *Blood Adv*, 3 (23): 4021–4033. doi:10.1182/bloodadvances.2019000617.

Gollomp, K., Kim, M., Johnston, I., et al. (2018) Neutrophil accumulation and NET release contribute to thrombosis in HIT. *JCI Insight*, 3 (18): 1–14. doi:10.1172/jci.insight.99445.

Gollomp, K., Sarkar, A., Harikumar, S., et al. (2020) Fc-modified HIT-like monoclonal antibody as a novel treatment for sepsis. *Blood*, 135 (10): 743–754. doi:10.1182/blood.2019002329.

Gonthier, M.-C., Gendron, N., Eloy, P., et al. (2021) Heparin-induced Thrombocytopenia Diagnosis: A Retrospective Study Comparing Heparin-induced Platelet Activation Test to 14C-serotonin Release Assay. *TH Open*, 05 (04): e507–e512. doi:10.1055/a-1653-5065.

Google DeepMind (n.d.) *AlphaFold Server Beta*. Available at: https://alphafoldserver.com/ (Accessed: 5 January 2025).

Goswami, A., Noirault, E., Coombs, E.J., et al. (2022) Attenuated evolution of mammals through the Cenozoic. *Science*, 378 (6618): 377–383. doi:10.1126/science.abm7525.

Gouwy, M., Ruytinx, P., Radice, E., et al. (2016) CXCL4 and CXCL4L1 differentially affect monocyte survival and dendritic cell differentiation and phagocytosis. *PLoS ONE*, 11 (11): 1–24. doi:10.1371/journal.pone.0166006.

Graca, F.A., Stephan, A., Minden-Birkenmaier, B.A., et al. (2023) Platelet-derived chemokines promote skeletal muscle regeneration by guiding neutrophil recruitment to injured muscles. *Nat Commun*, 14 (1). doi:10.1038/s41467-023-38624-0.

Gray, A.L., Karlsson, R., Roberts, A.R.E., et al. (2023) Chemokine CXCL4 interactions with extracellular matrix proteoglycans mediate widespread immune cell recruitment independent of chemokine receptors. *Cell Rep*, 42 (1): 111930. doi:10.1016/j.celrep.2022.111930.

Greinacher, A., Eichler, P., Lubenow, N., et al. (2000) Heparin-induced thrombocytopenia with thromboembolic complications: meta-analysis of 2 prospective trials to assess the value of parenteral treatment with lepirudin and its therapeutic aPTT range. *Blood*, 96 (3): 846–851. doi:10.1182/blood.V96.3.846.

Greinacher, A., Gopinadhan, M., Günther, J.U., et al. (2006) Close approximation of two platelet factor 4 tetramers by charge neutralization forms the antigens recognized by HIT antibodies. *Arterioscl Thromb Vasc Biol*, 26 (10): 2386–2393. doi:10.1161/01.ATV.0000238350.89477.88.

Greinacher, A., Schönborn, L., Siegerist, F., et al. (2022) Pathogenesis of vaccine-induced immune thrombotic thrombocytopenia (VITT). *Semin Hematol*, 59 (2): 97–107. doi:10.1053/j.seminhematol.2022.02.004.

Greinacher, A., Selleng, K. and Warkentin, T.E. (2017) Autoimmune heparin-induced thrombocytopenia. *J Thromb Haemost*, 15 (11): 2099–2114. doi:10.1111/jth.13813.

Greinacher, A., Thiele, T., Warkentin, T.E., et al. (2021) Thrombotic Thrombocytopenia after ChAdOx1 nCov-19 Vaccination. *N Engl J Med*, 384 (22): 2092–2101. doi:10.1056/nejmoa2104840.

Greinacher, A. and Warkentin, T.E. (2023) Platelet factor 4 triggers thrombo-inflammation by bridging innate and adaptive immunity. *Int J Lab Hematol*, 45 (S2): 11–22. doi:10.1111/ijlh.14075.

Gremmel, T., Frelinger, A.L. and Michelson, A.D. (2024) Platelet Physiology. *Sem Thromb Haemost*, 50 (08): 1173–1186. doi:10.1055/s-0044-1786387.

Gröger, M., Sarmay, G., Fiebiger, E., et al. (1996) Dermal microvascular endothelial cells express CD32 receptors in vivo and in vitro. *J Immunol*, 156 (4): 1549–56.

Grommes, J., Alard, J.E., Drechsler, M., et al. (2012) Disruption of platelet-derived chemokine heteromers prevents neutrophil extravasation in acute lung injury. *Am J Respir Crit Care Med*, 185 (6): 628–636. doi:10.1164/rccm.201108-1533OC.

Gutierrez, M.J. and Desiderio, S. (2024) “The chemistry, structure, and function of immunoglobulins.” In Niederhuber, J.E. (ed.) *Clinical Immuno-Oncology*. Amsterdam: Elsevier. pp. 15-40.e4. doi:10.1016/B978-0-323-87763-3.00011-3.

Hagedorn, M., Zilberberg, L., Lozano, R.M., et al. (2001) A short peptide domain of platelet factor 4 blocks angiogenic key events induced by FGF-2. *FASEB J*, 15 (3): 550–552. doi:10.1096/fj.00-0285fje.

Hamers-Casterman, C., Atarhouch, T., Muyldermans, S., et al. (1993) Naturally occurring antibodies devoid of light chains. *Nature*, 363 (6428): 446–448. doi:10.1038/363446a0.

Hammond, W.P., Wun, T., Kaplan, A., et al. (1998) High Concentrations of Thrombopoietin Activate Platelets In Vitro. *CATH*, 4 (3): 170–178. doi:10.1177/107602969800400306.

Handin, R.I. and Cohen, H.J. (1976) Purification and binding properties of human platelet factor four. *J Biol Chem*, 251 (14): 4273–4282. doi:10.1016/S0021-9258(17)33292-1.

Handtke, S., Wolff, M., Zaninetti, C., et al. (2021) A flow cytometric assay to detect platelet-activating antibodies in VITT after ChAdOx1 nCov-19 vaccination. *Blood*, 137 (26): 3656–3659. doi:10.1182/blood.2021012064.

Hanlon, A. and Brander, D.M. (2020) Managing toxicities of phosphatidylinositol-3-kinase (PI3K) inhibitors. *Hematology Am Soc Hematol Educ Program*, 2020 (1): 346–356. doi:10.1182/hematology.2020000119.

Harmsen, M.M. and De Haard, H.J. (2007) Properties, production, and applications of camelid single-domain antibody fragments. *Appl Microbiol Biotechnol*, 77 (1): 13–22. doi:10.1007/s00253-007-1142-2.

Haseley, L.A., Wisnieski, J.J., Denburg, M.R., et al. (1997) Antibodies to C1q in systemic lupus erythematosus: Characteristics and relation to FcγRIIA alleles. *Kidney Int*, 52 (5): 1375–1380. doi:10.1038/ki.1997.464.

Hayes, V., Johnston, I., Arepally, G.M., et al. (2017) Endothelial antigen assembly leads to thrombotic complications in heparin-induced thrombocytopenia. *J Clin Invest*, 127 (3): 1090–1098. doi:10.1172/JCI90958.

Heijnen, H. and van der Sluijs, P. (2015) Platelet secretory behaviour: As diverse as the granules... or not? *J Thromb Haemost*, 13 (12): 2141–2151. doi:10.1111/jth.13147.

Herbert, J.M., Savi, P., Jeske, W.P., et al. (1998) Effect of SR121566A, a potent GP IIb-IIIa antagonist, on the HIT serum/heparin-induced platelet mediated activation of human endothelial cells. *Thromb Haemost*, 80 (2): 326–331.

Herrera-Comoglio, R. and Lane, S. (2022) Vaccine-Induced Immune Thrombocytopenia and Thrombosis after the Sputnik V Vaccine. *N Engl J Med*, 387 (15): 1431–1432. doi:10.1056/NEJMc2210813.

Herrera-Galeano, J.E., Becker, D.M., Wilson, A.F., et al. (2008) A Novel Variant in the Platelet Endothelial Aggregation Receptor-1 Gene Is Associated With Increased Platelet Aggregability. *Arterioscler Thromb Vasc Biol*, 28 (8): 1484–1490. doi:10.1161/ATVBAHA.108.168971.

Hitchcock, I.S., Hafer, M., Sangkhae, V., et al. (2021) The thrombopoietin receptor: revisiting the master regulator of platelet production. *Platelets*, 32 (6): 770–778. doi:10.1080/09537104.2021.1925102.

Hitchcock, I.S. and Kaushansky, K. (2014) Thrombopoietin from beginning to end. *Br J Haematol*, 165 (2): 259–268. doi:10.1111/bjh.12772.

Hobbs, C.M., Manning, H., Bennett, C., et al. (2013) JAK2V617F leads to intrinsic changes in platelet formation and reactivity in a knock-in mouse model of essential thrombocythemia. *Blood*, 122 (23): 3787–3797. doi:10.1182/blood-2013-06-501452.

Hoffman, R.C., Andersen, H., Walker, K., et al. (1996) Peptide, Disulfide, and Glycosylation Mapping of Recombinant Human Thrombopoietin from Ser1 to Arg246. *Biochemistry*, 35 (47): 14849–14861. doi:10.1021/bi961075b.

Hogarth, P.M., Anania, J.C. and Wines, B.D. (2014) The FcγR of Humans and Non-human Primates and Their Interaction with IgG: Implications for Induction of Inflammation, Resistance to Infection and the Use of Therapeutic Monoclonal Antibodies. *Curr Top Microbiol Immunol*, 382: 321–352. doi:10.1007/978-3-319-07911-0_15.

Hu, X., li, J., Fu, M., et al. (2021) The JAK/STAT signaling pathway: from bench to clinic. *Signal Transduct Target Ther*, 6 (1): 402. doi:10.1038/s41392-021-00791-1.

Huang, J., Swieringa, F., Solari, F.A., et al. (2021) Assessment of a complete and classified platelet proteome from genome-wide transcripts of human platelets and megakaryocytes covering platelet functions. *Sci Rep*, 11 (1): 12358. doi:10.1038/s41598-021-91661-x.

Huang, Z.-Y., Chien, P., Indik, Z.K., et al. (2011) Human platelet FcγRIIA and phagocytes in immune-complex clearance. *Mol Immunol*, 48 (4): 691–696. doi:10.1016/j.molimm.2010.11.017.

Hughes, C.E. and Nibbs, R.J.B. (2018) A guide to chemokines and their receptors. *FEBS J*, 285 (16): 2944–2971. doi:10.1111/febs.14466.

Humphries, D.E., Wong, G.W., Friend, D.S., et al. (1999) Heparin is essential for the storage of specific granule proteases in mast cells. *Nature*, 400: 769–772.

Von Hundelshausen, P., Koenen, R.R., Sack, M., et al. (2005) Heterophilic interactions of platelet factor 4 and RANTES promote monocyte arrest on endothelium. *Blood*, 105 (3): 924–930. doi:10.1182/blood-2004-06-2475.

Hursting, M.J., Pai, P.J., McCracken, J.E., et al. (2010) Platelet factor 4/heparin antibodies in blood bank donors. *Am J Clin Path*, 134 (5): 774–780. doi:10.1309/AJCPG0MNR5NGKNFX.

Huynh, A., Arnold, D.M., Ivetic, N., et al. (2023) Antibodies against platelet factor 4 and the risk of cerebral venous sinus thrombosis in patients with vaccine-induced immune thrombotic thrombocytopenia. *J Thromb Haemost*, 21 (10): 2833–2843. doi:10.1016/j.jtha.2023.06.026.

Huynh, A., Kelton, J.G., Arnold, D.M., et al. (2021) Antibody epitopes in vaccine-induced immune thrombotic thrombocytopaenia. *Nature*, 596 (7873): 565–569. doi:10.1038/s41586-021-03744-4.

IQ Products (n.d.) *HITAlert™ Kit*. Available at: https://www.iqproducts.nl/products/hit/hitalert-kit/ (Accessed: 28 November 2024).

Izquierdo, I., Barrachina, M.N., Hermida-Nogueira, L., et al. (2020) A Comprehensive Tyrosine Phosphoproteomic Analysis Reveals Novel Components of the Platelet CLEC-2 Signaling Cascade. *Thromb Haemost*, 120 (2): 262–276. doi:10.1055/s-0039-3400295.

Janus-Bell, E. and Mangin, P.H. (2023) The relative importance of platelet integrins in hemostasis, thrombosis and beyond. *Haematologica*, 108 (7): 1734–1747. doi:10.3324/haematol.2022.282136.

Johansen, S., Lægreid, I.J., Ernstsen, S.L., et al. (2022) Thrombosis and thrombocytopenia after HPV vaccination. *J Thromb Haemost*, 20 (3): 700–704. doi:10.1111/jth.15604.

Johnston, I., Sarkar, A., Hayes, V., et al. (2020) Recognition of PF4-VWF complexes by heparin-induced thrombocytopenia antibodies contributes to thrombus propagation. *Blood*, 135 (15): 1270–1280. doi:10.1182/blood.2018881607.

De Jong, E.K., De Haas, A.H., Brouwer, N., et al. (2008) Expression of CXCL4 in microglia in vitro and in vivo and its possible signaling through CXCR3. *J Neurochem*, 105: 1726–1736. doi:10.1111/j.1471-4159.2008.05267.x.

Jouan, V., Canron, X., Alemany, M., et al. (1999) Inhibition of In Vitro Angiogenesis by Platelet Factor-4–Derived Peptides and Mechanism of Action. *Blood*, 94 (3): 984–993.

Jourdi, G., Ramström, S., Sharma, R., et al. (2023) Consensus report on flow cytometry for platelet function testing in thrombocytopenic patients: communication from the SSC of the ISTH. *J Thromb Haemost*, 21 (10): 2941–2952. doi:10.1016/j.jtha.2023.07.006.

Juhl, D., Eichler, P., Lubenow, N., et al. (2006) Incidence and clinical significance of anti-PF4/heparin antibodies of the IgG, IgM, and IgA class in 755 consecutive patient samples referred for diagnostic testing for heparin-induced thrombocytopenia. *Eur J Haematol*, 76 (5): 420–426. doi:10.1111/j.1600-0609.2005.00621.x.

Jumper, J., Evans, R., Pritzel, A., et al. (2021) Highly accurate protein structure prediction with AlphaFold. *Nature*, 596 (7873): 583–589. doi:10.1038/s41586-021-03819-2.

Kalucka, J., de Rooij, L.P.M.H., Goveia, J., et al. (2020) Single-Cell Transcriptome Atlas of Murine Endothelial Cells. *Cell*, 180 (4): 764-779.e20. doi:10.1016/j.cell.2020.01.015.

Kanack, A.J., Bayas, A., George, G., et al. (2022) Monoclonal and oligoclonal anti-platelet factor 4 antibodies mediate VITT. *Blood*, 140 (1): 73–77. doi:10.1182/blood.2021014588.

Kanack, A.J., Leung, N. and Padmanabhan, A. (2024) Diagnostic Complexity in Monoclonal Gammopathy of Thrombotic Significance. *N Engl J Med*, 391 (20): 1961–1963. doi:10.1056/NEJMc2409428.

Kardeby, C., Evans, A., Campos, J., et al. (2023) Heparin and heparin proteoglycan-mimetics activate platelets via PEAR1 and PI3Kβ. *J Thromb Haemost*, 21 (1): 101–116. doi:10.1016/j.jtha.2022.10.008.

Kardeby, C., Fälker, K., Haining, E.J., et al. (2019) Synthetic glycopolymers and natural fucoidans cause human platelet aggregation via PEAR1 and GPIba. *Blood Adv*, 3 (3): 275–287. doi:10.1182/bloodadvances.2018024950.

Karnes, J.H., Cronin, R.M., Rollin, J., et al. (2015) A genome-wide association study of heparin-induced thrombocytopenia using an electronic medical record. *Thromb Haemost*, 113 (4): 772–781. doi:10.1160/TH14-08-0670.

Kasper, B., Brandt, E., Brandau, S., et al. (2007) Platelet Factor 4 (CXC Chemokine Ligand 4) Differentially Regulates Respiratory Burst, Survival, and Cytokine Expression of Human Monocytes by Using Distinct Signaling Pathways. *J Immunol*, 179 (4): 2584–2591. doi:10.4049/jimmunol.179.4.2584.

Kasthuri, R.S., Glover, S.L., Jonas, W., et al. (2012) PF4/heparin-antibody complex induces monocyte tissue factor expression and release of tissue factor positive microparticles by activation of FcγRI. *Blood*, 119 (22): 5285–93. doi:10.1182/blood-2011-06-359430.

Kauskot, A., Di Michele, M., Loyen, S., et al. (2012) A novel mechanism of sustained platelet αIIbβ3 activation via PEAR1. *Blood*, 119 (17): 4056–4065. doi:10.1182/blood-2011-11-392787.

Kelton, J.G., Sheridan, D., Santos, A., et al. (1988) Heparin-induced thrombocytopenia: laboratory studies. *Blood*, 72 (3): 925–30.

Khairy, M., Lasne, D., Amelot, A., et al. (2004) Polymorphonuclear leukocyte and monocyte activation induced by plasma from patients with heparin-induced thrombocytopenia in whole blood. *Thromb Haemost*, 92 (6): 1411–1419. doi:10.1160/TH03-10-0649.

Khairy, M., Lasne, D., Brohard-Bohn, B., et al. (2001) A new approach in the study of the molecular and cellular events implicated in heparin-induced thrombocytopenia. Formation of leukocyte-platelet aggregates. *Thromb Haemost*, 85 (6): 1090–6.

Khan, A.O., Maclachlan, A., Lowe, G.C., et al. (2020) High-throughput platelet spreading analysis: a tool for the diagnosis of platelet-based bleeding disorders. *Haematologica*, 105 (3): e124–e128. doi:10.3324/haematol.2019.225912.

Kim, L.C., Cook, R.S. and Chen, J. (2017) MTORC1 and mTORC2 in cancer and the tumor microenvironment. *Oncogene*. 36 (16) pp. 2191–2201. doi:10.1038/onc.2016.363.

Kizlik-Masson, C., Vayne, C., McKenzie, S.E., et al. (2017) 5B9, a monoclonal antiplatelet factor 4/heparin IgG with a human Fc fragment that mimics heparin-induced thrombocytopenia antibodies. *J Thromb Haemost*, 15 (10): 2065–2075. doi:10.1111/jth.13786.

Kong, F.M.S., Zhao, L., Wang, L., et al. (2017) Ensuring sample quality for blood biomarker studies in clinical trials: A multicenter international study for plasma and serum sample preparation. *Transl Lung Cancer Res*, 6 (6): 625–634. doi:10.21037/tlcr.2017.09.13.

Kowalska, M.A., Mahmud, S.A., Lambert, M.P., et al. (2007) Endogenous platelet factor 4 stimulates activated protein C generation in vivo and improves survival after thrombin or

lipopolysaccharide challenge. *Blood*, 110 (6): 1903–1905. doi:10.1182/blood-2007-03-081901.

Kowalska, M.A., Rauova, L. and Poncz, M. (2010) Role of the platelet chemokine platelet factor 4 (PF4) in hemostasis and thrombosis. *Thromb Res*, 125 (4): 292–296. doi:10.1016/j.thromres.2009.11.023.

Krauel, K., Pötschke, C. and Weber, C. (2011) Platelet factor 4 binds to bacteria-inducing antibodies cross-reacting with the major antigen in heparin-induced thrombocytopenia. *Blood*, 117 (21): 5783. doi:10.1182/blood-2011-04-347740.

Krauel, K., Weber, C., Brandt, S., et al. (2012) Platelet factor 4 binding to lipid A of Gram-negative bacteria exposes PF4/heparin-like epitopes. *Blood*, 120 (16): 3345–3352. doi:10.1182/blood-2012-06-434985.

Kreimann, M., Brandt, S., Krauel, K., et al. (2014) Binding of anti–platelet factor 4/heparin antibodies depends on the thermodynamics of conformational changes in platelet factor 4. *Blood*, 124 (15): 2442–2449. doi:10.1182/blood-2014-03-559518.

Kristinsson, S.Y., Pfeiffer, R.M., Björkholm, M., et al. (2010) Arterial and venous thrombosis in monoclonal gammopathy of undetermined significance and multiple myeloma: a population-based study. *Blood*, 115 (24): 4991–4998. doi:10.1182/blood-2009-11-252072.

Kuo, J., Chen, Y., Liu, J., et al. (2013) Alternative C-terminal helix orientation alters chemokine function: structure of the anti-angiogenic chemokine, CXCL4L1. *J Biol Chem*, 288 (19): 13522–13533. doi:10.1074/jbc.M113.455329.

Kuter, D.J. (2013) The biology of thrombopoietin and thrombopoietin receptor agonists. *Int J Hematol*, 98 (1): 10–23. doi:10.1007/s12185-013-1382-0.

Lambert, M.P., Wang, Y., Bdeir, K.H., et al. (2009) Platelet factor 4 regulates megakaryopoiesis through low-density lipoprotein receptor-related protein 1 (LRP1) on megakaryocytes. *Blood*, 114 (11): 2290–2298. doi:10.1182/blood-2009-04-216473.

Lambert, M.P. and Warkentin, T.E. (2025) Mini-clusters of postadenovirus VITT. *Res Pract Thromb Haemost*, 9 (1): 102641. doi:10.1016/j.rpth.2024.102641.

Lamrani, L., Lacout, C., Ollivier, V., et al. (2014) Hemostatic disorders in a JAK2V617F-driven mouse model of myeloproliferative neoplasm. *Blood*, 124 (7): 1136–1145. doi:10.1182/blood-2013-10-530832.

Lande, R., Lee, E.Y., Palazzo, R., et al. (2019) CXCL4 assembles DNA into liquid crystalline complexes to amplify TLR9-mediated interferon-α production in systemic sclerosis. *Nat Commun*, 10 (1). doi:10.1038/s41467-019-09683-z.

Langer, F., Ingersoll, S., Amirkhosravi, A., et al. (2005) The role of CD40 in CD40L- and antibody-mediated platelet activation. *Thromb Haemost*, 93 (06): 1137–1146. doi:10.1160/TH04-12-0774.

Lasagni, L., Francalanci, M., Annunziato, F., et al. (2003) An alternatively spliced variant of CXCR3 mediates the inhibition of endothelial cell growth induced by IP-10, Mig, and I-TAC, and acts as functional receptor for platelet factor 4. *J Exp Med*, 197 (11): 1537–1549. doi:10.1084/jem.20021897.

Lasagni, L., Grepin, R., Mazzinghi, B., et al. (2007) PF-4/CXCL4 and CXCL4L1 exhibit distinct subcellular localization and a differentially regulated mechanism of secretion. *Blood*, 109 (10): 4127–4134. doi:10.1182/blood-2006-10-052035.

Lau, E.K., Paavola, C.D., Johnson, Z., et al. (2004) Identification of the glycosaminoglycan binding site of the CC chemokine, MCP-1: Implications for structure and function in vivo. *J Biol Chem*, 279 (21): 22294–22305. doi:10.1074/jbc.M311224200.

Lebeurier, I., Raclet, L., Amiral, J., et al. (1996) Carboxyterminal peptides with the dimeric form of PF4 retain the inhibitory effect on the growth of human megakaryoblastic cell lines. *J Lab Clin Med*, 127 (2): 179–85. doi:10.1016/s0022-2143(96)90076-1.

Lee, C.S.M., Huguenin, Y., Pillois, X., et al. (2024) In vitro characterization of rare anti-αIIbβ3 isoantibodies produced by patients with Glanzmann thrombasthenia that severely block fibrinogen binding and generate procoagulant platelets via complement activation. *Res Pract Thromb Haemost*, 8 (1): 102253. doi:10.1016/j.rpth.2023.102253.

Lee, R.H. and Bergmeier, W. (2016) Platelet immunoreceptor tyrosine-based activation motif (ITAM) and hemITAM signaling and vascular integrity in inflammation and development. *J Thromb Haemost*, 14 (4): 645–654. doi:10.1111/jth.13250.

Lee-Sundlov, M.M., Rivadeneyra, L., Falet, H., et al. (2022) Sialic acid and platelet count regulation: Implications in immune thrombocytopenia. *Res Pract Thromb Haemost*, 6 (3). doi:10.1002/rth2.12691.

Leiter, O., Brici, D., Fletcher, S.J., et al. (2023) Platelet-derived exerkine CXCL4/platelet factor 4 rejuvenates hippocampal neurogenesis and restores cognitive function in aged mice. *Nat Commun*, 14 (1): 4375. doi:10.1038/s41467-023-39873-9.

Lejeune, J., Brachet, G. and Watier, H. (2019) Evolutionary story of the low/medium-affinity IgG Fc receptor gene cluster. *Front Immunol*, 10 (JUN). doi:10.3389/fimmu.2019.01297.

Lenting, P.J., Denis, C. V. and Christophe, O.D. (2024) How unique structural adaptations support and coordinate the complex function of von Willebrand factor. *Blood*, 144 (21): 2174–2184. doi:10.1182/blood.2023023277.

Leung, H.H.L., Ahmadi, Z., Lee, B., et al. (2024) Antithrombotic efficacy and bleeding risks of vaccine-induced immune thrombotic thrombocytopenia treatments. *Blood Adv*, 8 (22): 5744–5752. doi:10.1182/bloodadvances.2024013883.

Leung, H.H.L., Perdomo, J., Ahmadi, Z., et al. (2022) NETosis and thrombosis in vaccine-induced immune thrombotic thrombocytopenia. *Nat Commun*, 13 (1). doi:10.1038/s41467-022-32946-1.

Levy, J.H., Ghadimi, K., Kizhakkedathu, J.N., et al. (2023) What's fishy about protamine? Clinical use, adverse reactions, and potential alternatives. *J Thromb Haemost*, 21 (7): 1714–1723. doi:10.1016/j.jtha.2023.04.005.

Lewis, B.E., Wallace, D.E., Leya, F., et al. (2003) Argatroban Anticoagulation in Patients With Heparin-Induced Thrombocytopenia. *Arch Int Med*, 163 (15): 1849. doi:10.1001/archinte.163.15.1849.

Lewis, B.E., Wallis, D.E., Berkowitz, S.D., et al. (2001) Argatroban Anticoagulant Therapy in Patients With Heparin-Induced Thrombocytopenia. *Circulation*, 103 (14): 1838–1843. doi:10.1161/01.CIR.103.14.1838.

Lin, T.-C., Fu, P.-A., Hsu, Y.-T., et al. (2023) Vaccine-Induced Immune Thrombotic Thrombocytopenia following BNT162b2 mRNA COVID-19 Booster: A Case Report. *Vaccines*, 11 (6): 1115. doi:10.3390/vaccines11061115.

Lindhoff-Last, E., Schönborn, L., Zaninetti, C., et al. (2023) Rescue Therapy in Chronic Prothrombotic Autoimmune Anti-PF4 Disorder. *N Engl J Med*, 389 (14): 1339–1341. doi:10.1056/NEJMc2309016.

Lishko, V.K., Yakubenko, V.P., Ugarova, T.P., et al. (2018) Leukocyte integrin Mac-1 (CD11b/CD18,M2, CR3) acts as a functional receptor for platelet factor 4. *J Biol Chem*, 293 (18): 6869–6882. doi:10.1074/jbc.RA117.000515.

Liu, C.Y., Battaglia, M., Lee, S.H., et al. (2005) Platelet Factor 4 Differentially Modulates CD4 + CD25 + (Regulatory) versus CD4 + CD25 − (Nonregulatory) T Cells. *J Immunol*, 174 (5): 2680–2686. doi:10.4049/jimmunol.174.5.2680.

Liu, Q., Miao, H., Li, S., et al. (2022) Anti-PF4 antibodies associated with disease severity in COVID-19. *Proc Natl Acad Sci U S A*, 119 (47): e2213361119. doi:10.1073/pnas.2213361119.

Lo, G., Juhl, D., Warkentin, T., et al. (2006) Evaluation of pretest clinical score (4 T's) for the diagnosis of heparin-induced thrombocytopenia in two clinical settings. *J Thromb Haemost*, 4 (4): 759–765. doi:10.1111/j.1538-7836.2006.01787.x.

Lord, M.S., Cheng, B., Farrugia, B.L., et al. (2017) Platelet factor 4 binds to vascular proteoglycans and controls both growth factor activities and platelet activation. *J Biol Chem*, 292 (10): 4054–4063. doi:10.1074/jbc.M116.760660.

Loscalzo, J., Melnick, B. and Handint, R.I. (1985) The Interaction of Platelet Factor Four and Glycosaminoglycans. *Arch Biochem Biophys*, 240 (1): 446–455.

Lu, W.J., Lin, K.C., Huang, S.Y., et al. (2014) Role of a Janus kinase 2-dependent signaling pathway in platelet activation. *Thromb Res*, 133 (6): 1088–1096. doi:10.1016/j.thromres.2014.03.042.

Lupia, E., Bosco, O., Bergerone, S., et al. (2006) Thrombopoietin Contributes to Enhanced Platelet Activation in Patients With Unstable Angina. *J Am Coll Cardiol*, 48 (11): 2195–2203. doi:10.1016/j.jacc.2006.04.106.

Lupia, E., Bosco, O., Mariano, F., et al. (2009) Elevated thrombopoietin in plasma of burned patients without and with sepsis enhances platelet activation. *Journal of Thrombosis and Haemostasis*, 7 (6): 1000–1008. doi:10.1111/j.1538-7836.2009.03348.x.

Lupia, E., Capuano, M., Vizio, B., et al. (2022) Thrombopoietin participates in platelet activation in COVID-19 patients. *eBioMedicine*, 85: 104305. doi:10.1016/j.ebiom.2022.104305.

Maharaj, S. and Chang, S. (2018) Anti-PF4/heparin antibodies are increased in hospitalized patients with bacterial sepsis. *Thromb Res*, 171: 111–113. doi:10.1016/j.thromres.2018.09.060.

Maier, M., Geiger, E. V., Henrich, D., et al. (2009) Platelet factor 4 is highly upregulated in dendritic cells after severe trauma. *Mol Med*, 15 (11–12): 384–391. doi:10.2119/molmed.2009.00074.

Maione, T.E., Gray, G.S., Hunt, A.J., et al. (1991) Inhibition of tumor growth in mice by an analogue of platelet factor 4 that lacks affinity for heparin and retains potent angiostatic activity. *Cancer Res*, 51 (8): 2077–83.

Maione, T.E., Gray, G.S., Petro, J., et al. (1989) Inhibition of Angiogenesis by Recombinant Human Platelet Factor-4 and Related Peptides. *Science*, 68 (C): 77–79. doi:doi: 10.1126/science.1688470.

Makar, R.S., Zhukov, O.S., Sahud, M.A., et al. (2013) Thrombopoietin levels in patients with disorders of platelet production: Diagnostic potential and utility in predicting response to TPO Receptor agonists. *Am J Hematol*, 88 (12): 1041–1044. doi:10.1002/ajh.23562.

Martel, N., Lee, J. and Wells, P.S. (2005) Risk for heparin-induced thrombocytopenia with unfractionated and low-molecular-weight heparin thromboprophylaxis: a meta-analysis. *Blood*, 106 (8): 2710–5. doi:10.1182/blood-2005-04-1546.

Martin, E.M., Clark, J.C., Montague, S.J., et al. (2024) Trivalent nanobody-based ligands mediate powerful activation of GPVI, CLEC-2, and PEAR1 in human platelets whereas FcγRIIA requires a tetravalent ligand. *J Thromb Haemost*, 22 (1): 271–285. doi:10.1016/j.jtha.2023.09.026.

Maurer, B., Kollmann, S., Pickem, J., et al. (2019) STAT5A and STAT5B—Twins with Different Personalities in Hematopoiesis and Leukemia. *Cancers*, 11 (11): 1726. doi:10.3390/cancers11111726.

Mayo, K.H. and Chen, M.J. (1989) Human platelet factor 4 monomer-dimer-tetramer equilibria investigated by 1H NMR spectroscopy. *Biochemistry*, 28 (24): 9469–78. doi:10.1021/bi00450a034.

Mazzeffi, M., Clark, M., Grazioli, A., et al. (2021) Platelet factor-4 concentration in adult veno-arterial ECMO patients. *Perfusion*, 36 (7): 688–693. doi:10.1177/0267659120965104.

McGowan, K.E., Makari, J., Diamantouros, A., et al. (2016) Reducing the hospital burden of heparin-induced thrombocytopenia: impact of an avoid-heparin program. *Blood*, 127 (16): 1954–1959. doi:10.1182/blood-2015-07-660001.

McMorran, B.J., Wieczorski, L., Drysdale, K.E., et al. (2012) Platelet Factor 4 and Duffy Antigen Required for Platelet Killing of Plasmodium falciparum. *Science*, 338 (6112): 1348–1351. doi:10.1126/science.1228892.

Medicines and Healthcare products Regulatory Agency (2020) *Oxford University/AstraZeneca vaccine authorised by UK medicines regulator*. Available at: https://www.gov.uk/government/news/oxford-universityastrazeneca-vaccine-authorised-by-uk-medicines-regulator (Accessed: 22 November 2024).

Medicines and Healthcare products Regulatory Agency (2022) *Coronavirus Vaccines - summary of Yellow Card reporting*. Available at: http://www.nationalarchives.gov.uk/doc/open-government-licence/.

Mehta, P., Ciurtin, C., Scully, M., et al. (2020) JAK inhibitors in COVID-19: The need for vigilance regarding increased inherent thrombotic risk. *Eur Respir J*, 56 (3): 10–12. doi:10.1183/13993003.01919-2020.

Menni, C., Klaser, K., May, A., et al. (2021) Vaccine side-effects and SARS-CoV-2 infection after vaccination in users of the COVID Symptom Study app in the UK: a prospective observational study. *Lancet Infect Dis*, 21 (7): 939–949. doi:10.1016/S1473-3099(21)00224-3.

Mertens, G., Cassiman, J.J., Van Den Berghe, H., et al. (1992) Cell surface heparan sulfate proteoglycans from human vascular endothelial cells: Core protein characterization and

antithrombin III binding properties. *J Biol Chem*, 267 (28): 20435–20443. doi:10.1016/s0021-9258(19)88721-5.

Meyer, S.C., Keller, M.D., Woods, B.A., et al. (2014) Genetic studies reveal an unexpected negative regulatory role for Jak2 in thrombopoiesis. *Blood*, 124 (14): 2280–2284. doi:10.1182/blood-2014-03-560441.

Meyer, T., Robles-Carrillo, L., Robson, T., et al. (2009) Bevacizumab immune complexes activate platelets and induce thrombosis in FCGR2A transgenic mice. *J Thromb Haemost*, 7 (1): 171–181. doi:10.1111/j.1538-7836.2008.03212.x.

De Michele, M., Piscopo, P., Crestini, A., et al. (2022) Vaccine-induced immune thrombotic thrombocytopenia: a possible pathogenic role of ChAdOx1 nCoV-19 vaccine-encoded soluble SARS-CoV-2 spike protein. *Haematologica*, 107 (7): 1687–1692. doi:10.3324/haematol.2021.280180.

Miyakawa, Y., Drachman, J.G., Gallis, B., et al. (2000) A structure-function analysis of serine/threonine phosphorylation of the thrombopoietin receptor, c-Mpl. *J Biol Chem*, 275 (41): 32214–32219. doi:10.1074/jbc.M005080200.

Miyakawa, Y., Oda, A., Druker, B.J., et al. (1995) Recombinant thrombopoietin induces rapid protein tyrosine phosphorylation of Janus kinase 2 and Shc in human blood platelets. *Blood*, 86 (1): 23–27. doi:10.1182/blood.v86.1.23.bloodjournal86123.

Miyakawa, Y., Oda, A., Druker, B.J., et al. (1996) Thrombopoietin induces tyrosine phosphorylation of Stat3 and Stat5 in human blood platelets. *Blood*, 87 (2): 439–446. doi:10.1182/blood.v87.2.439.bloodjournal872439.

Montague, S.J., Smith, C.W., Lodwick, C.S., et al. (2022) Anti-platelet factor 4 immunoglobulin G levels in vaccine-induced immune thrombocytopenia and thrombosis: Persistent positivity through 7 months. *Res Pract Thromb Haemost*, 6 (3): 1–8. doi:10.1002/rth2.12707.

Moore, S., Pepper, D.S. and Cash, J.D. (1975) Platelet antiheparin activity. The isolation and characterisation of platelet factor 4 released from thrombin-aggregated washed human platelets and its dissociation into subunits and the isolation of membrane-bound antiheparin activity. *Biochim Biophys Acta*, 379 (2): 370–84.

Moore, S.F., Hunter, R.W., Harper, M.T., et al. (2013) Dysfunction of the PI3 kinase/Rap1/integrin aIIbb3 pathway underlies ex vivo platelet hypoactivity in essential thrombocythemia. *Blood*, 121 (7): 1209–1219. doi:10.1182/blood-2012-05-431288.

Moore, S.F., Smith, N.R., Blair, T.A., et al. (2019) Critical roles for the phosphatidylinositide 3-kinase isoforms p110β and p110γ in thrombopoietin-mediated priming of platelet function. *Sci Rep*, 9 (1): 1468. doi:10.1038/s41598-018-37012-9.

Morel-Kopp, M. -C., Mullier, F., Gkalea, V., et al. (2016) Heparin-induced multi-electrode aggregometry method for heparin-induced thrombocytopenia testing: communication from the SSC of the ISTH. *J Thromb Haemost*, 14 (12): 2548–2552. doi:10.1111/jth.13516.

Mosnier, L.O. (2011) Platelet Factor 4 Inhibits Thrombomodulin-dependent Activation of Thrombin-activatable Fibrinolysis Inhibitor (TAFI) by Thrombin. *J Biol Chem*, 286 (1): 502–510. doi:10.1074/jbc.M110.147959.

Mueller, A., Meiser, A., McDonagh, E.M., et al. (2008) CXCL4-induced migration of activated T lymphocytes is mediated by the chemokine receptor CXCR3. *Journal of Leukocyte Biology*, 83 (4): 875–882. doi:10.1189/jlb.1006645.

Müller, J., Sperl, B., Reindl, W., et al. (2008) Discovery of Chromone-Based Inhibitors of the Transcription Factor STAT5. *Chembiochem*, 9 (5): 723–727. doi:10.1002/cbic.200700701.

Müller, L., Dabbiru, V.A.S., Schönborn, L., et al. (2024) Therapeutic strategies in FcγIIA receptor-dependent thrombosis and thromboinflammation as seen in heparin-induced thrombocytopenia (HIT) and vaccine-induced immune thrombocytopenia and thrombosis (VITT). *Expert Opin Pharmacother*, 25 (3): 281–294. doi:10.1080/14656566.2024.2328241.

Mulloy, B., Hogwood, J., Gray, E., et al. (2016) Pharmacology of Heparin and Related Drugs. *Pharmacol Rev*, 68 (1): 76–141. doi:10.1124/pr.115.011247.

Mumford, A.D., Dawood, B.B., Daly, M.E., et al. (2010) A novel thromboxane A2 receptor D304N variant that abrogates ligand binding in a patient with a bleeding diathesis. *Blood*, 115 (2): 363–369. doi:10.1182/blood-2009-08-236976.

Nanda, N., Bao, M., Lin, H., et al. (2005) Platelet Endothelial Aggregation Receptor 1 (PEAR1), a Novel Epidermal Growth Factor Repeat-containing Transmembrane Receptor, Participates in Platelet Contact-induced Activation. *J Biol Chem*, 280 (26): 24680–24689. doi:10.1074/jbc.M413411200.

National Health Service Blood and Transplant (2023) *INF136/8.3 – User Guide for Histocompatibility and Immunogenetics Diagnostics Services*. Available at: https://nhsbtdbe.blob.core.windows.net/umbraco-assets-corp/29939/inf136.pdf (Accessed: 26 December 2024).

National Institute for Health and Care Research (2021) *NIHR135073: Understanding Mechanisms of Thrombosis and Thrombocytopenia in COVID-19 and with SARS-CoV-2 Vaccines*.

Nazy, I., Elliott, T.D. and Arnold, D.M. (2020) Platelet factor 4 inhibits ADAMTS13 activity and regulates the multimeric distribution of von Willebrand factor. *Br J Haematol*, 190 (4): 594–598. doi:10.1111/bjh.16553.

Nesmelova, I. V., Sham, Y., Dudek, A.Z., et al. (2005) Platelet factor 4 and interleukin-8 CXC chemokine heterodimer formation modulates function at the quaternary structural level. *J Biol Chem*, 280 (6): 4948–4958. doi:10.1074/jbc.M405364200.

Nevzorova, T.A., Mordakhanova, E.R., Daminova, A.G., et al. (2019) Platelet factor 4-containing immune complexes induce platelet activation followed by calpain-dependent platelet death. *Cell Death Discov*, 5 (1): 106. doi:10.1038/s41420-019-0188-0.

Ngo, A.T.P., Skidmore, A., Oberg, J., et al. (2023) Platelet factor 4 limits neutrophil extracellular trap- and cell-free DNA-induced thrombogenicity and endothelial injury. *JCI Insight*, 8 (22): e171054. doi:10.1172/jci.insight.171054.

Nguyen, K.T.P., Volkman, B., Dréau, D., et al. (2022) A new obligate CXCL4-CXCL12 heterodimer for studying chemokine heterodimer activities and mechanisms. *Sci Rep*, 12 (1): 17204. doi:10.1038/s41598-022-21651-0.

Nguyen, T., Medvedev, N., Delcea, M., et al. (2017) Anti-platelet factor 4/polyanion antibodies mediate a new mechanism of autoimmunity. *Nat Commun*, 8 (14945): 1–12. doi:10.1038/ncomms14945.

Nguyen, T.-H., Chen, L.-Y., Khan, N.Z., et al. (2024) The Binding of the SARS-CoV-2 Spike Protein to Platelet Factor 4: A Proposed Mechanism for the Generation of Pathogenic Antibodies. *Biomolecules*, 14 (3): 245. doi:10.3390/biom14030245.

Nguyen, T.H., Greinacher, A. and Delcea, M. (2015) Quantitative description of thermodynamic and kinetic properties of the platelet factor 4/heparin bonds. *Nanoscale*, 7 (22): 10130–10139. doi:10.1039/c5nr02132d.

Nicolson, P.L., Abrams, S.T., Amirthalingam, G., et al. (n.d.) Understanding Mechanisms of Thrombosis and Thrombocytopenia with Adenoviral SARS-CoV-2 Vaccines: A Comprehensive Synopsis. *Efficacy and Mechanism Evaluation*, (in press).

Nicolson, P.L., Montague, S.J., Buka, R.J., et al. (2025) Anti-PF4 mediated thrombocytopenia and thrombosis associated with acute cytomegalovirus infection displays both HIT-like and VITT-like characteristics. *Br J Haematol*, (Online ahead of print). doi:10.1111/bjh.20092.

Nilius, H., Cuker, A., Haug, S., et al. (2022) A machine-learning model for reducing misdiagnosis in heparin-induced thrombocytopenia: A prospective, multicenter, observational study. *EClinicalMedicine*, 55. doi:10.1016/j.eclinm.2022.101745.

Niu, C., Yang, Y., Huynh, A., et al. (2020) Platelet Factor 4 Interactions with Short Heparin Oligomers: Implications for Folding and Assembly. *Biophys J*, 119 (7): 1371–1379. doi:10.1016/j.bpj.2020.04.012.

Nomiyama, H., Osada, N. and Yoshie, O. (2013) Systematic classification of vertebrate chemokines based on conserved synteny and evolutionary history. *Genes Cells*, 18 (1): 1–16. doi:10.1111/gtc.12013.

Nuyttens, B.P., Thijs, T., Deckmyn, H., et al. (2011) Platelet adhesion to collagen. *Thromb Res*, 127 (Suppl 2): S26–S29. doi:10.1016/S0049-3848(10)70151-1.

Offermanns, S. (2006) Activation of Platelet Function Through G Protein–Coupled Receptors. *Circ Res*, 99 (12): 1293–1304. doi:10.1161/01.RES.0000251742.71301.16.

Okayama, M., Oguri, K., Fujiwara, Y., et al. (1986) Purification and characterization of human platelet proteoglycan. *Biochem J*, 233 (1): 73–81. doi:10.1042/bj2330073.

Olivieri A and Manzione L (2007) Dasatinib: a new step in molecular target therapy. *Ann Oncol*, 18: vi42–vi46. doi:10.1093/annonc/mdm223.

Olson, J.D., Arkin, C.F., Brandt, J.T., et al. (1998) College of American Pathologists Conference XXXI on laboratory monitoring of anticoagulant therapy: laboratory monitoring of unfractionated heparin therapy. *Arch Pathol Lab Med*, 122 (9): 782–98.

Van Os, E., Wu, Y.P., Pouwels, J.G., et al. (2003) Thrombopoietin increases platelet adhesion under flow and decreases rolling. *Br J Haematol*, 121 (3): 482–490. doi:10.1046/j.1365-2141.2003.04292.x.

Van Den Oudenrijn, S., Bruin, M., Folman, C.C., et al. (2000) Mutations in the thrombopoietin receptor, mpl, in children with congenital amegakaryocytic thrombocytopenia. *Br J Haematol*, 110 (2): 441–448. doi:10.1046/j.1365-2141.2000.02175.x.

Pabmanabhan, A., Splinter, N., Mauch, E., et al. (2024) Platelet-Activating Anti-PF4 Antibodies in MGUS Patients with Thrombosis. *Blood*, 144 (Supplement 1): 3996–3996. doi:10.1182/blood-2024-207999.

Pachitariu, M. and Stringer, C. (2022) Cellpose 2.0: how to train your own model. *Nat Methods*, 19 (12): 1634–1641. doi:10.1038/s41592-022-01663-4.

Padmanabhan, A., Jones, C.G., Bougie, D.W., et al. (2015) Heparin-independent, PF4-dependent binding of HIT antibodies to platelets: Implications for HIT pathogenesis. *Blood*, 125 (1): 155–161. doi:10.1182/blood-2014-06-580894.

Padmanabhan, A., Jones, C.G., Curtis, B.R., et al. (2016) A Novel PF4-Dependent Platelet Activation Assay Identifies Patients Likely to Have Heparin-Induced Thrombocytopenia/Thrombosis. *Chest*, 150 (3): 506–515. doi:10.1016/j.chest.2016.02.641.

Parker, Z.F., Rux, A.H., Riblett, A.M., et al. (2016) Platelet Factor 4 Inhibits and Enhances HIV-1 Infection in a Concentration-Dependent Manner by Modulating Viral Attachment. *AIDS Res Hum Retroviruses*, 32 (7): 705–717. doi:10.1089/aid.2015.0344.

Parra-Izquierdo, I., Melrose, A.R., Pang, J., et al. (2022) Janus kinase inhibitors ruxolitinib and baricitinib impair glycoprotein-VI mediated platelet function. *Platelets*, 33 (3): 404–415. doi:10.1080/09537104.2021.1934665.

Pasquet, J.M., Gross, B.S., Gratacap, M.P., et al. (2000) Thrombopoietin potentiates collagen receptor signaling in platelets through a phosphatidylinositol 3-kinase-dependent pathway. *Blood*, 95 (11): 3429–3434. doi:10.1182/blood.v95.11.3429.

Pavord, S., Scully, M., Hunt, B.J., et al. (2021) Clinical Features of Vaccine-Induced Immune Thrombocytopenia and Thrombosis. *N Engl J Med*, 385 (18): 1680–1689. doi:10.1056/nejmoa2109908.

Perdomo, J., Leung, H.H.L., Ahmadi, Z., et al. (2019) Neutrophil activation and NETosis are the major drivers of thrombosis in heparin-induced thrombocytopenia. *Nature Communications*, 10 (1). doi:10.1038/s41467-019-09160-7.

Perrella, G., Nagy, M., Watson, S.P., et al. (2021) Platelet GPVI (Glycoprotein VI) and Thrombotic Complications in the Venous System. *Arterioscler Thromb Vasc Biol*, 41 (11): 2681–2692. doi:10.1161/ATVBAHA.121.316108.

Pervushina, O., Scheuerer, B., Reiling, N., et al. (2004) Platelet Factor 4/CXCL4 Induces Phagocytosis and the Generation of Reactive Oxygen Metabolites in Mononuclear Phagocytes Independently of Gi Protein Activation or Intracellular Calcium Transients. *J Immunol*, 173 (3): 2060–2067. doi:10.4049/jimmunol.173.3.2060.

Petersen, F., Bock, L., Flad, H.D., et al. (1998) A chondroitin sulfate proteoglycan on human neutrophils specifically binds platelet factor 4 and is involved in cell activation. *J Immunol*, 161 (8): 4347–4355.

Petersen, F., Brandt, E., Lindahl, U., et al. (1999) Characterization of a neutrophil cell surface glycosaminoglycan that mediates binding of platelet factor 4. *J Biol Chem*, 274 (18): 12376–12382. doi:10.1074/jbc.274.18.12376.

Petersen, F., Ludwig, A., Flad, H.D., et al. (1996) TNF-alpha renders human neutrophils responsive to platelet factor 4. Comparison of PF-4 and IL-8 reveals different activity profiles of the two chemokines. *J Immunol*, 156 (5): 1954–1962.

Pishko, A.M., Lefler, D.S., Gimotty, P., et al. (2019) The risk of major bleeding in patients with suspected heparin-induced thrombocytopenia. *J Thromb Haemost*, 17 (11): 1956–1965. doi:10.1111/jth.14587.

Poncz, M., Surrey, S., LaRocco, P., et al. (1987) Cloning and characterization of platelet factor 4 cDNA derived from a human erythroleukemic cell line. *Blood*, 69 (1): 219–223. doi:10.1182/blood.v69.1.219.219.

Preston, R.J.S., Tran, S., Johnson, J.A., et al. (2009) Platelet factor 4 impairs the anticoagulant activity of activated protein C. *J Biol Chem*, 284 (9): 5869–5875. doi:10.1074/jbc.M804703200.

Proteintech (n.d.) *HumanKine® recombinant human TPO (Thrombopoietin) protein*. Available at: https://www.ptglab.com/products/recombinant-human-tpo.htm?srsltid=AfmBOoomrBmICD20yzKzgkIXoL_z-G87bdbmKlaNGYLbu29r17Ave6uM (Accessed: 4 November 2024).

Pula, G., Schuh, K., Nakayama, K., et al. (2006) PKCδ regulates collagen-induced platelet aggregation through inhibition of VASP-mediated filopodia formation. *Blood*, 108 (13): 4035–4044. doi:10.1182/blood-2006-05-023739.

Quintás-Cardama, A., Vaddi, K., Liu, P., et al. (2010) Preclinical characterization of the selective JAK1/2 inhibitor INCB018424: therapeutic implications for the treatment of myeloproliferative neoplasms. *Blood*, 115 (15): 3109–17. doi:10.1182/blood-2009-04-214957.

Raschke, R.A., Gallo, T., Curry, S.C., et al. (2017) Clinical effectiveness of a Bayesian algorithm for the diagnosis and management of heparin-induced thrombocytopenia. *J Thromb Haemost*, 15 (8): 1640–1645. doi:10.1111/jth.13758.

Rauova, L., Hirsch, J.D., Greene, T.K., et al. (2010) Monocyte-bound PF4 in the pathogenesis of heparin-induced thrombocytopenia. *Blood*, 116 (23): 5021–31. doi:10.1182/blood-2010-03-276964.

Rauova, L., Zhai, L., Kowalska, M.A., et al. (2006) Role of platelet surface PF4 antigenic complexes in heparin-induced thrombocytopenia pathogenesis: Diagnostic and therapeutic implications. *Blood*, 107 (6): 2346–2353. doi:10.1182/blood-2005-08-3122.

Rayes, J. and Brill, A. (2024) Hot under the clot: venous thrombogenesis is an inflammatory process. *Blood*, 144 (5): 477–489. doi:10.1182/blood.2023022522.

Rayes, J., Watson, S.P. and Nieswandt, B. (2019) Functional significance of the platelet immune receptors GPVI and CLEC-2. *J Clin Invest*, 129 (1). doi:10.1172/JCI122955.

R&D Systems (2016) *Quantikine ® ELISA Human CXCL4/PF4 Immunoassay DPF40*. Available at: https://resources.rndsystems.com/pdfs/datasheets/dpf40.pdf.

Reilly, M.P., Sinha, U., André, P., et al. (2011) PRT-060318, a novel Syk inhibitor, prevents heparin-induced thrombocytopenia and thrombosis in a transgenic mouse model. *Blood*, 117 (7): 2241–2246. doi:10.1182/blood-2010-03-274969.

Reilly, M.P., Taylor, S.M., Hartman, N.K., et al. (2001) Heparin-induced thrombocytopenia/thrombosis in a transgenic mouse model requires human platelet factor 4 and platelet activation through FcyRIIA. *Blood*, 98 (8): 2442–2447.

Reitsma, S., Slaaf, D.W., Vink, H., et al. (2007) The endothelial glycocalyx: composition, functions, and visualization. *Pflügers Arch*, 454 (3): 345–359. doi:10.1007/s00424-007-0212-8.

Ren, X., Duan, L., He, Q., et al. (2010) Identification of Niclosamide as a New Small-Molecule Inhibitor of the STAT3 Signaling Pathway. *ACS Med Chem Lett*, 1 (9): 454–459. doi:10.1021/ml100146z.

Robles-Carrillo, L., Meyer, T., Hatfield, M., et al. (2010) Anti-CD40L Immune Complexes Potently Activate Platelets In Vitro and Cause Thrombosis in FCGR2A Transgenic Mice. *J Immunol*, 185 (3): 1577–1583. doi:10.4049/jimmunol.0903888.

Rodríguez-Liñares, B. and Watson, S.P. (1994) Phosphorylation of JAK2 in thrombin-stimulated human platelets. *FEBS Lett*, 352 (3): 335–338. doi:10.1016/0014-5793(94)00983-X.

Rollin, J., Pouplard, C., Gratacap, M.-P., et al. (2012) Polymorphisms of protein tyrosine phosphatase CD148 influence FcγRIIA-dependent platelet activation and the risk of heparin-induced thrombocytopenia. *Blood*, 120 (6): 1309–1316. doi:10.1182/blood-2012-04-424044.

Rollin, J., Pouplard, C., Sung, H.C., et al. (2015) Increased risk of thrombosis in FcγRIIA 131RR patients with HIT due to defective control of platelet activation by plasma IgG2. *Blood*, 125 (15): 2397–404. doi:10.1182/blood-2014-09-594515.

Rollins, B.J. (1997) Chemokines. *Blood*, 90 (3): 909–28.

Romagnani, P., Maggi, L., Mazzinghi, B., et al. (2005) CXCR3-mediated opposite effects of CXCL10 and CXCL4 on TH1 or TH2 cytokine production. *J Allergy Clin Immunol*, 116 (6): 1372–9. doi:10.1016/j.jaci.2005.09.035.

Rybak, M., Gimbrone, M.J., Davies, P., et al. (1989) Interaction of platelet factor four with cultured vascular endothelial cells. *Blood*, 73 (6): 1534–1539. doi:10.1182/blood.V73.6.1534.1534.

Sachais, B., Higazi, A.A.-R., Cines, D., et al. (2004) Interactions of Platelet Factor 4 with the Vessel Wall. *Sem Thromb Haemost*, 30 (03): 351–358. doi:10.1055/s-2004-831048.

Sachais, B.S., Kuo, A., Nassar, T., et al. (2002) Platelet factor 4 binds to low-density lipoprotein receptors and disrupts the endocytic itinerary, resulting in retention of low-density lipoprotein on the cell surface. *Blood*, 99 (10): 3613–3622. doi:10.1182/blood.V99.10.3613.

Sachais, B.S., Turrentine, T., McKenna, J.M.D., et al. (2007) Elimination of platelet factor 4 (PF4) from platelets reduces atherosclerosis in C57Bl/6 and apoE-/- mice. *Thromb Haemost*, 98 (5): 1108–1113. doi:10.1160/TH07-04-0271.

Salanga, C.L., Dyer, D.P., Kiselar, J.G., et al. (2014) Multiple glycosaminoglycan-binding epitopes of monocyte chemoattractant protein-3/CCL7 enable it to function as a non-oligomerizing chemokine. *J Biol Chem*, 289 (21): 14896–14912. doi:10.1074/jbc.M114.547737.

Salih, F., Schönborn, L., Kohler, S., et al. (2021) Vaccine-Induced Thrombocytopenia with Severe Headache. *N Engl J Med*, 385 (22): 2103–2105. doi:10.1056/NEJMc2112974.

Salmasi, G., Murray, D.L. and Padmanabhan, A. (2024) Myeloma Therapy for Monoclonal Gammopathy of Thrombotic Significance. *N Engl J Med*, 391 (6): 570–571. doi:10.1056/NEJMc2406453.

Sangli, S., Virani, A., Cheronis, N., et al. (2021) Thrombosis With Thrombocytopenia After the Messenger RNA–1273 Vaccine. *Ann Int Med*, 174 (10): 1480–1482. doi:10.7326/L21-0244.

Sattler, M., Durstin, M., Frank, D., et al. (1995) The thrombopoietin receptor c-MPL activates JAK2 and TYK2 tyrosine kinases. *Exp Hematol*, 23 (9): 1040–8.

Saur, S.J., Sangkhae, V., Geddis, A.E., et al. (2010) Ubiquitination and degradation of the thrombopoietin receptor c-Mpl. *Blood*, 115 (6): 1254–1263. doi:10.1182/blood-2009-06-227033.An.

Savi, P., Chong, B.H., Greinacher, A., et al. (2005) Effect of fondaparinux on platelet activation in the presence of heparin-dependent antibodies: a blinded comparative multicenter study with unfractionated heparin. *Blood*, 105 (1): 139–144. doi:10.1182/blood-2004-05-2010.

Schaffner, A., Rhyn, P., Schoedon, G., et al. (2005) Regulated expression of platelet factor 4 in human monocytes - role of PARs as a quantitatively important monocyte activation pathway. *J Leuk Biol*, 78 (1): 202–209. doi:10.1189/jlb.0105024.

Scheuerer, B., Ernst, M., Dürrbaum-Landmann, I., et al. (2000) The CXC-chemokine platelet factor 4 promotes monocyte survival and induces monocyte differentiation into macrophages. *Blood*, 95 (4): 1158–1166. doi:10.1182/blood.v95.4.1158.004k31_1158_1166.

van Schie, R.C.A.A. and Wilson, M.E. (2000) Evaluation of Human FcγRIIA (CD32) and FcγRIIIB (CD16) Polymorphisms in Caucasians and African-Americans Using Salivary DNA. *Clin Diagn Lab Immunol*, 7 (4): 676–681. doi:10.1128/CDLI.7.4.676-681.2000.

Schindelin, J., Arganda-Carreras, I., Frise, E., et al. (2012) Fiji: an open-source platform for biological-image analysis. *Nat Methods*, 9 (7): 676–682. doi:10.1038/nmeth.2019.

Schönborn, L., Esteban, O., Wesche, J., et al. (2023) Anti-PF4 immunothrombosis without proximate heparin or adenovirus vector vaccine exposure. *Blood*, 142 (26): 2305–2314.

Schönborn, L., Pavord, S., Chen, V.M.Y., et al. (2024) Thrombosis with thrombocytopenia syndrome (TTS) and vaccine-induced immune thrombocytopenia and thrombosis (VITT): Brighton Collaboration case definitions and guidelines for data collection, analysis, and presentation of immunisation safety data. *Vaccine*, 42 (7): 1799–1811. doi:10.1016/j.vaccine.2024.01.045.

Schultz, N.H., Sørvoll, I.H., Michelsen, A.E., et al. (2021) Thrombosis and Thrombocytopenia after ChAdOx1 nCoV-19 Vaccination. *N Engl J Med*, 384 (22): 2124–2130. doi:10.1056/nejmoa2104882.

Schulz, O., Hammerschmidt, S.I., Moschovakis, G.L., et al. (2016) Chemokines and Chemokine Receptors in Lymphoid Tissue Dynamics. *Annual Review of Immunology*. 34 pp. 203–242. doi:10.1146/annurev-immunol-041015-055649.

Schust, J., Sperl, B., Hollis, A., et al. (2006) Stattic: A Small-Molecule Inhibitor of STAT3 Activation and Dimerization. *Chem Biol*, 13 (11): 1235–1242. doi:10.1016/j.chembiol.2006.09.018.

Schwartz, K.L., Richardson, S.E., MacGregor, D., et al. (2019) Adenovirus-Associated Central Nervous System Disease in Children. *J Pediatr*, 205: 130–137. doi:10.1016/j.jpeds.2018.09.036.

Scully, M., Cataland, S.R., Peyvandi, F., et al. (2019) Caplacizumab treatment for acquired thrombotic thrombocytopenic purpura. *N Engl J Med*, 380 (4): 335–346. doi:10.1056/NEJMoa1806311.

Scully, M., Singh, D., Lown, R., et al. (2021) Pathologic Antibodies to Platelet Factor 4 after ChAdOx1 nCoV-19 Vaccination. *N Engl J Med*, 384 (23): 2202–2211. doi:10.1056/nejmoa2105385.

Seavey, M.M. and Dobrzanski, P. (2012) The many faces of Janus kinase. *Biochem Pharmacol*, 83 (9): 1136–1145. doi:10.1016/j.bcp.2011.12.024.

See, I., Lale, A., Marquez, P., et al. (2022) Case Series of Thrombosis With Thrombocytopenia Syndrome After COVID-19 Vaccination—United States, December 2020 to August 2021. *Ann Intern Med*, 175 (4): 513–522. doi:10.7326/M21-4502.

Selleckchem (n.d.) *SH-4-54*. Available at: https://www.selleckchem.com/products/sh-4-54.html (Accessed: 5 January 2025).

Shi, G., Field, D.J., Ko, K.A., et al. (2014) Platelet factor 4 limits Th17 differentiation and cardiac allograft rejection. *J Clin Invest*, 124 (2): 543–552. doi:10.1172/JCI71858.

Silva-Cardoso, S.C., Affandi, A.J., Spel, L., et al. (2017) CXCL4 Exposure Potentiates TLR-Driven Polarization of Human Monocyte-Derived Dendritic Cells and Increases Stimulation of T Cells. *J Immunol*, 199 (1): 253–262. doi:10.4049/jimmunol.1602020.

Slungaard, A., Fernandez, J.A., Griffin, J.H., et al. (2003) Platelet factor 4 enhances generation of activated protein C in vitro and in vivo. *Blood*, 102 (1): 146–151. doi:10.1182/blood-2002-11-3529.

Slungaard, A. and Key, N.S. (1994) Platelet factor 4 stimulates thrombomodulin protein C-activating cofactor activity: A structure-function analysis. *J Biol Chem*, 269 (41): 25549–25556. doi:10.1016/s0021-9258(18)47284-5.

Smith, C.W., Montague, S.J., Kardeby, C., et al. (2021) Antiplatelet drugs block platelet activation by VITT patient serum. *Blood*, 138 (25): 2733–2740. doi:10.1182/blood.2021012641.

Sokolovic, M., Pratt, A.K., Vukicevic, V., et al. (2016) Platelet Count Trends and Prevalence of Heparin-Induced Thrombocytopenia in a Cohort of Extracorporeal Membrane Oxygenator Patients. *Crit Care Med*, 44 (11): e1031–e1037. doi:10.1097/CCM.0000000000001869.

St Charles, R., Walz, D.A. and Edwards, B.F. (1989) The three-dimensional Structure of Bovine Platelet Factor 4 at 3.0-A Resolution. *J Biol Chem*, 264 (4): 2092–2099. doi:10.1016/S0021-9258(18)94146-3.

Stanger, L., Yamaguchi, A. and Holinstat, M. (2023) Antiplatelet strategies: past, present, and future. *J Thromb Haemost*, 21 (12): 3317–3328. doi:10.1016/j.jtha.2023.09.013.

Stegner, D., Göb, V., Krenzlin, V., et al. (2022) Foudroyant cerebral venous (sinus) thrombosis triggered through CLEC-2 and GPIIb/IIIa dependent platelet activation. *Nat Cardiovasc Res*, 1 (2): 132–141. doi:10.1038/s44161-021-00017-1.

Stimpfle, F., Bauer, M., Rath, D., et al. (2018) Variants of PEAR1 Are Associated With Outcome in Patients With ACS and Stable CAD Undergoing PCI. *Front Pharmacol*, 9. doi:10.3389/fphar.2018.00490.

Stolla, M., Stefanini, L., André, P., et al. (2011) CalDAG-GEFI deficiency protects mice in a novel model of FcγRIIA-mediated thrombosis and thrombocytopenia. *Blood*, 118 (4): 1113–1120. doi:10.1182/blood-2011-03-342352.

Stringer, S., Wray, N.R., Kahn, R.S., et al. (2011) Underestimated Effect Sizes in GWAS: Fundamental Limitations of Single SNP Analysis for Dichotomous Phenotypes. *PLoS ONE*, 6 (11): e27964. doi:10.1371/journal.pone.0027964.

Stringer, S.E. and Gallagher, J.T. (1997) Specific binding of the chemokine platelet factor 4 to heparan sulfate. *J Biol Chem*, 272 (33): 20508–20514. doi:10.1074/jbc.272.33.20508.

Struyf, S., Burdick, M.D., Proost, P., et al. (2004) Platelets release CXCL4L1, a nonallelic variant of the chemokine platelet factor-4/CXCL4 and potent inhibitor of angiogenesis. *Circ Res*, 95 (9): 855–7. doi:10.1161/01.RES.0000146674.38319.07.

Sulpice, E., Bryckaert, M., Lacour, J., et al. (2002) Platelet factor 4 inhibits FGF2-induced endothelial cell proliferation via the extracellular signal – regulated kinase pathway but not by the phosphatidylinositol 3 – kinase pathway. *Blood*, 100 (9): 3087–3094. doi:10.1182/blood.V100.9.3087.

Sulpice, E., Contreres, J.-O., Lacour, J., et al. (2004) Platelet factor 4 disrupts the intracellular signalling cascade induced by vascular endothelial growth factor by both KDR dependent and independent mechanisms. *Eur J Biochem*, 271 (16): 3310–8. doi:10.1111/j.1432-1033.2004.04263.x.

Sun, Y., Vandenbriele, C., Kauskot, A., et al. (2015) A Human Platelet Receptor Protein Microarray Identifies the High Affinity Immunoglobulin E Receptor Subunit α (FcεR1α) as an Activating Platelet Endothelium Aggregation Receptor 1 (PEAR1) Ligand. *Mol Cell Proteomics*, 14 (5): 1265–1274. doi:10.1074/mcp.M114.046946.

Tardy-Poncet, B., Montmartin, A., Piot, M., et al. (2021) Functional Flow Cytometric Assay for Reliable and Convenient Heparin-Induced Thrombocytopenia Diagnosis in Daily Practice. *Biomedicines*, 9 (4): 332. doi:10.3390/biomedicines9040332.

Taylor, S.M., Reilly, M.P., Schreiber, A.D., et al. (2000) Thrombosis and shock induced by activating antiplatelet antibodies in human Fc gamma RIIA transgenic mice: the interplay among antibody, spleen, and Fc receptor. *Blood*, 96 (13): 4254–60.

ThermoFisher Scientific (n.d.) *Invitrogen c-Mpl Polyclonal Antibody*. Available at: https://www.thermofisher.com/antibody/product/c-Mpl-Antibody-Polyclonal/PA5-47042 (Accessed: 31 October 2024).

Tran, H.A., Deng, L., Wood, N., et al. (2023) The clinicopathological features of thrombosis with thrombocytopenia syndrome following ChAdOx1-S (AZD1222) vaccination and case outcomes in Australia: a population-based study. *Lancet Reg Health West Pac*, 40: 100894. doi:10.1016/j.lanwpc.2023.100894.

Trimm, E. and Red-Horse, K. (2023) Vascular endothelial cell development and diversity. *Nat Rev Cardiol*, 20 (3): 197–210. doi:10.1038/s41569-022-00770-1.

Trist, H.M., Tan, P.S., Wines, B.D., et al. (2014) Polymorphisms and Interspecies Differences of the Activating and Inhibitory FcγRII of Macaca nemestrina Influence the Binding of Human IgG Subclasses. *J Immunol*, 192 (2): 792–803. doi:10.4049/jimmunol.1301554.

Tsutsumi, N., Masoumi, Z., James, S.C., et al. (2023) Structure of the thrombopoietin-MPL receptor complex is a blueprint for biasing hematopoiesis. *Cell*. doi:10.1016/j.cell.2023.07.037.

Tunnacliffe, A., Majumdar, S., Yan, B., et al. (1992) Genes for β-thromboglobulin and platelet factor 4 are closely linked and form part of a cluster of related genes on chromosome 4. *Blood*, 79 (11): 2896–2900. doi:10.1182/blood.v79.11.2896.2896.

Ueland, T., Hausberg, I., Mørtberg, T.V., et al. (2022) Anti-PF4/polyanion antibodies in COVID-19 patients are associated with disease severity and pulmonary pathology. *Platelets*, 33 (4): 640–644. doi:10.1080/09537104.2022.2042238.

Urbanus, R.T., Pennings, M.T.T., Derksen R.H.W.M., et al. (2008) Platelet activation by dimeric β2-glycoprotein I requires signaling via both glycoprotein Ibα and apolipoprotein E receptor 2′. *J Thromb Haemost*, 6 (8): 1405–1412. doi:10.1111/j.1538-7836.2008.03021.x.

Uzun, G., Zlamal, J., Althaus, K., et al. (2023) Cerebral venous sinus thrombosis and thrombocytopenia due to heparin independent anti-PF4 antibodies after adenovirus infection. *Haematologica*, pp. 2010–2015. doi:10.3324/haematol.2023.284127.

Valentini, G., Riccardi, A., Vettori, S., et al. (2017) CXCL4 in undifferentiated connective tissue disease at risk for systemic sclerosis (SSc) (previously referred to as very early SSc). *Clin Exp Med*, 17 (3): 411–414. doi:10.1007/s10238-016-0437-y.

Vandercappellen, J., Liekens, S., Bronckaers, A., et al. (2010) The COOH-terminal peptide of platelet factor-4 variant (CXCL4L1/PF- 4var47-70) strongly inhibits angiogenesis and suppresses B16 melanoma growth in vivo. *Mol Cancer Res*, 8 (3): 322–334. doi:10.1158/1541-7786.MCR-09-0176.

Vandercappellen, J., Noppen, S., Verbeke, H., et al. (2007) Stimulation of angiostatic platelet factor-4 variant (CXCL4L1/PF-4var) versus inhibition of angiogenic granulocyte chemotactic protein-2 (CXCL6/GCP-2) in normal and tumoral mesenchymal cells. *J Leuk Biol*, 82 (6): 1519–1530. doi:10.1189/jlb.0407206.

Varga-Szabo, D., Braun, A. and Nieswandt, B. (2009) Calcium signaling in platelets. *J Thromb Haemost*, 7 (7): 1057–1066. doi:10.1111/j.1538-7836.2009.03455.x.

Vassilev, A.O., Lorenz, D.R., Tibbles, H.E., et al. (2002) Role of the Leukemia-associated Transcription Factor STAT3 in Platelet Physiology. *Leuk Lymphoma*, 43 (7): 1461–1467. doi:10.1080/1042819022386716.

Vayne, C., Guéry, E., Charuel, N., et al. (2020) Evaluation of functional assays for the diagnosis of heparin induced thrombocytopenia using 5B9, a monoclonal IgG that mimics human antibodies. *J Thromb Haemost*, 18 (4): 968–975. doi:10.1111/jth.14749.

Vayne, C., May, M.-A., Bourguignon, T., et al. (2019) Frequency and Clinical Impact of Platelet Factor 4-Specific Antibodies in Patients Undergoing Extracorporeal Membrane Oxygenation. *Thromb Haemost*, 119 (07): 1138–1146. doi:10.1055/s-0039-1688827.

Vayne, C., Nguyen, T.-H., Rollin, J., et al. (2021a) Characterization of New Monoclonal PF4-Specific Antibodies as Useful Tools for Studies on Typical and Autoimmune Heparin-Induced Thrombocytopenia. *Thromb Haemost*, 121 (03): 322–331. doi:10.1055/s-0040-1717078.

Vayne, C., Palankar, R., Billy, S., et al. (2021b) The Deglycosylated Form of 1E12, a Monoclonal Anti-PF4 IgG, Strongly Inhibits Antibody-Triggered Cellular Activation in

Vaccine-Induced Thrombotic Thrombocytopenia, and Is a Potential New Treatment for VITT. *Blood*, 138 (Supplement 1): 582–582. doi:10.1182/blood-2021-147922.

Vayne, C., Rollin, J., Clare, R., et al. (2024) The use of 1E12, a monoclonal anti-platelet factor 4 antibody, to improve the diagnosis of vaccine-induced immune thrombotic thrombocytopenia. *J Thromb Haemost*. doi:10.1016/j.jtha.2024.05.005.

Vettori, S., Irace, R., Riccardi, A., et al. (2016) Serum CXCL4 increase in primary Sjögren's syndrome characterizes patients with microvascular involvement and reduced salivary gland infiltration and lymph node involvement. *Clin Rheumatol*, 35 (10): 2591–2596. doi:10.1007/s10067-016-3386-7.

Vidarsson, G., Dekkers, G. and Rispens, T. (2014) IgG Subclasses and Allotypes: From Structure to Effector Functions. *Front Immunol*, 5. doi:10.3389/fimmu.2014.00520.

Visentin, G.P., Ford, S.E., Scott, J.P., et al. (1994) Antibodies from patients with heparin-induced thrombocytopenia/thrombosis are specific for platelet factor 4 complexed with heparin or bound to endothelial cells. *J Clin Invest*, 93 (1): 81–88. doi:10.1172/JCI116987.

Wang, M., Hao, H., Leeper, N.J., et al. (2018) Thrombotic Regulation From the Endothelial Cell Perspectives. *Arterioscler Thromb Vasc Biol*, 38 (6). doi:10.1161/ATVBAHA.118.310367.

Warkentin, T.E. (2023a) Autoimmune Heparin-Induced Thrombocytopenia. *J Clin Med*, 12: 6921. doi:10.3390/jcm12216921.

Warkentin, T.E. (2023b) Heparin-induced thrombocytopenia (and autoimmune heparin-induced thrombocytopenia): an illustrious review. *Res Pract Thromb Haemost*, 7 (8): 102245. doi:10.1016/j.rpth.2023.102245.

Warkentin, T.E., Arnold, D.M., Nazi, I., et al. (2015) The platelet serotonin-release assay. *Am J Haematol*, 90 (6): 564–572. doi:10.1002/ajh.24006.

Warkentin, T.E., Arnold, D.M., Sheppard, J.A.I., et al. (2023a) Investigation of anti-PF4 versus anti-PF4/heparin reactivity using fluid-phase enzyme immunoassay for 4 anti-PF4 disorders: classic heparin-induced thrombocytopenia (HIT), autoimmune HIT, vaccine-induced immune thrombotic thrombocytopenia, and spontaneous HIT. *J Thromb Haemost*. doi:10.1016/j.jtha.2023.04.034.

Warkentin, T.E., Baskin-Miller, J., Raybould, A.L., et al. (2023b) Adenovirus-Associated Thrombocytopenia, Thrombosis, and VITT-like Antibodies. *N Engl J Med*, 389 (6): 574–577. doi:10.1056/NEJMc2307721.

Warkentin, T.E., Cook, R.J., Marder, V.J., et al. (2005a) Anti–platelet factor 4/heparin antibodies in orthopedic surgery patients receiving antithrombotic prophylaxis with fondaparinux or enoxaparin. *Blood*, 106 (12): 3791–3796. doi:10.1182/blood-2005-05-1938.

Warkentin, T.E. and Greinacher, A. (2022) Laboratory testing for VITT antibodies. *Semin Hematol*, 59 (2): 80–88. doi:10.1053/j.seminhematol.2022.03.003.

Warkentin, T.E., Hayward, C.P., Smith, C.A., et al. (1992) Determinants of donor platelet variability when testing for heparin-induced thrombocytopenia. *J Lab Clin Med*, 120 (3): 371–9.

Warkentin, T.E., Makris, M., Jay, R.M., et al. (2008a) A Spontaneous Prothrombotic Disorder Resembling Heparin-induced Thrombocytopenia. *Am J Med*, 121 (7): 632–636. doi:10.1016/j.amjmed.2008.03.012.

Warkentin, T.E., Roberts, R.S., Hirsh, J., et al. (2005b) Heparin-Induced Skin Lesions and Other Unusual Sequelae of the Heparin-Induced Thrombocytopenia Syndrome. *Chest*, 127 (5): 1857–1861. doi:10.1378/chest.127.5.1857.

Warkentin, T.E., Sheppard, J.A., Horsewood, P., et al. (2000) Impact of the patient population on the risk for heparin-induced thrombocytopenia. *Blood*, 96 (5): 1703–1708.

Warkentin, T.E., Sheppard, J.I., Moore, J.C., et al. (2008b) Quantitative interpretation of optical density measurements using PF4-dependent enzyme-immunoassays. *J Thromb Haemost*, 6 (8): 1304–1312. doi:10.1111/j.1538-7836.2008.03025.x.

Warmerdam, P.A., van de Winkel, J.G., Gosselin, E.J., et al. (1990) Molecular basis for a polymorphism of human Fc gamma receptor II (CD32). *J Exp Med*, 172 (1): 19–25. doi:10.1084/jem.172.1.19.

Watson, O.J., Barnsley, G., Toor, J., et al. (2022) Global impact of the first year of COVID-19 vaccination: a mathematical modelling study. *Lancet Infect Dis*, 22 (9): 1293–1302. doi:10.1016/S1473-3099(22)00320-6.

Weismann, R.E. and Tobin, R.W. (1958) Arterial Embolism Occurring During Systemic Heparin Therapy. *AMA Arch Surg*, 76 (2): 219. doi:10.1001/archsurg.1958.01280200041005.

Van Willigen, G., Gorter, G. and Akkerman, J.W.N. (2000) Thrombopoietin increases platelet sensitivity to α-thrombin via activation of the ERK2-cPLA2 pathway. *Thromb Haemost*, 83 (4): 610–616. doi:10.1055/s-0037-1613872.

Wilson, W.W., Wade, M.M., Holman, S.C., et al. (2001) Status of methods for assessing bacterial cell surface charge properties based on zeta potential measurements. *J Microbiol Methods*, 43 (3): 153–164. doi:10.1016/S0167-7012(00)00224-4.

Winkler, E.A., Kim, C.N., Ross, J.M., et al. (2022) A single-cell atlas of the normal and malformed human brain vasculature. *Science*, 375 (6584): eabi7377. doi:10.1126/science.abi7377.

Witte, L.D., Kaplan, K.L., Nossel, H.L., et al. (1978) Studies of the release from human platelets of the growth factor for cultured human arterial smooth muscle cells. *Circ Res*, 42 (3): 402–9. doi:10.1161/01.res.42.3.402.

Witzemann, A., Pelzl, L., Wolska, N., et al. (2023) Anti-PF4/Heparin Monoclonal Antibodies Induce Thrombus Formation in an Ex Vivo Endothelialized Microfluidic System. *Blood*, 142 (Supplement 1): 1199–1199. doi:10.1182/blood-2023-189626.

Worth, R.G., Chien, C.D., Chien, P., et al. (2006) Platelet FcγRIIA binds and internalizes IgG-containing complexes. *Exp Hematol*, 34 (11): 1490–1495. doi:10.1016/j.exphem.2006.06.015.

Woulfe, D.S., Lilliendahl, J.K., August, S., et al. (2008) Serglycin proteoglycan deletion induces defects in platelet aggregation and thrombus formation in mice. *Blood*, 111 (7): 3458–67. doi:10.1182/blood-2007-07-104703.

Wymann, M.P., Bulgarelli-Leva, G., Zvelebil, M.J., et al. (1996) Wortmannin Inactivates Phosphoinositide 3-Kinase by Covalent Modification of Lys-802, a Residue Involved in the Phosphate Transfer Reaction. *Mol Cell Biol*, 16 (4): 1722–1733. doi:10.1128/MCB.16.4.1722.

Xi, X., Caen, J.P., Fournier, S., et al. (1996) Direct and reversible inhibition of platelet factor 4 on megakaryocyte development from CD34+ cord blood cells: comparative studies with transforming growth factor β1. *Br J Haematol*, 93 (2): 265–272. doi:10.1046/j.1365-2141.1996.4901032.x.

Xiao, Z. and Théroux, P. (1998) Platelet Activation With Unfractionated Heparin at Therapeutic Concentrations and Comparisons With a Low-Molecular-Weight Heparin and With a Direct Thrombin Inhibitor. *Circulation*, 97 (3): 251–256. doi:10.1161/01.CIR.97.3.251.

Xu, D. and Esko, J.D. (2014) Demystifying heparan sulfate-protein interactions. *Annu Rev Biochem*, 83: 129–57. doi:10.1146/annurev-biochem-060713-035314.

Yamada, M., Komatsu, N., Okada, K., et al. (1995) Thrombopoietin Induces Tyrosine Phosphorylation and Activation of Mitogen-Activated Protein Kinases in a Human

Thrombopoietin-Dependent Cell Line. *Biochem Biophys Res Commun*, 217 (1): 230–237. doi:10.1006/BBRC.1995.2768.

Yang, C., Bachu, M., Du, Y., et al. (2022) CXCL4 synergizes with TLR8 for TBK1-IRF5 activation, epigenomic remodeling and inflammatory response in human monocytes. *Nature Commun*, 13 (1): 3426. doi:10.1038/s41467-022-31132-7.

Yao, H.HY. and Kahr, W.HA. (2024) Molecular basis of platelet granule defects. *J Thromb Haemost*. doi:10.1016/j.jtha.2024.11.016.

Ye, L., Zhang, Y.P., Yu, N., et al. (2017) Serum platelet factor 4 is a reliable activity parameter in adult patients with inflammatory bowel disease. *Medicine (Baltimore)*, 96 (11). doi:10.1097/MD.0000000000006323.

Yin, L., Xu, J., Wu, W., et al. (2023) Dual inhibition of STAT3 and STAT5 may overcome imatinib resistance in chronic myeloid leukemia. *Hematology*, 28 (1). doi:10.1080/16078454.2023.2224625.

Yu, G., Rux, A.H., Ma, P., et al. (2005) Endothelial expression of E-selectin is induced by the platelet-specific chemokine platelet factor 4 through LRP in an NF-κB-dependent manner. *Blood*, 105 (9): 3545–3551. doi:10.1182/blood-2004-07-2617.

Yu, K., Toral-Barza, L., Shi, C., et al. (2009) Biochemical, Cellular, and In vivo Activity of Novel ATP-Competitive and Selective Inhibitors of the Mammalian Target of Rapamycin. *Cancer Res*, 69 (15): 6232–6240. doi:10.1158/0008-5472.CAN-09-0299.

Zhang, S., Ayemoba, C., Di Staulo, A.M., et al. (2024) “Platelet Factor 4 (PF4) Regulates Hematopoietic Stem Cell Aging.” In *Blood*. 2024. pp. 2–2. doi:10.1182/blood-2024-205355.

Zhang, X., Chen, L., Bancroft, D.P., et al. (1994) Crystal structure of recombinant human platelet factor 4. *Biochemistry*, 33 (27): 8361–8366. doi:10.1021/BI00193A025.

Zhao, X., Feng, X., Wu, Z., et al. (2018) Persistent elevation of plasma thrombopoietin levels after treatment in severe aplastic anemia. *Exp Hematol*, 58: 39–43. doi:10.1016/j.exphem.2017.09.006.

Zheng, Y., Yu, M., Podd, A., et al. (2013) Critical role for mouse marginal zone B cells in PF4/heparin antibody production. *Blood*, 121 (17): 3484–3492. doi:10.1182/blood-2013-01-477091.

Zhou, T., Georgeon, S., Moser, R., et al. (2014a) Specificity and mechanism-of-action of the JAK2 tyrosine kinase inhibitors ruxolitinib and SAR302503 (TG101348). *Leukemia*, 28 (2): 404–407. doi:10.1038/leu.2013.205.

Zhou, T., Georgeon, S., Moser, R., et al. (2014b) Specificity and mechanism-of-action of the JAK2 tyrosine kinase inhibitors ruxolitinib and SAR302503 (TG101348). *Leukemia*, 28 (2): 404–407. doi:10.1038/leu.2013.205.

Zhou, Y., Abraham, S., Andre, P., et al. (2015) Anti–miR-148a regulates platelet FcγRIIA signaling and decreases thrombosis in vivo in mice. *Blood*, 126 (26): 2871–2881. doi:10.1182/blood-2015-02-631135.

Zhou, Y., Abraham, S., Renna, S., et al. (2016) TULA-2 (T-Cell Ubiquitin Ligand-2) Inhibits the Platelet Fc Receptor for IgG IIA (FcγRIIA) Signaling Pathway and Heparin-Induced Thrombocytopenia in Mice. *Arterioscler Thromb Vasc Biol*, 36 (12): 2315–2323. doi:10.1161/ATVBAHA.116.307979.

Zhou, Z., Gushiken, F.C., Bolgiano, D., et al. (2013) Signal transducer and activator of transcription 3 (STAT3) regulates collagen-induced Platelet aggregation independently of its transcription factor activity. *Circulation*, 127 (4): 476–485. doi:10.1161/CIRCULATIONAHA.112.132126.

Zhu, W., Zheng, Y., Yu, M., et al. (2024) Prothrombotic Antibodies Targeting the Spike Protein's Receptor-Binding Domain in Severe COVID-19. *Blood Journal*. doi:10.1182/blood.2024025010.

Zon, R.L., Sylvester, K.W., Rubins, D., et al. (2024) Electronic alerts to improve management of heparin-induced thrombocytopenia. *Res Pract Thromb Haemost*, 8 (4). doi:10.1016/j.rpth.2024.102423.

Appendix 1

References for information events described in Figure 1.1.

1948: Existence first postulated as heparin neutralising agent (Conley et al., 1948)
1957: First purification (Deutsch et al., 1957)
1958: First report of HIT (Weismann and Tobin, 1958)
1976: Tetrameric form discovered (Handin and Cohen, 1976)
1976: GAG binding properties described (Handin and Cohen, 1976)
1977: Amino acid sequence identified (Deuel et al., 1977)
1978: Discovered in platelet alpha granules (Witte et al., 1978)
1985: Potentiates platelet activation (Capitanio et al., 1985)
1986: Structure of PF4 with heparin (Cowan et al., 1986)
1987: Gene cloned (Poncz et al., 1987)
1989: First crystal structure (bovine) (St Charles et al., 1989)
1990: Comparison with PF4alt gene (Eisman et al., 1990)
1991: Amino acids for heparin binding confirmed (Maione et al., 1991)
1994: Structure of human PF4 (Zhang et al., 1994)
1998: Neutrophil activation by PF4 dependent on GAGs (Petersen et al., 1998)
2003: CXCR3b identified as an endothelial PF4 receptor (Lasagni et al., 2003)
2008: First description of autoimmune HIT (Warkentin et al., 2008a)
2009: LRP1 identified as a megakaryocyte PF4 receptor (Lambert et al., 2009)
2010: Structural basis for difference between PF4 and PF4var (Kuo et al., 2013)
2012: Binding to bacterial lipid A exposes HIT epitopes (Krauel et al., 2012)
2014: MK secretion of PF4 regulates stem cell quiescence (Bruns et al., 2014)
2015: Atomic description of HIT immune complex (Cai et al., 2015)
2021: First reports of VITT (Schultz et al., 2021; Greinacher et al., 2021; Scully et al., 2021)
2023: c-Mpl identified as platelet PF4 receptor (Buka et al., 2024)
2023: Endothelial GAG binding recruits leukocytes (Gray et al., 2023)